Department of Pharmacology

Wellcome Trust 4-year PhD Programme in Neuroscience

University College London

An electrophysiological study of synaptic glutamate receptors in cerebellar Golgi cells during development

by

Man Hin Mok

2003

A thesis submitted for the Degree of
Doctor of Philosophy
University of London

Supervisor: Professor Stuart G. Cull-Candy FRS

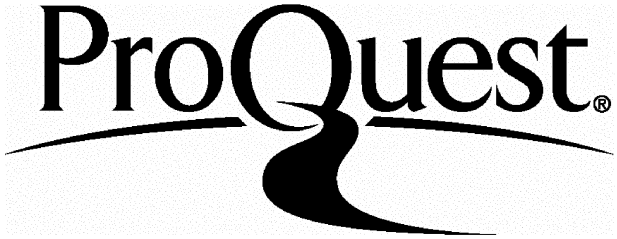

ABSTRACT

N-methyl-D-aspartate receptors (NMDARs) are assemblies of NR1 and NR2 (NR2A-2D) subunits and their kinetic and pharmacological properties depend on the NR2 subunits expressed. We examined developmental changes in NMDAR-mediated excitatory postsynaptic currents (EPSCs) in mouse cerebellar Golgi cells in acute thin slices. Further, we investigated whether NMDAR subtypes are differentially distributed at synaptic and extrasynaptic sites.

EPSCs were recorded under whole-cell voltage-clamp. EPSC decay kinetics and pharmacology were studied at postnatal days (P)7-8 and P15-18. We found EPSCs at P7-8 to be highly sensitive to the NR2B-selective antagonist ifenprodil. At P15-18, EPSCs were shorter in duration, less ifenprodil-sensitive but more sensitive to TPEN, an agent affecting NR2A-NMDARs. Taken together, these observations suggest a developmental switch from NR2B- to NR2A-NMDARs.

We next examined whether similar changes occur extrasynaptically. Extrasynaptic NMDARs, activated by a high-frequency train of stimuli, were compared with synaptic NMDARs activated by a single stimulus. Single- and trains of EPSCs at P7-8 were highly ifenprodil-sensitive, suggesting NR2B-NMDARs are present both synaptically and extrasynaptically. At P15-18, train-generated EPSCs were slower and more ifenprodil-sensitive than single EPSCs. Ifenprodil sensitivity was further increased after blockade of synaptic NMDARs with the channel-blocker MK801. This supports the idea that the NR2B-to-NR2A switch is restricted to the synapse.

NR2D-containing NMDARs are present on the soma of Golgi cells. To investigate whether NR2D-NMDARs are involved in synaptic transmission, we compared EPSCs from wild-type and NR2D-ablated mice at P7-10. We found no apparent differences in EPSC properties, suggesting NR2D is restricted to extrasynaptic sites.

In conclusion, cerebellar Golgi cells express several NMDAR subtypes which are differentially distributed within the cell and developmentally regulated. At P7-8, NR2B-receptors are present at and peripheral to the synapse and NR2D-receptors are in the soma. By P15-18, NR2A-NMDARs are targeted to synapses while NMDARs in the vicinity remain of the NR2B subtype.

TABLE OF CONTENTS

LIST OF FIGURES

LIST OF TABLES

COMMUNICATIONS AND PUBLICATIONS

Mok MHS, Liu SQJ & Cull-Candy SG (2002) Changes in the properties of NMDA receptor-mediated EPSCs during development of mouse cerebellar Golgi cells. Meeting of The Physiological Society, Liverpool, UK. Journal of Physiology, 543:29P

Mok MHS, Liu SQJ & Cull-Candy SG (2002) Changes in subunits contributing to synaptic NMDA receptors during development of mouse cerebellar Golgi cells. 32nd Annual Meeting for the Society for Neuroscience, Orlando, USA. Abstract 244.15.

Mok MHS, Liu SQJ & Cull-Candy SG (2002) Developmental changes in subunits contributing to synaptic NMDA receptors in cerebellar Golgi cells. 3rd Forum of European Neuroscience, FENS, Paris, France. Abstract 077.4.

Misra C, Brickey SG, Mok MHS, Mishina M & Cull-Candy SG (2002) NMDAR channels subunits in cerebellar Golgi cell of wild-type and NR2D-ablated mice. Meeting of The Physiological Society, London, UK. Journal of Physiology, 547:39P

Brickey SG, Misra C, Mok MHS, Mishina M & Cull-Candy SG. NR2B and NR2D subunits co-assemble in cerebellar Golgi cells to form a distinct NMDAR subtype restricted to extrasynaptic sites. In Press (Journal of Neuroscience).

ACKNOWLEDGMENTS

I thank my supervisor Stuart Cull-Candy for his generous and unwavering support. His door was always open when I needed guidance, encouragement or just a friendly chat. It has been a memorable experience, a time full of learning and discovery.

Also a big thank you to June Liu for her time, care and friendship. Much appreciated and thoroughly enjoyed were the long (late-evening) discussions, the countless laughs and the happy explorations of London's theatres, galleries and restaurants.

Thank you to Stephen Brickley for his support, his advice and for introducing me to the Golgi cell. I would also like to thank Laurence Cathala. Further thanks to Charu Misra, Christine Gebhardt, Lorna Medhurst, Mark Farrant and Beverley Clark for all their help and support.

I am grateful to the Wellcome Trust and to the committee members of the 4-year PhD Programme in Neuroscience at UCL, in particular David Attwell and Alasdair Gibb, for their generous support.

To my parents and sister, your love and steadfast faith made it possible.

To my dearest, I am forever grateful for your patience and understanding.

CHAPTER 1

GENERAL

INTRODUCTION

1.1 *Classification of ionotropic glutamate receptors*

The majority of fast excitatory synaptic transmission in the vertebrate central nervous system is mediated by the amino acid L-glutamate. The excitatory and depolarising effects of glutamate were discovered in the 1950's and the following two to three decades saw tremendous efforts in establishing glutamate as a neurotransmitter and the classification of glutamate receptors (see Lodge, 1988; Wheal and Thomson, 1991; Collingridge and Watkins, 1994). In the 1960's, J.C. Watkins and others led a series of studies on the structure-activity relationships of analogues and homologues of glutamate (reviewed in Watkins and Evans, 1981; McLennan, 1983). By the late 1970s and early 1980s, development and testing of these compounds indicated a family of mammalian ionotropic glutamate receptors. Compounds similar in structure to L-glutamate (both naturally-occurring and synthetic) displayed varying degrees of agonist and antagonist affinities at these receptors. The ionotropic receptors are thus classified according to and named after relatively selective agonists. A subset of receptors is activated by the synthetic analogue of aspartic acid, *N*-methyl-D-aspartate (NMDA), and responses through NMDA receptors (NMDARs) are strongly inhibited by the antagonist D-2-amino-5-phosphonopentanoic acid (D-AP5). NMDA-insensitive or non-NMDA receptors were initially termed quisqualate and/or kainate receptors, after the agonist actions of these compounds. These receptors are now divided into α-amino-3-hydroxy-5-methyl-isoxazolepropionic acid (AMPA) receptors and kainate receptors. Both AMPA- and kainate receptors are sensitive to the antagonist 6-cyano-7-nitro-quinoxaline-2,3-dione (CNQX) but are not susceptible to inhibition by D-AP5.

By the mid 1980's, the properties of the NMDAR ion channel were being elucidated (reviewed in Collingridge and Lester, 1989). The NMDAR is highly permeable to Ca^{2+}, in addition to the Na^{+} influx and K^{+} efflux on receptor activation (MacDermott *et al*, 1986). The receptor is subject to a voltage-dependent channel block by Mg^{2+}, with the channel being blocked at negative membrane potentials (Nowak *et al*, 1984; Mayer and Westbrook, 1985). Single-channel openings induced by glutamate were also being investigated (Cull-Candy and Usowisz, 1987; Jahr and Stevens, 1987).

The demonstration of synaptic plasticity in the hippocampus was a milestone in the study of synaptic transmission (Bliss and Lømo, 1973). Termed long-term potentiation (LTP), this phenomenon was shown to involve the NMDAR (Collingridge *et al*, 1983). The conditional activation of the receptor, requiring the coincidence of presynaptic glutamate release and postsynaptic depolarisation to remove the Mg^{2+} block, underlies the role of the NMDAR in inducing associative synaptic plasticity (for reviews, Bliss and Collingridge, 1993; Bear and Malenka, 1994). In addition to its role in fast synaptic transmission and plasticity, the NMDAR is involved in a variety of processes during neuronal development, including synaptogenesis (Rabacchi *et al*, 1992), neuronal cell migration (Komura and Rakic, 1993) and neurite growth (Fischer *et al*, 2000; Sin *et al*, 2002).

On the other hand, excessive activation of NMDARs can lead to over-excitation and cell death, and this has been indicated in pathological conditions such as cerebral ischaemia, hypoxia, epilepsy, neuropathic pain syndromes and chronic neurodegenerative diseases (for reviews, Lodge, 1988; Dingledine *et al*, 1990; Meldrum and Garthwaite, 1990; Choi, 1995; Cull-Candy *et al*, 2001). Understanding the properties and functions of the NMDAR is of immense

importance, and three developments have culminated in major advances in the field: the molecular cloning of glutamate receptor subunits, the patch-clamp technique, and the availability of selective pharmacological agents.

1.2 *Molecular cloning of glutamate receptor subunits*

The cloning of cDNAs encoding glutamate receptor subunits in the early 1990s has propelled the research and knowledge of glutamate receptors forward with immense speed. By expression cloning and sequence homology studies, the pharmacological distinction of the three types of mammalian ionotropic glutamate receptors was given a molecular basis (reviewed by Hollmann and Heinemann, 1994). AMPA receptors are encoded for by a single gene family, kainate receptors by two and NMDA receptors by three. All glutamate receptor subunits are structurally similar. There are three lipophilic transmembrane regions M1, M3 and M4, with M2 being a re-entrant loop and most likely lining the channel pore (Hollmann *et al*, 1994; Bennett and Dingledine, 1995; Kuner and Schoepfer, 1996).

The AMPA receptors subunits (GluR1 to GluR4) can form both homomeric assemblies and heteromeric complexes, generating many possible combinations (reviewed by Bettler and Mulle, 1996; Borges and Dingledine, 1998). All copies of GluR2 are post-transcriptionally edited at the 'Q/R' site in M2 and the presence of an arginine (R) residue at this site confers low Ca^{2+}-permeability (Hume, Dingledine & Heinemann, 1991; Burnashev *et al*, 1992a; reviewed by Seeburg, 1996). The diversity of AMPA receptors is further increased by alternative splicing, such as that of the flip/flop cassette which affects channel deactivation and desensitisation (Sommer *et al*, 1990; Monyer *et al*, 1991). AMPA receptors

have deactivation kinetics at the millisecond level, a property which makes them suitable for their role in rapid synaptic transmission (Silver *et al*, 1992).

The first NMDA receptor subunit, NR1, was cloned by Moriyoshi *et al* (1991). Further studies have described the alternative splicing of exons 5, 21 and 22, generating at least eight known functional splice variants to date (Durand *et al*, 1992; Sugihara *et al*, 1992; Zukin and Bennett, 1995). A family of four cDNA clones, NR2A to NR2D, was further isolated (Monyer *et al*, 1992; Ishii *et al*, 1993). The NR2 subunits are 50-70% homologous to each other, but have only 15-20% homology with NR1. Equivalent cDNAs have been cloned from mouse brain, and are named ζ1 (NR1) and ϵ1-4 (NR2A-D; Kutsuwada *et al*, 1992; Meguro *et al*, 1992). Functional receptors are readily formed by co-expression of NR1 and at least one type of NR2 subunit (Monyer *et al*, 1994). In the M2 region of NR2 subunits, a conserved asparagine residue at a position analogous to the Q/R site of GluR1-4 subunits is partly responsible for the characteristic voltage-dependent Mg^{2+} block and permeability to divalent cations (Burnashev *et al*, 1992b; Mori *et al*, 1992; Kuner and Schoepfer, 1996). The less well-characterised NR3 subunit does not form functional channels on its own, but can co-assemble with NR1 and NR2 subunits to form NR1/NR2/NR3 complexes (Ciabarra *et al*, 1995; Sucher *et al*, 1995; Das *et al*, 1998).

In situ hybridisation studies have elucidated clear spatial and developmental profiles in the expression patterns of NR2 (or ε) subunits in the rat and mouse brain (Monaghan and Cotman, 1986; Akazawa *et al*, 1994; Monyer *et al*, 1994; Watanabe *et al*, 1994; Zhong *et al*, 1995; Wenzel *et al*, 1997; Monaghan *et al*, 1998). In general, the NR2B and NR2D subunits are expressed prenatally and are

abundant at early stages of postnatal development. Their expression levels tend to taper off as the brain matures. On the other hand, the expression of NR2A and NR2C begins after birth and increases with age. NR2A and NR2B are prominent in the hippocampus and cortical structures, while NR2C is mainly restricted to the cerebellum. The NR2D subunit appears to be localised in interneurons and in midbrain structures. Both NR1 splice variants and the NR3A subunit are also subject to developmental and regional regulation (Laurie and Seeburg, 1994a; Ciabarra *et al*, 1995; Sucher *et al*, 1995; Prybylowski and Wolfe, 2000).

1.3. *Functional properties of NMDARs*

The patch-clamp electrophysiology technique is used to examine the properties of synaptic currents and single-channel openings (Hamill *et al*, 1981; Neher and Sakmann, 1995). High-resolution single-channel openings of agonist-activated NMDARs have been resolved by excising patches of membrane in the outside-out configuration (for example, Cull-Candy and Usowicz, 1987; Farrant *et al*, 1994; Momiyama *et al*, 1996; Wyllie *et al*, 1998; Misra *et al*, 2000b). In the whole-cell configuration and under voltage-clamp, the kinetics and pharmacological sensitivities of agonist-evoked and synaptic currents through recombinant and native NMDARs can be studied (for example, Hestrin, 1992; Monyer *et al*, 1994; Kirson and Yaari, 1996; Vicini *et al*, 1998; Misra *et al*, 2000b; Cathala *et al*, 2000).

NMDARs have several characteristic properties, the majority of which are dependent on the NR2 subunit present within the receptor assembly (for reviews, McBain and Mayer, 1994; Dingledine *et al*, 1999). The affinity for glutamate is slightly different for recombinant receptors comprising the four different NR2

subunits (Table 1.1; Ikeda *et al*, 1992; Kutsuwada *et al*, 1992; Laurie and Seeburg 1994b; Priestley *et al*, 1995). Also, NR1/NR2A- and NR1/NR2B-diheteromers are subject to a stronger voltage-dependent block by Mg^{2+} than NR2C- and NR2D-receptors (Kutsuwada *et al*, 1992; Monyer *et al*, 1994; Kuner and Schoepfer, 1996). NMDARs require glycine as a co-agonist (Johnson and Ascher, 1987; Kleckner and Dingledine, 1988) and NR2A-containing receptors have a lower affinity for glycine compared with NR2B-, NR2C- and NR2D-containing receptors (Ikeda *et al*, 1992; Kutsuwada *et al*, 1992; Laurie and Seeburg, 1994b; Priestley *et al*, 1995). However, the permeability to Ca^{2+} appears to be comparable between the four receptor subtypes (MacDermott *et al*, 1986; Monyer *et al*, 1994). NMDARs are also sensitive to a number of modulators, including protons, Zn^{2+}, and polyamines (see section 1.4). A summary of the differential functional properties for different NMDAR subtypes can be found in Table 1.1.

Table 1.1 *Functional properties of recombinant NMDA receptors**

	NR2A	NR2B	NR2C	NR2D
Glutamate affinity (EC_{50}; μM)	1.7[d], 3.7[b]	0.8[d]	0.7[d], 1.0[b]	0.4[a]
Glycine affinity (EC_{50}, μM)	2.1[d]	0.3[d]	0.2[d]	0.1[a]
Mg^{2+} sensitivity[c] (at -100mV; IC_{50}, μM)	2.4	2.1	14.2	10.2
Ifenprodil sensitivity[j] (IC_{50}, μM)	161	0.47	No effect	No effect
Zn^{2+} sensitivity[g] (at -50mV, Mg^{2+}-free; IC_{50}, nM)	10	490	14,000	Not determined
Single-channel conductance (pS)	50 / 40[h,k]	50 / 40[h]	38 / 18[h]	38 / 18[k]
Asymmetry of transitions	no asymmetry	no asymmetry	no asymmetry	67% from 38 to 18pS
Decay kinetics of whole-cell currents (τ, ms) #	120[f], 180[k]	400[f]	380[f]	3000[e], 4800[f], 4400[k], 1600[i]

* co-expressed with NR1-1a

currents were measured in Mg^{2+}-free solutions, at -60mV except (i) which was measured at -50mV

EC_{50}: concentration which generates a half-maximal response

IC_{50} : concentration which blocks 50% of the maximal response

Values are taken from a number of studies ([a]Ikeda *et al*, 1992; [b]Ishii *et al*, 1992; [c]Kuner and Schoepfer, 1996; [d]Kutsuwada *et al*, 1992; [e]Misra *et al*, 2000b; [f]Monyer *et al*, 1994; [g]Paoletti *et al*, 1997; [h]Stern *et al*, 1992; [i]Vicini *et al*, 1998; [j]Williams, 1993; [k]Wyllie *et al*, 1998)

1.3.1 *Single-channel conductance*

The single-channel conductance of NMDARs is now known to be dependent on the NR2 subunit expressed in the receptor assembly (reviewed in Cull-Candy *et al*, 1998). Early reports of single-channel recordings showed that glutamate receptors open to multiple conductance levels (Cull-Candy and Usowisz, 1987; Jahr and Stevens, 1987; Gibb and Colquhoun, 1992). Following the molecular cloning of NMDAR subunits, an attempt was made to work out the subunit composition of native NMDARs by combining information of mRNA expression from *in situ* hybridisation experiments with single-channel conductance levels. For example, *in situ* hybridisation studies showed the expression of NR2D in rat cerebellar Purkinje cells (Akazawa *et al*, 1994; Monyer *et al*, 1994) and NMDA-activated single-channel openings of 18 and 38pS were observed (Momiyama *et al*, 1996).

Characterisation of recombinant receptors made the identification of native NMDAR subtypes more straight-forward by generating 'fingerprints' of NMDAR single-channel conductance levels. Outside-out patches containing recombinant NR1/NR2A and NR1/NR2B receptors have 'high' conductance level openings of ~50 and ~40pS, while NR1/NR2C and NR1/NR2D receptors displayed 'low' single-channel conductance levels of ~38 and ~18pS (Stern *et al*, 1992; Wyllie *et al*, 1996, 1998). Outside-out patches excised from the soma of internal granule cells in rat cerebellar slices have NMDA-activated single-channel openings of 18, 30, 40 and 48pS (Farrant *et al*, 1994). *In situ* hybridisation studies indicate the expression of NR1, NR2A, NR2B and NR2C subunits in these cells (Monyer *et al*, 1994; Akazawa *et al*, 1994). Taken together, the low conductance channels observed in these cells are most likely NR2C-containing NMDARs while the high

conductance openings reflect activation of NR1/NR2A and NR1/NR2B. Furthermore, NR1/NR2D openings exhibit asymmetry of transitions between conductance levels - 67% of openings going from the 38pS to the 18pS state (Wyllie *et al*, 1996). This behaviour has been observed in single-channel openings in patches from cerebellar Purkinje cells and Golgi cells (Momiyama *et al*, 1996; Misra *et al*, 2000). To date, the single-channel properties and possible subunit composition of native NMDA receptors have been examined in the rat cerebellum (Momiyama *et al*, 1996; Rumbaugh and Vicini, 1999; Cathala *et al*, 2000; Misra *et al*, 2000a; Billups *et al*, 2002), in the rat forebrain (Plant *et al*, 1997), in the rat hippocampus (Gibb and Colquhoun, 1992; Piña-Crespo and Gibb, 2002) and in the rat spinal cord (Momiyama *et al*, 1996; Momiyama, 2000).

Genetically-engineered mice have also played a role in the determination of NMDAR subunit composition in native neurons and the influence of subunit composition on receptor properties (Ebralidze *et al*, 1996; Takahashi *et al*, 1996; Tovar and Westbrook, 2000; also see Chapter 5). For example, the demonstration of high-conductance channels in cerebellar granule cells from young NR2A-knockout mice indicated the expression of NR2B-containing NMDA receptors in these cells (Takahashi *et al*, 1996). Whether disruption or enhancement of NR2 subunit expression affects synaptic plasticity and behaviour (e.g. motor co-ordination, learning and memory) has also received much interest (Ikeda *et al*, 1995; Sakimura *et al*, 1995; Kadotani *et al*, 1996; Kiyama *et al*, 1998; Okabe *et al*, 1998; Tang *et al*, 1999; Philpot *et al*, 2001b).

1.3.2 *Decay kinetics of whole-cell and synaptic currents*

Although single-channel conductance is useful in determining the subunit composition of receptors in outside-out patches excised from cell bodies, it is not

a parameter easily resolvable for whole-cell and synaptic currents (but see Clark *et al*, 1997). Another property of the NMDAR channel that is dependent on the NR2 subunit expressed is the decay kinetics of macroscopic currents. Monyer *et al* (1992, 1994) demonstrated that whole-cell currents through NR1/NR2A receptors expressed in HEK293 cells have the fastest decay time-course (time constant τ, ~100ms; Table 1.1). At the other end of the spectrum, currents through NR1/NR2D receptors decay approximately 400 times more slowly. The decay time-course of currents through NR1/NR2B and NR1/NR2C receptors is intermediate, with τ values of around 400ms. Other studies using rapid agonist applications and concentration jumps have shown similar values of decay time constants (Vicini *et al*, 1998; Wyllie *et al*, 1998). It is of note that NR1 splice variants can also affect the average decay time-course when co-expressed with NR2B but not when accompanied by NR2A (Rumbaugh *et al*, 2000; Vicini *et al*, 1998).

Following release from the presynaptic terminal, glutamate is rapidly cleared from the synaptic cleft and the duration of the glutamate transient is thought to be about 1ms (Clements *et al*, 1992; Clements, 1996; Diamond and Jahr, 1997; Bergles *et al*, 1999; but see Kinney *et al*, 1997). The decay kinetics of NMDAR-mediated synaptic currents is therefore unlikely to be dependent on the glutamate profile in the synapse and can thus provide an indication of the NR2 subunit expressed. Further molecular or pharmacological evidence is required to support the identification of NMDAR subunit composition. Experiments such as the examination of mice lacking the NR2A subunit (Takahashi *et al*, 1996) and the correlation of the decay kinetics with the relative amount of NR2A expressed (Flint *et al*, 1997) have demonstrated that NR2A expression is positively

correlated with faster-decaying currents in native systems. Synaptic currents in cerebellar granule cells from mice lacking the NR2A subunit exhibited slower decay kinetics (τ ~170ms compared with τ ~100ms for wild-type cells; Takahashi *et al*, 1996). Conversely, the presence of NR2B increased the duration of synaptic currents, as shown by comparing wild-type and NR2B-knockout mice (τ ~80ms and τ ~50ms, respectively; Tovar and Westbrook, 2000). Also, the kinetic properties of currents through native NMDA receptors have been shown to change during development (Carmignoto and Vicini, 1992; Hestrin, 1992). This phenomenon is thought to reflect the developmental regulation of NR2 subunit expression (Akazawa *et al*, 1994; Monyer *et al*, 1994; Watanabe *et al*, 1994) and will be discussed further in section 1.6.

1.4 *Pharmacology and modulation of NMDARs*

A unique property of the NMDA receptor is the strong voltage-sensitive channel block by Mg^{2+}. Monyer *et al* (1992, 1994) showed that recombinant NR1/NR2A and NR1/NR2B receptors are more sensitive to Mg^{2+} than NR1/NR2C and NR1/NR2D receptors. Similarly, the open channel blocker MK801 has a higher affinity for NR2A- and NR2B-containing receptors (Kutsuwada *et al*, 1992; Laurie and Seeburg, 1994b).

The NMDA receptor is sensitive to a wide range of compounds. Polyamines exert complex effects on NMDA receptors, including voltage-dependent inhibition and glycine-independent enhancement of currents (Benveniste and Mayer, 1993; Williams, 1994; reviewed by McBain and Mayer, 1994). Protons inhibit NMDARs and the extent of this inhibition is dependent on the NR1 splice variant

expressed (Traynelis and Cull-Candy, 1991; 1995). NMDA receptors have also been reported to be susceptible to modulation by: redox agents (Aizenman *et al*, 1989; Köhr *et al*, 1994; Brimecombe *et al*, 1997), nitric oxide (Lei *et al*, 1992; Lipton *et al*, 1993; Kim *et al*, 1999), ethanol (Kuner *et al*, 1993), intracellular Ca^{2+} (Clark *et al*, 1990; Legendre *et al*, 1993; Medina *et al*, 1995; Krupp *et al*, 1996), intracellular Na^{+} (Yu and Salter, 1998); light (Leszkiewicz *et al*, 2000) and changes in temperature (Feldmeyer and Cull-Candy, 1993). Furthermore, NR1, NR2A and NR2B subunits can be directly phosphorylated by cAMP-dependent protein kinase (PKA) and protein kinase C (PKC) at different sites (Hall and Soderling, 1997; Leonard and Hell, 1997; Tingley *et al*, 1997), and the NR2A and NR2B subunits are also susceptible to phosphorylation by tyrosine kinases (Moon *et al*, 1994; Lau and Huganir, 1995; Köhr and Seeburg, 1996; Zheng *et al*, 1998). These phosphorylation systems are thought to be important in the functional regulation of NMDA receptors (Chen and Huang, 1992; Wang and Salter, 1994; Wang *et al*, 1994; Raman *et al*, 1996; Lan *et al*, 2001; Vissel *et al*, 2001; Li *et al*, 2002).

1.4.1 *Ifenprodil: an antagonist selective for NR2B-NMDARs*

Although there are many known modulators for the NMDAR, there is still a dearth of specific agents which differentiate between the four receptor subtypes. The development of the phenylethanolamines (ifenprodil, haloperidol and CP101,606) was a milestone in the study of NMDAR subunit composition as this class of compounds proved very effective in inhibiting currents through NR2B receptors (Williams, 1993; Chenard *et al*, 1995; Ilyin *et al*, 1996). Ifenprodil is 400 times more selective for NR1/NR2B receptors than for NR1/NR2A receptors

(IC_{50} (concentration which blocks 50% of the maximal response), 0.34μM and 146μM, respectively; Williams, 1993) and has no effect on NMDARs with low single-channel conductance (i.e. NR2C- or NR2D-containing receptors; Williams, 1995; Mott *et al*, 1998; Misra *et al*, 2000a; Momiyama, 2000). Ifenprodil also has no effects on currents through AMPA and kainate receptors (Mott *et al*, 1998).

Ifenprodil is an atypical non-competitive antagonist and several mechanisms of action have been proposed. An interference with polyamine binding in the amino terminal domain was originally thought to be involved (Carter *et al*, 1990) but subsequent work using site-directed mutagenesis showed that ifenprodil binds to a distinct site (Gallagher *et al*, 1996). There was also evidence to suggest that ifenprodil stabilises a channel state that has a lower open probability (Legendre and Westbrook, 1991; Kew *et al*, 1996). Recently, it was demonstrated phenylethanolamines act by enhancing proton inhibition (Mott *et al*, 1998). Point mutation experiments also indicated an allosteric interaction between the glutamate and ifenprodil binding sites (analogous to the interaction between glutamate and Zn^{2+} binding sites on NR2A; see section 1.4.2). Glutamate binding may enhance ifenprodil binding, in turn enhancing the binding of protons and shifting more receptors into closed states (Zheng *et al*, 2001). Ifenprodil, haloperidol and CP101-606 have been widely used in elucidating the subunit composition of NMDA receptors on the cell bodies and at synapses in central neurons (Williams *et al*, 1993; Kirson and Yaari, 1996; Rumbaugh and Vicini, 1999; Cathala *et al*, 2000; Misra *et al*, 2000a; this study)

1.4.2 *TPEN: removal of the NR2A-selective high-affinity Zn^{2+} inhibition*

It was shown over a decade ago that Zn^{2+} inhibits NMDARs (Peters *et al*, 1987; Westbrook and Mayer, 1987; Mayer *et al*, 1989; Christine and Choi, 1990; Legendre and Westbrook, 1990; reviewed in Dingledine *et al*, 1999). It has been known since the 1980s that Zn^{2+} is present in high concentrations in the brain, especially in the synaptic vesicles of mossy fibres in the hippocampus, and is released during neuronal activity (Frederickson *et al*, 1983; Assaf and Chung, 1984; Howell *et al*, 1984; Perez-Clausell and Danscher, 1985). It is therefore very plausible that modulation of NMDARs by Zn^{2+} would alter synaptic activity.

Receptors containing NR2A have a higher affinity for Zn^{2+} and this sensitivity is influenced by NR1 alternative splicing and possibly also by Src tyrosine phosphorylation (Hollmann *et al*, 1993; Paoletti *et al*, 1997; Traynelis *et al*, 1998; Zheng *et al*, 1998; but see Xiong *et al*, 1999). The inhibition involves a voltage-dependent and a voltage-independent component, with 40% of the Zn^{2+} inhibition at NR1/NR2A receptors being voltage-independent and having an IC_{50} value in the nanomolar range (Williams, 1996; Chen *et al*, 1997). The remaining 60% is inhibited in a voltage-dependent manner, mediated by a channel block similar to but weaker than the block by Mg^{2+}, with an IC_{50} value of 45-80μM. The compound *N,N,N',N'*-tetrakis-(2-pyridylmethyl)-ethylene-diamine (TPEN) is a high-affinity chelator for heavy metal ions such as Zn^{2+}, Cu^{2+} and Mn^{2+}, but has a poor affinity for Ca^{2+} (Arslan *et al*, 1985). Contaminant levels of Zn^{2+} in recording solutions are sufficient for a tonic block of NR2A receptors as bath application of TPEN (1μM) enhanced currents through NR1a/NR2A receptors by 50-300%, but had no significant effects on NR1a/NR2B channels (Paoletti *et al*, 1997).

Similar to ifenprodil inhibition of NR1/NR2B receptors, Zn^{2+} inhibits NR1/NR2A by enhancing the tonic proton inhibition at physiological pH (Choi and Lipton, 1999; Low *et al*, 2000). Zn^{2+} has been shown to bind with high affinity to the amino terminal of the NR2A subunit (Fayyazuddin *et al*, 2000; Paoletti *et al*, 2000) and an allosteric interaction between the glutamate and Zn^{2+} binding sites may underlie the fast-onset desensitisation observed in NR1/NR2A receptors (Zheng *et al*, 2001). Glutamate binding increases Zn^{2+} affinity, and Zn^{2+} binding in turn promotes inhibition by enhancing proton binding to pH-sensitive gating elements. Indeed, mutation of residues in the amino terminal of the NR1 subunit which control proton sensitivity also affects Zn^{2+} inhibition (Traynelis *et al*, 1998). Furthermore, polyamines and redox modulation may regulate the sensitivity of NR1/NR2A receptors to Zn^{2+} (Paoletti *et al*, 1997; Traynelis *et al*, 1998; Berger and Rebernik, 1999; Choi *et al*, 2001). This is of possible physiological significance as Zn^{2+} is present in presynaptic vesicles at some synapses, can be released into the synapse during neuronal activity, and may affect the size of the glutamate-induced postsynaptic response (Lu *et al*, 2000; Vogt *et al*, 2000; Li *et al*, 2001; Lin *et al*, 2001).

1.5 *Receptor stoichiometry and co-assembly of NR2 subunits*

It may appear that a substantial amount of information has been gathered regarding the link between the NR2 subunit expressed in a receptor complex and the functional properties of this NMDA receptor, but two fundamental questions remain largely unanswered. How many subunits make up the receptor channel? And do different NR2 subunits co-assemble (with NR1) to form functional channels with unique properties? A tetrameric structure is likely although there is also evidence for a pentameric structure. It is thought the NMDAR complex

contains two or three copies of NR1 (Béhé *et al*, 1995; Premkumar and Auerbach, 1997) and two copies of NR2 (Premkumar and Auerbach, 1997; Laube *et al*, 1998; reviewed by Dingledine *et al*, 1999).

The co-assembly of different NR2 subtypes within a single receptor complex has been implicated in several studies (Wafford *et al*, 1993; Chazot *et al*, 1994; Sheng *et al*, 1994; Luo *et al*, 1997). Single-channel analysis of membrane patches from *Xenopus* oocytes injected with cRNAs for NR1, NR2A and NR2D revealed an additional conductance level between the conventional high and low conductance states (Cheffings and Colquhoun, 2000). A recent study of neonatal hippocampal neurons reported a novel negative coupling between high and low conductance states (Piña-Crespo and Gibb, 2002). A single NMDA receptor population appears to switch between high and low conductance levels, indicating the possibility of triheteromeric NR1/NR2B/NR2D receptors. Indeed, an immunoprecipitation study by Dunah *et al* (1998) supports the co-existence of NR2D with NR1 and NR2A or NR2B.

Several pharmacological studies also support the formation of triheteromeric NMDA receptors. Vicini *et al* (1998) reported that some cells transfected with NR1, NR2A and NR2B exhibited currents that had slow deactivation times characteristic of NR1/NR2B receptors, but were not affected by the NR2B-selective antagonist haloperidol. Tovar and Westbrook (1999) reported that co-transfection of NR1, NR2A and NR2B produced currents with reduced sensitivity to ifenprodil, but the kinetics of recovery from ifenprodil block differed from that of NR1/NR2B receptors. This result was inconsistent with a mixed population of NR1/NR2A and NR1/NR2B receptors, and provided evidence for the formation of triheteromeric assemblies. The same study also showed that NMDA receptor-

mediated excitatory postsynaptic currents (EPSCs) in cultured hippocampal neurons exhibited two components of ifenprodil sensitivity. The highly ifenprodil-sensitive component was attributed to NR1/NR2B receptors, while the component of lower sensitivity is speculated to arise from NR1/NR2A/NR2B triheteromeric receptors. Dual components of ifenprodil sensitivity had also previously been observed in native neurons by Williams *et al* (1993) and Kirson and Yaari (1996). However, Kew *et al* (1998) proposed that triheteromeric NR1/NR2A/NR2B receptors might have a high affinity for ifenprodil: if the binding of ifenprodil to a single high-affinity site is sufficient, then the presence of a single NR2B subunit would be enough to confer sensitivity. The assembly of triheteromeric receptors is supported by the co-immunoprecipitation of NR1, NR2A and NR2B (Sheng *et al*, 1994; Chazot and Stephenson, 1997; Luo *et al*, 1997), and the overlap of NR2A and NR2B signals in imaging studies (Li *et al*, 1998; Luo *et al*, 2002). In Chapter 5 of this thesis, we address the possibility of NR2B and NR2D co-assembly in the cell bodies of cerebellar Golgi cells. We put forward evidence for the co-assembly of these two subunits at somatic sites.

1.6 *Developmental profile of NMDAR subunit composition*

Functional evidence for changes in NMDAR-mediated synaptic currents during development was initially demonstrated in the superior colliculus (Hestrin, 1992) and in the visual cortex (Carmignoto and Vicini, 1992). *In situ* hybridisation experiments subsequently provided a possible molecular mechanism for this phenomenon. The mRNA and protein expression of NR2 subunits exhibit distinct and dynamic patterns during development (Akazawa *et al*, 1994; Monyer *et al*, 1994; Sheng *et al*, 1994; Watanabe *et al*, 1994). It was thus suggested that the shortening of EPSCs during maturation, as characterised by the two functional

studies, reflected the developmental switch between NR2B and NR2A expression in many areas of the brain.

A number of studies have addressed this proposal by correlating the shortening of synaptic currents during development with changes in the expression or pharmacology of NR2 subunits (Kirson and Yaari, 1996; Takahashi *et al*, 1996; Flint *et al*, 1997; Stocca and Vicini, 1998; Rumbaugh and Vicini, 1999; Tovar and Westbrook, 1999; Cathala *et al*, 2000). The genetically-engineered ablation of NR2A expression resulted in slower EPSCs at the cerebellar mossy fibre-granule cell synapse in mice (Takahashi *et al*, 1996). Flint *et al* (1997) found a correlation between NR2A expression (as determined by single-cell RT-PCR) and faster EPSC decay kinetics, and showed that even low levels of NR2A expression in rat neocortical neurons were sufficient to affect the decay time-course of synaptic currents.

Reduced inhibition by the NR2B-selective antagonists ifenprodil, haloperidol and CP101,606 also correlate with faster decay kinetics during development (Williams *et al*, 1993; Kirson and Yaari, 1996; Stocca and Vicini, 1998; Tovar and Westbrook, 1999; Cathala *et al*, 2000). The whole-cell and synaptic currents of 'immature' cultured hippocampal neurons (1-3 days *in vitro*) displayed the same ifenprodil sensitivity as those from cells transfected with NR1a and NR2B. However, EPSCs from 'mature' cells (5-7 days *in vitro*) were less susceptible to ifenprodil inhibition (Tovar and Westbrook, 1999). Furthermore, the reduction in ifenprodil or haloperidol sensitivity observed during development appeared to be restricted to the synapse (Stocca and Vicini, 1998; Rumbaugh and Vicini, 1999; Tovar and Westbrook, 1999; but see Cathala *et al*, 2000).

1.7 *Functional importance of changes in NMDAR properties*

1.7.1 *Ca^{2+} entry*

There has been a recent explosion in the study of interactions between the NMDAR and the postsynaptic density (PSD; for reviews, Ziff, 1997; Grant and O'Dell, 2001; Sheng and Kim, 2002). The PSD is a complex structure containing a multitude of signalling and scaffolding proteins, and is important for receptor clustering and anchoring at synaptic sites. The carboxyl terminals of NR2 subunits and some isoforms of NR1 can bind to proteins in the PSD via PDZ domains (e.g. PSD-95, SAP102, calmodulin and CaMKII; Kornau *et al*, 1995; Niethammer *et al*, 1996; Steigerwald *et al*, 2000; Roche *et al*, 2001; Scott *et al*, 2001), and the NMDAR is thereby directly or indirectly linked to a number of signalling pathways (including the Ras-MAPK pathway, the nitric oxide pathway, and (de)phosphorylation). The NMDAR can also bind directly to cytoskeletal elements such as α-actinin and NF-L (Ehlers *et al*, 1998; Lei *et al*, 2001). Due to the proximity of the NMDAR with so many (Ca^{2+}-sensitive) signalling molecules, the influx of Ca^{2+} through the open NMDAR can thus affect a myriad of intracellular processes.

In addition to the associative or conditional activation of the NMDAR, Ca^{2+} entry through this receptor channel also plays an important role in the induction of synaptic plasticity (Bliss and Collingridge, 1993; Bear and Malenka, 1994). The delivery and insertion of AMPA receptors to the membrane of hippocampal spines during long-term potentiation (LTP; Shi *et al*, 1999; Lu *et al*, 2001), as well as the removal of these receptors during long-term depression (LTD; Carroll *et al*,

1999), requires NMDAR activation and increases in the intracellular Ca^{2+} concentration. Changes in synaptic strength and structure (e.g. spine growth, the number of synapses) are thought to be mediated by Ca^{2+} entry through the NMDA receptor via the activation of phosphatases and kinases (for example, Sin *et al*, 2002). Furthermore, the relative amount and temporal profile of Ca^{2+} entering the neuron may determine the direction of change: large elevations in the intracellular Ca^{2+} concentration triggers LTP by protein kinase activation while modest changes lead to LTD via activation of protein phosphatases (Bear and Malenka, 1994; Cummings *et al*, 1996; Zucker, 1999; Lüscher *et al*, 2000; Soderling and Derkach, 2000; Grosshans *et al*, 2002; Sheng and Kim, 2002).

In light of this, it was hypothesised that developmental changes in NMDAR subunit composition may underlie the abated ability for LTP in adult animals. The acceleration in the decay kinetics of NMDAR-mediated synaptic currents brought about by a developmental switch from NR2B to NR2A expression means a reduction in charge transfer and Ca^{2+} influx through the NMDAR channel. However, evidence is mounting against this hypothesis. Recent studies demonstrated that NR2A expression and the acceleration in decay kinetics occur at the beginning rather than at the end of the critical period for plasticity in the visual system (Roberts and Ramoa, 1999; Barth and Malenka, 2001). Furthermore, the critical period for thalamocortical LTP was unchanged in NR2A-knockout mice (Lu *et al*, 2001).

Ca^{2+} permeability is also a crucial property for the NMDAR's participation in developmental processes such as neurite growth, cell migration, synaptogenesis and synapse elimination (Rabacchi *et al*, 1992; Komura and Rakic, 1993; Durand *et al*, 1996; Wu *et al*, 1996; Lin and Constantine-Paton, 1998; Fischer *et al*, 2000;

Kakizawa *et al*, 2000; Lüthi *et al*, 2001; Sin *et al*, 2002). Neuronal survival, via the transcription factor cAMP-response-element-binding-protein (CREB) and the neurotrophin brain-derived neurotrophic factor (BDNF), also appears to be dependent on Ca^{2+} flux through the NMDAR (Hardingham *et al*, 2002). Although NMDAR activation is necessary for many physiological processes, over-excitation of NMDARs is neurotoxic and excessive Ca^{2+} entry is thought to be one of the mechanisms of excitotoxicity (for reviews, Choi, 1995; Hardingham and Bading, 2003). Depending on the intensity of the glutamate insult, the loss of Ca^{2+} homeostasis can activate the signalling pathway for apoptosis or lead to necrotic cell death.

1.7.2 *Contribution to cell excitability*

The magnitude and time-course of the cationic influx through the open NMDAR channel will shape neuronal excitation and affect the firing of action potentials. For example, the contribution of NMDARs to synaptic activation in adult hippocampal CA1 pyramidal cells is minimal while NMDAR-dependent burst firing occurs in hippocampal radiatum giant cells where the NMDAR-mediated component of the EPSC is larger, more slowly-decaying and less sensitive to Mg^{2+} block (Kirson and Yaari, 2000).

The voltage-dependent activation and the deactivation kinetics of the NMDAR predict that repetitive high-frequency afferent stimuli may lead to non-linear summation of the postsynaptic response, mediating the integration of several inputs, triggering jittery firing or even blocking the generation of action potentials (Gabbiani *et al*, 1994; D'Angelo *et al*, 1995; Harsch and Robinson, 2000; Imamura *et al*, 2000; Lei and McBain, 2002; Maccaferri and Dingledine, 2002).

The acceleration in the decay kinetics of NMDAR-mediated synaptic currents during development is thought to improve the temporal precision of network activity. This has been elegantly demonstrated in the auditory system, where reliable and sustained firing at high frequencies is of necessity. The acquisition of high-fidelity transmission at the calyx of Held synapse is activity-dependent, requiring the downregulation of NMDARs and a reduction in the NMDAR-EPSC duration (Futai *et al*, 2001; Taschenberger and von Gersdorff, 2000). However, it is important to keep in mind that many other changes may occur simultaneously to affect overall cell excitability. Changes in intrinsic membrane properties of the postsynaptic neuron (e.g. expression levels and properties of K^+ and Na^+ channels), in presynaptic release profiles (e.g. release probability, presynaptic Ca^{2+} channels, vesicle pool size) and in neurotransmitter profile in the synaptic cleft (e.g. synapse morphology, activity of clearance systems) can all influence cell excitability and the relationship between presynaptic and postsynaptic activity (Taschenberger and von Gersdorff, 2000; Renger *et al*, 2001; reviewed in Conti and Weinberg, 1999; Magee, 2003). Of course, the excitation of a neuron also depends on the sum total of its inhibitory and excitatory inputs and the temporal interaction between these inputs will also shape neuronal firing (Mainen and Sejnowski, 1995; Stevens and Zador, 1998; Carter and Regehr, 2002).

1.8 *Differential localisation of NMDARs*

Not only is there a developmental or *temporal* profile of NMDAR expression, there are also *spatial* considerations. For example, NR2D receptors are transiently expressed on the soma of the cerebellar Purkinje cell during early postnatal development but no functional NMDARs have been documented at synapses in this cell type (Kano *et al*, 1988; Hirano, 1990; Perkel *et al*, 1990; Momiyama *et*

al, 1996). Indeed, NR2D-containing receptors have been shown to be expressed extrasynaptically in several cell types but do not appear to be involved in synaptic transmission (Misra *et al*, 2000a, 2000b; Momiyama, 2000; Clark and Cull-Candy, 2002; Piña-Crespo and Gibb, 2002; Chapter 5). Furthermore, at a developmental stage when NR2A-containing receptors are present at hippocampal or cerebellar synapses, NR2B-NMDARs are thought to remain abundant in the extrasynaptic membrane (Rumbaugh and Vicini, 1999; Tovar and Westbrook, 1999; Sinor *et al*, 2000; Chapter 4). A recent study suggests that NMDARs are able to move between synaptic and extrasynaptic locations in cultured hippocampal neurons (Tovar and Westbrook, 2002).

NMDARs expressed at synaptic sites contribute to excitatory transmission and synaptic plasticity but what are the possible functions of extrasynaptic NMDARs? It was demonstrated more than a decade ago that NMDARs in the extrasynaptic membrane are tonically active in hippocampal pyramidal cells and that this tonic depolarising current acts to enhance the coupling between afferent input and action potential firing (Sah *et al*, 1989). Although synaptically-released glutamate is thought to be largely cleared from the synaptic cleft within 1ms by high-affinity glutamate transporters and passive diffusion (Clements, 1996; Diamond and Jahr, 1997), diffusion simulations predict that the glutamate concentration may decay very slowly when it falls below the affinity of glial glutamate uptake (K_d ~13μM; Bergles and Jahr, 1997; Rusakov and Kullmann, 1998). The glutamate concentration in the extracellular fluid may therefore be sufficient to tonically activate NMDARs (with glutamate affinity of EC_{50} 0.4 to 4μM; Table 1.1).

Manipulating the expression of extrasynaptic receptors, either in terms of receptor number or receptor subtype, may provide a means of regulating cell excitability or cell survival. Extrasynaptic NMDARs appear to be more susceptible to use-dependent rundown than synaptic ones (Li *et al*, 2002), providing a possible mechanism for maintaining robust synaptic transmission while toning down overall excitability. NMDARs at somatic sites have also been implicated in mediating glutamate-induced neurotoxicity (Sinor *et al*, 2000) and a recent report indicated the contrasting roles of synaptic and extrasynaptic NMDARs in cell survival. While synaptic NMDAR activity promotes the activity of the transcription factor CREB and the subsequent production of the neuroprotective BDNF, activation of extrasynaptic NMDARs oppose CREB activity and can lead to cell death (Hardingham *et al*, 2002; Hardingham and Bading, 2003).

With its higher affinity for glutamate and its lower affinity to Mg^{2+} block, the extrasynaptically-located NR2D-containing receptors are more likely to be activated by ambient glutamate. Long-lasting NMDAR-mediated currents in thalamic neurons (with a decay time constant of around 3 seconds) have been linked to spontaneous Ca^{2+} oscillations in surrounding astrocytes (Parri *et al*, 2001). The authors suggest that Ca^{2+}-induced glutamate release from astrocytes may activate extrasynaptic NR2D-containing receptors abundantly expressed in these neurons (at the developmental stage studied).

1.9 *Diffuse synaptic transmission: Spillover*

The classic model of synaptic transmission is mainly that of 'point-to-point' transmission between a presynaptic terminal and the postsynaptic density. However, there is increasing evidence that transmission may be more diffuse than

previously thought and this has implications for the possible function of extrasynaptic receptors. The term 'spillover' is used to describe the diffusion of neurotransmitter beyond the space separating the presynaptic release sites and the opposing postsynaptic membrane, leading to activation of receptors either at neighbouring synapses or in the extrasynaptic membrane (Kullmann and Asztely, 1998; Bergles *et al*, 1999; Diamond, 2002; Otis, 2002). Spillover was first demonstrated in the hippocampus (Asztely *et al*, 1997), providing an alternative explanation for NMDAR-only 'silent synapses' (Isaac *et al*, 1995; Liao *et al*, 1995; see also Gasparini *et al*, 2000). The recording of NMDAR-only responses was initially thought to reflect the absence of AMPARs at certain synapses. However, spillover of low concentrations of glutamate into quiescent synapses containing both AMPARs and NMDARs could also generate NMDAR-only responses since NMDARs have a much higher affinity for glutamate than AMPARs.

Increased or repetitive afferent activity would be expected to increase the degree of spillover, with higher concentrations of glutamate accumulating in the synaptic cleft and perhaps even saturating glutamate uptake. For example, in hippocampal CA1 cells, a brief burst of afferent stimuli or inhibition of glutamate transporters led to the prolongation of the EPSC (Arnth-Jensen *et al*, 2002). What significance might this have on the synapse specificity thought to be so important for information processing and activity-dependent plasticity? It has been postulated that spillover may actually enhance synapse specificity in associative LTP: the postsynaptic Ca^{2+} influx through NMDARs is only sufficient to induce LTP at directly activated synapses and depression of synaptic strength may occur at neighbouring synapses where the Ca^{2+} signal is weaker (Diamond, 2002). AMPARs can be activated by spillover at the cerebellar mossy fibre to granule

cell synapse and modelling suggests that this spillover current would greatly affect the EPSP waveform by boosting the amplitude and slowing the decay of the EPSP (DiGregorio *et al*, 2002). This spillover is less prominent when presynaptic release probability is low. So, at higher firing frequencies where a reduction in release probability is likely, the EPSP would be smaller and faster allowing temporal precision to be maintained. The boosting of the EPSP may enhance the reliability of low-frequency transmission as threshold for action potential firing can be achieved more easily.

High-affinity glutamate transporters are important in shaping the glutamatergic response at some synapses (for example, Sarantis *et al*, 1993; Barbour *et al*, 1994; Isaacson, 1999; Overstreet *et al*, 1999; Carter and Regehr, 2000; Brasjno and Otis, 2001; Kinney *et al*, 1997; but see DiGregorio *et al*, 2002), and five subtypes have been cloned to date: GLT-1, GLAST, EAAT3, EAAT4 and EAAT5 (Kanai and Hediger, 1992; Pines *et al*, 1992; Storck *et al*, 1992; Arriza *et al*, 1994, 1997; Fairman *et al*, 1995). The glial transporters (GLT-1 and GLAST) are located both close to and away from synapses (Chaudry *et al*, 1995; Lehre *et al*, 1995; Minelli *et al*, 2001). EAAT3 is localised in pre- and postsynaptic neuronal structures in several brain regions while EAAT4 is enriched postsynaptically in cerebellar Purkinje cells (Rothstein *et al*, 1994; Lehre *et al*, 1995; Furuta *et al*, 1997a). The expression of transporter subtypes has also been shown to increase with age (Furuta *et al*, 1997a), so spillover might be expected to be more prominent early in development.

In addition to activating receptors at neighbouring synapses, diffusion of neurotransmitter out of the synapse can activate receptors located in the extrasynaptic membrane and anatomically-defined extrasynaptic receptors could

still participate in synaptic transmission. At an 'AMPAR-only' synapse in the cerebellum, trains of afferent stimuli generated an NMDAR-mediated current indicating activation of extrasynaptic NMDARs by glutamate spillover (Clark and Cull-Candy, 2002). In retinal ganglion layer cells, evoked EPSCs exhibited both AMPAR- and NMDAR-mediated components while spontaneously-occurring EPSCs were mediated only by AMPARs (Chen and Diamond, 2002). The NMDARs are likely to be located extrasynaptically as an additional NMDAR-mediated component was observed in spontaneous EPSCs on inhibition of glutamate uptake. Furthermore, extrasynaptic NMDARs may directly affect neuronal excitability as Ca^{2+} influx through these receptors can activate co-localised Ca^{2+}-activated K^+ channels (Isaacson and Murphy, 2001). Metabotropic glutamate receptors (mGluRs), situated away from synaptic sites and having similar glutamate affinities as NMDARs, can also be activated by synaptically-released glutamate, suggesting a role for spillover in modulating synaptic transmission on a slower time-scale (Baude *et al*, 1993; Conn and Pin, 1997; Petralia *et al*, 1997; Brasnjo and Otis, 2001).

It was mentioned in section 1.8 that NMDAR subtypes can be differentially distributed within a neuron. It is thus possible that glutamate spillover activates extrasynaptic NMDARs which differ in their properties from those at synapses. This possibility is investigated in Chapter 4.

1.10 *Cerebellum: cell types and connectivity*

The cerebellum is a protruding structure located at the base of the brain, sitting on the brainstem between the cerebrum and the spinal cord. It is a convoluted structure which can be divided into two cauliflower-like hemispheres separated by

the vermis. The cerebellum plays a pivotal role in the coordination of posture and locomotion, hand and eye movements, and a wide range of routine and skilled motor activities (see Kandel *et al*, 1991; Mauk *et al*, 2000). Although not essential in muscle contraction or somatosensory perception, the cerebellum appears to be involved in the regulation of movement and posture by adjusting the output of descending motor pathways. It receives information from all parts of the body: from skin, muscles, joints and visceral organs; from the visual, auditory and vestibular systems; and from higher motor centres. The efferent pathways ultimately affect the motor system, via the motor nuclei in the brainstem and/or via forebrain motor structures. The cerebellum also plays an important role in the learning of motor tasks (see Mauk, 1997). The most striking symptom of cerebellar disease is the loss of muscle coordination (ataxia), affecting speech and movements in the limbs, extremities, and the eyes. Posture, balance and muscle tone can also be affected.

The cerebellum is composed of the cerebellar cortex (an outer layer of grey matter), internal white matter and three pairs of deep cerebellar nuclei. Three layers are distinct in the cerebellar cortex and the arrangement of neurons is highly regular (Figures 1.1 and 1.2A; see Eccles *et al*, 1967; Palay and Chan-Palay, 1974; Ramón y Cajal, 1911). The *molecular layer* lies directly under the pial surface and consists primarily of densely-packed axon fibres and dendrites. The thin axon fibres run parallel along the longitudinal axis of the folium and are known as 'parallel fibres'. Two types of interneurons, the stellate cell and basket cell, are present in the molecular layer. The *Purkinje cell layer* is a sheet of large cell bodies that separates the molecular layer and the granule cell layer, with axonal and dendritic processes running between the Purkinje cell bodies. The *granule cell layer* is densely packed with small granule cells, and also contains the

bulb-like structures called glomeruli where granule cell axon terminals, mossy fibre axon terminals and Golgi cell dendrites and axon terminals come together and form synaptic contacts. Sparsely distributed within the granule cell layer, the Golgi cell, the unipolar brush cell and the Lugaro cell can be distinguished from granule cells by their larger cell bodies. Also visible in the granule cell layer are numerous axons. These include ascending projections from the white matter to terminate in glomeruli or on Purkinje cells, and descending Purkinje cell axons.

1.10.1 *The granule cell*

The most abundant neuronal cell type in the cerebellar cortex is the granule cell. These cells have small spherical cell bodies of 5-8μm in diameter and are densely packed in the granule cell layer. Each granule cell extends 3-5 dendrites in the granule cell layer, where they form part of the glomerulus and make synaptic contacts with mossy fibres and Golgi cell axon terminals.

The axons of granule cells extend towards the surface of the cerebellum to form the molecular layer. After passing through the Purkinje cell layer, each axon splits into two and the branches run along the axis of the folium in opposite directions. The position of the granule cell is in direct geometric relation to the position of the parallel fibre in the molecular layer: superficial granule cells (close to the Purkinje cell layer) give rise to superficial parallel fibres (towards the pial surface) while deep granule cells (near the white matter) give rise to deep parallel fibres (by the Purkinje cell layer). After bifurcation, parallel fibres extend for 1-2mm in both directions and make *en passant* synaptic contacts with dendrites of Purkinje cells,

Golgi cells, stellate cells and basket cells (see Eccles *et al*, 1967; Pichitpornchai *et al*, 1994).

1.10.2 *The Purkinje cell*

The Purkinje cell has a large cell body of transverse diameter 30-35μm and vertical diameter 50-70μm, and possesses a flat but highly elaborate dendritic tree which sits in the molecular layer perpendicular to the parallel fibres (i.e. in the parasagittal plane). Parallel fibres make *en passant* synaptic contacts onto densely distributed dendritic spines, and over 200,000 parallel fibres are thought to run through the dendritic tree of the Purkinje cell in the cat and monkey (Eccles *et al*, 1967; Napper and Harvey, 1988). The axons of the stellate and basket interneurons make inhibitory contacts onto the Purkinje cell dendrites. Each Purkinje cell is also contacted by a climbing fibre (originating from the inferior olive), which wraps around the Purkinje cell dendritic tree like ivy. Side branches of the climbing fibre end in boutons, forming synapses with the Purkinje cell and possibly also with stellate, basket and Golgi cells. Purkinje cell axons start at the base of the cell bodies, extend through the granule cell layer to the deep cerebellar nuclei or to extracerebellar structures, and form the only efferent pathway from the cerebellar cortex.

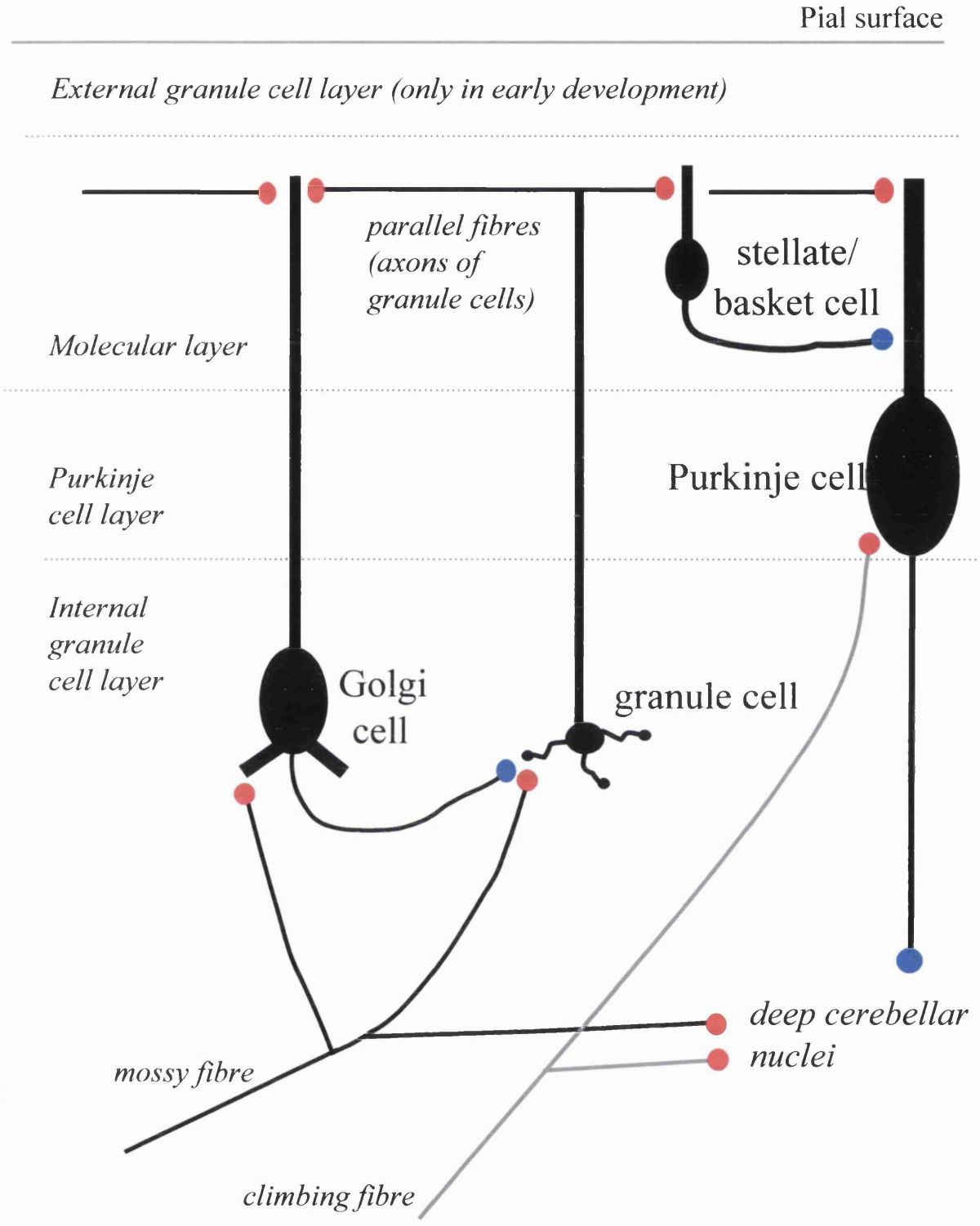

Figure 1.1 *Schematic diagram of the cerebellar circuitry*

The cerebellar cortex is divided into the external granule cell layer (only in early development), the molecular layer, the Purkinje cell layer and the internal granule cell layer. *Red* dots indicate excitatory synapses while *blue* dots indicate inhibitory connections.

A

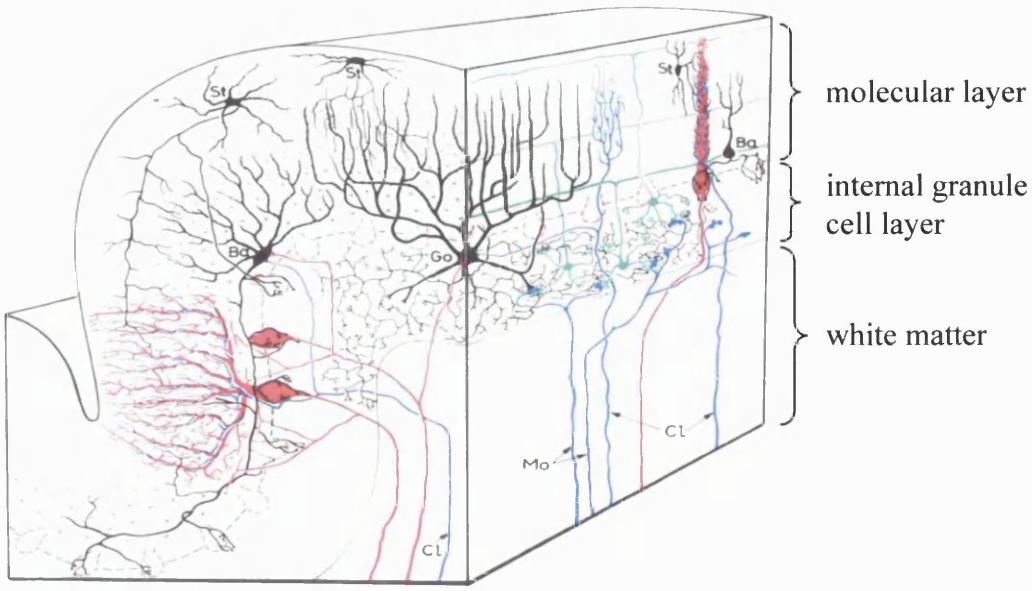

B

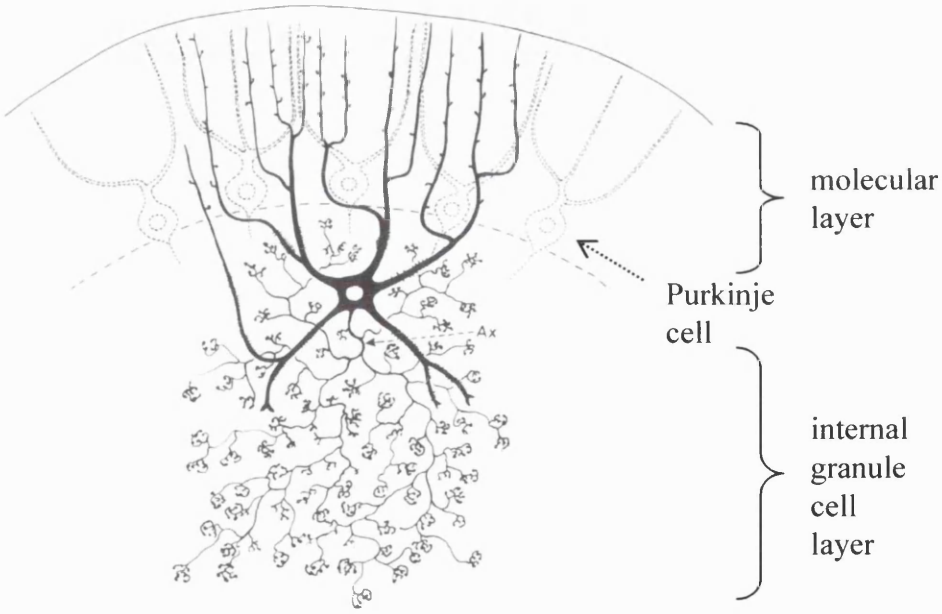

Figure 1.2 *The Golgi cell in the cerebellar cortex*

A, Stereodiagram of the cerebellar cortex, illustrating the afferent fibres in *blue* (mossy fibres (Mo) and climbing fibres (Cl) and the main neuronal cell types. The Purkinje cell is shown in *red*, granule cell in *green*, and the three main inhibitory cells in *black*: Golgi cell (Go), stellate cell (St) and basket cell (Ba). (Eccles *et al*, 1967, Figure 1, p. 5.)

B, The typical arborisation and location of the Golgi cell. The arborisations extend in all directions. The axon (Ax) branches extensively amongst the internal granule cells and form synaptic contacts within glomeruli. (Eccles *et al*, 1967, Figure 13, p. 23.)

1.10.3 *The Golgi cell*

The round or polygonal cell bodies of Golgi cells are typically located in the top half of the granule cell layer and with diameters of 20-25μm, they are readily distinguishable from the surrounding granule cells (Ramón y Cajal, 1911; Palay and Chan-Palay, 1974). Golgi cells are sparsely distributed, being outnumbered by Purkinje cells at a ratio of 10:1 (Eccles *et al*, 1967). Their density has been reported to be slightly greater in the vermis than in the hemispheres (Altman and Bayer, 1997).

Golgi cells extend a number of apical dendrites into the molecular layer, resulting in a span approximately three times wider than that of the Purkinje cell dendritic tree (Figure 1.2B). However, unlike the Purkinje cell, the apical dendrites of the Golgi cell extend equally in all directions and can therefore receive parallel fibre inputs from a large volume of the molecular layer. Also, there appears to be little or no overlap between the dendritic trees of neighbouring Golgi cells. The tertiary dendrites have irregularly-distributed, sparse, blunt and stiff spines onto which parallel fibres make synaptic contacts. Basal dendritic processes in the granule cell layer make direct contacts with mossy fibres in the glomerulus and the span of the basal dendritic tree is somewhat smaller than that of the apical one. Some Golgi cells located deep in the granule cell layer extend few if any dendrites into the molecular layer, with the mossy fibres forming their main or only input.

The axons of Golgi cells originate at the base of the cell body and form extended arborisations throughout the depth of the granule cell layer (with a span as wide as that of the apical dendritic tree; Figure 1.2B). The axon arborisations form

synapses with granule cell dendrites in the glomerulus (Hámori and Szentágothai, 1966), resulting in a connection loop between the granule cell and the Golgi cell. The cell body of the Golgi cell is also covered with synaptic contacts, with climbing fibre collaterals and Purkinje cell axon collaterals thought to be the presynaptic elements (Eccles *et al*, 1967).

In addition to Golgi cells, there are at least two other neuronal cell types with large- or medium-sized cell bodies located in the granule cell layer. The three cell types can be distinguished by the shape and size of their cell bodies, their location within the granule cell layer and by immunochemical markers (such as calretinin, somatostatin and the antigen Rat-303; Ramón y Cajal, 1911; Geurts *et al*, 2001). The *unipolar brush cell* (Mugnaini and Floris, 1994; Rossi *et al*, 1995) is mainly found in the posterior vestibulo-cerebellum and has a rounded cell body, intermediate in size between the granule cell and the Golgi cell. Its single thick dendrite has the shape of a paintbrush, with the bunch of dendritic branches at the tip forming synaptic contacts with one or two mossy fibre terminals. The contorted and branched axons of unipolar brush cells appear to remain in the granule cell layer, with the rosette-like terminals contacting granule cell dendrites and dendrites of other unipolar brush cells (Diño *et al*, 2000). The *Lugaro cell*, with its fusiform cell body, is located in the upper third of the granule cell layer and is found to be scattered throughout the cerebellar cortex (Sahin and Hockfield, 1990; Lainé and Axelrad, 2002). The poorly-ramified dendrites appear to follow a variable trajectory: the dendrites of some cells ramify into the molecular layer while dendrites of others extend in the granule cell or Purkinje cell layers. Lugaro cells receive excitatory serotonergic inputs (Dieudonné and Dumoulin, 2000), while their axon arborisations in the molecular layer form inhibitory contacts with

stellate cells, basket cells and Golgi cells (but not with Purkinje cells; Dieudonné and Dumoulin, 2000; Dumoulin *et al*, 2001).

1.10.4 *The mossy fibre-granule cell-Golgi cell microcircuit*

Originating from the spinal cord, the vestibular system, the reticular formation and the pontine nuclei, mossy fibres branch extensively in the white matter and in the granule cell layer and form contacts with the dendrites of several granule cells in complex synapses called glomeruli (Hámori and Szentágothai, 1966). In the centre of the glomerulus lies the enlarged mossy fibre terminal (or rosette), onto which granule cell dendrites and Golgi cell basal dendrites make contact. Golgi axon terminals form small beaded synaptic contacts with granule cell dendrites either at the outer side of granule cell dendrites opposite to the contact with the mossy fibre or somewhat adjacent to the mossy fibre-granule cell synapse.

Two pathways can be dissected from the connections made in the glomerulus (Ramón y Cajal, 1911; Palay and Chan-Palay, 1974). The mossy fibre forms an excitatory synapse with the granule cell, which extends its axon (parallel fibre) through the molecular layer to excite a Golgi cell at its apical dendrites. The Golgi cell axon then forms an inhibitory synapse back onto the mossy fibre to granule cell synapse. This connectivity forms a simple negative feedback loop (Eccles *et al*, 1966). Secondly, glutamate release at the mossy fibre terminal will activate synapses at the basal dendrites of the Golgi cell. The Golgi cell axon then forms an inhibitory connection with the granule cell, generating feedforward inhibition on the mossy fibre to granule cell connection.

1.10.5 *The possible functional role of the cerebellar Golgi cell*

The cerebellum is thought to regulate and coordinate movement by functioning as a computing machine, processing the information it receives from various parts of the body and sending the processed output directly or indirectly to the motor system. The cerebellum is also one of the main brain structures involved in motor learning. The discovery and establishment of synaptic plasticity in the cerebellum (Ito and Kano, 1982; Ito *et al*, 1982; Ekerot and Kano, 1985) provided the memory elements required by any computational machine (Marr, 1969; Albus, 1971). The Purkinje cell receives inputs from parallel fibres and from a climbing fibre. On coincident excitation of both parallel fibre and climbing fibre inputs, the parallel fibre to Purkinje cell relay undergoes long-term depression (LTD). As Purkinje cells form inhibitory connections onto neurons in the deep cerebellar nuclei, this LTD would effectively increase excitation in the system. Blockade of LTD impairs motor adaptation and learning (Chapman *et al*, 1992; Li *et al*, 1995; Shibuki *et al*, 1996; De Zeeuw *et al*, 1998; Ichise *et al*, 2000), supporting the view that this heterosynaptic LTD constitutes a major mechanism in cerebellar learning. The cerebellar learning hypothesis also proposes that the climbing fibre input represents an error message (see Ito, 2000, 2001). In simple situations such as reflexes, climbing fibres are excited in response to pain or a sudden loud sound. Although the model becomes much more complex for voluntary movements, most observations for simple situations support the view that LTD is driven by the error signals arising from the repeated exercise of a movement and that LTD reshapes the neuronal circuit of the cerebellum in the direction which minimises these errors (see Ito, 2000, 2001). In future, the hypothesis for cerebellar learning will have to be modified to incorporate the new findings of plasticity in other cerebellar cell types (D'Angelo et al, 1999; Liu and Cull-Candy, 2000).

Golgi cells, by its connectivity, most likely play a role in controlling the excitation of granule cells and thereby regulating the main input relay of the cerebellar cortex between mossy fibres and granule cells. This in turn affects the activity of the parallel fibres and ultimately the output of the cerebellar cortex via Purkinje cells. Golgi cells fire spontaneously (Edgley and Lidierth, 1987) and it has been proposed that Golgi cells exert a tonic inhibition on granule cells. The classic theories of Marr-Albus-Ito proposed the feedback inhibition exerted by Golgi cells may set the activation threshold for granule cell firing. It had been contemplated that Golgi cells may only fire when excited by both parallel fibre and mossy fibre inputs (Hámori and Szentágothai, 1966), but Eccles *et al* (1967) showed that activation of either pathway was sufficient. The large dendritic tree would integrate signals from many granule cells and conversely, excitation of a Golgi cell would lead to an inhibition of many granule cells. It is therefore possible that Golgi cells focus the excitation of granule cells. Granule cells receiving direct mossy fibre stimulation will be sufficiently excited to overcome the inhibition exerted by Golgi cells and will be able to fire. However, surrounding granule cells innervated by the same Golgi cell axon will be inhibited (Eccles *et al*, 1967). Recently, computer modelling has put forward the possible role of Golgi cells in regulating the timing of granule cell firing and in mediating oscillations in cerebellar activity (Hartmann and Bower, 1998). Work by the group of Maex and de Schutter showed that mossy fibre inputs lead to rhythmic and oscillatory firing of granule and Golgi cells (Maex and de Schutter, 1998). Furthermore, synchronised firing occurs in Golgi cells located in the longitudinal plane (i.e. along the parallel fibres; Vos *et al*, 1999).

The functional role played by the Golgi cell in the cerebellar circuitry is further complicated by its connections with climbing fibre collaterals, Purkinje cell axon

collaterals, the molecular layer interneurons, and the Lugaro cell. Although little information is currently available concerning these connections, the role of the Golgi cell in cerebellar function is likely to be a significant one. Ablation of the Golgi cell by genetic means proved detrimental to compound motor coordination, resulting in compromised balance and an ataxic gait (Watanabe *et al*, 1998). Although some recovery of balance was observed over several days, motor coordination and adaptation remained disabled. The ablation of Golgi cells not only removed the inhibition onto granule cells, it also led to the loss of NMDAR expression in granule cells (Imamura *et al*, 2000).

1.10.6 *Profile of cerebellar development*

The cerebellum undergoes a lot of its development after birth (Altman and Bayer, 1997) and this growth can be divided into: (1) the neonate and infantile phase, and (2) the juvenile and young-adult phase. In the rat, the first phase stretches from birth (embryonic day (E)22 or postnatal day (P)0) to P21 when weaning typically takes place in laboratory settings. The cerebellum as a whole increases in volume by over 20 times, the fissures deepen and the convoluted appearance becomes more and more prominent. It is during this period that cell migration, growth of dendrites and axons, synapse formation and the maturation of the circuitry take place. The second phase extends from P21 to P60. Synaptic organisation continues but the changes are far more subtle and much less understood.

Purkinje cells and deep cerebellar nuclei neurons in the rat develop in the cerebellum during the late embryonic stage, and Golgi cells begin to be discernable at E19. There is very little or no molecular layer during the first few days after birth. Granule cells migrate from the external granule cell layer, leaving

their newly-formed axons to form the molecular layer. They pass through the Purkinje cell layer and into the internal granule cell layer. The molecular layer interneurons and Golgi cells migrate from the white matter, and the generation of Golgi cells has already slowed considerably by P4 (Zhang and Goldman, 1996).

In the slices from mouse cerebellum used in this study, the molecular layer was almost indiscernible at P5, with Purkinje cells sitting between the external and internal granule cell layer. Although Golgi cells could be identified and patched at P5, only few spontaneous synaptic responses were observed. By P7, one could clearly delineate the molecular layer and synaptic responses were readily evoked by stimulation of the molecular layer, indicating that synapses with parallel fibres had already formed. Furthermore, mossy fibre-to-granule cell and Golgi cell-to-granule cell synaptic responses can be evoked at P7 (Cathala L, Brickley S, personal communication). At this age, the mouse pup barely moved. By P15-18, the pups were inquisitive and running around the cages. The molecular layer as observed in slices was thick and the external granule cell layer was hardly visible. The internal granule cells were more tightly packed and the degree of myelination was higher.

1.11 *Aims of the present study*

This aim of this study was to examine the subunit composition of NMDARs participating in synaptic transmission in the mouse cerebellar Golgi cell. The differential localisation of NMDAR subtypes at synaptic and extrasynaptic sites was also investigated. Whether NMDAR subunit composition and differential localisation changes during postnatal development of the Golgi cell was further considered.

In **Chapter 3**, an investigation of the properties of functional NMDARs at Golgi cell synapses was carried out using the whole-cell patch-clamp technique. The amplitude and decay kinetics of NMDAR-mediated synaptic currents have been characterised. The possible subunit composition of the synaptic NMDA receptors was further examined using NR2 subunit-selective agents. The biophysical and pharmacological properties of synaptic NMDA receptors were then compared in Golgi cells at different ages.

Chapter 4 investigates whether the developmental changes in NMDAR subunit composition observed with synaptic NMDA receptors in the Golgi cell also occurred at extrasynaptic sites. Brief high-frequency trains of stimuli were used to increase glutamate release, generating diffusion of the neurotransmitter away from the synapse and thereby activating extrasynaptic NMDA receptors. The kinetic and pharmacological properties of those currents generated by a train of stimuli were compared with those generated by a single stimulus.

Golgi cells are known to express NR2B- and NR2D-receptors in the cell body (Misra *et al*, 2000a). **Chapter 5** addresses whether these two subunits co-

assemble to form functional triheteromeric NR1/NR2B/NR2D assemblies with different properties. The strategy used was to compare the properties of NMDARs in wild-type and NR2D-knockout mice. The conductance, kinetic and pharmacological properties of NMDA-activated single-channels in outside-out patches excised from Golgi cells were compared between wild-type and NR2D-knockout mice. Furthermore, we investigated whether the NR2D subunit participates in synaptic transmission by examining the properties of NMDAR-mediated synaptic currents in the two animal strains.

CHAPTER 2

METHODS

AND MATERIALS

2.1 *Acute slice preparation*

Coronal and parasagittal cerebellar slices were prepared from C57BL/6 mice at postnatal days 7-8 (P7-8), 15-18 (P15-18) and 36-39 (P36-39; Harlan, UK; colonies also maintained in-house by Biological Services, UCL). For single-channel recordings, P7-10 C57BL/6 and NR2D-knockout (-/-) mice (Ikeda *et al*, 1995; see section 2.7) were used. Following decapitation (in accordance with the UK Animals (Scientific Procedures) Act 1986), the head was immersed in ice-cold (0-4°C) 'slicing' solution oxygenated with 95%CO_2 and 5%O_2. The brain was quickly removed and placed in a fresh beaker of slicing solution. With a razor blade, the cerebellum was dissected from the cerebrum and the brainstem, and the cerebellar hemispheres were removed. Gently, pial membranes were peeled off with fine forceps. The dissected cerebellar vermis was then glued onto the stage (embedded in ice) of a vibrating microslicer (DTK-1000 Dosaka Co. Ltd, Kyoto, Japan) and bathed in fresh ice-cold slicing solution. Slices of 150-300μm thickness were cut and transferred to a bathing chamber containing oxygenated slicing solution at room temperature (18-22°C) or at 31°C. The bathing chamber consisted of a glass beaker with a suspended sheet of nylon mesh or surgical gauze on which the slices rest. A mixture of 95%CO_2 and 5%O_2 was bubbled in a separate compartment, with the slicing solution being in free flow within the beaker. The slices were incubated at room temperature or at 31°C for one hour, and subsequently maintained at room temperature for up to 9 hours.

2.2 *Drugs and solutions*

The composition of the slicing solution was (mM): NaCl, 125; KCl, 2.5; $CaCl_2$, 1; $MgCl_2$, 4; $NaHCO_3$, 26; NaH_2PO_4, 1.25; glucose, 25; pH 7.4 when bubbled with 95%CO_2 and 5%O_2. The solution was made on the day of use by

dilution of a 'ten-times' concentrated stock solution of NaCl, KCl, $NaHCO_3$ and NaH_2PO_4. $CaCl_2$, $MgCl_2$ and glucose were added before the solution was diluted to the appropriate volume. To reduce cell damage, the competitive NMDAR antagonist D-AP5 (10-25μM) or the competitive non-specific glutamate receptor antagonist kynurenic acid (1mM) was included in the slicing solution used during slicing and incubation. After the slicing procedure, the cerebellar slices were maintained in slicing solution containing 2mM $MgCl_2$ (instead of 4mM $MgCl_2$ used during slicing). This was to facilitate the removal of Mg^{2+}, necessary for the recording of currents through NMDARs at negative holding potentials (see Section 2.4 and Figure 2.2).

The bathing solution used for the recording of synaptic currents was of similar composition, except that $CaCl_2$ was increased to 2mM and $MgCl_2$ was omitted. For outside-out patch recordings, the bathing solution was the same as the slicing solution, except that $MgCl_2$ was omitted. Solutions were bubbled with 95%CO_2 and 5%O_2 for at least 20mins before use or perfusion. Solutions were bath-applied to the recording chamber via gravity feed with a flow rate of 1-1.5ml/min. The recording chamber contained approximately 1.5ml of solution and drugs were allowed to equilibrate for at least 4 minutes before recordings were made in the presence of the drug. The internal solution used for whole-cell recordings contained (in mM): CsF, 95; CsCl, 45; *N*-2-hydroxy-ethylpiperazine-*N'*-2-ethanesulphonic acid (HEPES), 10; ethyleneglycol-bis(b-aminoethylether)-*N,N,N',N'*-tetraacetic acid (EGTA), 10; NaCl, 2; Mg-ATP, 2; QX-314, 1; TEA-Cl, 5; adjusted to pH 7.2 with CsOH; 270-290mOsM. For outside-out patch recordings, an internal solution of the following composition was used (in mM): CsCl, 140; NaCl, 4; $CaCl_2$, 0.5; HEPES, 10; EGTA, 5; Mg-ATP, 2 (adjusted to pH 7.3 with CsOH). Aliquots of internal solution were thawed on the day of use and stored at -20°C for no more than one month.

Drugs were dissolved in de-ionised water, with the exception of 6-cyano-7-dinitro-quinoxaline-dione (CNQX), 2,3-Dioxo-6-nitro-1,2,3,4-tetrahydrobenzo-quinoxaline-7-sulfonamide (NBQX) and *N,N,N',N'*-tetrakis-(2-pyridylmethyl)-ethylenediamine (TPEN) which were dissolved in DMSO. Drugs were made up and stored as stock solutions at 1000 times the final concentration. Aliquots were stored at -20°C and thawed on the day of use. All drugs were purchased from Tocris (Bristol, UK), Sigma-Aldrich (Dorset, UK) or Research Biomedicals Inc. (Natick, MA, USA).

2.3 *Patch electrodes*

Patch pipettes were made from thick-walled borosilicate glass capillary tubing (GC-150F; Clark Electromedical, Pangbourne, UK, or Harvard Apparatus Ltd, Edenbridge, UK) on a two-stage puller (Narashige, Japan) on the day of use. The glass capillary tubing was lightly fire-polished at both ends before pulling: this was to minimise the scraping of the AgCl layer on the wire electrode when mounting the patch pipette onto the pipette holder. The necks of patch pipette tips were coated with Sylgard (Dow Corning 184). As calculated from the current during a 5mV step (generated by the amplifier), patch pipettes for whole-cell recordings had tip resistances of 5-10MΩ in solution. Pipettes of the same dimensions, but without the Sylgard coating, were used as stimulation pipettes. For outside-out patch recordings, pipettes had tip resistances of ~10MΩ and the tips were fire-polished.

2.4 *Identification of Golgi cells*

Golgi cells are located in the internal granule cell layer (Ramón y Cajal, 1911; Palay and Chan-Palay, 1974; Dieudonné, 1995, 1998; Misra *et al*, 2000a). They were easily distinguished from surrounding granule cells by their larger

round cell bodies, approximately three to six times the size of granule cells or about half to two-thirds of the size of Purkinje cell bodies. The trunk of the ascending dendritic tree, in the direction of the molecular layer, was often visible. At P15-18, the granule cell layer was densely packed and only Golgi cells near the surface of the slice could be visualised. At P36-39, the high degree of myelination further reduced visibility and the probability of finding Golgi cells in slices was very low indeed. Golgi cells appeared to be more fragile than Purkinje cells and very often did not survive in acute slices (at P15-18 and P36-39). As their dendritic and axonal trees are so extensive and spanning in all directions (see section 1.10.3 and Figure 1.2), Golgi cells may be easily susceptible to damage by mechanical stress.

In cell-attached mode, Golgi cells were observed to fire spontaneously and regularly with a mean frequency of 8.2 ± 0.7Hz (n=59; Figure 2.1; c.q. 3.0 ± 0.4Hz in rat slices (Dieudonné, 1998) and 14.5 ± 0.6Hz in extracellular recordings in cats (Edgley and Lidierth, 1987). No differences in the rate of spiking were observed between Golgi cells at different ages (P7-8, 7.4 ± 1.3Hz, n=14; P15-18, 8.4 ± 1.1Hz, n=35; P36-39, 9.3 ± 1.4Hz, n=9; $p > 0.5$, one-way ANOVA). Golgi cells were further distinguished from surrounding granule cells by their relatively slow current transients in response to a 5mV voltage step when patched in whole-cell configuration. The mean whole-cell capacitance (as determined directly from the amplifier settings) of P7-8 Golgi cells was 18.0 ± 0.5pF (n=72). Golgi cells at ages P15-19 and P36-39 had similar mean capacitances (respectively, 18.6 ± 0.4pF (n=91) and 16.6 ± 0.6pF (n=11); $p>0.1$, one-way ANOVA).

2.5 *Recording procedures*

Slices were transferred to a recording chamber on a fixed-stage Axioskop-FS microscope (Zeiss, Welwyn Garden City, UK), and were visualised using a 40x or a 60x water-immersion objective (total magnification, 400-960x) and Nomarski differential interference contrast (DIC) optics. All experiments were conducted at room temperature (18-22°C).

Slices were washed in Mg^{2+}-free recording solution for at least 45 minutes before cells were patched. The NMDAR-mediated component was readily recorded at a holding potential of -80mV after washing the slice for over 45 minutes in nominally Mg^{2+}-free recording solution (Figure 2.2). The channel block by Mg^{2+} occurs at negative potentials, as shown by the 'J'- or tick-shaped current-voltage (I-V) relationship in Figure 2.2A (right panel). The linear I-V plot after an hour of washing indicates successful removal of Mg^{2+} and no further change in the I-V relationship was observed at two hours after washing (Figure 2.2B and C, right panels).

All recordings were made using an Axopatch 200A amplifier (Axon Instruments, Foster City, CA, USA). Golgi cell spike spontaneously (Dieudonné, 1998) and the firing of Golgi cells were sometimes recorded in the cell-attached configuration. Golgi cells were examined in the whole-cell configuration and were voltage-clamped at -80mV (unless otherwise stated). Series resistance and capacitance measures were determined directly from the amplifier settings during 5mV steps in command voltage, and were checked every 5-20mins during recording. Recordings were not included in the analysis if the series resistance changed for more than 20% during the recording. On average, Golgi cells in the whole-cell mode had a capacitance of 18.2 ± 0.3pF and series resistance of 15.0 ± 0.3MΩ (n=174). The series resistance of

Figure 2.1 *Properties of spontaneous firing*

A, Recording of spontaneous action potential spiking in cell-attached mode from a P15 Golgi cell.

B, Analysis of the firing pattern. Histogram of interspike intervals for 437 spikes from the recording shown in A. The mean firing frequency was 15.2Hz. Inset, stability plot of the interspike interval.

C, Autocorrelation of the action potentials shown in A. The distinct and regularly distributed peaks indicate the regularity in action potential firing.

D, The frequency of spontaneous firing in Golgi cells appeared to have a similar variance at different ages. There was no significant difference in the mean firing frequency between P7-8 (7.4 ± 1.3Hz, n=14), P15-18 (8.4 ± 1.1Hz, n=35) and P35-39 (9.3 ± 1.4Hz, n=9; $p > 0.5$, one-way ANOVA). The mean ± S.E.M. values are plotted at the median of each age group.

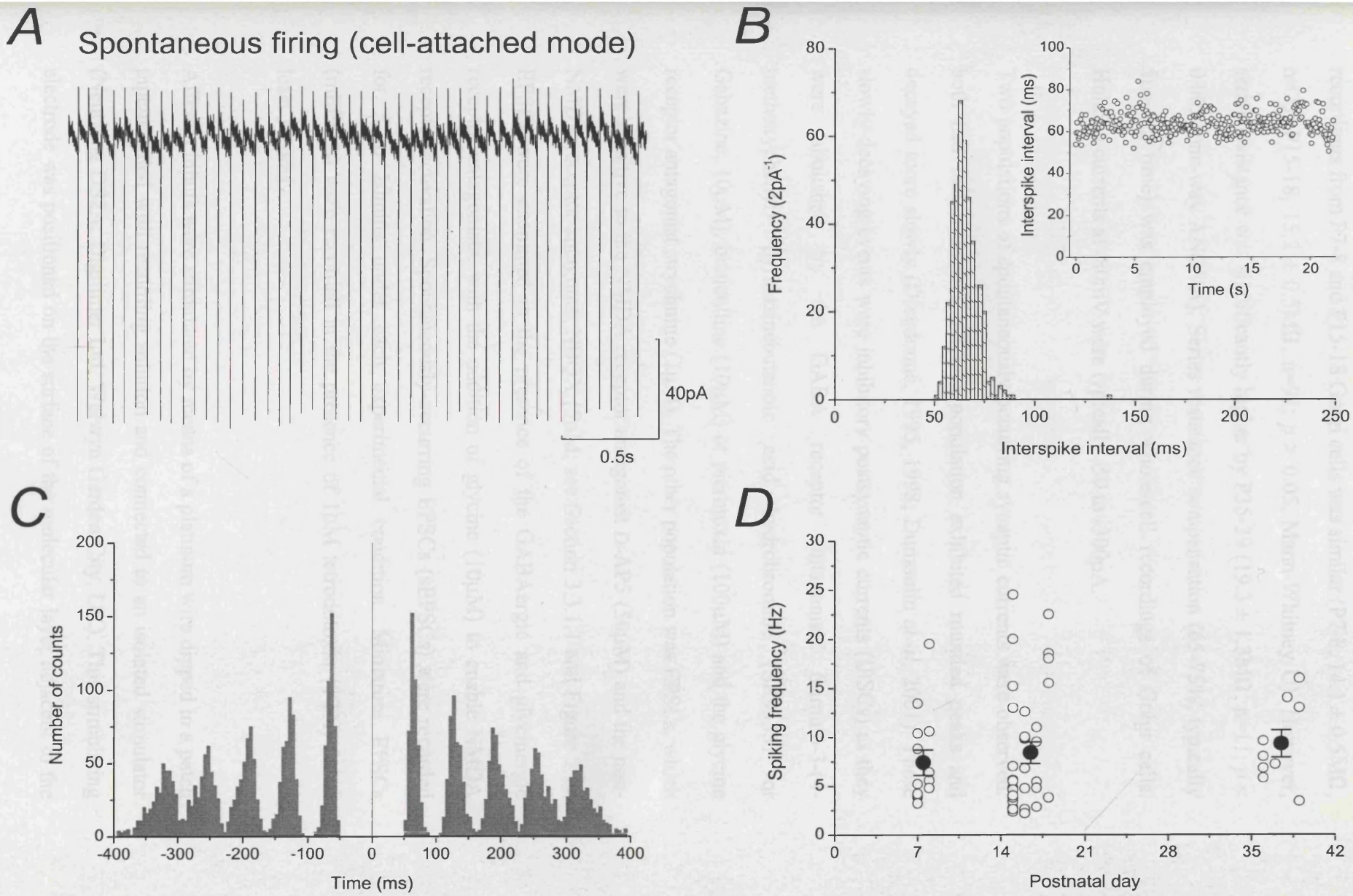
A
Spontaneous firing (cell-attached mode)
40pA
0.5s
B
Frequency (2pA^{-1})
Interspike interval (ms)
Interspike interval (ms)
Time (s)
C
Number of counts
Time (ms)
D
Spiking frequency (Hz)
Postnatal day

recordings from P7-8 and P15-18 Golgi cells was similar (P7-8, 14.1 ± 0.5MΩ, n=25; P15-18, 15.2 ± 0.5MΩ, n=91; $p > 0.05$, Mann-Whitney U). However, series resistance was significantly higher by P35-39 (19.3 ± 1.3MΩ, n=11; $p < 0.005$, one-way ANOVA). Series resistance compensation (65-75%, typically 5μs lag time) was employed during whole-cell recordings of Golgi cells. Holding currents at -80mV were typically -50 to -300pA.

Two populations of spontaneously-occurring synaptic currents were observed: both had fast rise-times but one population exhibited rounded peaks and decayed more slowly (Dieudonné, 1995, 1998; Dumoulin *et al*, 2001). These slowly-decaying events were inhibitory postsynaptic currents (IPSCs) as they were abolished by the GABA receptor antagonists 6-imino-3-(4-methoxyphenyl)-1-pyridazinebutanoic acid hydrobromide (SR93351 or Gabazine, 10μM), bicuculline (10μM) or picrotoxin (100μM) and the glycine receptor antagonist strychnine (1μM). The other population was EPSCs, which were sensitive to the NMDA receptor antagonist D-AP5 (50μM) and the non-NMDA receptor antagonist NBQX (5μM; see Section 3.3.1.1 and Figure 3.1). EPSCs were examined in the presence of the GABAergic and glycinergic receptor antagonists, with the addition of glycine (10μM) to enable NMDA receptor activation. Spontaneously-occurring EPSCs (sEPSCs) were recorded for 5 to 20mins under each experimental condition. Miniature EPSCs (mEPSCs) were recorded in the presence of 1μM tetrodotoxin (TTX) for at least 30mins.

Afferent inputs were stimulated by means of a platinum wire dipped in a patch pipette filled with recording solution and connected to an isolated stimulator (Neurolog DS2A; Digitimer Ltd, Welwyn Garden City, UK). This stimulating electrode was positioned on the surface of the molecular layer adjacent to the

Figure 2.2 *Removal of Mg^{2+} revealed an NMDAR-mediated component at -80mV*

A, Parallel fibre-evoked EPSCs recorded from a P7 Golgi cell voltage-clamped at -80mV. *Left*, average parallel fibre-evoked EPSC at 10 minutes after perfusing Mg^{2+}-free recording solution (containing 10μM SR93351, 1μM strychnine and 10μM glycine; *black trace*). For comparison, the average EPSC in 50μM D-AP5 (recorded at the end of the experiment) is shown in *grey*. *Right*, I-V relationship of the NMDAR-mediated current for the same cell at 5 to 15 minutes after perfusion of Mg^{2+}-free solution, showing that the NMDAR current was inhibited at negative potentials. NMDAR current amplitudes were measured at 20ms after the AP5-insensitive non-NMDAR EPSC peak.

B, *left*, average EPSC recorded from the same cell as shown in A, at 1 hour after perfusion of Mg^{2+}-free solution (*black*) and in 50μM D-AP5 (*grey*). The panel on the right shows the corresponding I-V relationship of the NMDAR-mediated component, which had become linear.

C, an hour later, there was no further change in the NMDAR-EPSC amplitude or in the NMDAR-EPSC I-V relationship.

A 10 minutes after perfusion of Mg^{2+}-free solution

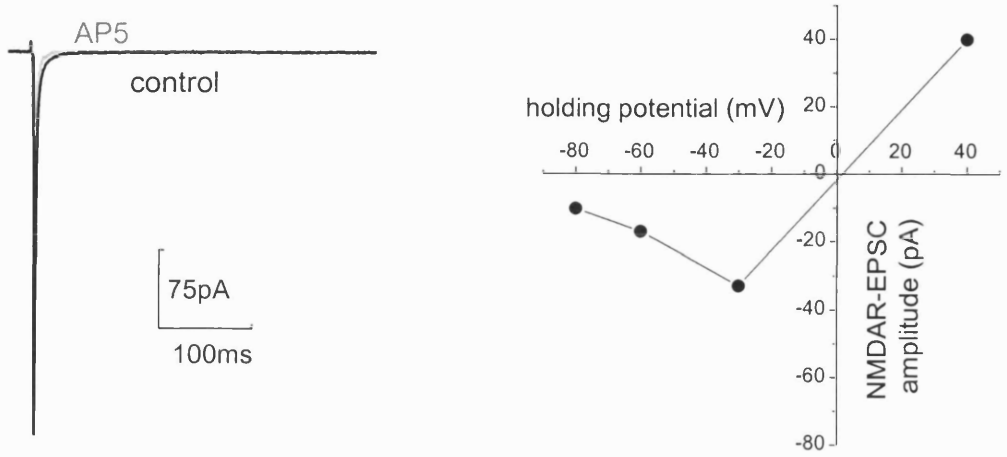

B 1 hour after perfusion of Mg^{2+}-free solution

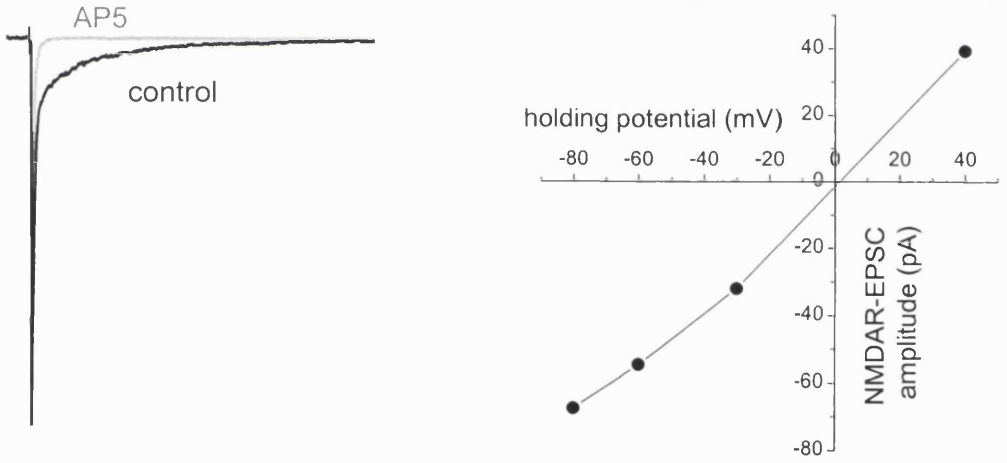

C 2 hours after perfusion of Mg^{2+}-free solution

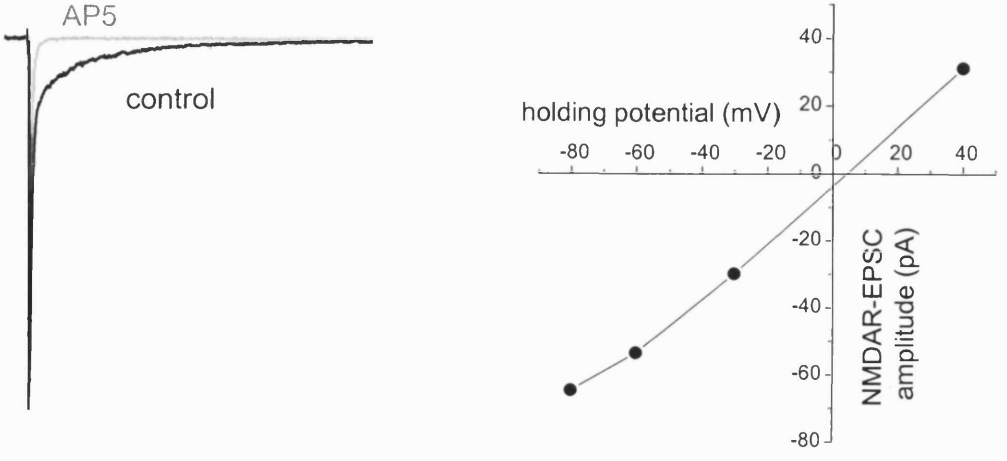

Figure 2.3 *Stability plot of parallel fibre-evoked EPSCs*

A, Average waveforms of parallel fibre-evoked EPSCs recorded at -80mV from a P7 Golgi cell at 5 minutes (*left*), 70 minutes (*middle*) and 150 minutes (*right*) from the beginning of the recording.

B, **i**, Stability plot of the non-NMDAR EPSC peak amplitude of individual EPSCs (*open circles*) over 2.5 hours. The mean values are shown as *filled circles*.

ii, stability plot of the holding current over the same period

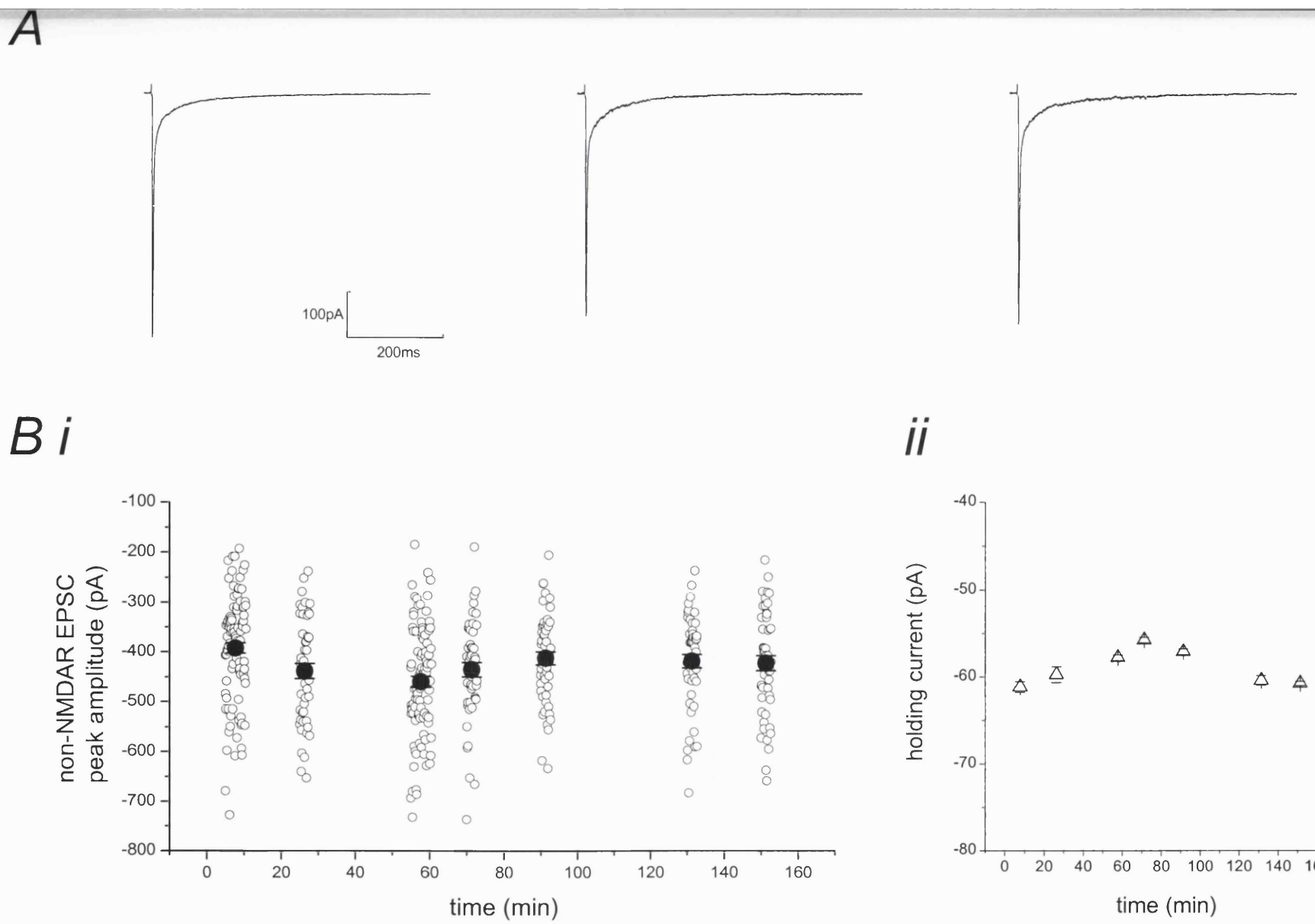
A
100pA
200ms
B i
non-NMDAR EPSC peak amplitude (pA)
-100
-200
-300
-400
-500
-600
-700
-800
0
20
40
60
80
100
120
140
160
time (min)
ii
holding current (pA)
-40
-50
-60
-70
-80
0
20
40
60
80
100
120
140
160
time (min)

recorded Golgi cell. The intensity and duration of the stimulation pulse (typically 15-35V and 40-200μs) were set such that the failure rate was 5-10% and at least half of the EPSCs produced exhibited a monophasic rise phase. Single stimuli were delivered at 0.3Hz and 100 sweeps were typically recorded under each experimental condition. For high-frequency train stimulation, the interval between each sweep was 10s and 10-20 sweeps were recorded under each condition. As illustrated in Figure 2.3, EPSC recordings remained stable and robust over two hours of recording.

2.6 *Data acquisition and analysis*

2.6.1 *Synaptic currents*

All current records were stored on digital tape (DTR-1204; BioLogic, Claix, France; DC-20kHz) with the amplifier filter (4-pole lowpass Bessel type) set at 10kHz. Records of sEPSCs and mEPSCs were replayed from tape, filtered at 2kHz (-3dB, 8-pole lowpass Bessel filter) and digitised at 10kHz or 20Hz (digidata 1200; Axotape or pClamp8, Axon Instruments). Evoked EPSCs were recorded directly onto computer and sampled at 10kHz (pClamp8).

sEPSCs were identified as rapid downward deflections (with a rise-time of approximately 1ms) from the digitised records and were analysed using 'N' version 5.0 software (written by Stephen Traynelis; Emory University, Atlanta, GA, USA). Records digitised at 20kHz were used for the analysis of non-NMDAR-mediated EPSCs. Average waveforms of sEPSCs and mEPSCs were constructed by aligning each event on their initial rising phase ('N' version 5). Parallel fibre-evoked EPSCs were aligned on the stimulus artefacts and average waveforms (at least 50 sweeps for single EPSCs and 10-20 sweeps for

EPSCs generated by a train of high-frequency stimuli) were constructed after baseline subtraction (pClamp8). EPSCs with multiphasic rises or multiple peaks were excluded from analysis.

The amplitude of the NMDAR-mediated component of sEPSCs was measured at 10ms after the non-NMDAR peak (average of 2ms) when the fast non-NMDAR-mediated component had returned to baseline. Because the non-NMDAR parallel fibre-evoked EPSC decayed more slowly than non-NMDAR sEPSCs, the NMDAR current amplitude of evoked EPSCs was measured at 20ms after the non-NMDAR current peak (average of 2ms). For NMDAR-EPSCs produced by high-frequency trains, the current amplitude was measured at 40ms after the final non-NMDAR EPSC peak. The charge transfer of the NMDAR-mediated sEPSCs and evoked EPSCs was measured by integrating from 10ms and 20ms after the non-NMDAR EPSC peak, respectively, for a duration of 1s and subtracting the charge transfer of the non-NMDAR EPSC (recorded in 50μM D-AP5). The charge transfer of EPSCs produced by high-frequency trains were integrated over 2.5s.

The decay waveforms of sEPSCs, evoked single EPSCs and EPSCs produced by a train of stimuli were fitted from 10ms, 20ms and 40ms after the non-NMDAR current peak, respectively. The decay time was fitted for 1-1.5s in the case of sEPSCs and evoked single EPSCS, and for 3s in the case of a train of EPSCs. To determine the decay kinetics of NMDAR-EPSCs, the decay waveforms of EPSCs were fitted using nonlinear least squares fitting (Origin 6.0, Microcal, Northampton, MA, USA). Most sEPSC and evoked EPSC decay waveforms (except sEPSCs at P15-18, see below) were best described by the sum of two exponential functions:

$$A(t) = A_{fast} \exp(-t/\tau_{fast}) + A_{slow} \exp(-t/\tau_{slow})$$

where τ_{fast} and τ_{slow} are the decay time constants of the fast and slow components, and A_{fast} and A_{slow} are their respective amplitudes. The weighted mean decay time constant (τ_w) was then calculated by:

$$\tau_w = [A_{fast} / (A_{fast} + A_{slow})] \tau_{fast} + [A_{slow} / (A_{fast} + A_{slow})] \tau_{slow}$$

sEPSCs at P15-18 were best described by a single exponential function:

$$A(t) = A \exp(-t/\tau)$$

where τ is the decay time constant and A is the amplitude. The fits were constrained to return to baseline. For comparison purposes, the mean decay time constant of NMDAR-EPSCs was also determined by a fit-independent method: by dividing the charge transfer of the EPSC by the amplitude.

2.6.2 *Single-channel current recordings*

Single-channel current records were collected on digital audiotape (DC - 20 kHz; DTR-1204; BioLogic, Claix, France), with the amplifier filter (4-pole Bessel type) set at 10 kHz. For analysis of single-channel currents, the records were replayed from tape, filtered at 2 kHz and digitized at 10 kHz (Axotape, pCLAMP 6.1, Axon Instruments).

The time-course fitting method was used to analyse the transitions between the various conductance levels in greater detail (Colquhoun and Sigworth, 1995; SCAN and EKDIST; http://www.ucl.ac.uk/Pharmacology/dc.html). For this

analysis, the currents were replayed from tape, filtered at 2 kHz and digitised at 10 kHz via a CED 1401+ interface (Cambridge Electronic Design, Cambridge, UK). Individual openings were then fitted with the step response function of the recording system. Events briefer than 2 filter rise times were excluded from the analysis of fitted amplitudes. In contrast to all-point amplitude distributions, the resulting fitted amplitude distributions convey no information regarding the time spent at any given amplitude. Kinetic information was obtained from analysis of open period and shut time distributions and the subsequent calculation of open probability.

The unbinned amplitude data were fitted to the sum of two or three Gaussian components, using the maximum likelihood method, to give mean amplitude levels of the single-channel currents. The Gaussian fits of the amplitude histogram were used to estimate the critical amplitude (A_{crit}) that would serve as a 'cut-off' between the 40 and the 50 pS conductance states (Howe *et al*, 1991). A_{crit} was chosen as the value that resulted in the least number of misclassified events within each group. This critical amplitude approach was chosen in order to analyze the open-period kinetics of high conductance openings (open-period$_{HIGH}$) and therefore calculate the open probability of this high conductance NMDAR population ($P_{OPEN(HIGH)}$) with little contamination from low conductance NR1/NR2D-like openings. For wild-type NMDAR openings, only a fraction of the 8±1 % misclassified events will arise from low conductance NR1/NR2D-like openings, as the majority of misclassified events will correspond to the sub-conductance state (~40 pS) of the high conductance openings (see section 5.3.1).

Ifenprodil inhibition curves were fitted with a modified form of the Hill equation with the fit weighted to the standard deviation at each concentration using Igor Pro (Wavemetrics, Lake Oswego, OR, USA):

$$I = I_{max}/(1 + ([A]/IC_{50})^n + (100 - I_{max})$$

Where I is the response magnitude, I_{max} is the maximal inhibition of the response, [A] is the concentration of ifenprodil, IC_{50} is the concentration of ifenprodil required to reduce the response to 50% of the maximum block, and n is the Hill slope.

A simple modification of this single component model (see Kew *et al.,* 1998) was applied to the data when attempting to describe the presence of a high ($IC_{50(H)}$) and a low affinity ($IC_{50(L)}$) ifenprodil inhibition:

$$I = [I_{max(H)}/(1 + ([A]/IC_{50(H)})^{n(H)})] + [I_{max(L)} / (1 + ([A]/IC_{50(L)})^{n(L)}] + [100 - I_{max(H)} - I_{max(L)}]$$

2.6.3 *Statistical analysis*

Average data are expressed as mean ± S.E.M. (n = number of cells). Error bars in graphs represent S.E.M.. The distribution of data groups was first tested for normality using the Shapiro-Wilks' W test (Statistica 5.1, StatSoft Inc, Tulsa, USA). Statistical significance between two groups of normally-distributed data was tested using the paired or unpaired two-tailed Student's t tests. Otherwise, the non-parametric Wilcoxon matched-pairs test or Mann-Whitney U test was used. For comparison of more than two data groups, the one-way ANOVA test was performed (Statistica 5.1 or Microsoft Excel). Correlations were tested for significance using the Spearman R coefficient and were illustrated by a linear regression (least squares fit) line. Statistical comparisons were considered significant at $p < 0.05$.

2.7 *NR2D-knockout mice*

NR2D-knockout (-/-) mice were a generous gift from Mishina's group (Ikeda *et al*, 1995) and were maintained in-house by Biological Services, UCL. Prior to performing this study, the genetic background of the NR2D-knockout strain had been purified by a series of seventeen backcrosses into the C57BL/6 strain, such that the NR2D-knockout strain was 99.99% genetically homogeneous with our wild-type controls (Takeuchi *et al*, 2001). We did not observe any gross differences in terms of behaviour or animal size compared with wild-type C57BL/6J mice. The general morphology of the cerebellar slices also appeared similar.

CHAPTER 3

PROPERTIES OF NMDAR- MEDIATED SYNAPTIC CURRENTS DURING CEREBELLAR GOLGI CELL DEVELOPMENT

3.1 Summary

1. To investigate the properties of NMDA receptors expressed at synapses in cerebellar Golgi cells, patch-clamp recordings were made from cells in acute thin cerebellar slices from mice. Golgi cells at three ages were studied: at 7-8 days after birth (P7-8), at 15-18 days (P15-18) and at 36-39 days (P36-39).

2. Spontaneously-occurring EPSCs (sEPSCs) were readily identified in whole-cell voltage-clamp recordings. The component mediated by NMDARs was found to decline in amplitude with age.

3. The decay kinetics of the NMDAR-mediated sEPSC became faster between P7-8 and P15-18. The weighted mean decay time constant was decreased from 70.4 ± 4.3ms (n=22) to 44.9 ± 5.0ms (n=13).

4. The acceleration in decay kinetics was accompanied by changes in the pharmacological properties of the NMDAR-mediated sEPSCs. Inhibition by the NR2B-selective antagonist ifenprodil (10μM) was reduced from 65.3 ± 2.4% (n=4) at P7-8 to 21.6 ± 3.5% (n=6) at P15-18. Sensitivity of NMDAR-mediated synaptic currents to the Zn^{2+} chelator TPEN (which affects NR2A-containing receptors; 1μM) was increased from 31.5 ± 6.6% (n=11) to 109.1 ± 59.8% (n=4) between P7-8 and P15-18.

5. Interestingly, the ifenprodil sensitivity of sEPSCs at P15-18 was higher when ifenprodil was applied in the presence of TPEN. This was not observed in sEPSCs recorded from P7-8 Golgi cells.

6. The parallel fibre to Golgi cell synapse was studied in isolation by stimulating afferent parallel fibres in the molecular layer. Parallel fibre-evoked EPSCs mediated by NMDARs displayed similar changes in decay kinetics and pharmacology between P7-8 and P15-18. Evoked EPSCs from older animals exhibited faster decay kinetics (P15-18, 79.9 ± 3.2, n=54; P7-8, 110.3 ± 4.7ms, n=24), were more sensitive to potentiation by TPEN (P15-18, 141.6 ± 68.1%, n=4; P7-8, 38.4 ± 19.2%, n=6), and were less susceptible to inhibition by ifenprodil (P15-18, 17.7 ± 4.6%, n=9; P7-8, 76.7 ± 4.6%, n=8).

7. It is concluded that the majority of NMDARs at Golgi cell synapses appear to display properties of the NR2B subtype at P7-8. A week later in development, the acceleration in decay kinetics, the decreased ifenprodil sensitivity and the increased effect of TPEN are consistent with the idea of an increased contribution of NR2A-containing receptors at these synapses.

3.2 Introduction

The NMDA receptor plays important roles in brain physiology. It is required for neuronal development and synapse formation, it can mediate a substantial component of synaptic currents to affect cell firing and it induces certain types of plasticity. Elucidating the properties of this subtype of ionotropic glutamate receptor, and how these properties develop as the brain matures, is essential to the understanding and study of excitatory synaptic transmission.

With the advent of molecular cloning, the *in situ* hybridisation and immuno-labelling techniques are often used to reveal the mRNA and protein expression of receptor subtypes in neurons. However, these techniques are less suitable when it comes to studying sparsely located cell types. The patch-clamp technique not only enables us to visually select the cell to be studied, it also provides us with information on *functional* receptors. With the availability of selective pharmacological agents, we can selectively manipulate receptor subtypes and hence identify the subunit composition of receptors expressed.

It has been shown that the properties of NMDAR-mediated whole-cell and synaptic currents change during development (Carmignoto and Vicini, 1992; Hestrin, 1992; Flint *et al*, 1996; Kirson and Yaari, 1996; Takahashi *et al*, 1996; Stocca and Vicini, 1998; Rumbaugh and Vicini, 1999; Cathala *et al*, 2000). Although the magnitude of NMDAR-mediated synaptic currents has been reported to increase, decrease or remain unchanged in various cell types, the decay kinetics of these currents generally becomes faster with age (Carmignoto and Vicini, 1992; Hestrin, 1992; Kirson and Yaari, 1996; Takahashi *et al*, 1996; Stocca and Vicini, 1998; but see Cathala *et al*, 2000). This developmental change in synaptic decay kinetics is thought to reflect the functional expression of different NR2 subunits in the NMDAR complex (Monyer *et al*, 1994; Flint *et al*, 1996; Plant *et al*, 1997; Tovar and Westbrook, 2000). This idea is further supported by changes in sensitivity of NMDAR-mediated synaptic currents to subunit-specific antagonists during development (Stocca and Vicini, 1998; Rumbaugh and Vicini, 1999; Tovar and Westbrook, 1999; Cathala *et al*, 2000).

Whether similar changes occur in inhibitory neurons during development has been less well studied. Golgi cells are GABAergic neurons located in the internal

granule cell layer of the cerebellar cortex. These cells are important in controlling the excitation of the numerous granule cells (Eccles *et al*, 1966; Maex and de Schutter, 1998; Vos *et al*, 1999; Watanabe *et al*, 1998). Although Golgi cells can be distinguished by their location and their large-sized cell bodies, they are greatly outnumbered by the surrounding granule cells. This renders the *in situ* hybridisation technique less effective in resolving the NMDAR subunits expressed in Golgi cells (unless they express subunits not present in granule cells).

Previous work on the rat cerebellar Golgi cell by Misra *et al* (2000a) demonstrated functional NMDARs in the cell soma and at synapses. Interestingly, other inhibitory neurons in the cerebellar cortex, the stellate/basket cell and the Purkinje cell, do not express synaptic NMDARs (Kano *et al*, 1988; Hirano 1990; Perkel *et al*, 1990; Clark and Cull-Candy, 2002). This chapter investigates the properties of NMDARs at Golgi cell synapses and whether these properties change with development. The characteristics of NMDAR-mediated synaptic currents recorded from mouse cerebellar Golgi cells will be described from animals at 7-8 (P7-8), 15-18 (P15-18) and 36-39 days old (P36-39). Various properties, including the amplitude, the decay time-course and the sensitivity to pharmacological agents selective for particular NR2 subunits, are compared.

3.3 Results

3.3.1 *Changes in the properties of spontaneous EPSCs during development*

As Golgi cells also receive GABAergic and glycinergic inputs (Dieudonné, 1995, 1998; Dumoulin *et al*, 2001), glutamatergic EPSCs were isolated in the presence of the $GABA_A$ receptor antagonist SR95531 (10μM) or picrotoxin (100μM), and the glycine receptor antagonist strychnine (500nM or 1μM). Glycine is required as a co-agonist for NMDAR activation (Johnson and Ascher, 1987; Kleckner and Dingledine, 1988) and 10μM glycine was included in the recording solution to facilitate NMDAR activation and to minimise variation in glycine concentrations between experiments. All EPSCs were recorded at the holding potential of -80mV and all experiments were conducted at room temperature (18-22°C).

3.3.1.1 *sEPSCs at P7-8*

Figure 3.1A shows a trace of sEPSCs recorded under control conditions from a P7 Golgi cell. The frequency of sEPSCs was typically 0.1-0.35Hz (0.22 ± 0.03Hz, n=20). As is apparent from the examples of individual sEPSCs and the average waveform of 178 sEPSCs shown in Figure 3.1D and 3.1E, sEPSCs in these cells displayed two components (Dieudonné, 1998; Misra *et al*, 2000a). As expected, the slow-decaying component was abolished by the competitive NMDAR antagonist D-AP5 (50μM; Figure 3.1B, D and E). The fast-decaying component was insensitive to D-AP5 (50μM) but was inhibited by the non-NMDAR antagonist NBQX (5μM; Figure 3.1C). This non-NMDAR-mediated component will be discussed in more detail in Section 3.3.2.

The amplitude of the slow-decaying NMDAR-mediated component was measured at 10ms after the non-NMDAR-mediated peak, by taking the average of 20 data points (2ms at 10 kHz sampling rate), and has a mean value of -5.96 ± 0.45pA (n=22) at P7-8. As is apparent from Figure 3.2A, the non-NMDAR component had returned to baseline within 10ms of the non-NMDAR peak (indicated by the vertical dotted line).

The decay time-course of the average NMDAR-sEPSC was obtained by fitting the current from 10ms after the non-NMDAR peak for 1 to 1.5 seconds. In 18 out of 22 cells, the decay time was best described by a sum of two exponential functions (Figure 3.2B). The mean decay time constants for the fast (τ_{fast}) and slow (τ_{slow}) components were 30.9 ± 5.5ms and 123.2 ± 10.9ms, respectively, with the fast component contributing 50.4 ± 6.0% to the total current amplitude. The weighted mean decay time constant (τ_w) for these 18 cells was 73.6 ± 5.0ms. In the remaining 4 cells, the decay phase of the average sEPSC was best fitted with a single exponential function. The mean decay time constant of these 4 cells was 57.0 ± 5.9ms. Taking all 22 cells together, the average (weighted mean) decay time constant for sEPSCs at P7-8 was 70.4 ± 4.3ms and was independent of the amplitude (Figure 3.2C; Spearman R = -0.253, $p > 0.2$). Similar mean decay time constants were obtained using a fit-independent measure (charge transfer divided by amplitude: 71.2 ± 5.7ms, n=22; $p > 0.5$, Mann-Whitney U).

Figure 3.1 *NMDAR sEPSCs from a P7 Golgi cell*

A, trace of a whole-cell recording under control conditions (in the presence of 10μM SR93351, 1μM strychnine and 10μM glycine) at holding potential -80mV. Events 1-4 are shown on an expanded scale in D.

B, sEPSCs in the presence of 50μM D-AP5 (NMDAR antagonist). Events 5 and 6 are shown on an expanded scale in D.

C, on perfusion of 50μM D-AP5 and 5μM NBQX (non-NMDAR antagonist), all sEPSCs were abolished. The same scale bars apply to B.

D, under control conditions, sEPSCs have a fast-rising, fast-decaying component and a slower-decaying component (traces 1-4, corresponding to 1-4 in A). The slow component was abolished in 50μM D-AP5 (traces 5 and 6, corresponding to 5 and 6 in B), indicating that this component was mediated by NMDARs. The fast component was mediated by non-NMDARs, as it was insensitive to 50μM D-AP5 but was abolished by NBQX (see C).

E, an average of 178 sEPSCs recorded under control conditions (*black*) and an average of 82 sEPSCs in 50μM D-AP5 (*grey*).

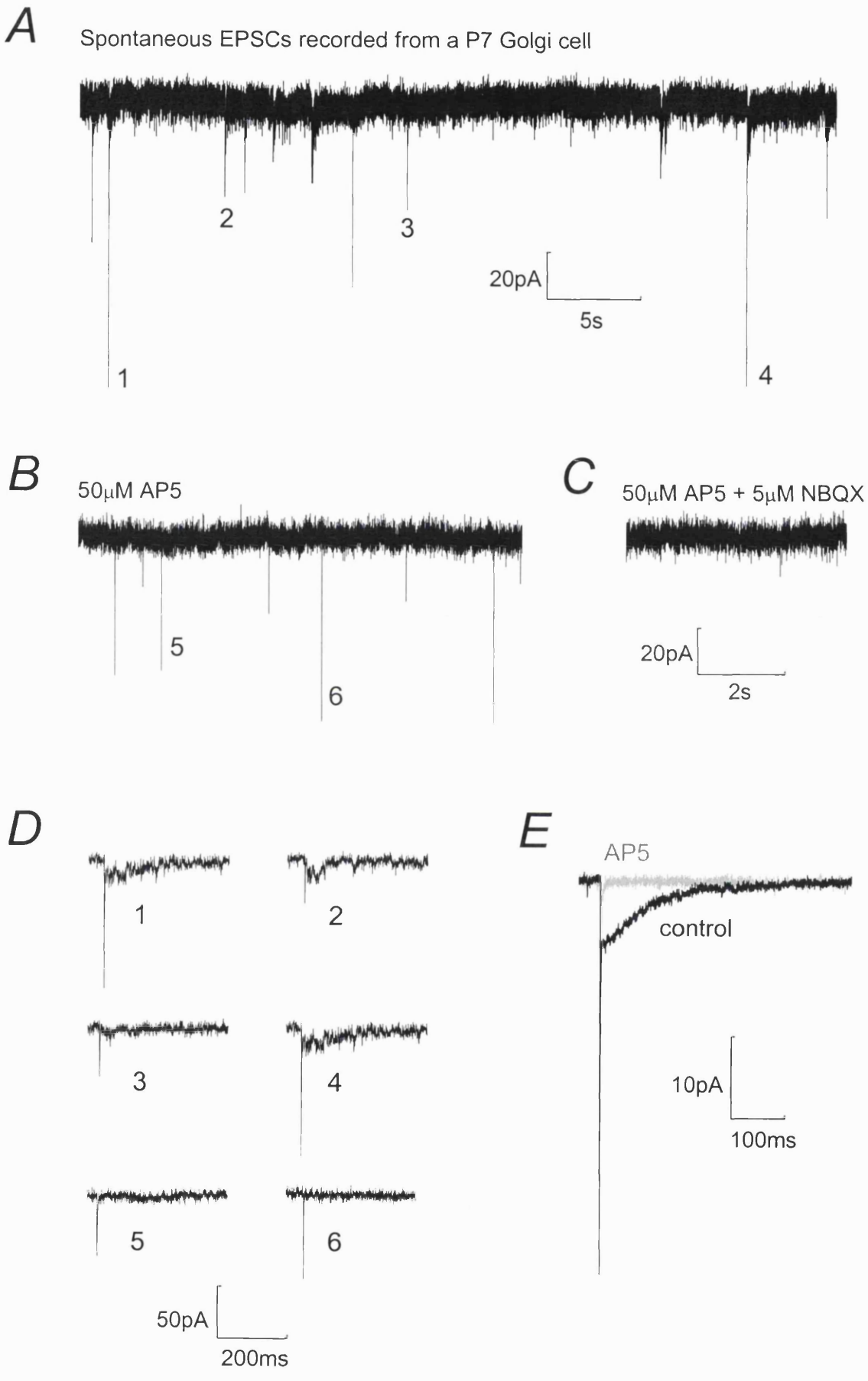
A
Spontaneous EPSCs recorded from a P7 Golgi cell
1
2
3
4
20pA
5s
B
50μM AP5
5
6
C
50μM AP5 + 5μM NBQX
20pA
2s
D
1
2
3
4
5
6
50pA
200ms
E
AP5
control
10pA
100ms

Figure 3.2 *Decay kinetics of sEPSCs from P7 Golgi cell*

A, average control sEPSC recorded at a holding potential of -80mV (*black*). The dotted vertical line indicates 10ms after the AP5-insensitive non-NMDAR EPSC peak. By this time, the non-NMDAR EPSC (*grey*) has returned to baseline. The NMDAR current amplitude (for sEPSCs) is measured at this time-point, average of 20 data points (2ms at 10kHz sampling rate).

B, the decay time-course of the NMDAR current is fitted from 10ms after the non-NMDAR EPSC peak. Best fitted with the sum of two exponential functions (described by τ_{fast} and τ_{slow}; *red*), the average sEPSC from this P7 cell displayed a weighted mean decay time constant (τ_w) of 101.8ms.

C, a plot of NMDAR current amplitude against weighted mean decay time constant (τ_w) for 22 cells at P7-8 shows that the decay time is independent of the current amplitude (*red,* linear regression, $R = 0.02$, $p > 0.9$).

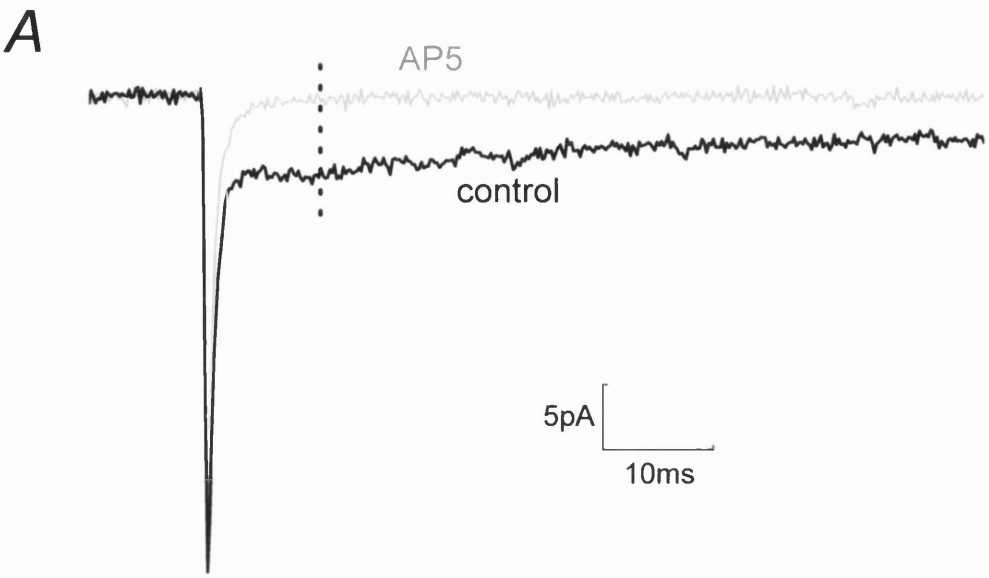
A
AP5
control
5pA
10ms

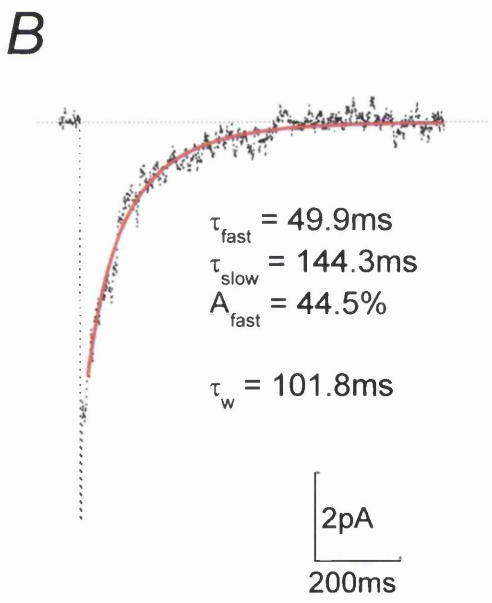
B
τfast = 49.9ms
τslow = 144.3ms
Afast = 44.5%
τw = 101.8ms
2pA
200ms

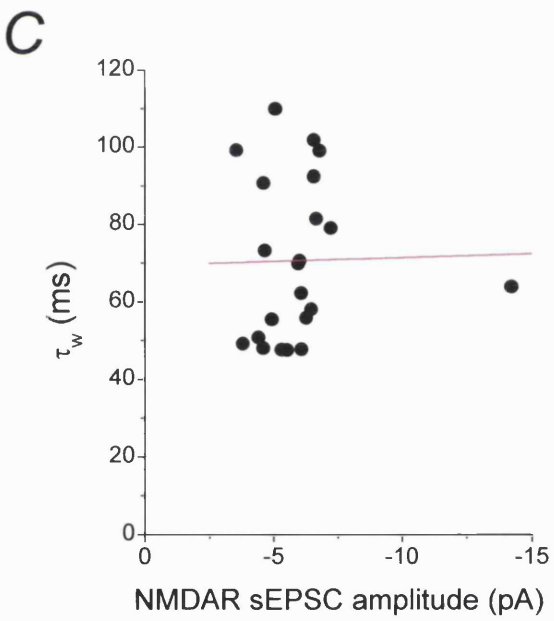
C
120
100
80
60
40
20
0
τw (ms)
0
-5
-10
-15
NMDAR sEPSC amplitude (pA)

3.3.1.2 *Properties of sEPSCs at P15-18*

Next, we examined the properties of sEPSCs a week later in development, at P15-18. Figure 3.3A shows a typical recording of sEPSCs under control conditions from a P15 Golgi cell. The mean frequency of sEPSCs from cells in this age group was not significantly different to that at P7-8 (0.19 ± 0.02Hz, n=15; $p > 0.4$, Mann-Whitney U). As with sEPSCs at P7-8, individual sEPSCs at P15 were made up of fast- and slow-decaying components (Figure 3.3B), with the average non-NMDAR component returned to baseline within 10ms (indicated by the vertical dotted line in Figure 3.3C). The mean amplitude of the AP5-sensitive slow-decaying component (measured at 10ms after the non-NMDAR peak) at this age was -4.64 ± 0.75pA (n=22).

Unlike at P7-8, the decay time-course of NMDAR-mediated currents at P15-18 was best fitted with a mono-exponential function (Figure 3.3D). Nine cells had NMDAR currents that were too small for their decay time-course to be accurately fitted, i.e. with amplitudes less than -3pA. The mean decay time constant of the other 13 cells was 44.9 ± 5.0ms. The fitted decay time constants were independent of the current amplitude (Figure 3.3E; Spearman $R = 0.058$, $p > 0.5$). Mean decay time constants obtained by dividing the charge transfer by the current amplitude were similar to the values obtained by fitting (46.8 ± 4.5ms, n=22; $p > 0.5$, Mann-Whitney U).

Figure 3.3 *sEPSCs from a P15 Golgi cell*

A, whole-cell recording from a P15 Golgi cell under control conditions. Examples of individual sEPSCs (1-4) are shown on an expanded scale in **B**.

C, average control waveform of 50 sEPSCs (*black*) and average waveform of 40 sEPSCs in 50μM D-AP5 (*grey*). As with sEPSCs at P7, the non-NMDAR synaptic current has returned to baseline levels by 10ms after the non-NMDAR peak (indicated by the vertical dotted line).

D, the decay time-course of the average sEPSC was fitted from 10ms after the non-NMDAR EPSC peak and was best described by a single exponential function (*red*). The decay time constant (τ) for the average waveform was 47.7ms.

E, the decay time-course was independent of the NMDAR current amplitude as shown in a plot of decay time constant (τ) against current amplitude for 13 Golgi cells at P15-18. *Red*, linear regression, $R = 0.075$, $p > 0.5$.

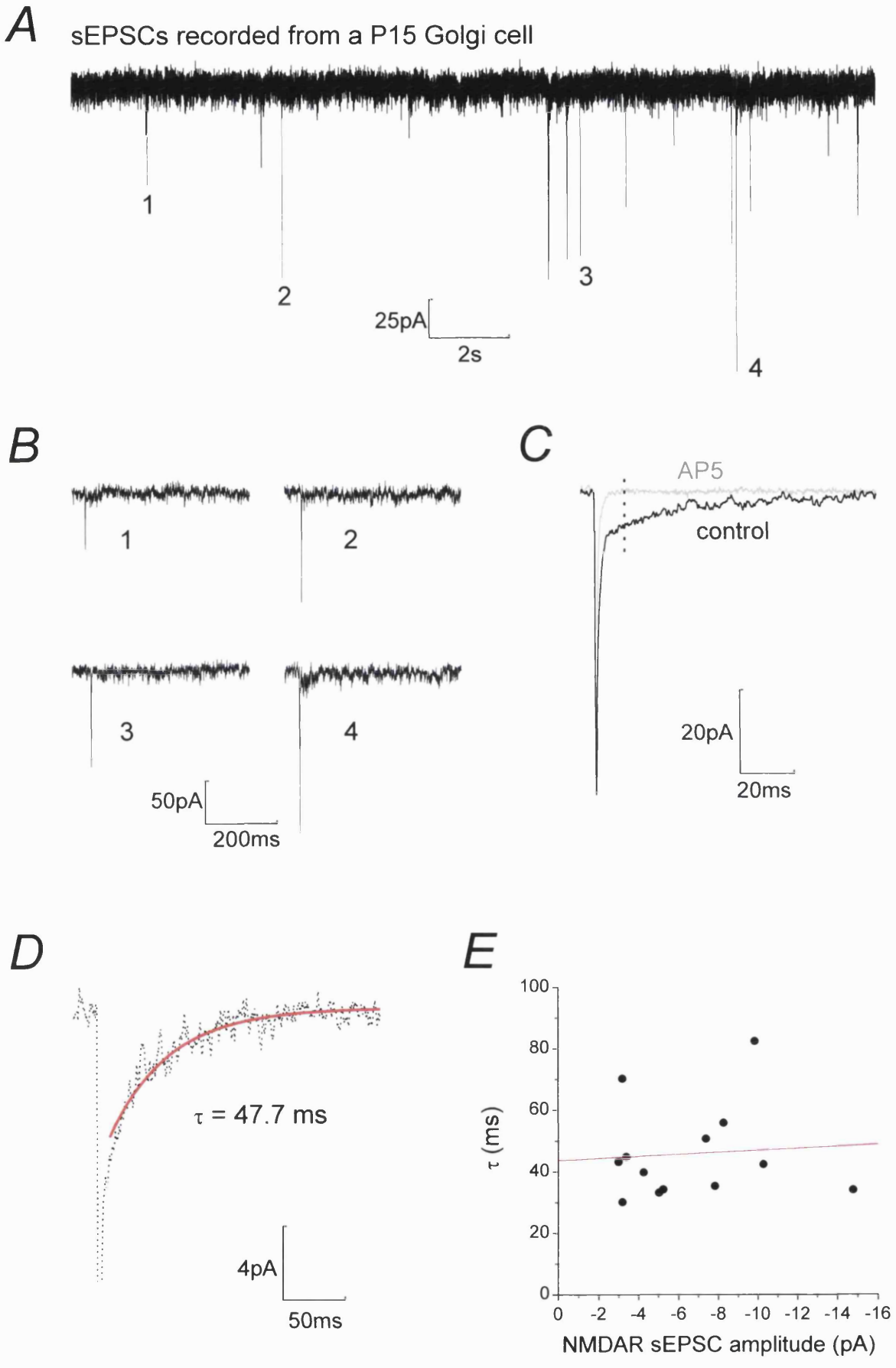
A
sEPSCs recorded from a P15 Golgi cell
1
2
3
4
25pA
2s
B
1
2
3
4
50pA
200ms
C
AP5
control
20pA
20ms
D
τ = 47.7 ms
4pA
50ms
E
τ (ms)
100
80
60
40
20
0
0
-2
-4
-6
-8
-10
-12
-14
-16
NMDAR sEPSC amplitude (pA)

Figure 3.4 *Comparing sEPSCs recorded from Golgi cells at P7-8, P15-18 and P36-39*

A, average sEPSCs under control conditions (*black*) and in 50μM D-AP5 (*grey*) recorded from a P7 (*left*), P15 (*middle*) and P38 (*right*) Golgi cell.

B, the mean NMDAR current amplitude declined between P7-8 (n=22), P15-18 (n=22), and P36-39 (n=5). The *open circles* denote measurements from individual cells and the *filled circle* is the mean amplitude ± S.E.M. for each age group plotted at the median age. *, $p = 0.01$, one-way ANOVA.

C, the decay time-course of the NMDAR sEPSC became faster between P7-8 (n=22) and P15-18 (n=13). Readings from individual cells (*open circles*) and mean decay time constant ± S.E.M. (*filled circles*) plotted at the median age. #, $p < 0.0005$, Mann-Whitney U.

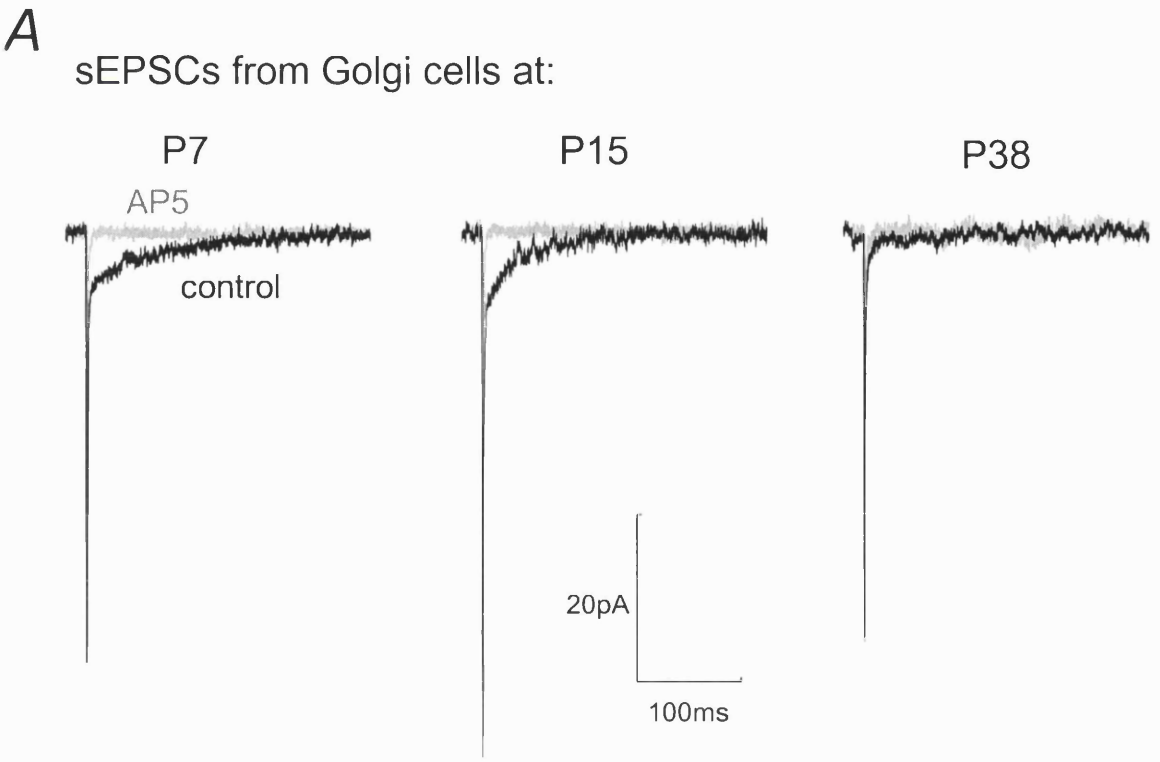
A
sEPSCs from Golgi cells at:
P7
P15
P38
AP5
control
20pA
100ms

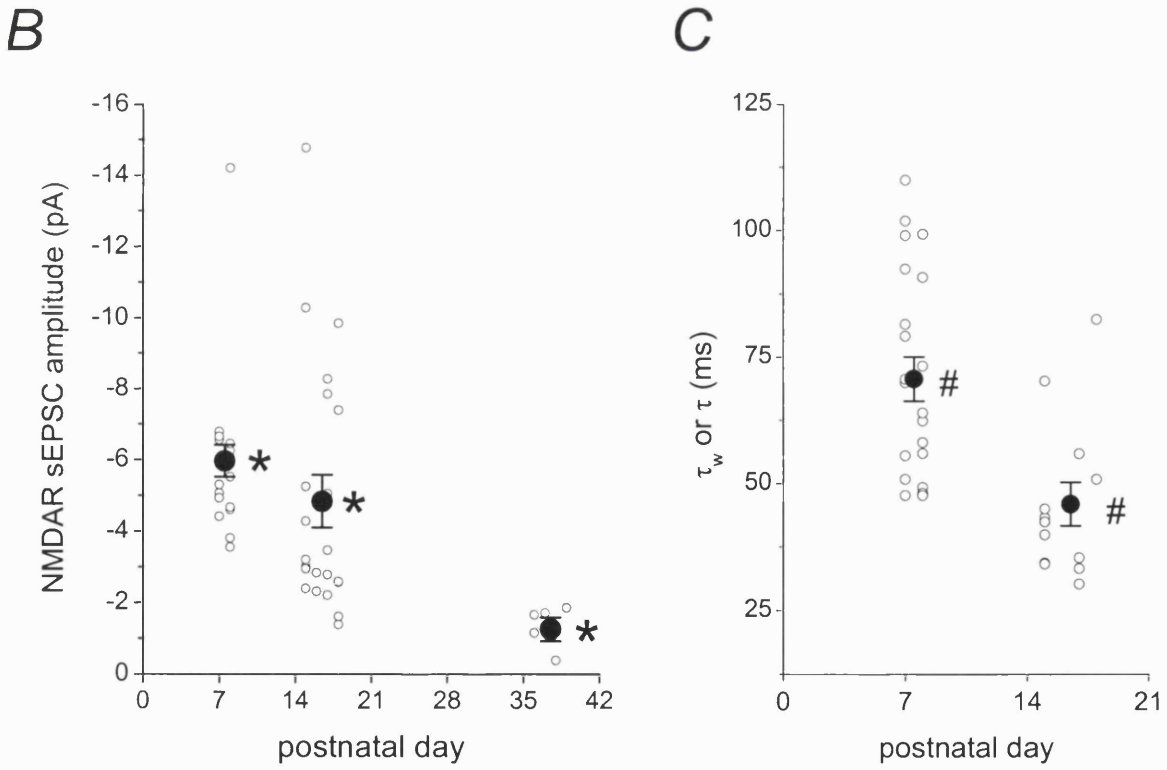
B
NMDAR sEPSC amplitude (pA)
-16
-14
-12
-10
-8
-6
-4
-2
0
0
7
14
21
28
35
42
postnatal day
*
*
*
C
τw or τ (ms)
125
100
75
50
25
0
7
14
21
postnatal day
#
#

3.3.1.3 *Comparison of sEPSCs at P7-8, P15-18 and P36-39*

The amplitude of the NMDAR synaptic current decreased with age (Figure 3.4A and B). At P36-39, the mean NMDAR-sEPSC amplitude was -1.25 ± 0.33pA (n=5), and the overall change in amplitude between P7 and P39 was statistically significant (p = 0.01, one-way ANOVA). The difference in amplitude between P7-8 and P15-18 was also significant (-5.96 ± 0.45pA and -4.64 ± 0.75pA, respectively, n=22 for each age group; $p < 0.05$, Mann-Whitney U).

Furthermore, the duration of the NMDAR synaptic current became significantly shorter during the course of the second postnatal week (Figure 3.4C and Table 3.1). The decay time constant was reduced from 70.4 ± 4.3ms (n=22) to 44.9 ± 5.0ms (n=13; $p < 0.0005$, Mann-Whitney U) between P7-8 and P15-18. The decay kinetics of sEPSCs at P36-39 could not be accurately determined: the currents were too small for an accurate fit and the signal-to-noise ratio was too high for an accurate measure of the charge transfer.

3.3.2 *Properties of non-NMDAR sEPSCs*

The fast-decaying non-NMDAR component was examined in isolation in the presence of the NMDAR antagonist D-AP5 (50μM). Typical examples are shown in Figure 3.5A. At P7-8, the mean 10-90% rise-time and mean amplitude of the non-NMDAR sEPSC were 263.3 ± 8.0μsec and -57.0 ± 4.2pA, respectively (n=21). The decay time-course of the non-NMDAR current was best fitted with the sum of two exponential functions (Figure 3.5D), giving a weighted mean time constant (τ_w) of 1.16 ± 0.06ms (τ_{fast}, 0.93 ± 0.06ms; τ_{slow}, 8.10 ± 1.49ms; A_{fast},

94.2 ± 1.0%). The τ_w between cells was independent of the mean EPSC amplitude (Figure 3.5E; Spearman $R = 0.07, p > 0.7$).

Since the Golgi cell has extensive apical dendritic arborisations extending through the molecular layer (Ramón y Cajal, 1911; Palay and Chan-Palay, 1974; Dieudonne, 1998), the distortion of EPSC amplitude and kinetics by dendritic filtering is likely. In the P7 Golgi cell illustrated in Figure 3.5, a significant positive correlation was found between the 10-90% rise-time and the mean decay of individual non-NMDAR sEPSCs (Figure 3.5C; Spearman $R = 0.28$, $p < 0.005$). Of the 21 recordings made, a significant correlation was found between these two parameters in 13 cells (Spearman $R = 0.38 \pm 0.03$). (In the other 8 cells, the rise- and decay times were independent of each other; Spearman R = 0.07 ± 0.06.) However, the current amplitude was independent of the 10-90% rise-time (data not shown; Spearman $R = -0.04 \pm 0.04$, n=21).

In contrast to the NMDAR-mediated component, sEPSCs mediated by non-NMDARs showed no changes in current amplitude between P7 and P39 (Figure 3.6A and B). There were also no significant differences in the 10-90% rise time, τ_{fast}, τ_{slow}, %fast or τ_w ($0.07 < p < 0.75$, one-way ANOVA; Figure 3.6C and D). A summary of values for all parameters is given in Table 3.1. Similar to the observations at P7-8, individual non-NMDAR sEPSCs at P15-18 exhibited a positive correlation between the 10-90% rise-time and the mean decay time (data not shown; 12 of 16 cells, Spearman $R = 0.4 \pm 0.05$) but the amplitude was independent of the 10-90% rise-time for all cells (Spearman R = 0.03 ± 0.05, n=16).

Figure 3.5 *Non-NMDAR sEPSCs recorded from a P7 Golgi cell*

A, examples of individual sEPSCs mediated by non-NMDARs recorded from a P7 Golgi cell in the presence of 50μM D-AP5.

B, amplitude histogram for 105 non-NMDAR sEPSCs from the same recording.

C, there was a significant correlation between the 10-90% rise-time and the mean decay time of individual EPSCs (*red*, linear regression, R = 0.27, $p < 0.005$), indicating dendritic filtering.

D, average waveform of 105 sEPSCs. The decay time-course was best fitted with the sum of two exponentials (described by τ_{fast} and τ_{slow}), giving a weighted mean time constant (τ_w) of 0.97ms (*red*).

E, a plot of the weighted mean decay time constant against the non-NMDAR sEPSC amplitude (n=21). Linear regression (*red*) showed no significant correlation (R = 0.065, $p > 0.7$).

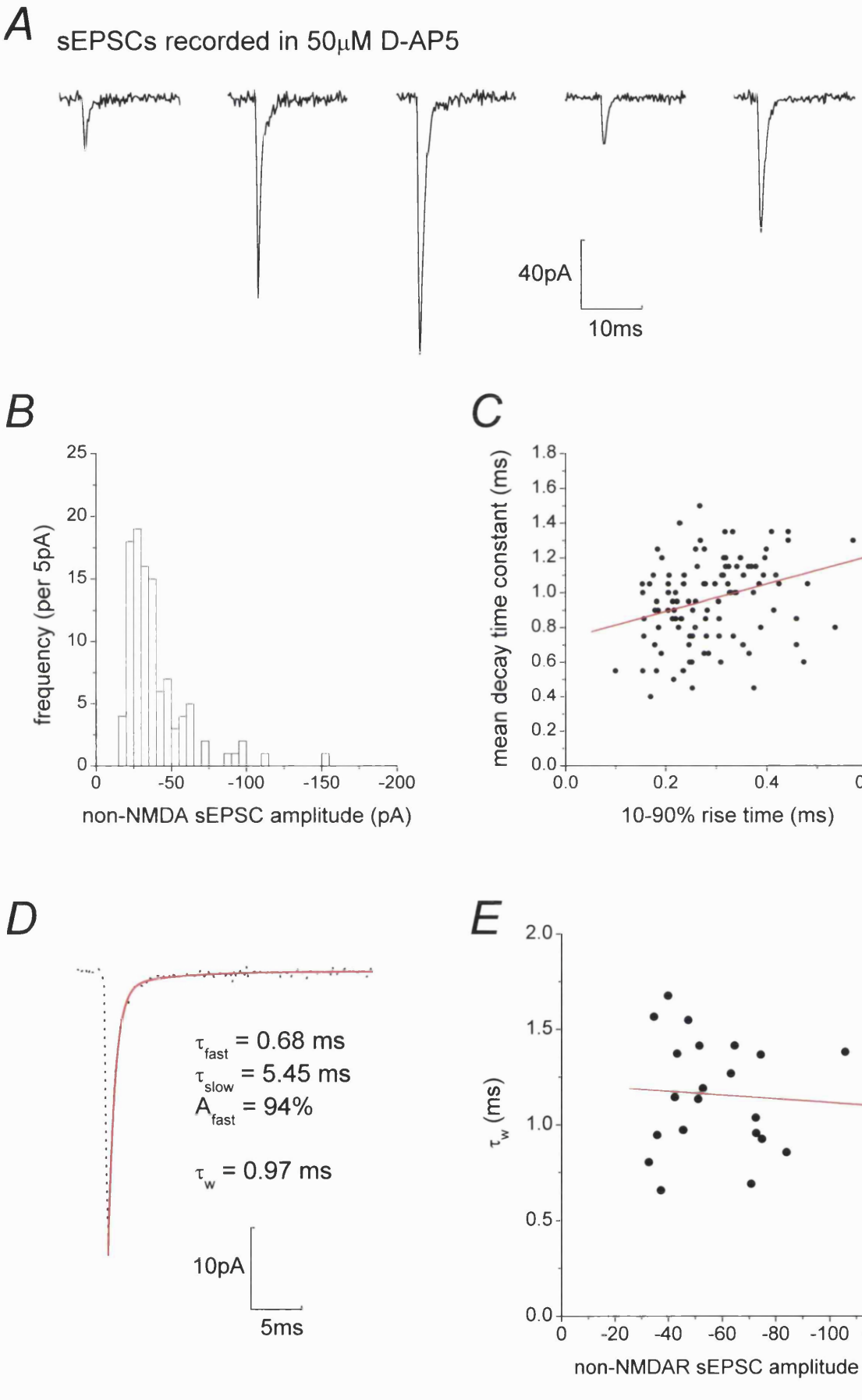
A
sEPSCs recorded in 50μM D-AP5
40pA
10ms
B
frequency (per 5pA)
non-NMDA sEPSC amplitude (pA)
C
mean decay time constant (ms)
10-90% rise time (ms)
D
τfast = 0.68 ms
τslow = 5.45 ms
Afast = 94%
τw = 0.97 ms
10pA
5ms
E
τw (ms)
non-NMDAR sEPSC amplitude (pA)

Figure 3.6 *Comparison of non-NMDAR sEPSCs at P7-8, P15-18 and P36-39*

A, average sEPSCs recorded in the presence of 50μM D-AP5 from a P7 (*left*), P15 (*middle*) and P38 (*right*) Golgi cell.

There were no significant changes in (**B**) the non-NMDAR current amplitude, (**C**) the 10-90% rise-time, and (**D**) the weighted mean decay time constant between P7 and P39 ($0.05 < p < 0.75$, one-way ANOVA). The mean values ± S.E.M. (*filled circles*) are plotted at the median of each age group (P7-8, n=21; P15-18, n=15; P36-39, n=4).

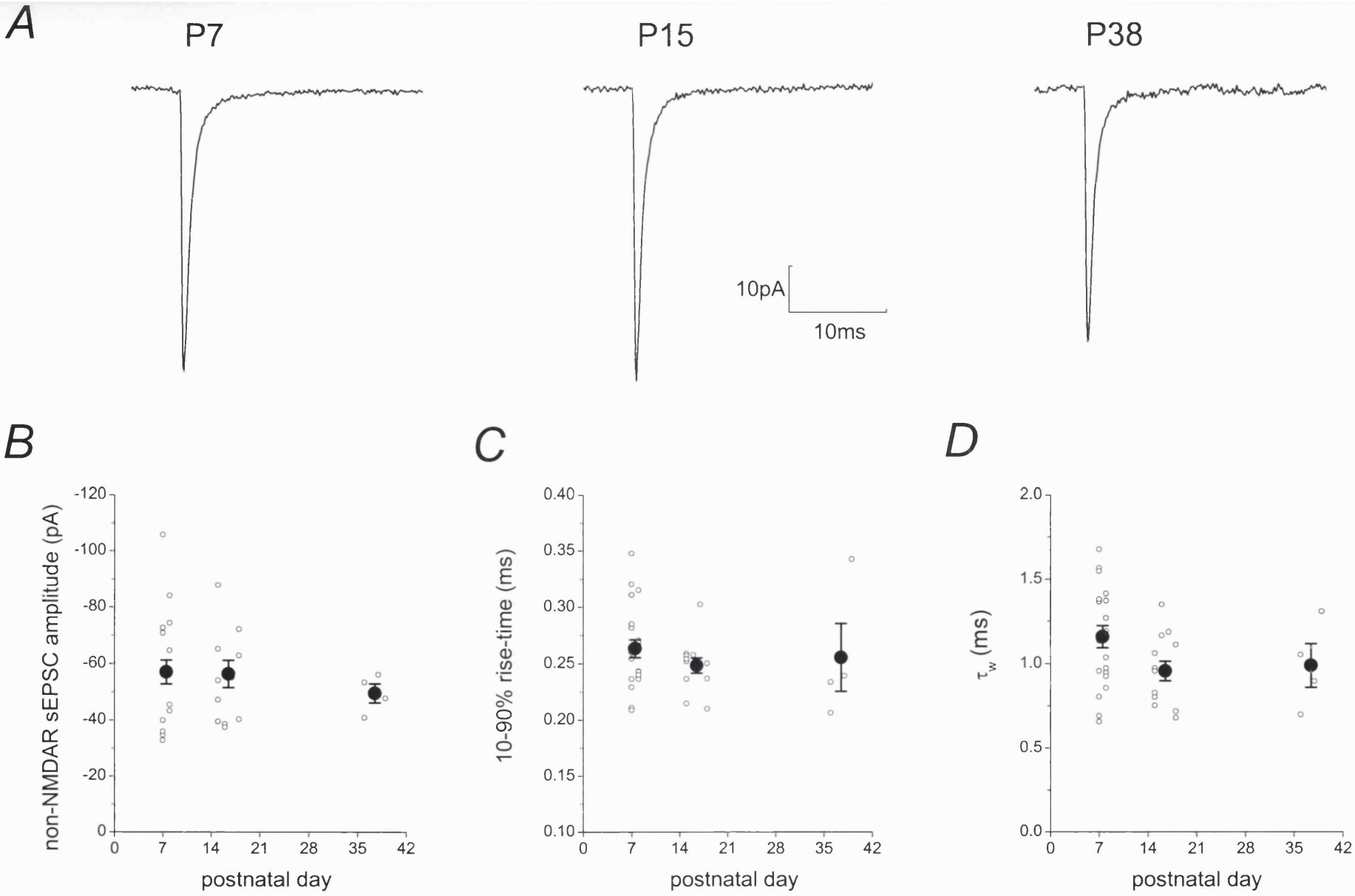
A
P7
P15
P38
10pA
10ms
B
non-NMDAR sEPSC amplitude (pA)
-120
-100
-80
-60
-40
-20
0
0
7
14
21
28
35
42
postnatal day
C
10-90% rise-time (ms)
0.40
0.35
0.30
0.25
0.20
0.15
0.10
postnatal day
D
τ_w (ms)
2.0
1.5
1.0
0.5
0.0
postnatal day

Table 3.1 *Properties of sEPSCs at three ages*

		P7-8	P15-18	P36-39
NMDAR-EPSC amplitude[a] (pA)		-5.96 ± 0.45 (22)* †	-4.64 ± 0.75 (22)* †	-2.61 ± 0.56 (5)*
NMDAR decay kinetics	τ_{fast} (ms)	30.9 ± 5.5 (22)		Not determined
	τ_{slow} (ms)	123.2 ± 10.9		
	A_{fast} (%)	50.4 ± 6.0		
	τ_w or τ (ms)	70.4 ± 4.3**	44.9 ± 5.0 (13)**	
non-NMDAR EPSC peak amplitude (pA)		-57.01 ± 4.20 (21)	-57.43 ± 4.30 (15)	-49.51 ± 3.37 (4)
non-NMDAR decay kinetics	τ_{fast} (ms)	0.93 ± 0.06 (21)	0.74 ± 0.04 (15)	0.84 ± 0.14 (4)
	τ_{slow} (ms)	8.10 ± 1.49	6.00 ± 1.57	3.94 ± 0.95
	A_{fast} (%)	94.2 ± 1.0	77.4 ± 7.7	93.2 ± 2.5
	τ_w (ms)	1.16 ± 0.06	0.99 ± 0.06	0.98 ± 0.13
non-NMDAR 10-90% rise time (μs)		263 ± 8 (21)	249 ± 8 (15)	255 ± 30 (4)

Cells were voltage-clamped at -80mV.

Mean values ± S.E.M. (number of cells)

[a], measured at 10ms after non-NMDAR peak, average of 2ms

†, $p < 0.05$, Mann-Whitney U

*, $p = 0.01$, one-way ANOVA

**, $p < 0.0005$, Mann-Whitney U

3.3.3 *Parallel fibre-evoked EPSCs*

Although Golgi cells receive inputs from both mossy- and parallel fibres (see sections 1.10.3 and 1.10.4), mossy fibres are severed in the slice preparation and the sEPSCs recorded most likely reflect release from parallel fibres (Dieudonné, 1998). To study the parallel fibre to Golgi cell synapse in isolation, we further examined EPSCs generated by stimulation in the molecular layer. The mossy fibre to Golgi cell synapse could not be studied in isolation as stimulation within the internal granule cell layer resulted in a complex response (see Misra *et al*, 2000a). The combination of direct mossy fibre activation and indirect activation of parallel fibres via excitation of granule cells led to poly-synaptic responses that were not amenable to analysis.

3.3.3.1 *Comparison of evoked EPSCs at P7-8 and P15-18*

We used a 'minimal' level of focal stimulation which generated evoked EPSCs with a fast monophasic rise (indicating synchronous release) and a failure rate of less than 10%. This intensity was typically 5V above threshold. Events with a multiphasic rise or multiple (non-NMDAR) peaks were not included in the analysis. The amplitude of the NMDAR component of evoked EPSCs was measured at 20ms after the non-NMDAR peak and the decay time-course was fitted from 20ms after the non-NMDAR peak (as opposed to the 10ms previously used for sEPSCs).

The amplitude of parallel fibre-evoked synaptic currents is dependent on the number of fibres activated (Carter and Regehr, 2000), so comparing absolute values could be misleading. If one increased the number of parallel fibres

activated, either by increasing the stimulation intensity or by using a stimulation electrode with a tip of greater diameter, the magnitude of both the non-NMDAR and NMDAR components were increased (Figure 3.7A and B). However, the ratio of the NMDAR to non-NMDAR current amplitude remained unchanged (Figure 3.7C). One could therefore use this ratio for comparison of the NMDAR-mediated current magnitude between the age groups. Because the non-NMDAR component of sEPSCs did not change with age (section 3.3.2), any change in the NMDAR:non-NMDAR amplitude ratio of evoked currents would indicate a change in the size of the NMDAR component. The NMDAR to non-NMDAR amplitude ratio was smaller at P15-18 (0.095 ± 0.01; NMDAR amplitude, -18.5 ± 1.8pA; non-NMDAR amplitude, -220.6 ± 14.2pA; n=58; Figure 3.8B) than at P7-8 (0.13 ± 0.01; NMDAR amplitude, -22.0 ± 3.4pA; non-NMDAR amplitude, -155.4 ± 15.5pA; n=27; p = 0.01, Mann-Whitney U). This is comparable to the change in NMDAR-sEPSC amplitudes between the two ages (evoked EPSCs, %decrease = 26.9%; sEPSCs, %decrease = 22.1%; section 3.3.1.3).

As with spontaneous events, parallel fibre-evoked NMDAR-EPSCs became faster between P7-8 and P15-18 (Figure 3.8A and C). The currents were best fitted by two exponentials at both ages; the value of τ_w for the NMDAR-EPSCs was 110.3 ± 4.7ms (τ_{fast}, 59.2 ± 7.1ms; τ_{slow}, 311.0 ± 44.4ms; A_{fast}, 73.2 ± 3.9%; n=24) and 79.9 ± 3.2 (τ_{fast}, 40.2 ± 3.8ms; τ_{slow}, 163.3 ± 9.4ms; A_{fast}, 69.5 ± 3.5%; n=54) at P7-8 and P15-18, respectively. The values of τ_w, τ_{fast} and τ_{slow} were significantly different between the two age groups (τ_w, $p < 5x10^{-7}$, unpaired t test; τ_{fast}, p = 0.005, Mann-Whitney U; and τ_{slow}, $p < 0.001$, Mann-Whitney U). Fit-independent calculation of the mean decay time constant gave similar values (P7, 123.9 ± 5.6ms, n=8; P15, 75.6 ± 12.4, n=6).

Figure 3.7 *Stimulation conditions affect the amplitude of the non-NMDAR and NMDAR components of evoked EPSCs but not the ratio between the two components*

A, B, Increasing the stimulation intensity by 15V (above 'minimal' stimulation) generated larger EPSCs, for both non-NMDAR (*circles*) and NMDAR (*triangles*) components. Using a larger stimulation electrode and stimulating at 'minimal' stimulation intensity also increased the size of the evoked EPSC. This indicates that the amplitude of EPSCs is dependent on the number of afferent parallel fibres activated. The mean ± S.E.M. values (*filled*) are calculated from four P7-8 and four P15-18 recordings (*open*). *, #, $p < 0.05$ for both data sets, one-way ANOVA.

C, the ratio of NMDAR to non-NMDAR current amplitude was not significantly affected ($p > 0.3$, one-way ANOVA), indicating that using a higher intensity or a larger electrode produced parallel increases in the non-NMDAR and NMDAR components.

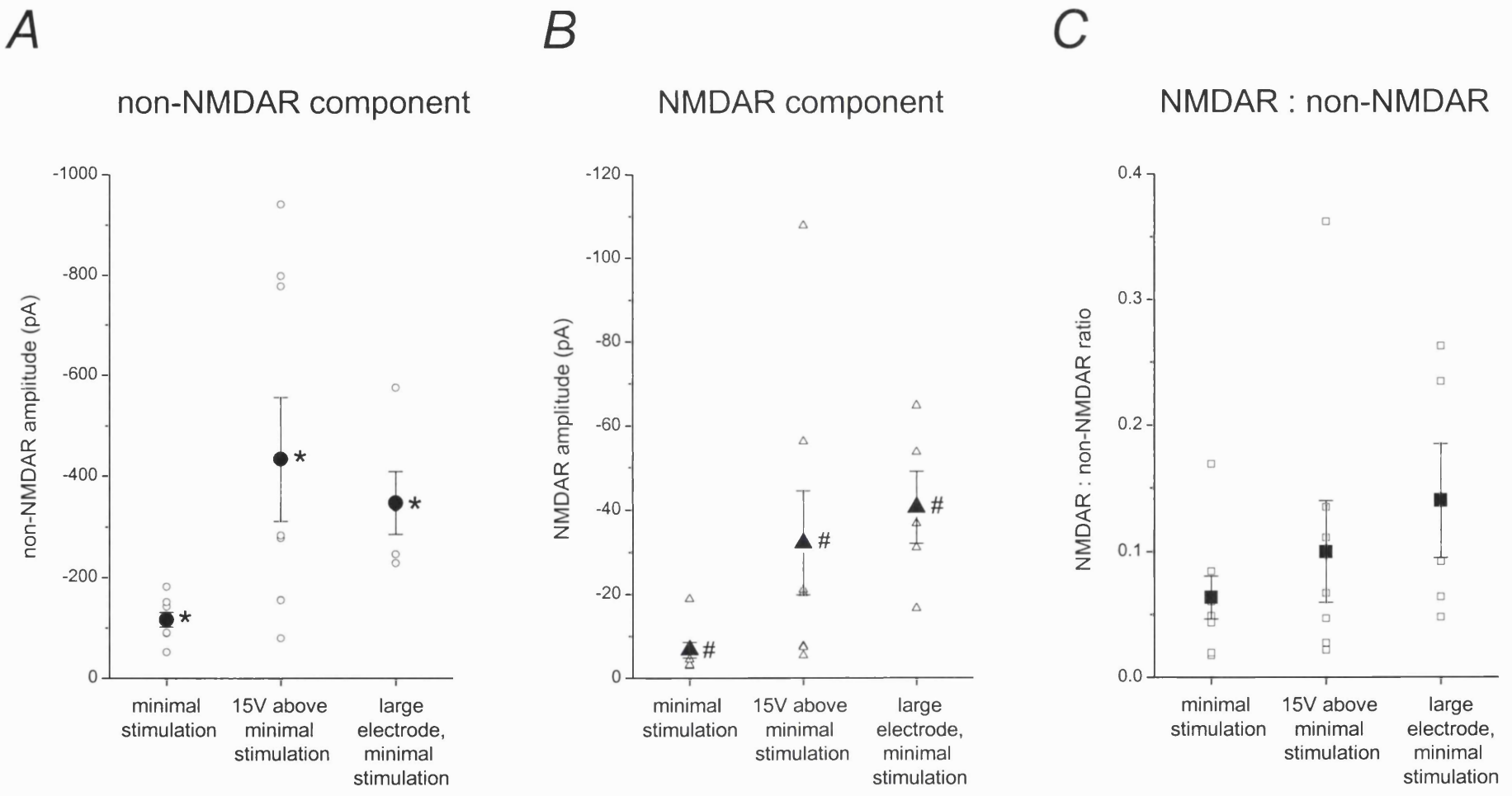
A
non-NMDAR component
non-NMDAR amplitude (pA)
-1000
-800
-600
-400
-200
0
*
*
*
minimal stimulation
15V above minimal stimulation
large electrode, minimal stimulation
B
NMDAR component
NMDAR amplitude (pA)
-120
-100
-80
-60
-40
-20
0
#
#
#
minimal stimulation
15V above minimal stimulation
large electrode, minimal stimulation
C
NMDAR : non-NMDAR
NMDAR : non-NMDAR ratio
0.4
0.3
0.2
0.1
0.0
minimal stimulation
15V above minimal stimulation
large electrode, minimal stimulation

Figure 3.8 *Parallel fibre-evoked EPSCs at P7-8 and at P15-18*

A, average EPSC waveforms recorded under control conditions (*black*) and in 50μM D-AP5 (*grey*). The panel on the left shows traces from a P7 Golgi cell, with the arrow indicating where the stimulation artefact has been removed. The decay phase of the NMDAR-mediated component was best described by the sum of two exponentials (described by τ_{fast} and τ_{slow}; inset), giving a weighted mean decay time constant (τ_w) in this example of 106.2ms. The panel on the right shows EPSCs recorded from a P15 Golgi cell. At this age, the decay time-course was also best fitted with the sum of two exponentials (inset), giving a τ_w of 60.1ms.
B, the ratio of the NMDAR to non-NMDAR EPSC amplitudes was smaller at P15-18 than at P7-8 (*, p = 0.01, Mann-Whitney U). The open circles represent measurements from individual cells; the filled circles denote the mean value ± S.E.M. plotted at the median age for each age group (P7-8, n=28; P15-18, n=58).
C, the decay time-course of parallel fibre-evoked NMDAR-EPSCs was significantly faster by P15-18 (n=54) compared with EPSCs at P7-8 (n=25; # $p < 5x10^{-7}$, unpaired t test).

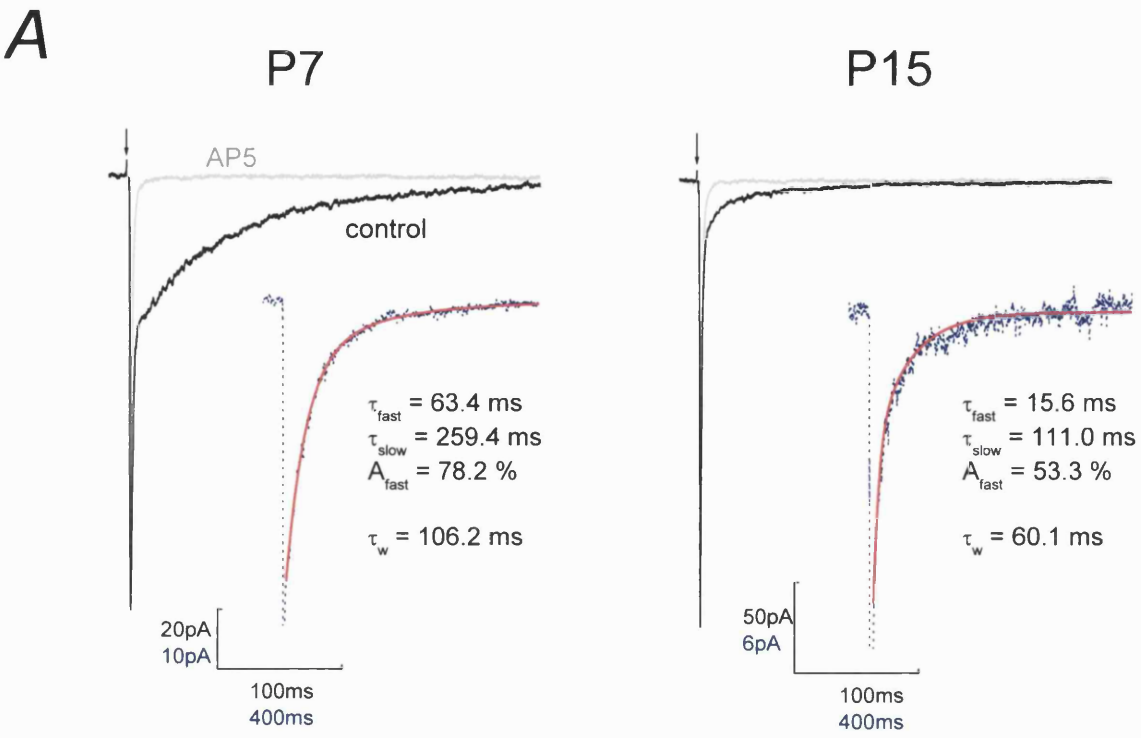
A
P7
P15
AP5
control
τfast = 63.4 ms
τslow = 259.4 ms
Afast = 78.2 %
τw = 106.2 ms
20pA
10pA
100ms
400ms
τfast = 15.6 ms
τslow = 111.0 ms
Afast = 53.3 %
τw = 60.1 ms
50pA
6pA
100ms
400ms

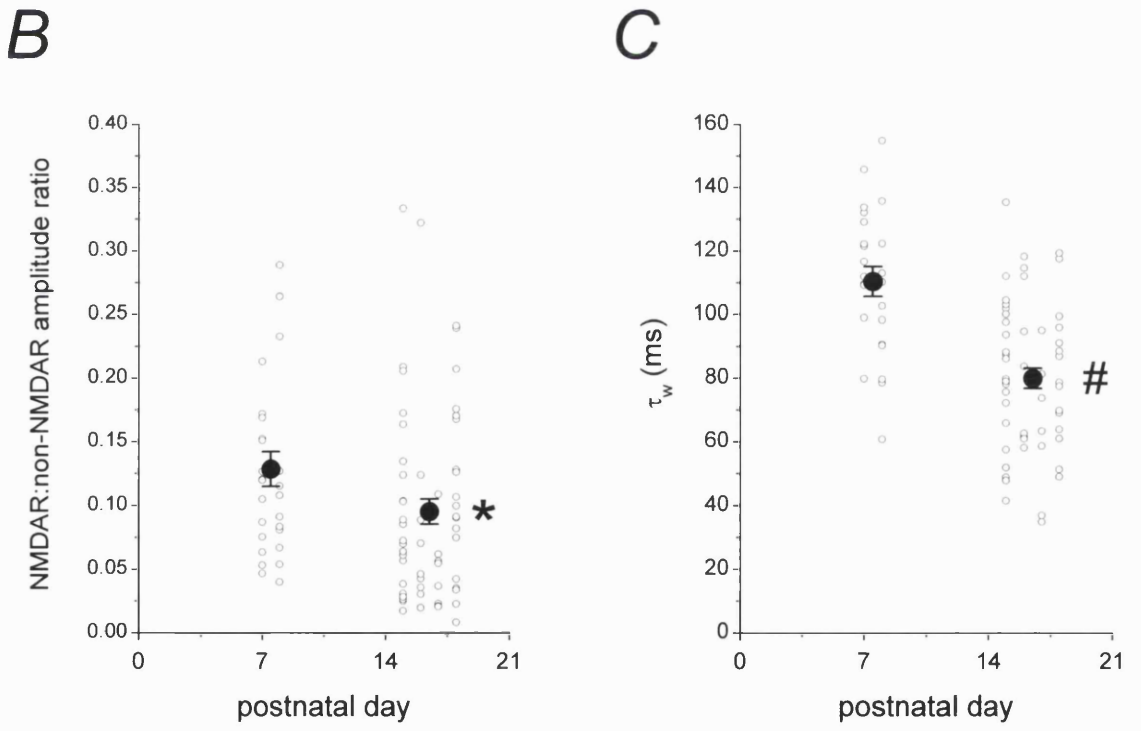
B
NMDAR:non-NMDAR amplitude ratio
0.40
0.35
0.30
0.25
0.20
0.15
0.10
0.05
0.00
0
7
14
21
postnatal day
*
C
τw (ms)
160
140
120
100
80
60
40
20
0
0
7
14
21
postnatal day
#

The decay time of evoked EPSCs was slower than that of sEPSCs at both ages (Table 3.3). Golgi cell sEPSCs are likely to be quantal events (Dieudonné, 1998; also see section 5.3.2.2) and stimulation of parallel fibres is likely to result in multi-vesicular release or activation of several synapses since evoked non-NMDAR EPSCs are ~3 times the size of non-NMDAR-sEPSCs. The slower decay of evoked EPSCs is likely to reflect the prolonged glutamate profile in the synapse following multivesicular release at a single synapse or overlap of activation at multiple synapses.

3.3.4 *Developmental changes in pharmacological properties*

What is the molecular mechanism underlying the shortening of NMDAR synaptic currents during development of the Golgi cell? One possibility is a change in the subunits making up the NMDAR assembly. Recombinant studies have shown that currents through NR1/NR2A NMDARs have faster decay times compared with NR1/NR2B receptor currents (Monyer *et al*, 1994; Table 1.1). The idea of a developmentally regulated switch in subunit composition, from mainly NR2B(ε2)-containing NMDARs to a larger proportion of NR2A(ε1)-containing ones, could explain the acceleration in decay kinetics observed between P7-8 and P15-18.

To investigate this possibility, we used two pharmacological agents, ifenprodil and TPEN, to identify the presence of NR2B and NR2A, respectively. Ifenprodil is an atypical non-competitive antagonist selective for NR1/NR2B receptors (Williams, 1993). The Zn^{2+} chelator TPEN potentiates currents through NR2A-

containing receptors by relieving a high-affinity tonic inhibition by Zn^{2+} (Paoletti *et al*, 1997; Traynelis *et al*, 1998).

3.3.4.1 *Effects of ifenprodil and TPEN on NMDAR-mediated sEPSCs*

The NR2B-selective antagonist ifenprodil (10μM) significantly inhibited sEPSCs by 65.3 ± 2.4% in P7-8 recordings (n=4; $p < 0.05$, Wilcoxon matched-pairs; Figure 3.9). A week later in development (P15-18), ifenprodil at the same concentration inhibited synaptic currents by only 21.6 ± 3.5% (n=6; $p < 0.05$, Wilcoxon matched-pairs). The statistically significant decrease in ifenprodil sensitivity between P7-8 and P15-18 ($p = 0.01$, Mann-Whitney U) is in accordance with the idea that a decrease in NR2B expression underlies the shortening of synaptic currents.

At both P7-8 and P15-18, NMDAR sEPSCs were significantly potentiated by 1μM TPEN (P7-8, 31.5 ± 6.6%, n=11; $p < 0.05$, Wilcoxon's matched pairs; P15-18, 109.1 ± 59.8%, n=7; $p < 0.01$, Wilcoxon's matched pairs; Figure 3.9B). The increase in TPEN sensitivity between the two age groups was significant ($p < 0.02$, Mann-Whitney U), consistent with the idea of an increase in the contribution of NR2A to synaptic NMDARs in Golgi cells. As neither ifenprodil nor TPEN affected the sEPSC frequency or the non-NMDAR peak amplitude (Table 3.2), the effects observed on the NMDAR-mediated current most likely reflect direct action on postsynaptic receptors rather than presynaptic manipulation (e.g. by inhibition of voltage-gated Ca^{2+} channels; Church *et al*, 1994).

3.3.4.2 *Pharmacological properties of parallel fibre-evoked EPSCs*

Ifenprodil and TPEN had similar effects on parallel fibre-evoked EPSCs as on sEPSCs (Figure 3.10). The sensitivity to ifenprodil (10μM) decreased from 76.7 ± 4.6% to 17.7 ± 4.6% between P7-8 and P15-18 (n=8 and n=9, respectively; $p <$ 0.001, Mann-Whitney U). TPEN (1μM) had a greater effect on evoked EPSCs recorded from older animals, potentiating currents by 38.4 ± 19.2% at P7-8 (n=6) and by 141.6 ± 68.1% at P15-18 (n=4; $p < 0.05$, Mann-Whitney U). The actions of TPEN and ifenprodil on evoked EPSCs are also likely to be postsynaptic as neither drug affected the peak amplitude of the non-NMDAR component (Table 3.2).

Taken together, the pharmacology is consistent with a relative decrease in NR2B expression and an increase in NR2A contribution to NMDARs at Golgi cell synapses. In support of this, the reduction in NR2B expression correlated with the acceleration in the decay time of synaptic currents at the parallel fibre to Golgi cell synapse (Figure 3.11; Spearman $R = 0.68$; $p < 0.005$). Because the amplitude of the NMDAR component did not increase with age (see sections 3.2.1.3 and 3.2.4.1), NR2A-containing receptors are likely to be replacing NR2B ones at Golgi cell synapses between P7 and P15. A comparison of decay and pharmacological properties of sEPSCs and evoked EPSCs is shown in Table 3.3.

Figure 3.9 *Effects of TPEN and ifenprodil on NMDAR sEPSCs*

A, effect of 10μM ifenprodil (*blue*) on NMDAR sEPSCs from a P8 (*top left*) and from a P15 (*bottom left*) Golgi cell. Ifenprodil significantly inhibited NMDAR currents at both ages. However, the level of inhibition was higher at P7-8 (n=4) than at P15-18 (n=6; $p = 0.01$, Mann-Whitney U).

B, effect of 1μM TPEN (*red*) on NMDAR sEPSCs from a P8 (*top left*) and from a P18 (*bottom left*) Golgi cell. On average, TPEN potentiated sEPSCs at both P7-8 (n=11) and P15-18 (n=7), but the degree of potentiation was significantly greater at P15-18 ($p < 0.02$, Mann-Whitney U).

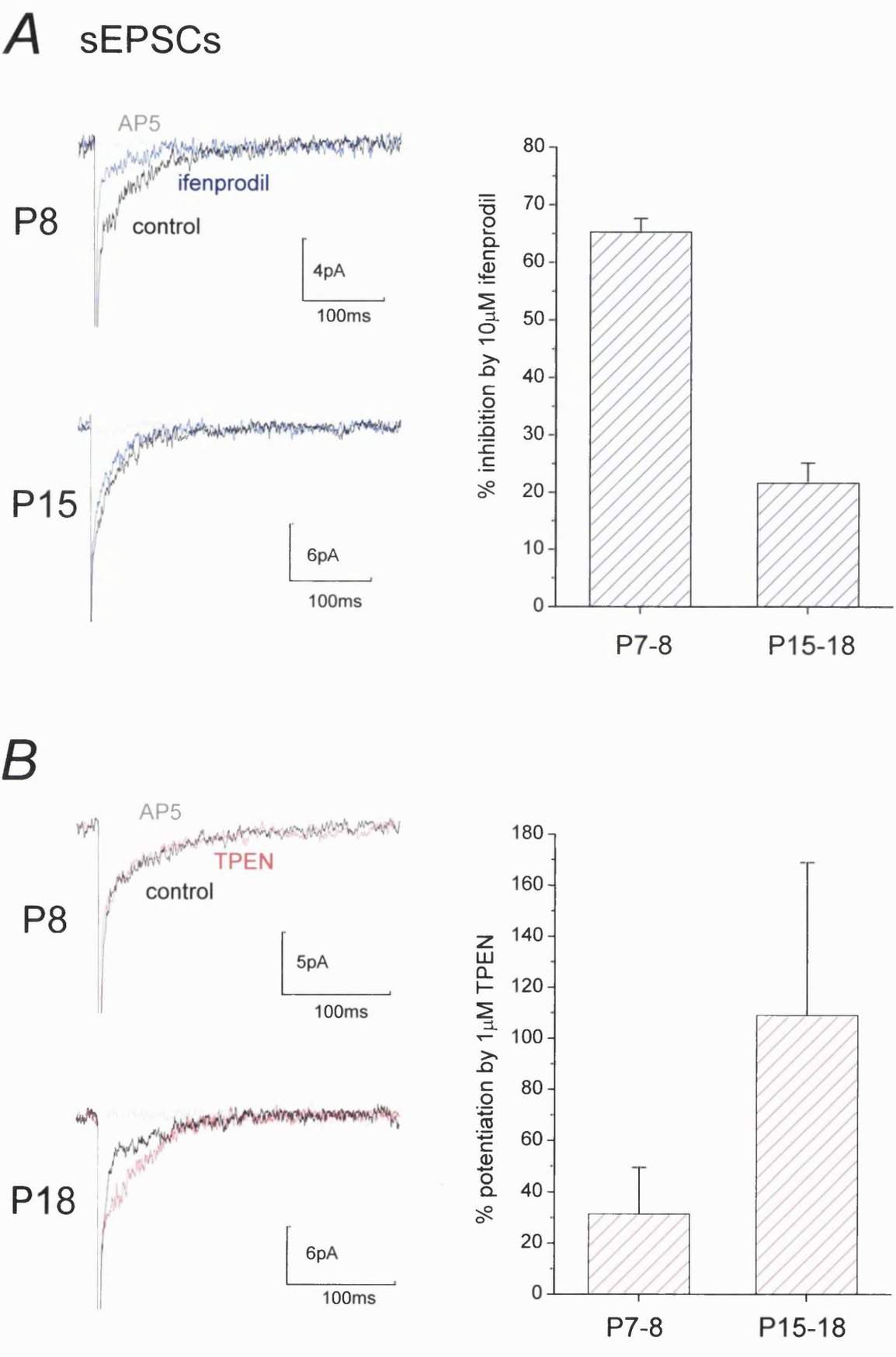
A
sEPSCs
AP5
ifenprodil
control
P8
4pA
100ms
P15
6pA
100ms
% inhibition by 10μM ifenprodil
80
70
60
50
40
30
20
10
0
P7-8
P15-18
B
AP5
TPEN
control
P8
5pA
100ms
P18
6pA
100ms
% potentiation by 1μM TPEN
180
160
140
120
100
80
60
40
20
0
P7-8
P15-18

Table 3.2 *TPEN and ifenprodil had no effects on the sEPSC frequency or the non-NMDAR sEPSC peak amplitude at both ages.*

		control	TPEN (1μM)	ifenprodil (10μM)
P7-8	sEPSC frequency (Hz)	0.22 ± 0.03 (15)	0.21 ± 0.02 (11)	0.20 ± 0.02 (4)
	Non-NMDAR sEPSC peak (pA)	-64.0 ± 4.4 (15)	-72.7 ± 7.2 (11)	-69.6 ± 4.6 (4)
	Non-NMDAR eEPSC peak (pA)	-179.2 ± 23.6 (14)	-148.5 ± 26.5 (6)	-199.3 ± 45.7 (8)
P15-18	sEPSC frequency (Hz)	0.18 ± 0.02 (13)	0.15 ± 0.02 (7)	0.17 ± 0.02 (6)
	Non-NMDAR sEPSC peak (pA)	-71.0 ± 5.5 (13)	-59.0 ± 6.4 (7)	-71.7 ± 7.1 (6)
	Non-NMDAR eEPSC peak (pA)	-190.6 ± 23.4 (13)	-223.2 ± 22.6 (4)	-222.8 ± 31.0 (9)

Mean values ± S.E.M. (number of cells).

sEPSC, spontaneous EPSC

eEPSC, parallel fibre-evoked EPSC

No statistical significance for each parameter between control and TPEN, and between control and ifenprodil ($0.1 < p < 0.7$, Wilcoxon's matched pairs).

3.3.4.3 *Are triheteromeric NR1/NR2A/NR2B receptors present at these synapses?*

An increase in NR2A expression at Golgi cell synapses could occur in the form of diheteromeric NR1/NR2A receptors or as triheteromeric NR1/NR2A/NR2B ones (Tovar and Westbrook, 1999). In the previous section, we used the Zn^{2+}-chelator TPEN and the antagonist ifenprodil to test for NR2A and NR2B expression, respectively. If NR2A- and NR2B-receptors are distinct diheteromeric populations, the sensitivities to TPEN and to ifenprodil should be independent of each other. We decided to test if synaptic NMDARs at Golgi cell synapses are indeed a mixed population of diheteromeric NR2A- and NR2B-receptors, by examining whether the ifenprodil sensitivity of NMDAR-EPSCs was affected by TPEN.

If NMDARs at P15-18 Golgi cell synapses are a mixed population of diheteromeric NR1/NR2A and NR1/NR2B receptors, the *absolute* amount of ifenprodil-sensitive current should not be affected by the presence of TPEN. However, at this age, the amplitude of NMDAR-EPSCs was larger in TPEN compared with control. Therefore, the *fractional* ifenprodil inhibition was expected to be lower in the presence of TPEN (ifenprodil-sensitive current divided by current in TPEN) than in the absence of TPEN (ifenprodil-sensitive current divided by control current). In contrast, TPEN had little effect on NMDAR-EPSCs at P7. The ifenprodil sensitivity of synaptic currents at this age was therefore expected to be independent of TPEN.

Our experiments showed that, at P7, the ifenprodil sensitivities of both sEPSCs and evoked EPSCs were independent of TPEN. The level of ifenprodil inhibition was 70% under both sets of conditions (Table 3.4; sEPSCs, $p > 0.3$; evoked

EPSCs, $p > 0.8$, Mann-Whitney U), consistent with the expression of mainly NR1/NR2B receptors (Williams, 1993). For both spontaneous and evoked EPSCs at P15, the percentage inhibition by ifenprodil was 10-20% in the absence of TPEN. However, the percentage inhibition was *greater* in the presence of TPEN, averaging between 40-45%. This difference in ifenprodil sensitivity between the two conditions was significant (sEPSCs, $p < 0.05$; evoked EPSCs, $p < 0.02$, Mann-Whitney U).

Figure 3.10 *Pharmacological properties of parallel fibre-evoked EPSCs at P7-8 and P15-18*

A, ifenprodil (10μM; *blue*) had a greater effect on evoked EPSCs at P7 (*top left*) than at P15 (*bottom left*). The inhibition by ifenprodil was significantly different between the two age groups (P7-8, n=7; P15-18, n=9; $p < 0.001$, Mann-Whitney U).

B, in contrast, TPEN (1μM; *red*) had a greater effect on the average NMDAR evoked EPSC recorded from a P15 Golgi cell ($p < 0.05$, Mann-Whitney U). The bar chart shows a summary of the TPEN sensitivity for 6 cells at P7-8 and 4 cells at P15-18.

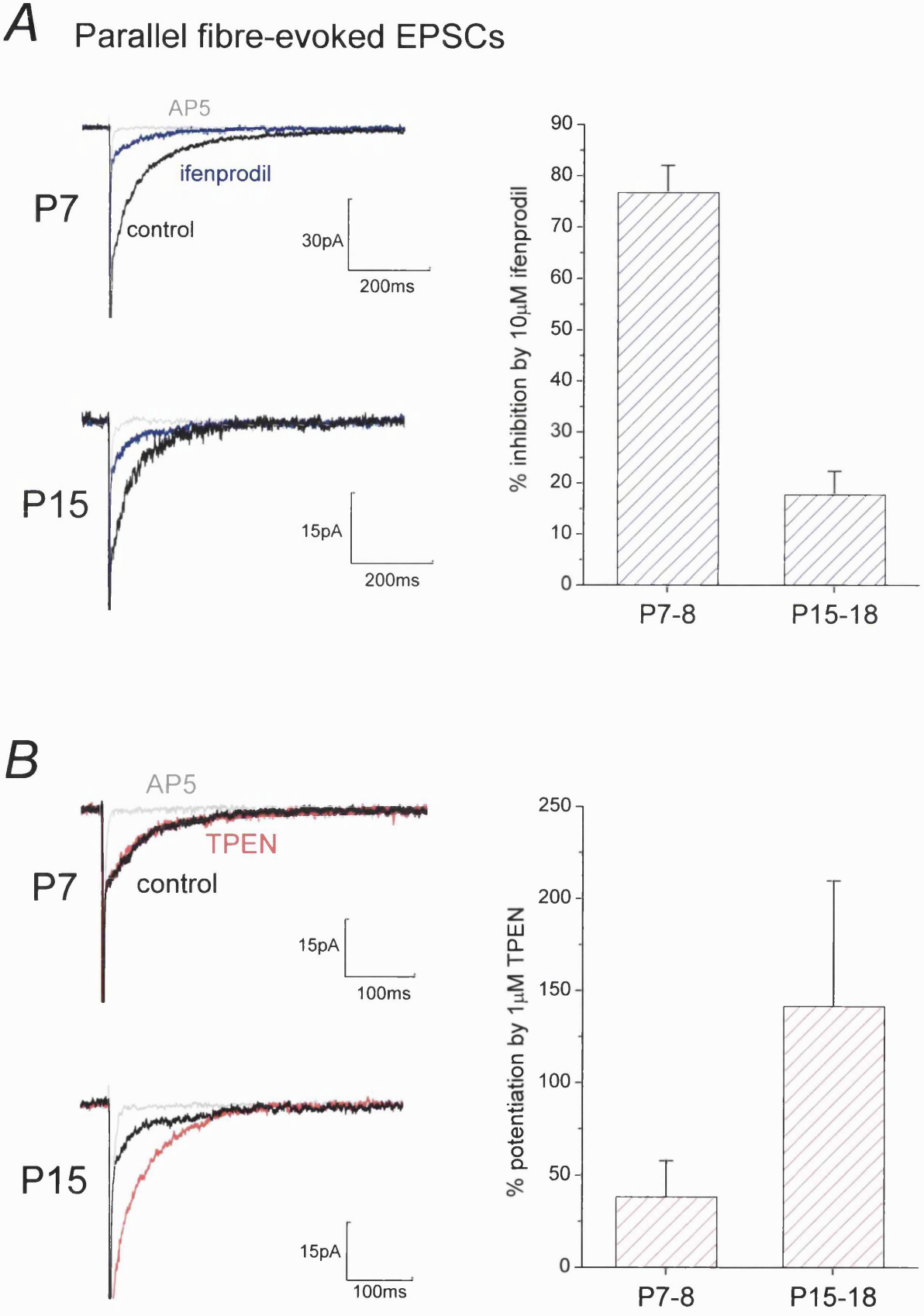
A
Parallel fibre-evoked EPSCs
AP5
ifenprodil
P7
control
30pA
200ms
P15
15pA
200ms
% inhibition by 10μM ifenprodil
90
80
70
60
50
40
30
20
10
0
P7-8
P15-18
B
AP5
TPEN
P7
control
15pA
100ms
P15
15pA
100ms
% potentiation by 1μM TPEN
250
200
150
100
50
0
P7-8
P15-18

Figure 3.11 *Slower decay kinetics are correlated with higher ifenprodil sensitivity*

A, *top*, evoked EPSCs from a P7 Golgi cell showing the decay kinetics (*left*) and the inhibition by ifenprodil (10μM; *right*, *blue*). EPSCs under control conditions and in the presence of 10μM ifenprodil from a P17 Golgi cell are shown (bottom panels).

B, grouping all data from evoked EPSC recordings of P7-8 and P15-18 cells, there was a significant positive correlation between lower ifenprodil sensitivity and faster EPSC decay kinetics (*red*, linear regression $R = 0.69$, $p < 0.005$). This indicates that lower NR2B expression is correlated with the shortening of EPSCs observed at the parallel fibre to Golgi cell synapse during development.

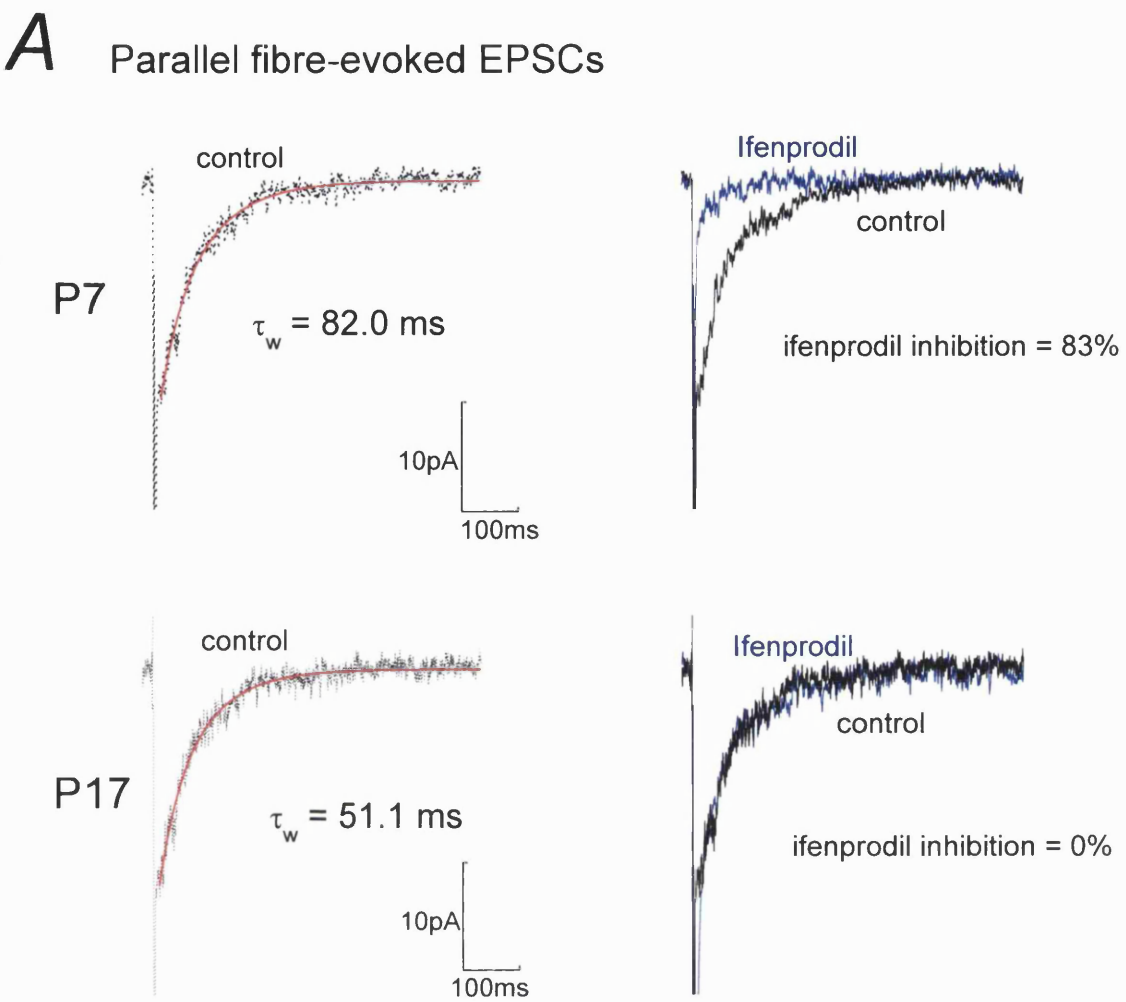
A
Parallel fibre-evoked EPSCs
control
P7
τ_w = 82.0 ms
10pA
100ms
Ifenprodil
control
ifenprodil inhibition = 83%
control
P17
τ_w = 51.1 ms
10pA
100ms
Ifenprodil
control
ifenprodil inhibition = 0%

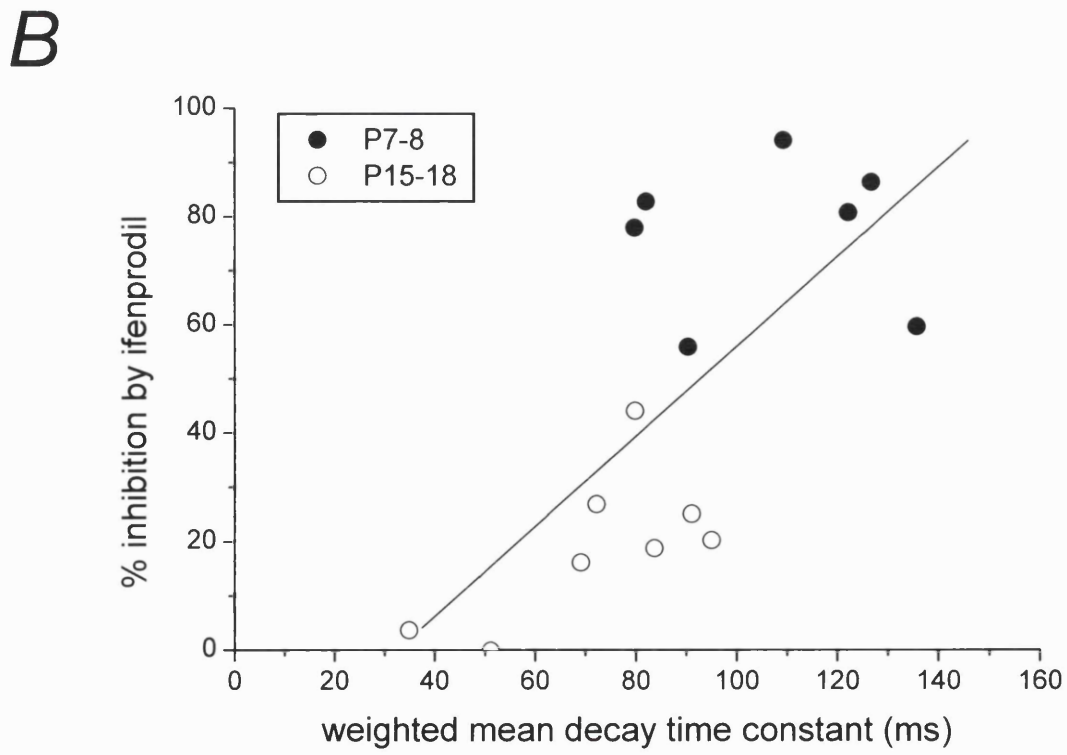
B
P7-8
P15-18
% inhibition by ifenprodil
weighted mean decay time constant (ms)
0
20
40
60
80
100
120
140
160

Table 3.3 *Comparison the properties of NMDAR-mediated sEPSC and parallel fibre-evoked EPSC*

			Spontaneous EPSCs	**Parallel fibre - evoked EPSCs**
P7-8	Amplitude (pA)	Non-NMDAR	-64.0 ± 4.4 (22)	-162.2 ± 16.6 (25)
		NMDAR	-6.0 ± 0.5	-16.9 ± 2.7
	Decay kinetics	τ_{fast} (ms)	30.9 ± 5.5 (22)	59.2 ± 7.1 (25)
		τ_{slow} (ms)	123.2 ± 10.9	311.0 ± 44.4
		A_{fast} (%)	50.4 ± 6.0	73.2 ± 3.9
		τ_w (ms)	70.4 ± 4.3 *	110.3 ± 4.7 *
	% Inhibition by ifenprodil		65.3 ± 2.4 (4)	73.2 ± 5.1 (6)
	% Potentiation by TPEN		31.5 ± 17.9 (11)	38.4 ± 19.2 (7)
P15-18	Amplitude (pA)	Non-NMDAR	-71.0 ± 5.5 (22)	-220.6 ± 14.2 (58)
		NMDAR	-4.8 ± 0.7	-18.5 ± 1.8
	Decay kinetics	τ_{fast} (ms)		40.2 ± 7.1
		τ_{slow} (ms)		163.3 ± 9.4
		A_{fast} (%)		69.5 ± 3.5
		τ_w (ms)	44.9 ± 5.0 (13) #	79.9 ±3.2 #
	% Inhibition by ifenprodil		21.6 ± 3.5 (6)	17.7 ± 4.6% (9)
	% Potentiation by TPEN		109.1 ± 59.8 (7)	141.6 ± 68.1 (4)

Mean ± S.E.M. (number of cells)

*, $p < 5 \times 10^{-6}$, Mann-Whitney U

#, $p < 5 \times 10^{-5}$, Mann-Whitney U

Table 3.4 *Ifenprodil sensitivity of synaptic currents at P15-18 is greater in the presence of TPEN*

		Ifenprodil %inhibition compared with control	**Ifenprodil + TPEN** %inhibition compared with TPEN
P7-8	sEPSC	65.3 ± 2.4 (4)	71.2 ± 3.2 (11)
	eEPSC	73.2 ± 5.1 (6)	69.8 ± 5.6 (7)
P15-18	sEPSC	21.6 ± 3.5 (6)*	42.3 ± 7.9 (7)*
	eEPSC	17.7 ± 4.6 (9)**	44.1 ± 6.8 (4)**

Mean values ± S.E.M. (number of cells).

sEPSC, spontaneous EPSC

eEPSC, parallel fibre-evoked EPSC

*, $p<0.05$ (Mann-Whitney U)

**, $p<0.02$ (Mann-Whitney U)

3.4 Discussion

3.4.1 *Summary of results*

Glutamatergic synaptic currents recorded from cerebellar Golgi cells, whether spontaneously-occurring or parallel-fibre evoked, consisted of two components corresponding to the activation of non-NMDARs and NMDARs. The amplitude of the NMDAR-mediated EPSC declined with age. In the course of the second postnatal week (from P7 to P15), the decay time-course of the NMDAR-mediated synaptic currents became significantly faster. This was accompanied by a decrease in sensitivity to the NR2B-selective drug ifenprodil and an increase in the effect of the Zn^{2+} chelator TPEN which affects NR2A-containing NMDARs. By the fifth postnatal week (P36-39), the NMDAR-sEPSC amplitude was almost undetectable. In contrast, the amplitude, decay kinetics and rise-time of sEPSCs mediated by non-NMDARs remained unaltered during this period of Golgi cell development.

3.4.2 *Developmental change in subunit composition of synaptic NMDARs*

The simplest explanation for the observed kinetic and pharmacological changes in NMDAR-EPSC properties is a change in subunit composition of the synaptic NMDAR population. Recombinant NR1/NR2A receptors exhibit faster decay kinetics than NR1/NR2B, NR1/NR2C or NR1/NR2D (Monyer *et al*, 1994; Table 1.1). The high degree of inhibition by the NR2B-selective antagonist ifenprodil at P7-8, together with the slower decay kinetics at this age, indicates a predominant NR2B contribution. Although NR2C- and NR2D-receptors also exhibit slow

decay kinetics (Monyer *et al*, 1994), these receptors are not sensitive to ifenprodil (Williams, 1995; Mott *et al*, 1998). A week later in development (P15-18), the faster decay time-course, the lower sensitivity to ifenprodil and the higher sensitivity to TPEN is consistent with an increase in the role of NR2A at Golgi cell synapses.

Tovar and Westbrook (1999) suggested that the developmental increase in NR2A at hippocampal synapses is likely to be in the form of triheteromeric NR1/NR2A/NR2B receptors. If a mixture of diheteromeric NR1/NR2A and NR1/NR2B receptors is expressed, then the decay of the relief from ifenprodil block should be the same as for NR1/NR2B receptors alone. However, the authors found that the kinetics of the relief from ifenprodil block was different at 'mature' NR2A-containing synapses compared with 'immature' NR2B-only synapses. We tried a different approach (section 3.3.4.3), postulating that if diheteromeric NR1/NR2A and NR1/NR2B receptors predominated at P15-18 Golgi cell synapses, the *percentage* ifenprodil inhibition of EPSC amplitude would be greater in the absence of TPEN (i.e. ifenprodil-sensitive current divided by the control current) than in the presence of TPEN (i.e. ifenprodil-sensitive current divided by the control current and the TPEN-sensitive current). However, we found that ifenprodil sensitivity of EPSCs was *higher* in the presence of TPEN. Although ifenprodil and Zn^{2+} inhibition had been found to be independent of each other in the rat hippocampus and parietal cortex, negative or positive interactions were observed in other areas such as the piriform cortex and amygdala (Berger and Rebernik, 1999). So, it is possible that ifenprodil sensitivity is not independent of Zn^{2+} inhibition in NR1/NR2A or NR1/NR2A/NR2B receptors; i.e. that these receptors are more sensitive to ifenprodil when the Zn^{2+} inhibition is removed. Since both Zn^{2+} inhibition and ifenprodil inhibition are now thought to

act through a similar mechanism - by altering proton sensitivity of the NMDAR - there is a possibility of interactions (Mott *et al*, 1998; Choi and Lipton, 1999; Low *et al*, 2000; Zheng *et al*, 2001). It would be useful to find out whether recombinant NR1/NR2A or NR1/NR2A/NR2B receptors are more sensitive to ifenprodil in the absence of Zn^{2+}. Without knowing more about these interactions, it is difficult to interpret our results.

Evidence of a developmental switch from NR2B to NR2A has been presented for several synapses. After the cloning of the NR2 subunits, *in situ* hybridisation studies by Monyer *et al* (1994), Akazawa *et al* (1994) and Watanabe *et al* (1994) revealed developmental and spatial expression profiles for the four NR2 subunits in the rat and mouse brain. A developmentally-regulated acceleration in current decay kinetics has been described in rat superior colliculus neurons (Hestrin, 1992), rat visual cortical neurons (Carmignoto and Vicini, 1992; Stocca and Vicini, 1998), mouse hippocampal CA1 pyramidal cells (Kirson and Yaari, 1996), and cerebellar granule cells (Takahashi *et al*, 1996; Cathala *et al*, 2000). The shortening of NMDAR-EPSC duration has been correlated with an increase in the amount of NR2A mRNA present in the neuron (Flint *et al*, 1997; Plant *et al*, 1997; Quinlan *et al*, 1999). Furthermore, the change in decay kinetics appeared to be accompanied by a decrease in the sensitivity to NR2B-selective antagonists (Kirson and Yaari, 1996; Stocca and Vicini, 1998; Tovar and Westbrook, 1999). However, the NR2B to NR2A switch may not occur at all synapses. NMDAR-mediated synaptic currents in the central nucleus of the amygdala were recently reported to remain highly sensitive to ifenprodil in three- to four-week old rats (Lopez de Armentia and Sah, 2002). It is also of interest to note that the switch from NR2B to NR2A expression may be reversible (Philpot *et al*, 2001a).

Neuronal injury has been reported to prolong the duration of NMDAR-EPSCs and increase ifenprodil sensitivity in rat vagal motoneurons (Nabekura *et al*, 2002).

Are there alternative explanations for the shortening of NMDAR-EPSCs with age? Changes in presynaptic release or the profile of glutamate in the synapse can affect the decay kinetics of synaptic currents (see Conti and Weinberg, 1999). Release probability is unlikely to have changed as the paired-pulse ratio was the same between the two ages (see Table 4.2; 10ms interpulse interval, P7-8, 1.00 ± 0.24, n=6; P15-18, 1.12 ± 0.11, n = 9; $p > 0.8$, unpaired *t* test). Changes in synapse morphology, glutamate profile or presynaptic vesicle content between P7-8 and P15-18 could contribute to the change in decay kinetics, but the pharmacological data argue for a change in subunit composition. Although it has been reported that inhibition by ifenprodil is dependent on agonist NMDA concentration (Kew *et al*, 1996; Zhang *et al*, 2000), the observed decrease from 70% to 20% inhibition is substantial and is unlikely to be caused solely by a change in glutamate concentration at the synapse.

Another issue that needs to be considered is the possible change in the expression of NR1 splice variants. A developmental change in the alternative splicing of NR1 in the cerebellum has been shown (Laurie and Seeburg, 1994a; Prybylowski and Wolfe, 2000) but whether this take place specifically in the Golgi cell is unknown. Vicini *et al* (1998) investigated the effect of different NR1 splice variants on the decay kinetics of recombinant NR1/NR2A receptors and found that there were no significant differences in the average decay time of currents through receptors comprising different NR1 splice variants. In contrast to NR2A receptors, the deactivation of currents through NR2B receptors is dependent on the NR1 isoform expressed. Expression of NR1a (splice variant lacking exon 5) significantly

slowed the decay kinetics compared with NR1b (containing exon 5; τ_w = 750ms *vs* 200ms, respectively; Rumbaugh *et al*, 2000).

Also, NR1 splice variants have been shown to affect the sensitivity of recombinant NR1/NR2A receptors to Zn^{2+}. The IC_{50} for Zn^{2+} inhibition of NR1a/NR2A receptors is 0.02μM, while that for NR1b/NR2A is 0.2μM (Traynelis *et al*, 1998). Ifenprodil sensitivity, however, is unlikely to be affected by NR1 alternative splicing. The binding of ifenprodil was reported to be independent of NR1 isoform expression (Gallagher *et al*, 1996). Furthermore, Mott *et al* (1998) showed that the IC_{50} of CP-101,606 (a derivative of ifenprodil) inhibition on agonist-evoked currents was the same for NR1a/NR2B and NR1b/NR2B receptors. Although it cannot be ruled out that a change in NR1 isoform expression contributes to the developmental change in decay kinetics and TPEN sensitivity, the observed decrease in ifenprodil sensitivity at Golgi cell synapses argues for a developmental change in the NR2 subunit rather than a change in the NR1 isoform alone.

The reduction in ifenprodil sensitivity between P7-8 and P15-18 is also unlikely to reflect increased expression of NR2C or NR2D. The faster decay kinetics and increased sensitivity to TPEN at P15-18 argues for the expression of NR2A but we cannot rule out the possibility of triheteromeric NR1/NR2A/NR2C or NR1/NR2A/NR2D receptors.

3.4.3 *Functional relevance of developmental changes in subunit composition*

The NMDAR has attracted much attention because of its crucial role in development and plasticity. For example, genetically-manipulated mice have been extensively studied to investigate whether the disruption or enhancement of NR2 subunit expression has any consequences on synaptic plasticity, behaviour and learning and memory (Kadotani *et al*, 1996; Kiyama *et al*, 1998; Okabe *et al*, 1998; Sakimura *et al*, 1995; Tang *et al*, 1999; Philpot *et al*, 2001b). The developmentally-regulated shortening of synaptic currents and change in ifenprodil sensitivity in the visual system requires sensory information (Carmignoto and Vicini, 1992; Quinlan *et al*, 1999; Philpot *et al*, 2001a), and it was long hypothesized that this activity-dependent change in NMDAR current duration may act as a brake, regulating and limiting plasticity.

However, several lines of evidence now argue against this theory. Roberts and Ramoa (1999) showed that NR2A expression and faster decay kinetics at visual cortical neurons occurred at the onset, rather than at the end, of the critical period for ocular dominance plasticity. Barth and Malenka (2001) also demonstrated that the loss of LTP at thalamocortical synapses was not correlated with a change in the kinetics of NMDAR synaptic currents. Further evidence that the end of the critical period for LTP does not require changes in the duration of NMDAR currents was supplied by Lu *et al* (2001): analysis of NMDAR currents at thalamocortical synapses of NR2A knockout mice showed that, while the shortening of EPSC duration and reduction in ifenprodil sensitivity was abolished, the critical period for LTP was unaffected. It appears from these studies that factors other than changes in the duration of NMDAR synaptic currents are responsible for abating LTP at these synapses.

Besides deactivation kinetics, changes in the NR2 subunit expressed will also affect the spatiotemporal profile of Ca^{2+} entry and the sensitivity and susceptibility of the receptor to various modulators. Recombinant receptors containing NR2A, NR2B or NR2C are differentially sensitive to redox conditions (Brimecombe *et al*, 1997). The activity of Ca^{2+}-sensitive enzymes linked to the NMDAR, such as CaMKII, may be affected. The potentiating effect of the endogenous Src kinase has been shown to be greater for NR1/NR2A than for receptors comprising NR2B, NR2C or NR2D (Köhr and Seeburg, 1996; Zheng *et al*, 1998). Tyrosine kinases and phosphatases, via PSD proteins, are also thought to regulate the properties of NMDARs (Wang and Salter, 1994; Wang *et al*, 1994; Vissel *et al*, 2001), and there are indications that tyrosine phosphorylation may be involved in LTP (O'Dell *et al*, 1991; Grant *et al*, 1992; Lu *et al*, 1998). Therefore, developmental changes in NMDAR subunit composition can affect a myriad of events downstream of receptor opening.

NMDAR receptors were recently reported to control the EPSP-spike coupling in hippocampal interneurons, thereby affecting the temporal properties of feedforward inhibition onto pyramidal cells (Maccaferri and Dingledine, 2002). 'Slow' interneurons, with a large and slowly-decaying NMDAR-mediated component, had slow EPSP-spike latencies and action potential firing in these cells could either precede or follow firing in simultaneously-activated pyramidal cells. On the other hand, 'fast' interneurons with a smaller and faster-decaying NMDAR component always fired action potentials before the pyramidal cells. The authors speculated that the differences in NMDAR decay kinetics between the two 'cell types' may reflect differences in subunit composition. Furthermore, Lei and McBain (2002) showed that hippocampal interneuron synapses with fast-decaying and ifenprodil-insensitive NMDAR components fired doublet or triplet

EPSPs when stimulated with a train of afferent stimuli. However, at those synapses where NMDARs were more ifenprodil sensitive and exhibited slower decay kinetics, the same stimulation protocol only generated single or doublet EPSPs. So it is possible that subunit changes in NMDAR composition during development affect the firing properties of neurons and thereby influence the activity in a neural network.

CHAPTER 4

COMPARISON OF SYNAPTIC AND EXTRASYNAPTIC NMDARs AT THE PARALLEL FIBRE – GOLGI CELL SYNAPSE

4.1 Summary

1. Parallel fibre-evoked EPSCs generated by a single stimulus and by a train of 3 stimuli at 100Hz were recorded from mouse cerebellar Golgi cells at P7-8 and P15-18.

2. The decay kinetics of the NMDAR-mediated component of single EPSCs and a train of EPSCs were compared. At P7-8, the decay time of EPSCs generated by the two stimulation conditions were similar (single, 110.2 ± 7.6ms; train, 127.8 ± 6.7ms, respectively; n=9). However, at P15-18, EPSCs generated by a train of stimuli were consistently slower (160.1 ± 9.8ms; single stimulus, 81.3 ± 3.7ms; n=36).

3. At P15-18, NMDAR-EPSCs produced by a train of stimuli also exhibited greater ifenprodil sensitivity. Ifenprodil (10μM) inhibited single EPSCs by 20.5 ± 6.0% and a train of EPSCs by 60.6 ± 3.8% (n=7). In contrast, at P7-8, there was no difference in ifenprodil sensitivity (single, 76.8 ± 5.3%; train, 85.9 ± 4.6%; n=7).

4. The NMDAR open-channel blocker MK801 was used to block synaptic receptors activated by a single stimulus. At P15-18, high-frequency train stimulation after MK801 treatment generated NMDAR-mediated currents with an even higher sensitivity to ifenprodil inhibition (87.1 ± 3.7%, n=9).

5. The glutamate transporter blocker TBOA had no effect on the amplitude or the decay kinetics of NMDAR-mediated synaptic currents at P7-8. In older animals,

the effect of TBOA was more heterogeneous and more detrimental to cells. It appeared that TBOA may slow the decay kinetics of NMDAR-EPSCs in a subset of Golgi cells.

6. These results demonstrate that NMDARs of different subunit composition are differentially located at parallel fibre-Golgi cell synapses. At a developmental stage when NR2A-containing receptors are present at synaptic sites, NMDARs located in the periphery of these synapses remain of the NR2B-subtype.

4.2 Introduction

The experiments described in Chapter 3 demonstrated that currents through synaptic NMDARs at the parallel fibre-Golgi cell synapse undergo changes in their kinetic and pharmacological properties during development. Do extrasynaptic NMDARs have properties similar to those of synaptic receptors? Is the developmentally-regulated change in subunit composition confined to synaptic NMDARs or does it also occur at extrasynaptic sites? This chapter will explore the properties of NMDARs activated during brief high-frequency trains. Under these stimulation conditions, glutamate is likely to diffuse to the extrasynaptic- or perisynaptic space and therefore can activate receptors located there.

The properties of NMDAR-mediated currents generated at the parallel fibre to Golgi cell synapse by a single stimulus and a high-frequency train of stimuli were compared. The decay kinetics and sensitivity to ifenprodil inhibition were

considered. The comparison of single EPSCs and a train of EPSCs was carried out at the two ages studied in Chapter 3, namely at P7-8 and P15-18.

Next, the NMDAR open channel blocker MK801 was used to selectively block synaptic NMDARs activated by a single stimulus. On subsequent train stimulation, the current through synaptic NMDARs would be excluded from the train-generated EPSC. The kinetic and pharmacological properties of the remaining current through extrasynaptic receptors were examined. In the final part of this chapter, we tried inhibiting glutamate clearance as an alternative method of activating extrasynaptic receptors. The effect of the glutamate transporter inhibitor TBOA on NMDAR-mediated synaptic currents at the parallel fibre-Golgi cell synapse was explored.

4.3 Results

4.3.1 *Devising a stimulation protocol for activating extrasynaptic receptors*

In the experiments described in Chapter 3, we used a single stimulus under focal 'minimal' stimulation conditions to generate an EPSC. Under these conditions, mainly receptors located at synaptic sites are activated by the synaptically-released glutamate. In order to activate a larger proportion of extrasynaptic or perisynaptic receptors, one needs to increase the glutamate concentration or prolong the presence of glutamate at the synapse such that sufficient glutamate diffuses out of the synaptic cleft onto more distant sites. To activate extrasynaptic receptors, we applied a brief high-frequency train of stimuli.

Other means of activating extrasynaptic NMDARs that were considered included: (1) increasing the stimulus intensity, (2) increasing external Ca^{2+} concentration to increase release probability, and (3) blocking the neurotransmitter clearance mechanism. Since our aim was to compare the properties of synaptic and perisynaptic receptors, the former two alternatives were not considered suitable for the following reasons. Increasing stimulation intensity recruits more afferent fibres (Tóth and McBain, 1998; Carter and Regehr, 2000; Clark and Cull-Candy, 2002), thereby activating additional synapses. As we wanted to compare synaptic and extrasynaptic receptors, we needed to minimise the chance of activating additional synaptic receptors. Increasing the external Ca^{2+} concentration to promote release was equally unsuitable as it complicates any comparison of currents at different external Ca^{2+} concentrations. The single-channel conductance through NMDARs is dependent on the concentration of external Ca^{2+} (Jahr and

Stevens, 1987; Gibb and Colquhoun, 1992; Billups *et al*, 2002) and NMDARs are regulated by Ca^{2+}-dependent desensitisation and Ca^{2+}-dependent kinases and phosphatases (Clark *et al*, 1990; Legendre *et al*, 1993; Dingledine *et al*, 1999). We did attempt to manipulate glutamate clearance as an alternative way to activate extrasynaptic receptors (section 4.3.5). Using a glutamate transporter inhibitor, we examined if transporters are involved in shaping the synaptic current at these synapses.

The frequency of stimulation in a train of stimuli will affect the extent of neurotransmitter diffusion out of the synaptic cleft. Although we cannot exclude spillover of neurotransmitter onto neighbouring synapses, it seemed likely that diffusion out of the synaptic cleft would also activate extrasynaptic receptors. The current generated by a brief high-frequency train of stimuli is the sum of the current through synaptic and extrasynaptic receptors. Figure 4.1 illustrates the relationship between the stimulus frequency and the NMDAR-EPSC amplitude. In the presence of 50μM D-AP5, the non-NMDAR EPSCs generated by three pulses at 10Hz returned to baseline within 20ms of the final peak of the non-NMDAR current. Therefore, the amplitude of the NMDAR-mediated current was measured 20ms after the final non-NMDAR current peak (an average of 20 data points). Applying this criterion to all stimulation conditions, the amplitude of the NMDAR-mediated current produced by a three-stimuli 100Hz train was measured at 40ms after the final peak of the non-NMDAR EPSC. The prolonged non-NMDAR current is likely to reflect spillover and delayed release (Atluri and Regehr, 1998; Carter and Regehr, 2000; Kreitzer and Regehr, 2000). The decay of a train of EPSCs was fitted for 3 to 4 seconds from 40ms after the final non-NMDAR EPSC peak. Figure 4.1C compares the frequency dependence of a train

of NMDAR-EPSCs at P7-8 and P15-18. As is apparent from the plots, increasing the frequency of a train of three stimuli from 5- to 10Hz did not affect the amplitude of the NMDAR-mediated EPSC. Further increasing the frequency from 10 to 100Hz did increase the amplitude of the NMDAR-mediated current at both ages.

4.3.2 *Decay kinetics of a train of EPSCs at P7-8 and at P15-18*

As glutamate diffuses out of the synaptic cleft, it would be expected to activate receptors located peripheral to the synapse. Figure 4.2 compares the NMDAR-EPSC produced by a single stimulus with that produced by a brief train of stimuli. Typical traces recorded from a P8 and a P18 cell are shown in panel A. A train of stimuli (3 at 100Hz) generated currents that were approximately 3.5 times larger than those generated by a single stimulus. At P7-8, the 'train-to-single' ratio was 3.4 ± 0.5 (n=7). The ratio was similar at P15-18 (3.5 ± 0.3; n=33; $p > 0.5$, Mann-Whitney U).

Golgi cell sEPSCs are similar to miniature EPSCs and are therefore likely to be quantal events (Dieudonne, 1998; see section 5.3.2.2). We can roughly estimate how many quanta are released in response to single- and train stimulation. Values are summarised in Table 4.1. It was mentioned in Chapter 3 that some spillover is already likely to occur in response to a single stimulus as the decay of evoked NMDAR-EPSCs was slower than that of sEPSCs (section 3.3.3.1 and Table 3.3). At both P7-8 and P15-18 synapses, a train of 3 stimuli at 100Hz further increased the NMDAR current by ~10 quanta.

Figure 4.1 *Increasing the stimulation frequency from 10Hz to 100Hz increased the parallel fibre-evoked NMDAR-EPSC amplitude*

A, Recording of parallel fibre-evoked EPSCs generated by a train of 3 stimuli at 10Hz (*top*) and at 100Hz (*bottom*) from a P8 Golgi cell. The non-NMDAR EPSC, recorded in the presence of 50μM D-AP5, is shown in grey.

B, EPSCs in response to a train of 3 pulses at 10Hz (*top*) and 100Hz (*bottom*) from a P15 Golgi cell. The same scale bar also applies to traces in panel A.

C, the EPSC generated by 3 stimuli at 10Hz was the same in amplitude compared with single EPSCs. Increasing the frequency to 100Hz generates NMDAR-EPSCs which were about 3 times greater in amplitude than EPSCs produced by a single stimulus.

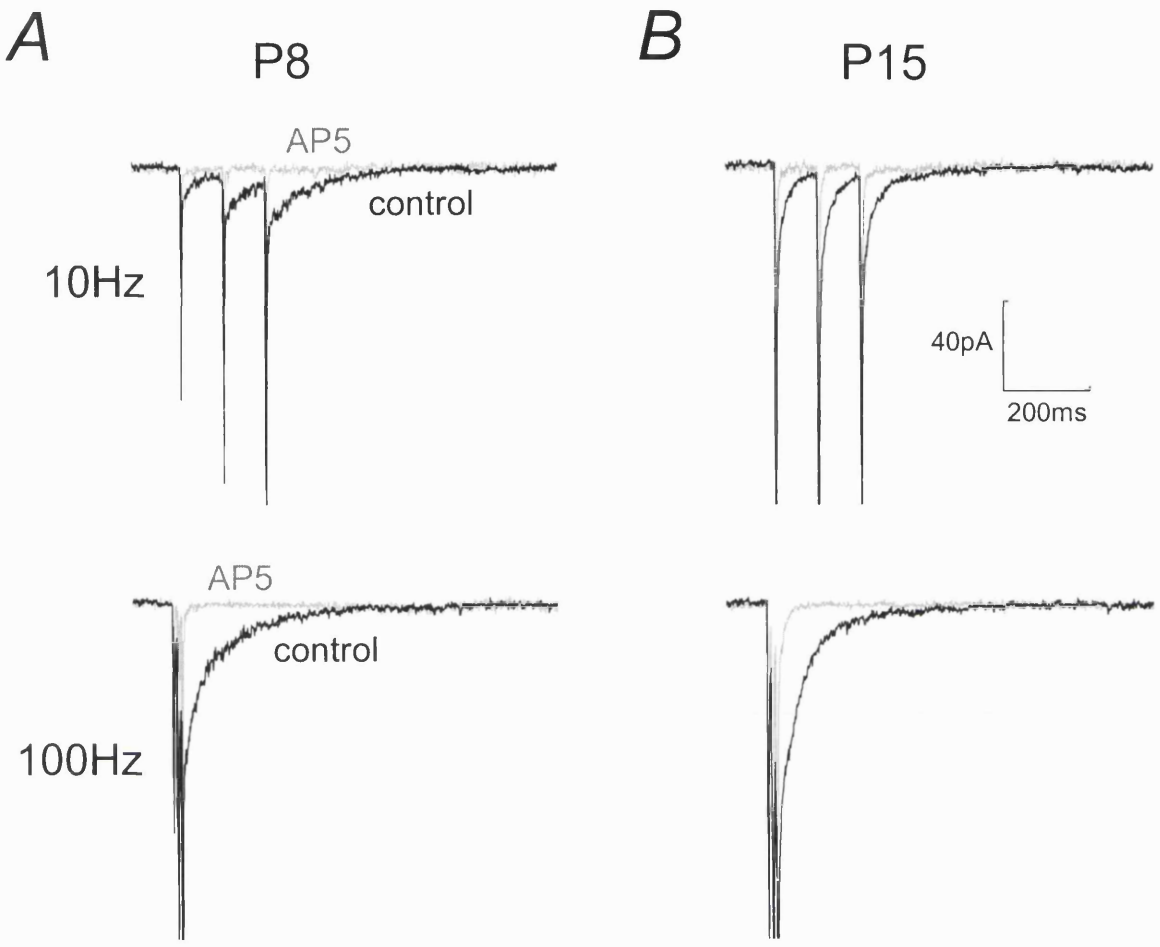
A
P8
B
P15
AP5
control
10Hz
40pA
200ms
AP5
control
100Hz

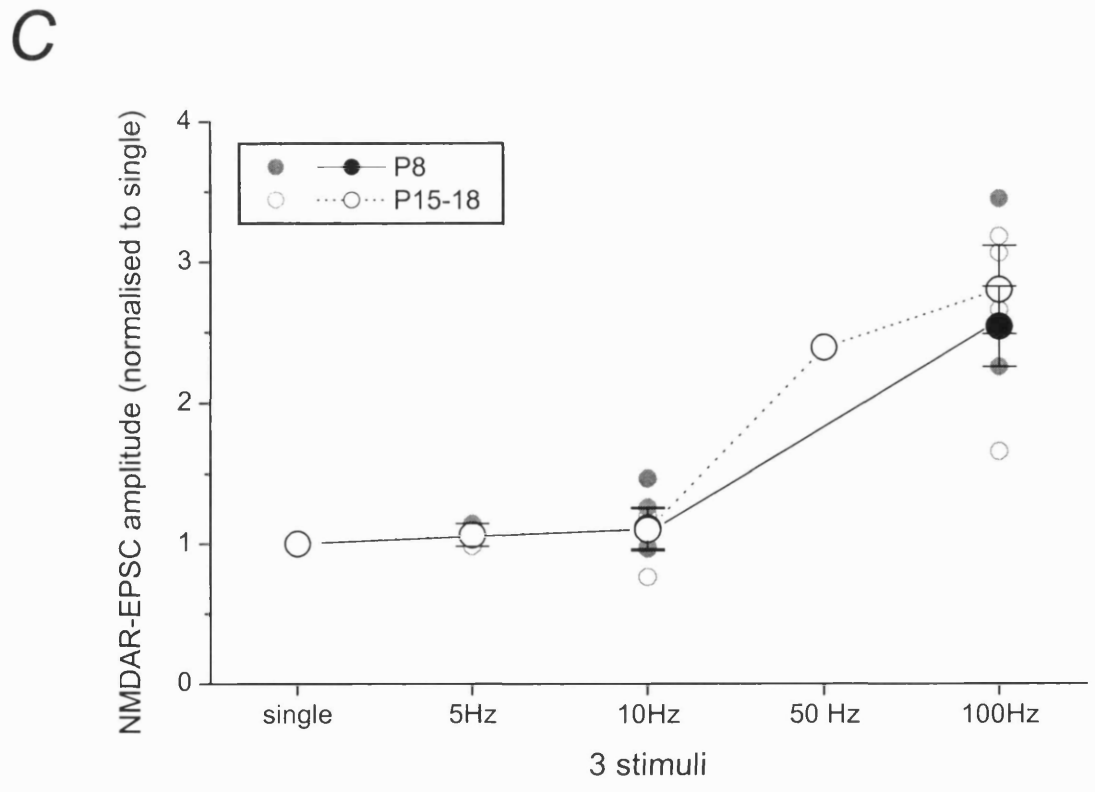
C
NMDAR-EPSC amplitude (normalised to single)
P8
P15-18
0
1
2
3
4
single
5Hz
10Hz
50 Hz
100Hz
3 stimuli

Table 4.1 *Comparing the amplitudes of single- and a train of EPSCs with those of spontaneous EPSCs*

		sEPSC	Evoked EPSC	
			Single	**Train**
P7-8	NMDAR-EPSC Amplitude (pA)	-6.0 ± 4.4 (22)	-31.7 ± 7.2 (8)	-82.9 ± 20.8 (8)
	Evoked: sEPSC ratio		5.3	15.5
P15-18	NMDAR-EPSC Amplitude (pA)	-4.8 ± 0.7 (22)	-20.5 ± 2.0 (36)	-70.2 ± 7.6 (36)
	Evoked: sEPSC ratio		4.2	14.5

Mean ± SEM (number of cells)

As with single NMDAR-EPSCs, the decay phase of NMDAR-EPSCs elicited by a train of stimuli was best fitted by the sum of two exponential functions. Figure 4.2A (bottom left panel) illustrates the decay phase of NMDAR-EPSCs produced by a single stimulus and a train of stimuli at P7-8 (average of 9 cells), normalised to the peak and overlaid on the same time-scale. No difference was observed between the decay kinetics of single EPSCs (τ_w, 110.2 ± 7.6 ms; τ_{fast}, 61.3 ± 8.7ms; τ_{slow}, 353.7 ± 60.2ms ms, A_{fast}, 78.5 ± 5.6%; n=9) and a train of EPSCs recorded from P7-8 Golgi cells (τ_w = 127.8 ± 6.7 ms; τ_{fast}, 74.8 ± 8.1ms; τ_{slow}, 360.7 ± 52.1ms, A_{fast}, 75.9 ± 5.9%; $p > 0.05$ for τ_w, τ_{fast}, τ_{slow} and A_{fast}, paired Student's *t* tests). Similar values were obtained using a fit-independent method (by dividing the charge transfer by current amplitude; single, τ_w = 123.8 ± 5.6; train, τ_w = 142.3 ± 6.6ms; $p > 0.2$ between fit and fit-independent measures, paired Student's *t* tests).

At P15-18, a high-frequency train of stimuli consistently and significantly slowed the EPSC decay time-course (τ_w, 153.8 ± 9.6ms, τ_{fast}, 79.2 ± 6.2ms; τ_{slow}, 586.5 ± 51.5ms; A_{fast}, 80.1 ± 2.6%; single EPSCs: τ_w, 81.3 ± 3.7ms, τ_{fast}, 41.8 ± 4.6ms; τ_{slow}, 175.7 ± 11.1ms; A_{fast}, 69.9 ± 3.8%; n=36; n=36; $p < 5x10^{-7}$, Wilcoxon's matched pairs). This is illustrated in the bottom right panel of Figure 4.2A, showing the average decay waveforms of single- and a train of EPSCs recorded from nine P15-18 Golgi cells. The EPSCs were scaled to the peak amplitude and the peaks were aligned. Similar values were obtained using a fit-independent analysis method on a random sample of cells (single EPSCs, τ_w = 75.6 ± 12.4ms; a train of EPSCs, τ_w = 145.8 ± 10.3ms; n=6; $p > 0.8$ between fit and fit-independent measures, paired Student's *t* test).

It is interesting to note that the decay time constant of the fast component (τ_{fast}) of a train of EPSCs at P15-18 was similar to the weighted mean decay time (τ_w) of single EPSCs (79.2 ± 6.2ms *vs* 81.3 ± 3.7 ms, respectively; $p > 0.1$, Mann-Whitney U). The slow component of the train of EPSCs had a decay time constant (τ_{slow}) of 586.5 ± 51.5ms, making up 19.9 ± 2.6% of the total amplitude. As the average amplitude was 70.2 ± 7.6pA (n=36), this slow-decaying component ranged between 10pA and 20pA in absolute terms. As also shown in Chapter 3, the difference in the decay-time of single NMDAR-EPSCs between P7-8 and P15-18 was significant ($p < 0.002$, unpaired Student's *t* test). However, although the mean decay time of a train of EPSCs at P7-8 appeared to be faster than that at P15-18 (Figure 4.2B), the difference was not significant (τ_w, 127.8 ± 6.7ms at P7-8 and 153.8 ± 9.6ms at P15-18; $p > 0.2$, Mann Whitney U).

On average, at P15-18, the decay time constant of EPSCs elicited by a train of 3 stimuli at 100Hz was twice that of single EPSCs (τ_w, 153.8 ± 9.6ms *vs* 81.3 ± 3.7 ms). Was this relationship uniform for all cells? We investigated this by plotting, for individual cells, the τ_w of single EPSCs against the percentage change in τ_w brought about by high-frequency train stimulation (i.e. the τ_w of a train of EPSCs expressed as a percentage change of the single EPSC τ_w). Illustrated in Figure 4.2C, the plot shows clearly that the proportional difference in the decay kinetics between single- and a train of EPSCs was greater for those cells with faster single EPSCs (Spearman R = -0.7, $p < 5x10^{-8}$). The correlation indicates that not all cells were affected by high-frequency stimulation to the same extent. Briefer single NMDAR-EPSCs displayed a greater degree of slowing of EPSC decay kinetics when a high-frequency train of stimuli was applied.

Figure 4.2 *High-frequency train stimulation slowed the NMDAR-EPSC at P15-18 but not at P7-8*

A, Parallel fibre-Golgi cell EPSCs recorded under control conditions (*black*) and in the presence of 50μM D-AP5 (*grey*). The top and middle panels on the left show typical recordings of single- and a train of EPSCs from a P8 Golgi cell. On the right, single- (*top*) and a train of (*middle*) EPSCs recorded from a P18 Golgi cell. *Bottom left and bottom right panels*, to compare the decay kinetics of EPSCs generated by the two stimulation conditions, EPSC decay waveforms were normalised to the NMDAR-EPSC amplitude (as measured at 20ms after the non-NMDAR peak for single stimuli and at 40ms after the non-NMDAR peak for train stimuli), and aligned on the same time-scale for better visual comparison. The normalised average single EPSC (*dotted black line*) and train-generated EPSC (*solid blue line*) are shown for P7-8 (n=9; *left*) and P15-18 Golgi cells (n=9; *right*).

B, the slower decay of train NMDAR-EPSCs was consistent for all P15-18 cells recorded (n=36; * $p < 5x10^{-7}$, Wilcoxon's matched pairs). The average data for P7-8 (n=9; *filled circles*) and P15-18 (*open circles*) are summarised in the plot.

C, the τ_w of single-pulse EPSCs of individual cells plotted against the corresponding τ_w of train EPSC (expressed as the percentage change of the τ_w of single EPSCs). The plot indicates that high-frequency train stimulation had a greater effect on slowing the decay kinetics of NMDAR-EPSCs in those cells with faster-decaying single-pulse EPSCs. The correlation between all the data points was statistically significant (linear regression, R = -0.63; $p < 5x10^{-6}$).

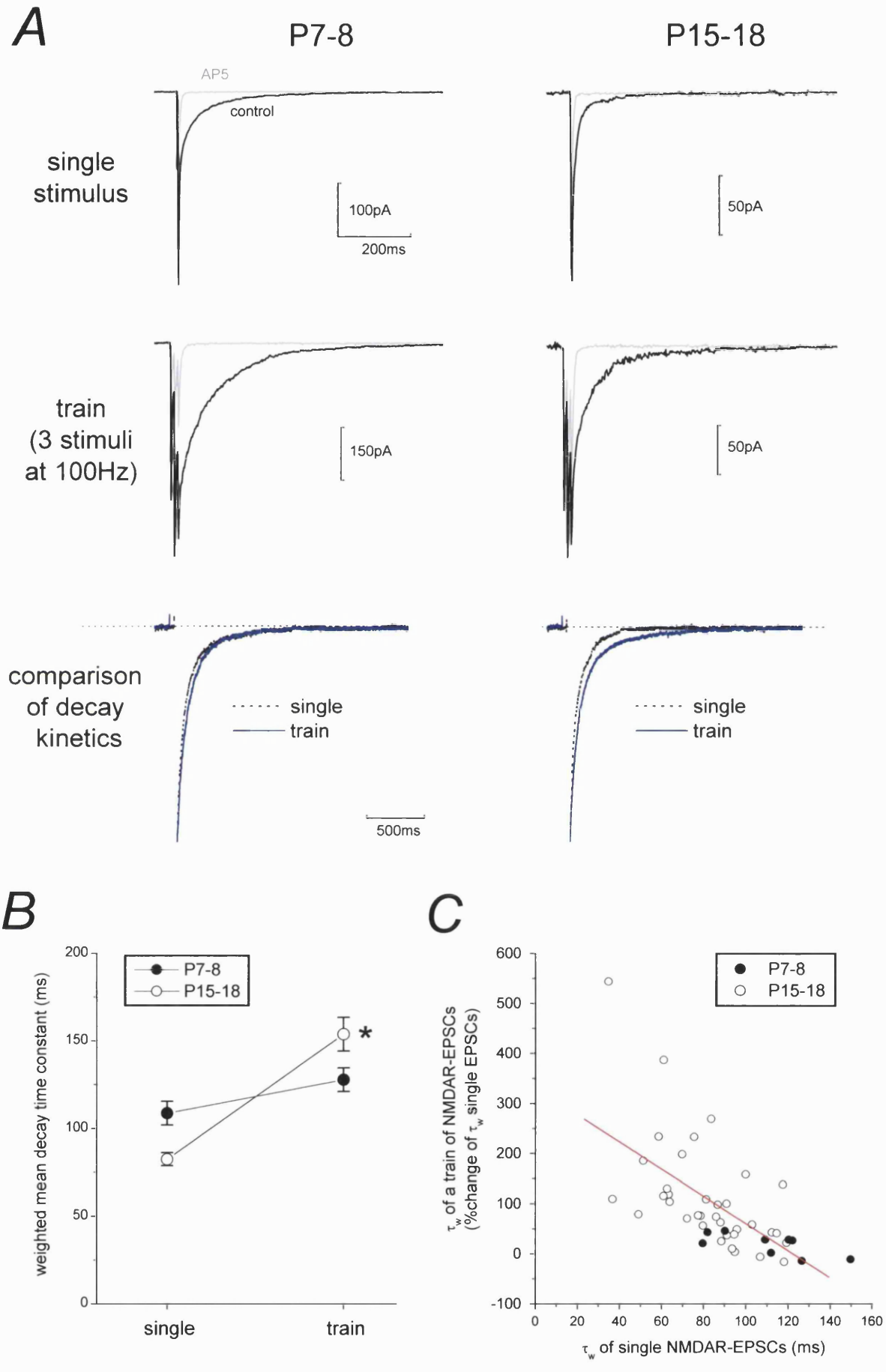
A
P7-8
P15-18
AP5
control
single stimulus
100pA
200ms
50pA
train (3 stimuli at 100Hz)
150pA
50pA
comparison of decay kinetics
single
train
500ms
single
train
B
weighted mean decay time constant (ms)
P7-8
P15-18
*
single
train
C
τw of a train of NMDAR-EPSCs (%change of τw single EPSCs)
P7-8
P15-18
τw of single NMDAR-EPSCs (ms)

4.3.3 *Ifenprodil sensitivity of a train of NMDAR-EPSCs*

In the previous section, we observed that NMDAR-EPSCs recorded from P15-18 Golgi cells exhibited a significantly slower decay time-course when elicited by a train of stimuli. In contrast, at P7-8, there was no difference between the decay kinetics of NMDAR-EPSCs produced by a train of stimuli *vs* a single stimulus.

What could underlie the slower decay of the NMDAR-current elicited by a train of stimuli at P15-18? Is it the delayed activation of receptors located further away from the synapse or the repeated activation of receptors caused by the persistence of glutamate at the synapse? Or is glutamate activating a distinct population of extrasynaptic receptors with slower deactivation kinetics? Perhaps, at P15-18, those NMDARs at perisynaptic sites are of a different subunit composition, and therefore exhibit different properties compared with receptors at synaptic sites.

We presented evidence in Chapter 3 for a developmental change in the subunit composition of NMDARs at the parallel fibre to Golgi cell synapse. The NMDAR-mediated synaptic current became shorter in duration and less sensitive to the NR2B-selective antagonist ifenprodil between P7-8 and P15-18. The kinetic and pharmacological properties of the synaptic current at P15-18 are consistent with a reduced contribution from the NR2B subunit and an increased functional expression of NR2A. What if the subunit composition of synaptic NMDARs changes during development, while that of perisynaptic receptors does not? If both synaptic and the extrasynaptic NMDARs are mainly of the NR2B-containing subtype at P7-8, this would explain the similarity in decay kinetics. If, by P15-18, the synaptic population of NMDARs comprise more NR2A-containing receptors while the extrasynaptic receptors remain unchanged, then activation of

extrasynaptic NR2B receptors during a train of stimuli could account for the slower EPSCs. To investigate this hypothesis further, we next compared the ifenprodil sensitivity between single- and a train of EPSCs.

Figure 4.3 compares the effect of 10μM ifenprodil on NMDAR-EPSCs produced by a single stimulus and a train of stimuli. The ifenprodil sensitivity of the train-generated NMDAR-EPSC amplitude at P15-18 was consistently higher: 60.6 ± 3.8% compared with 20.5 ± 6.0% for single EPSCs (Figure 4.3C; n=7; $p < 5x10^{-4}$, paired Student's *t* test). In contrast, at P7-8, the inhibition by 10μM ifenprodil was similar for single- and a train of stimuli. NMDAR-EPSC amplitudes were inhibited by 76.8 ± 5.3% and 85.9 ± 4.6%, respectively (n=7; $p > 0.05$, paired Student's *t* test). The action of ifenprodil at this concentration was most likely postsynaptic as it affected neither the non-NMDAR peak nor the paired-pulse ratio (Table 4.2).

The lack of a difference in ifenprodil inhibition between single- and a train of EPSCs at P7-8 supports the idea that synaptic and extrasynaptic NMDARs at the parallel fibre to Golgi cell connection are of the same subunit composition. The high degree of ifenprodil sensitivity indicates that these NMDARs are mainly of the NR2B subtype. In older animals at P15-18, single EPSCs were much less sensitive to ifenprodil. However, the ifenprodil sensitivity was three times higher when a train of stimuli was applied. The slower decay kinetics and higher ifenprodil sensitivity of a train of EPSCs at P15-18 support the idea that high-frequency stimulation leads to the activation of a distinct population of NMDARs. These perisynaptic NMDARs have properties indicative of NR2B receptors.

Figure 4.3 *A train of stimuli increased the ifenprodil sensitivity of the parallel fibre-Golgi cell EPSC at P15-18*

A, outline of the experimental procedure.

B, Parallel fibre-Golgi cell EPSCs recorded from a P7 (left) and P15 (right) Golgi cell. Ifenprodil (10μM; *blue*) almost completely inhibited NMDAR-EPSCs at P7. However, at P15, ifenprodil has a greater inhibitory effect on a train of EPSCs than on single EPSCs.

C, summary data of 7 cells in each age group. At P7-8, ifenprodil sensitivity was high under both stimulation conditions (*filled circles*). At P15-18, the inhibition by ifenprodil was significantly higher in response to a train than to a single stimulus (*open circles*; * $p < 5\text{x}10^{-4}$, paired Student's *t* test).

A

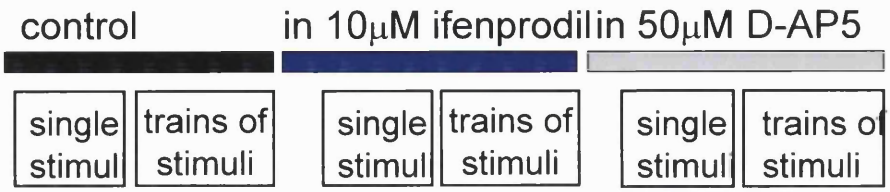
control
in 10μM ifenprodil
in 50μM D-AP5
single stimul
trains of stimuli
single stimul
trains of stimuli
single stimuli
trains of stimuli

B

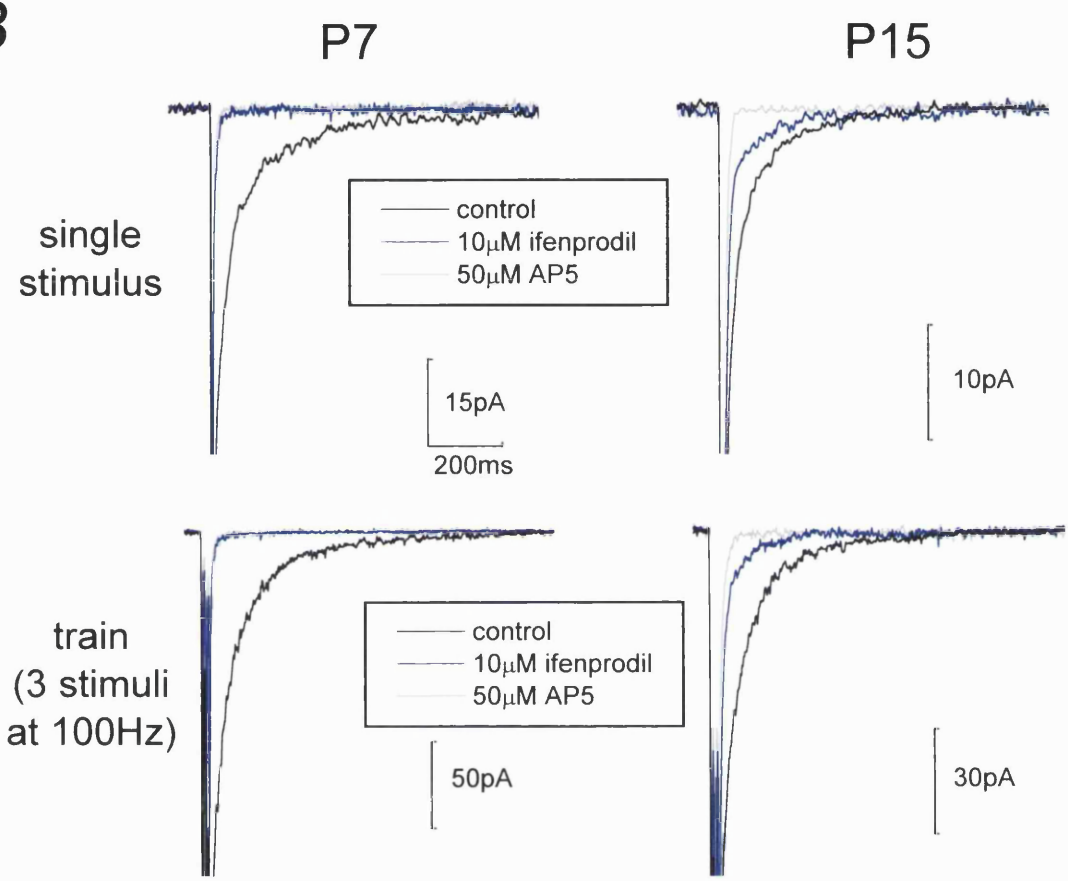
P7
P15
single stimulus
control
10μM ifenprodil
50μM AP5
15pA
200ms
10pA
train (3 stimuli at 100Hz)
control
10μM ifenprodil
50μM AP5
50pA
30pA

C

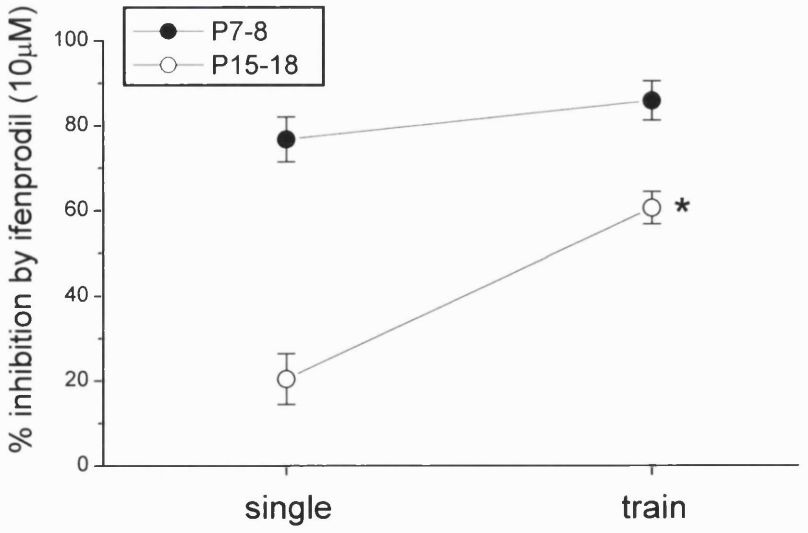
P7-8
P15-18
% inhibition by ifenprodil (10μM)
100
80
60
40
20
0
*
single
train

Table 4.2 *Ifenprodil did not affect the non-NMDAR peak amplitude nor the paired-pulse ratio*

		control	ifenprodil (10μM)	D-AP5 (50μM)
P7-8	Non-NMDAR amplitude (pA)	-255.3 ± 46.8 (6)	-218.8 ± 37.5	-180.6 ± 33.4
	Paired-pulse ratio	1.00 ± 0.24	1.18 ± 0.1	1.23 ± 0.16
	'Third-pulse' ratio	0.68 ± 0.21	0.71 ± 0.14	0.83 ± 0.21
P15-18	Non-NMDAR amplitude (pA)	-202.6 ± 15.9 (9)	-178.5 ± 16.6	-167.8 ± 19.7
	Paired-pulse ratio	1.12 ± 0.11	1.18 ± 0.12	1.18 ± 0.1
	'Third-pulse' ratio	0.81 ± 0.12	0.84 ± 0.12	0.86 ± 0.13

Mean values ± S.E.M. (number of cells)

Paired-pulse ratio: ratio between non-NMDAR amplitudes of the second and the first EPSCs of the train (3 stimuli at 100Hz)

'Third-pulse' ratio: ratio between non-NMDAR amplitudes of the third and the first EPSCs of the train (3 stimuli at 100Hz)

P7-8: no significant difference in non-NMDAR amplitude, paired-pulse or 'third-pulse' ratios between control, ifenprodil and D-AP5 ($0.9>p>0.4$, one-way ANOVA).

P15-18: no significant difference in non-NMDAR amplitude, paired-pulse or 'third-pulse' ratios between control, ifenprodil and D-AP5 ($1.0>p>0.3$, one-way ANOVA).

Also, no significant difference in paired-pulse or 'third-pulse' ratios (in control, ifenprodil or D-AP5) between P7-8 and P15-18 ($1.0>p>0.3$, Mann-Whitney U).

Figure 4.4 *MK801 blocked the NMDAR-mediated component of EPSCs elicited by single stimuli*

A, Parallel fibre-evoked EPSCs from a P18 Golgi cell. Ten single stimuli (one every 30s) were applied in the presence of the NMDAR open channel blocker MK801 (10μM). The NMDAR-mediated component was blocked by MK801 (*middle*) and subsequent perfusion 50μM D-AP5 had little effect.

B, time-course plot outlining the experimental protocol and the effect of MK801 on the parallel fibre-evoked NMDAR-EPSC. With the exception of the stimulation protocol in the presence of MK801 (*open circles*, second panel from the left), single stimuli were elicited at 0.3Hz and the data points shown are averages of 10 EPSCs (*solid circles*).

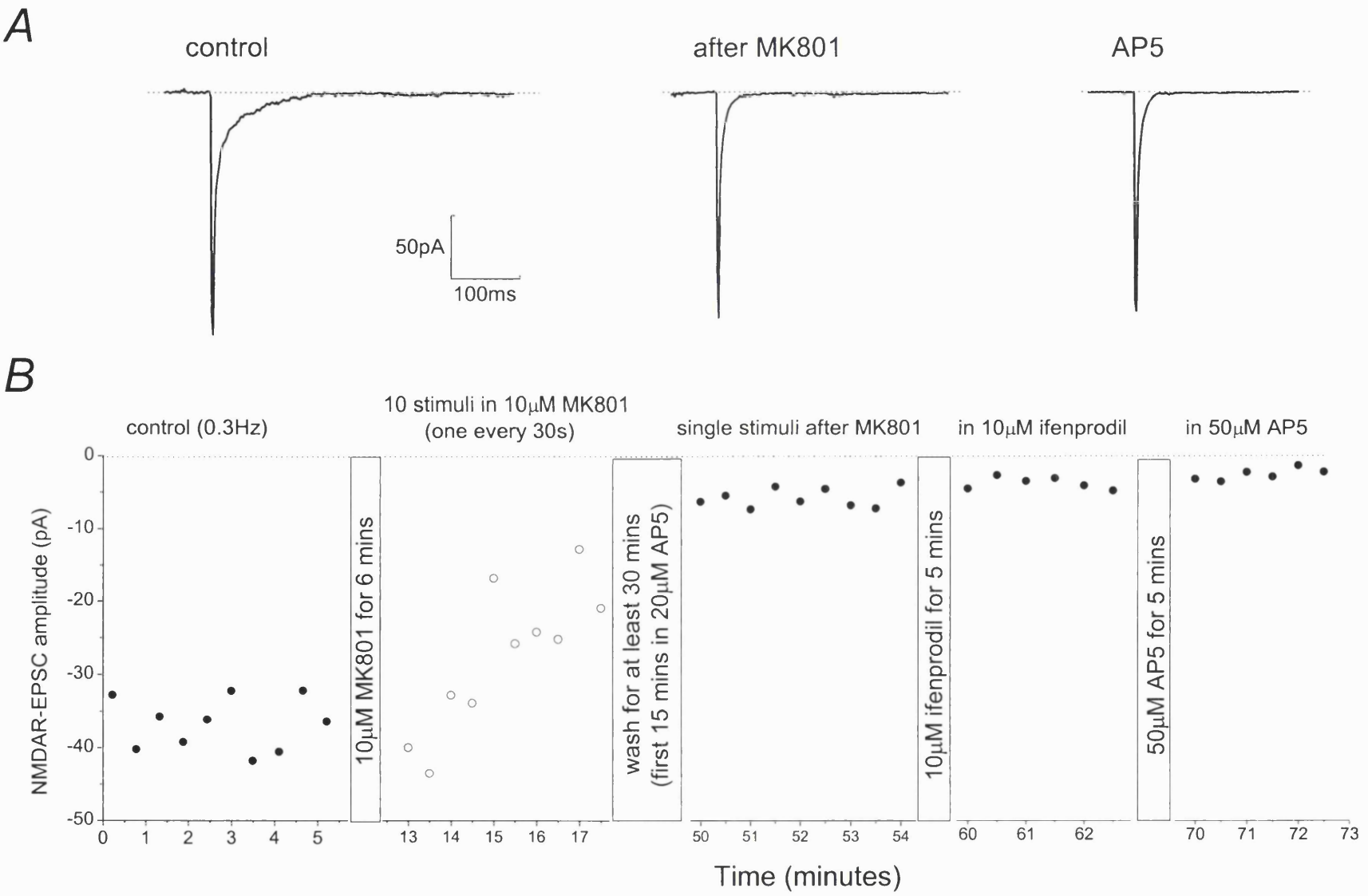
A
control
after MK801
AP5
50pA
100ms
B
control (0.3Hz)
10 stimuli in 10μM MK801
(one every 30s)
single stimuli after MK801
in 10μM ifenprodil
in 50μM AP5
NMDAR-EPSC amplitude (pA)
0
-10
-20
-30
-40
-50
10μM MK801 for 6 mins
wash for at least 30 mins
(first 15 mins in 20μM AP5)
10μM ifenprodil for 5 mins
50μM AP5 for 5 mins
0 1 2 3 4 5
13 14 15 16 17
50 51 52 53 54
60 61 62
70 71 72 73
Time (minutes)

4.3.4 *Using MK801 to isolate the current through extrasynaptic NMDARs*

MK801 produces a use-dependent block of NMDAR channels. It can therefore be used to selectively block NMDARs that are activated (Huettner and Bean, 1988; Jahr, 1992). We stimulated parallel fibres with single stimuli in the presence of MK801 to block the synaptic NMDA receptors. MK801 was then washed out of the recording chambre for at least 30 minutes. During the first 15 minutes of the wash period, 20-25μM D-AP5 was included in the bathing medium to prevent residual MK801 from blocking additional NMDARs during spontaneous activity. After MK801 washout, trains of stimuli (3 stimuli at 100Hz) were applied and the resultant EPSC was compared with those recorded before MK801 treatment. This allowed us to examine the decay kinetics and ifenprodil sensitivity of (predominately) extrasynaptic receptors that were not subjected to MK801 block.

Figure 4.4 shows an outline of the MK801 treatment procedure and the effect of MK801 on the NMDAR-mediated component of parallel fibre-evoked EPSCs recorded from a P18 Golgi cell. In the presence of 4 or 10μM MK801, single stimuli were applied every 30 seconds for 5 minutes (10 stimuli) and this was sufficient to block 80.6 ± 3.8% (n=9) of the NMDAR-mediated current. MK801 treatment inhibited the charge transfer of single NMDAR-EPSCs to a similar extent (72.3 ± 4.7%; $p > 0.2$, unpaired Student's t test). The NMDAR-mediated component showed no recovery after applying single stimuli (at 0.3Hz) for an hour after MK801 washout (n=2, data not shown). Also, the non-NMDAR peak amplitudes were not affected by MK801 (control, -250.4 ± 28.8pA; after MK801 treatment, -222.6 ± 21.8pA; n=10; $p > 0.2$, paired Student's t test).

4.3.4.1 *Exclusion of synaptic NMDARs by MK801 did not affect the decay kinetics of a train of EPSCs but increased the ifenprodil sensitivity*

In order to examine the amplitude and decay kinetics of currents through extrasynaptic NMDARs at P15-18, the NMDAR-EPSC generated by a train of 3 stimuli at 100Hz was recorded before and after the MK801 treatment. An outline of the experimental procedure is shown in Figure 4.5A. The ifenprodil sensitivity of NMDAR-EPSCs after MK801 treatment was compared with values from previous experiments where MK801 was not applied. In the example shown in Figure 4.5B, MK801 treatment reduced the amplitude of a train of NMDAR-EPSCs by 55.2%. The average block produced by 4 or 10μM MK801 in P15-18 Golgi cells was 68.3 ± 2.6% (before MK801, -129.8 ± 29.5pA; after MK801, -40.3 ± 6.9pA; n=9).

The decay waveforms of NMDAR-EPSCs generated by a train of stimuli in P15-18 Golgi cells were fitted with double exponentials and gave a τ_w value of 137.6 ± 9.4ms before MK801 treatment (τ_{fast}, 75.8 ± 6.9ms; τ_{slow}, 538.4 ± 83.2ms; A_{fast}, 84 ± 3%; n=9; Figure 4.5C). There was no significant change in the decay time-course after MK801 treatment (τ_w, 134.1 ± 4.5ms; τ_{fast}, 63.7 ± 6.4ms; τ_{slow}, 457.4 ± 49.1ms; A_{fast}, 79 ± 4%; $p > 0.7$, paired Student's *t* test). The values for τ_{fast}, τ_{slow} or A_{fast} also remained unchanged ($0.4 > p > 0.2$, paired Student's *t* tests for τ_{fast} and τ_{slow}, Wilcoxon's matched pairs for A_{fast}). Values are summarised in Table 4.3.

Figure 4.5 *After MK801 treatment to block synaptic NMDARs, ifenprodil almost completely abolished the current through extrasynaptic receptors*

A, outline of the experimental procedure.

B, Parallel fibre-Golgi cell EPSCs in response to a train of stimuli recorded from a P18 Golgi cell under control conditions (*black*), after MK801 treatment (*red*), in 10μM ifenprodil (*blue*) and in 50μM D-AP5 (*grey*).

C, summary data comparing the weighted mean decay time constants of EPSCs recorded from P15-18 Golgi cells (n=9) in response to a single stimulus, to a train of stimuli without MK801 treatment and to a train of stimuli after MK801 treatment. Exclusion of synaptic receptors by MK801 blockade did not affect the decay kinetics of train EPSCs.

D, Train stimulation increased the ifenprodil sensitivity of NMDAR-EPSCs (*, $p < 5x10^{-4}$, paired Student's *t* test). Blockade of synaptic NMDARs by MK801 treatment further increased the degree of inhibition by 10μM ifenprodil (#, $p < 5x10^{-4}$, unpaired Student's *t* test).

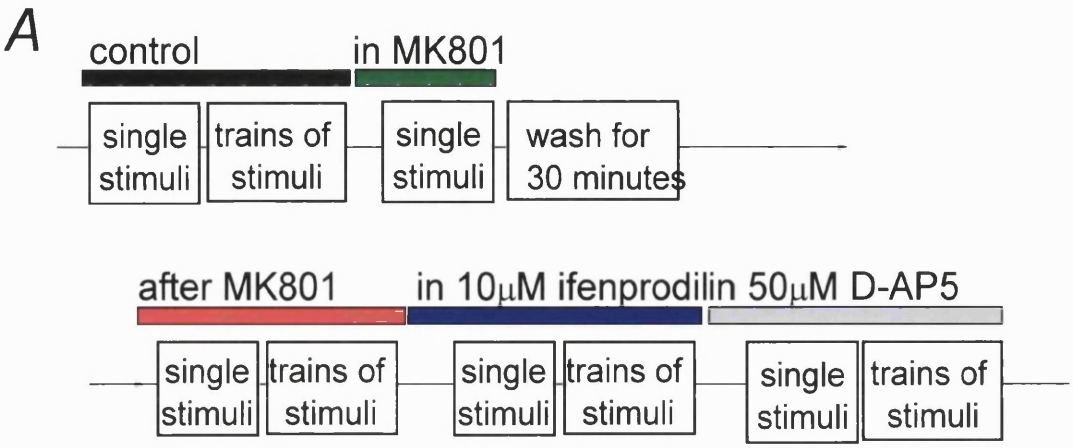
A
control
in MK801
single stimuli
trains of stimuli
single stimuli
wash for 30 minutes
after MK801
in 10μM ifenprodilin 50μM D-AP5
single stimuli
trains of stimuli
single stimuli
trains of stimuli
single stimuli
trains of stimuli

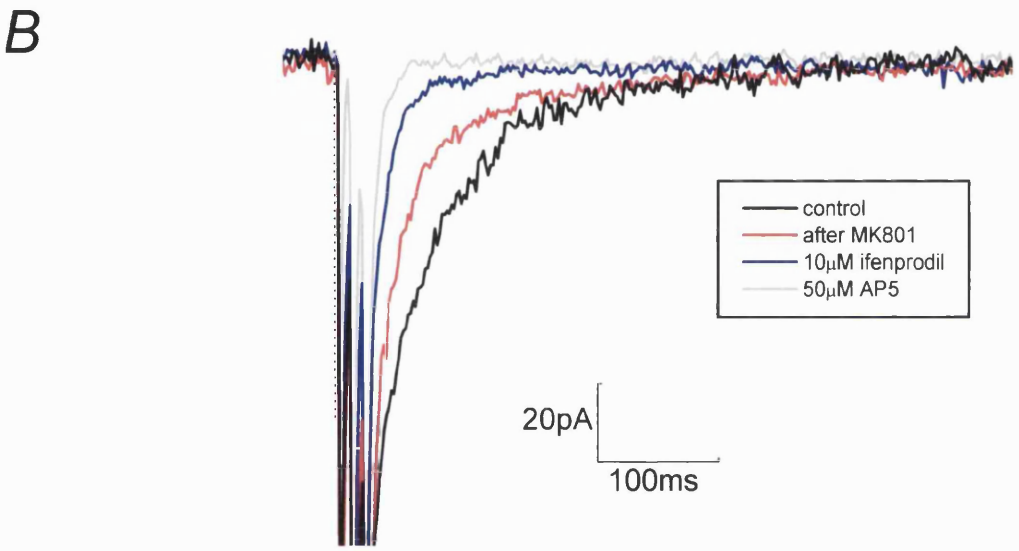
B
control
after MK801
10μM ifenprodil
50μM AP5
20pA
100ms

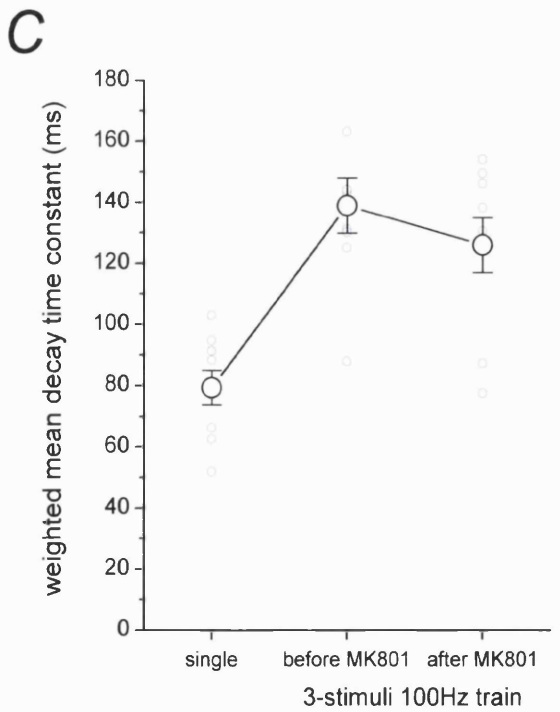
C
weighted mean decay time constant (ms)
180
160
140
120
100
80
60
40
20
0
single
before MK801
after MK801
3-stimuli 100Hz train

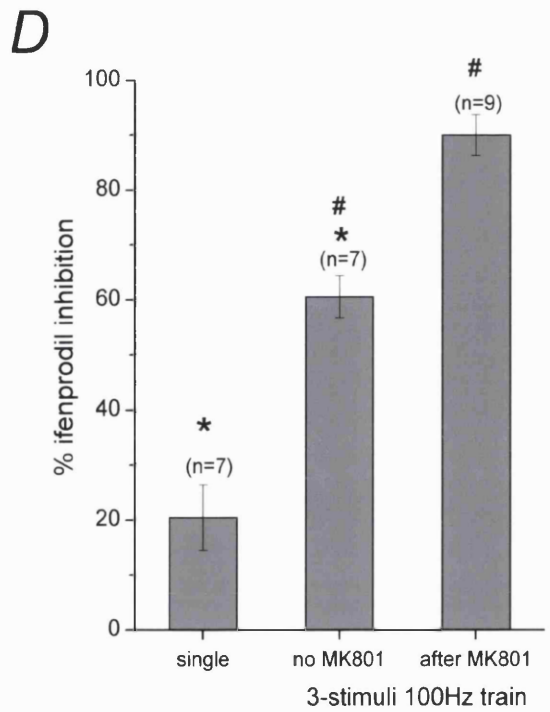
D
% ifenprodil inhibition
100
80
60
40
20
0
*
(n=7)
#
*
(n=7)
#
(n=9)
single
no MK801
after MK801
3-stimuli 100Hz train

Table 4.3 *Summary table of the kinetic and pharmacological properties of single and a train of NMDAR-EPSCs at P7-8 and P15-18*

		P7-8	P15-18
Single EPSCs	Decay τ_w (ms)	110.2 ± 7.6 (9)	81.3 ± 3.7 (36) *
	% inhibition of amplitude by ifenprodil	76.8 ± 5.3% (7) §	20.5 ± 6.0% (7) §, #
Train of EPSCs	Decay τ_w (ms)	127.8 ± 6.7 (9)	153.8 ± 9.6ms (36) *
	% inhibition of amplitude by ifenprodil	85.9 ± 4.6% (7)	60.6 ± 3.8% (7) #, †
	% inhibition of charge transfer by ifenprodil	82.1 ± 10.7 (7)	65.8 ± 6.6 (7) ††
Train of EPSCs after MK801 treatment	Decay τ_w (ms)	Not determined	Before MK801, 137.6 ± 9.4 After MK801, 134.1 ± 4.5 (9)
	% inhibition of amplitude by ifenprodil	Not determined	86.8 ± 4.0% (9) †
	% inhibition of charge transfer by ifenprodil	Not determined	87.7 ± 5.1 (9) ††

Mean ± S.E.M. (number of cells)

*, $p < 5\text{x}10^{-7}$, Wilcoxon's matched pairs

§, $p < 5\text{x}10^{-6}$, unpaired Student's *t* test

#, $p < 5\text{x}10^{-4}$, paired Student's *t* test

†, $p < 5\text{x}10^{-4}$, unpaired Student's *t* test

††, $p < 0.02$, Mann-Whitney U

With synaptic receptors blocked by MK801, the inhibition by 10μM ifenprodil of a train of NMDAR-EPSCs was even more pronounced (Figure 4.5D). Without MK801, ifenprodil inhibited EPSCs by 60.6 ± 3.8% (n=7; see section 4.3.3). After using MK801 to block the synaptic population of NMDARs, ifenprodil inhibited EPSCs by 86.8 ± 4.0% (n=9; $p < 5x10^{-4}$, unpaired Student's *t* test). Similar values were obtained for ifenprodil inhibition using charge transfer measurements (without MK801 treatment, 67.6 ± 6.1%, n=7; after MK801 treatment, 87.7 ± 5.1%, n=9). A summary of the kinetic and pharmacological properties of EPSCs generated by a single stimulus and a train of stimuli can be found in Table 4.3.

The results from this set of experiments are consistent with our hypothesis on the differential localisation of NMDARs at and surrounding the parallel fibre-Golgi cell synapse. After blockade of synaptic NMDA receptors with MK801, the ifenprodil sensitivity of a train of EPSCs was significantly higher. This supports the idea that, at P15-18, NR1/NR2B receptors are prominent at sites surrounding this synapse.

4.3.5 *The effect of the glutamate transporter inhibitor TBOA on synaptic currents*

Extrasynaptic receptors can also be activated by impeding the neurotransmitter clearance system (Barbour *et al*, 1994; Otis *et al*, 1996; Diamond, 2001). At the excitatory parallel fibre-Golgi cell synapse, blocking glutamate transporters may prolong the presence of glutamate or increase the glutamate concentration at the synapse if high-affinity transporters are important for the removal of glutamate after release. Inhibitors of glutamate transporters can be applied to elucidate the role of transporters in shaping EPSCs. The newly-available DL-*threo*-β-benzyl-

oxyaspartate (TBOA) is the glutamate transporter inhibitor most suitable for our purposes, as it is not transported and has negligible agonist action on glutamate receptors (LeBrun *et al*, 1997; Shimamoto *et al*, 1998).

4.3.5.1 *Effect of TBOA on NMDAR-EPSC amplitude*

We examined the effect of TBOA on parallel fibre-evoked single EPSCs. Figure 4.6A (left panel) shows that TBOA had no effect on parallel fibre-evoked EPSCs in P7-8 Golgi cells. The four cells tested showed no changes in baseline variance or holding current in the presence of TBOA (10 to 150μM; data not shown). At 20μM, TBOA had no effect on the NMDAR-EPSC current amplitude or charge transfer (98.2 ± 17% and 114.0 ± 24% of control, respectively). Furthermore, the peak amplitude of the non-NMDAR component of the EPSC was unchanged (102.4 ± 15% of control; $0.8 > p > 0.4$, Wilcoxon's matched pairs, Figure 4.6B, black bars).

At P15-18, 20μM TBOA had variable effects on single EPSCs. In 8 out of 17 cells examined, TBOA (10 or 20μM) caused a dramatic increase in the holding current and spontaneous EPSC frequency (data not shown). These cells deteriorated quickly and were not amenable to analysis. This detrimental effect of TBOA was never observed in slices from P7-8 mice. Recordings from the remaining nine P15-18 Golgi cells were analysed (but increasing the TBOA concentration beyond 30μM was detrimental to all P15-18 Golgi cells). Although there was often a visible increase in baseline variance on perfusion of TBOA, gross inspection (looking at the readings on the oscilloscope during experiments) suggested relatively little change in the holding current or the spontaneous EPSC

frequency. TBOA (20μM) had no significant effect on the NMDAR-EPSC amplitude (127.4 ± 15.9% of control; $p > 0.2$, Wilcoxon's matched pairs), charge transfer (147.4 ± 24.5% of control, $p > 0.6$, Wilcoxon's matched pairs), or non-NMDAR-EPSC current amplitude (105.2 ± 12.0% of control; $p > 0.6$, paired Student's *t* test; Figure 4.6B).

4.3.5.2 *Effect of TBOA on NMDAR-EPSC decay kinetics*

We next analysed the effect of TBOA on the decay kinetics of NMDAR-EPSCs. As illustrated in Figure 4.7, TBOA (20μM) had no apparent effect on the decay time-course of NMDAR-EPSCs at P7-8 (average of 4 cells). When fitted with the sum of two exponential functions, τ_w was 130.5 ± 16.8ms under control conditions (τ_{fast}, 82.6 ± 16.4ms; τ_{slow}, 501.3 ± 219.1ms; A_{fast}, 85.1 ± 6%) and 137.6 ± 14.0ms in the presence of 20μM TBOA (τ_{fast}, 68.3 ± 7.7ms; τ_{slow}, 486.0 ± 97.1ms; A_{fast}, 81.2 ± 4%). TBOA had no significant effect on τ_w, τ_{fast}, τ_{slow}, or A_{fast} at this age ($0.1<p<0.8$, Wilcoxon's matched pairs).

TBOA had a more variable effect on the NMDAR-EPSC decay kinetics at P15-18 (Figure 4.7). However, the overall effect was not statistically significant. The mean value for τ_w was 77.0 ± 7.1ms under control conditions (τ_{fast}, 42.3 ± 10.1ms; τ_{slow}, 146.3 ± 20.2ms; A_{fast}, 67.9 ± 9%; n=9) and 102.9 ± 9.7ms in the presence of 20μM TBOA (τ_{fast}, 48.4 ± 9.7ms; τ_{slow}, 416.5 ± 127.6ms; A_{fast}, 78.6 ± 5%). There was no significant change in τ_w, τ_{fast}, or A_{fast} in the presence of TBOA ($0.05<p<0.5$, paired Student's *t* test for τ_w, Wilcoxon's matched pairs for τ_{fast} and A_{fast}). However, the difference in τ_{slow} between control and in 20μM TBOA was significant ($p < 0.05$, Wilcoxon' matched pairs).

Although the effect of TBOA on τ_w was not significant overall, the decay kinetics appeared to be slowed by TBOA in 4 out of the 9 cells analysed. In these 4 cells, the τ_w value was below 70ms before perfusion of TBOA (Figure 4.7B). Grouping these 4 cells together gave an average τ_w of 59.2 ± 3.0ms under control conditions *vs* 112.9 ± 18.1ms in 20μM TBOA. However, this difference was not statistically significant ($p > 0.05$, Wilcoxon's matched pairs). For the remaining 5 cells, the average decay times were 91.3 ± 7.8ms in control and 94.8 ± 10.4ms in TBOA. So it appears likely that at P15-18, glutamate transporters may influence to a greater extent the decay time of synaptic currents in a sub-population of cells where the initial decay time was faster. Since diffusion and glutamate transport are temperature-dependent, the effect of TBOA may be more substantial at physiological temperatures.

Figure 4.6 *TBOA had no significant effect on the amplitude of NMDAR-EPSCs at both P7-8 and P15-18.*

A, average EPSCs of 4 recordings at P7-8 (*left*) and 9 recordings at P15-18 (*right*), under control conditions (*black*) and in the presence of 20μM TBOA (*red*). A range of TBOA concentrations was tried (P7-8, 20-150μM; P15-18, 10-30μM) and the concentration-response relationships are illustrated in the insets.
B, the effect of 20μM TBOA on NMDAR-EPSC amplitude, NMDAR-EPSC charge transfer and non-NMDAR EPSC amplitude at P7-8 (*black*; n=4) and at P15-18 (*grey*; n=9). There were no significant differences in the three parameters examined at both ages.

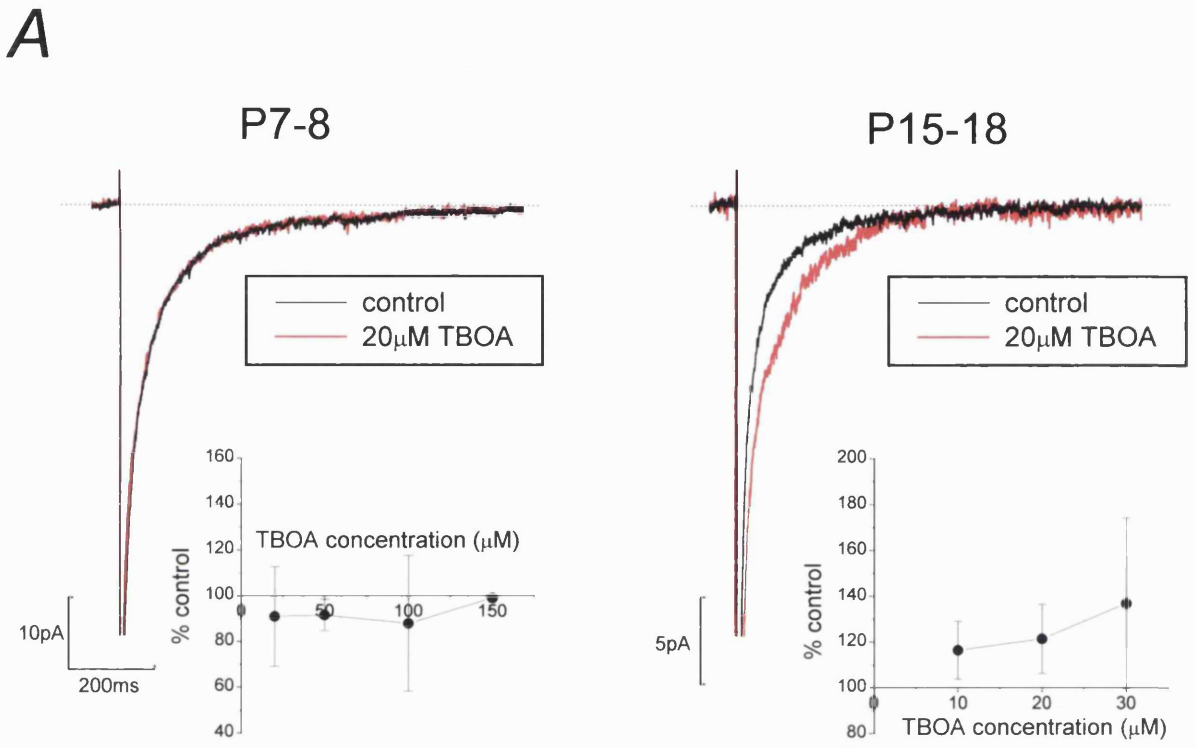
A
P7-8
control
20μM TBOA
10pA
200ms
% control
TBOA concentration (μM)
P15-18
control
20μM TBOA
5pA
% control
TBOA concentration (μM)

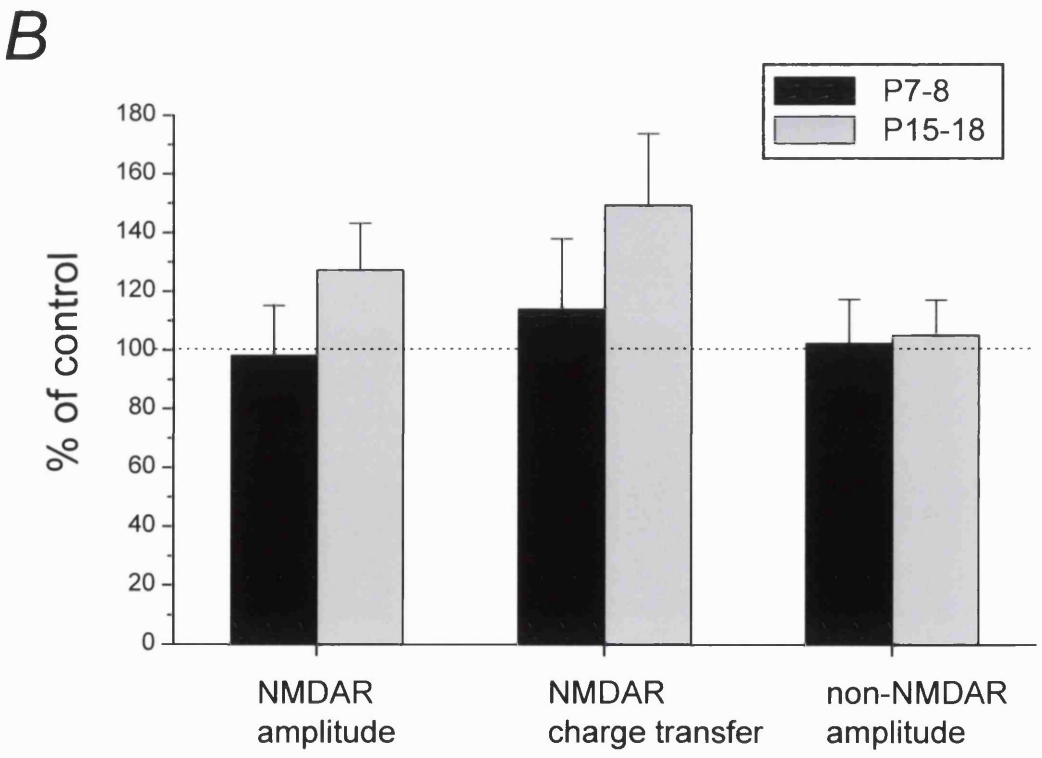
B
P7-8
P15-18
% of control
NMDAR amplitude
NMDAR charge transfer
non-NMDAR amplitude

Figure 4.7 *TBOA had no effect on the decay time-course of synaptic currents*

A, The effect of TBOA (20μM; *red*) on the decay time-course of parallel fibre-evoked EPSCs from P7-8 and P15-18 Golgi cells. The traces shown are average waveforms of P7-8 cells (n=4) and P15-18 cells (n=9). The traces are normalised to the NMDAR current amplitude (measured 20ms after the non-NMDAR peak). At both ages, there was no significant difference in the average weighted mean decay time constants under control conditions and in the presence of TBOA.

B, A plot illustrating the change in decay kinetics of individual cells brought about by TBOA. All four P7-8 cells (*filled circles*) and five of nine P15-18 cells (*open circles*) were not affected by TBOA, as these points lie close to the 'y=x' line (which indicates no change; *dotted line*). TBOA slowed the decay of four cells at P15-18: these four cells had the fastest decay kinetics under control conditions.

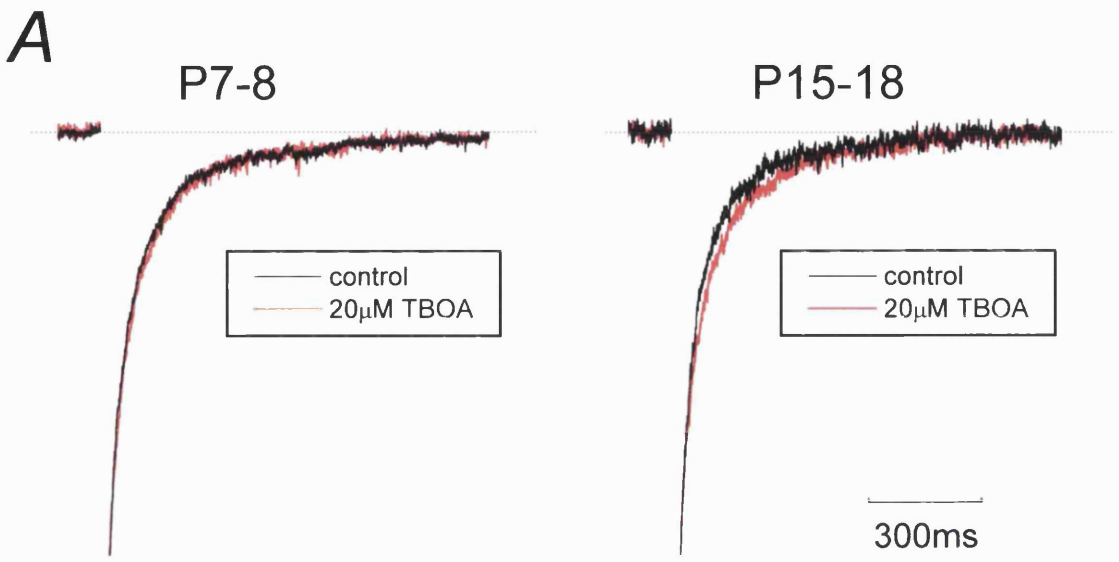
A
P7-8
P15-18
control
20μM TBOA
control
20μM TBOA
300ms

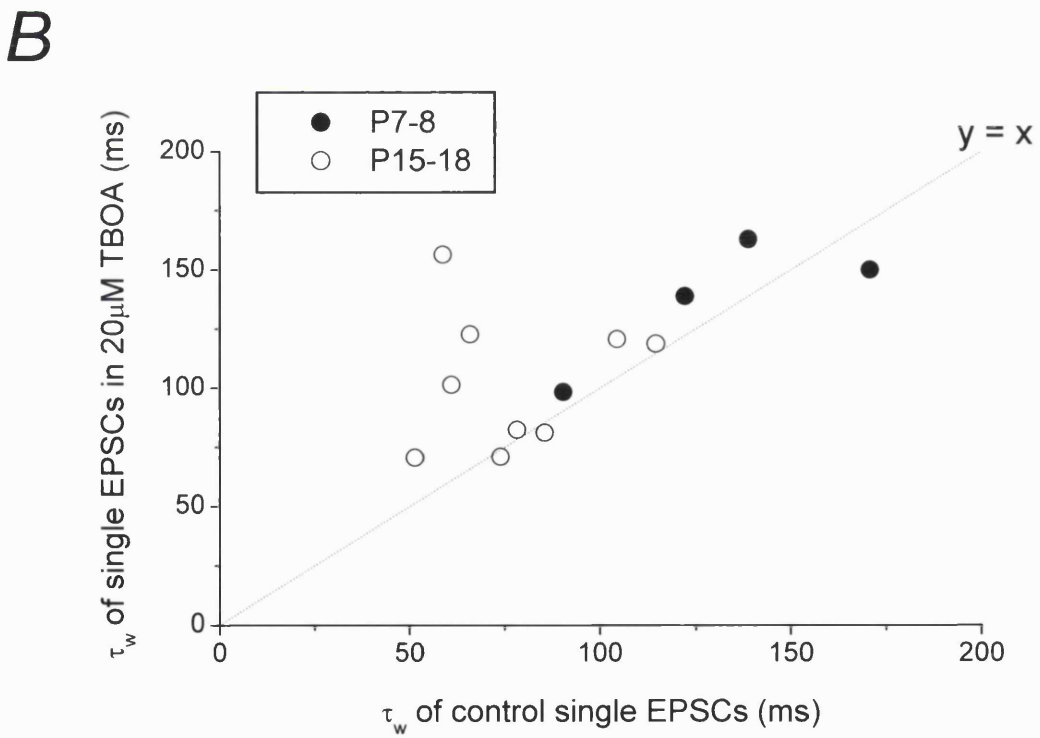
B
P7-8
P15-18
y = x
200
150
100
50
0
0
50
100
150
200
τw of single EPSCs in 20μM TBOA (ms)
τw of control single EPSCs (ms)

4.4 Discussion

4.4.1 *Summary of results*

In this chapter, we examined the properties of extrasynaptic NMDARs surrounding the parallel fibre to Golgi cell synapse. We investigated whether the properties of NMDA receptors located peripherally to this synapse also undergo the same developmental changes observed with synaptic NMDA receptors. Using a train of three stimuli at 100Hz to activate extrasynaptic receptors, the decay kinetics and ifenprodil sensitivity of the NMDAR-EPSCs produced by the train were compared with those EPSCs elicited by a single stimulus.

At P7-8, there was little difference in decay kinetics and ifenprodil sensitivity between NMDAR-EPSCs produced by single- and a train of stimuli. In contrast, at P15-18, the kinetic and pharmacological properties of NMDAR-EPSCs produced by a high-frequency train were significantly different to those of single EPSCs. The decay time-course was slower and the degree of ifenprodil inhibition was greater for a train of EPSCs. After using MK801 to block synaptic receptors, the current through extrasynaptic NMDARs was even more sensitive to inhibition by ifenprodil.

Figure 4.8 *Differential localisation of NMDARs at and surrounding the parallel fibre to Golgi cell synapse*

Early in postnatal development (P7-8), NMDARs at both synaptic and perisynaptic sites are mainly of the NR2B subtype. This is supported by the similar kinetic and pharmacological properties of currents elicited by a single stimulus and by a brief high-frequency train of stimuli (3 stimuli at 100Hz).

A week later in development (P15-18), NR2A-containing receptors are expressed at the synapse. However, NMDARs peripheral to synaptic sites appear to remain of the NR2B subtype. This is suggested by the slower decay kinetics and higher ifenprodil sensitivity of currents produced by a train of stimuli. After using MK801 to selectively block those receptors activated by a single stimulus, the remaining current through perisynaptic receptors was even more sensitive to ifenprodil. This further supports the targeting of NR2A-containing receptors to synaptic sites and the localisation of NR2B receptors further away from the synapse.

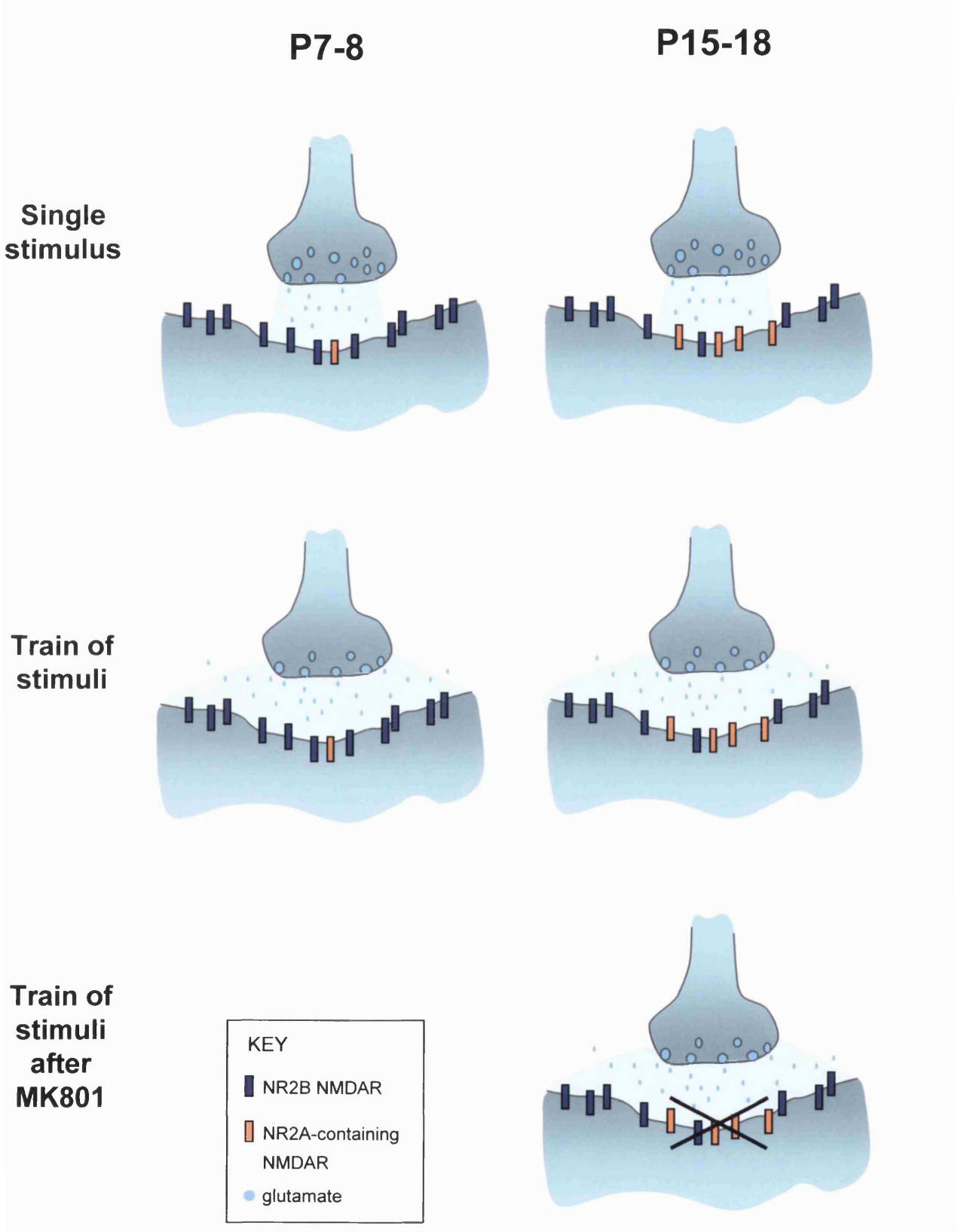
P7-8
P15-18
Single stimulus
Train of stimuli
Train of stimuli after MK801
KEY
NR2B NMDAR
NR2A-containing NMDAR
glutamate

4.4.2 *Differential localisation of NMDARs at the parallel fibre-Golgi cell synapse*

Taking together the results presented in Chapter 3 and in this chapter, our observations suggest that NR2B receptors are activated at both synaptic and perisynaptic sites by synaptically-released glutamate at P7-8. By P15-18, the synaptic NMDARs exhibit properties of NR2A-containing assemblies while perisynaptic NMDARs appear to be unchanged (Figure 4.8).

Can the differences in kinetic and pharmacological properties between single- and a train of NMDAR-EPSCs at P15-18 be explained by differences in the spatiotemporal profile of synaptically-released glutamate, rather than by differential localisation of postsynaptic NMDAR subtypes? Although the slower decay of a train of EPSCs could be alternatively attributed to diffusion and delayed receptor activation, the greater degree of ifenprodil inhibition of these EPSCs (both without and after MK801 treatment) is strong evidence in favour of differential localisation. If the synaptic and extrasynaptic receptors were of the same subunit composition, then a change in glutamate profile should not alter ifenprodil sensitivity.

On the other hand, there are reports that the inhibitory effect of ifenprodil is dependent on agonist concentration. Two studies have shown that ifenprodil potentiated agonist-evoked currents at low concentrations of agonist NMDA, but inhibited currents at higher agonist concentrations (Kew *et al*, 1996; Zhang *et al*, 2000). This could be due to an allosteric interaction between the glutamate and ifenprodil binding sites on the NR2B subunit (Zheng *et al*, 2001). However, the greater ifenprodil inhibition of a train of EPSCs (compared with single EPSCs) observed in this study is unlikely to be caused solely by higher concentrations of

glutamate. Mainly extrasynaptic receptors are activated by a train of stimuli after blocking synaptic receptors with MK801 and the glutamate concentration at extrasynaptic sites is most likely lower than the concentration at synaptic sites. If ifenprodil inhibition is reduced at lower agonist concentrations, then one might even expect ifenprodil inhibition of a train of EPSCs to be reduced after MK801 treatment. However, our experiments showed that ifenprodil sensitivity was increased by 30% after MK801 block of synaptic receptors. The ifenprodil inhibition after MK801 was the same as that at P7-8 synapses, supporting the idea that extrasynaptic NMDARs remain the same between P7-8 and P15-18. Even if there is substantial pooling of glutamate between adjacent synapses or release sites, the glutamate concentration at extrasynaptic sites is unlikely to exceed that at synaptic sites. Therefore, higher glutamate concentrations or changes in glutamate profile do not explain the different pharmacological properties between single- and a train of NMDAR-EPSCs. Furthermore, NR2A and NR2B receptor subtypes have similar affinities for MK801 (Kutsuwada *et al*, 1992; Laurie and Seeburg, 1994b) so it is unlikely that the increase in ifenprodil sensitivity after MK801 is due to selective blockade of NR2A-containing receptors.

Ca^{2+}-dependent inactivation has been shown to regulate the activity of NMDARs on the order of seconds and is more prominent for NR1/NR2A receptors (Clark *et al*, 1990; Legendre *et al*, 1993; Medina *et al*, 1995; Krupp *et al*, 1996; Dingledine et al, 1999). This could provide an alternative explanation for the difference in kinetics and ifenprodil sensitivity between single- and a train of EPSCs: NR2A receptors were being downregulated during the course of the experiment and by the time currents were measured in the presence of ifenprodil, the proportional contribution of NR2B receptors at the synapse had gone up. Although we cannot rule out the possibility that this occurred to some extent during our experiments,

the increased ifenprodil sensitivity after MK801 treatment still argues for the differential localisation of NR2A- and NR2B-containing receptors.

The differences in kinetic and pharmacological properties of NMDAR-EPSCs produced by single- and trains of stimuli are also unlikely to reflect the perisynaptic localisation of NR2C- or NR2D-containing receptors. Although NR1/NR2C and NR1/NR2D receptors have slow decay kinetics, they are not sensitive to ifenprodil (Williams, 1995; Mott *et al*, 1998; Misra *et al*, 2000a; Momiyama, 2000). However, one cannot rule out the possibility of ifenprodil-sensitive triheteromeric NR1/NR2B/NR2C or NR1/NR2B/NR2D receptors. In Chapter 5, we investigate the possible expression of triheteromeric NR1/NR2B/NR2D receptors in the perisynaptic membrane at the parallel fibre to Golgi cell synapse (section 5.3.2.4).

Golgi cells in the cerebellum have been shown to be immunopositive for the metabotropic glutamate receptors mGluR2 and mGluR5 (Neki *et al*, 1996). The mGluR2 receptors are located on the cell bodies and the proximal parts of their dendrites, while mGluR5 immunoactivity could be traced throughout the molecular layer (Neki *et al*, 1996). The expression of mGluRs on Golgi cells is supported by binding studies (Knoflach *et al*, 2001), and mGluRs play a role in synaptic transmission at the Golgi cell to granule cell synapse (Mitchell and Silver, 2000). As mGluRs are insensitive to D-AP5 (Shirasaki *et al*, 1994; Conn and Pin, 1997) and the ifenprodil sensitivity is calculated from the AP5-sensitive current, it is unlikely that mGluR activation was responsible for the slower decay of those EPSCs generated by a train of stimuli.

We also cannot rule out the possibility of differential expression of NR1 splice variants. Agonist-evoked currents through NR1a/NR2B receptors exhibit slower decay kinetics than NR1b/NR2B receptors (Rumbaugh *et al*, 2000). However, affinity of NMDARs to ifenprodil does not appear to be dependent on the NR1 splice variant expressed (Gallagher *et al*, 1996). Therefore it is unlikely that differential distribution of NR1 splice variants provides us with the simplest explanation for our observations.

4.4.3 *Possible involvement of glutamate transporters*

Immunohistochemical studies show intensive staining of the cerebellar cortex for expressed proteins of four cloned glutamate transporters: GLT-1, GLAST, EAAT3 and EAAT4. The first two are expressed on astrocytes, mainly on Bergmann glia which extend processes throughout the molecular layer. Immunopositive processes surround parallel fibre terminals and ensheath Purkinje cells in adult rat brain (Rothstein *et al*, 1994; Lehre *et al*, 1995). The neuronal EAAT3 and EAAT4 are also present in high density in the molecular layer and Purkinje cell layer. Of the four transporter subtypes, only EAAT3 is found in the granule cell layer but there is no evidence of presynaptic localisation in the parallel fibre terminals (Rothstein *et al*, 1994; Furuta *et al*, 1997a).

Our observations are in accordance with the reported developmental profile of glutamate transporter expression. Immunopositivity for glutamate transporters begins to occur around P14 in the rat cerebellum, reaching high levels around P24. There is little or no staining in P7 rats (Furuta *et al*, 1997b). We observed no apparent changes in P7-8 Golgi cell NMDAR-EPSCs in the presence of TBOA. Glutamate transporters are unlikely to play a major role in rapid removal of

glutamate at these synapses at this stage in development. However, TBOA had a heterogeneous effect on parallel fibre-evoked EPSCs at P15-18. More glutamate transporters may be expressed at this age than at P7-8. Alternatively, glutamate transporters may be expressed at the same levels between the two ages but changes in synapse geometry may increase effectiveness of glutamate transport (e.g. glial processes may wrap more tightly around synapses, increasing the proximity between transporters and the synaptic receptors).

If glutamate transporters do play a larger role in synaptic transmission at more mature synapses, then one might expect a correlation between faster decay kinetics of the NMDAR-EPSC and the effect of TBOA. There was some indication of this in Figure 4.7B, where the four cells with the fastest decay time-course under control conditions were most affected by TBOA. We intended to use TBOA as an alternative method of activating extraysnaptic receptors and since the experiments were conducted at room temperature, limited conclusions can be drawn about the physiological participation of glutamate transporters at this synapse.

The problem with manipulating glutamate clearance in the granule cell-Golgi cell system is that an increase in ambient glutamate can lead to excitation of many granule cells. This was observed in some experimental trials, where perfusion of TBOA brought about dramatic increases in spontaneous EPSC frequency and leak current, making the cell unviable for recording. Therefore, the cells used in the analysis may be a biased sample. The overall lack of effect by TBOA may reflect a bias towards less mature cells where the level of transporter expression was lower.

4.4.4 *Targeting of NR2A to synaptic sites*

The surface delivery of functional NR2A-containing NMDARs during development appears to be restricted to synaptic sites (Li *et al*, 1998; Rumbaugh and Vicini, 1999; Tovar and Westbrook, 1999; Momiyama, 2000) and the possible mechanisms underlying this targeting have received much interest. A sequence involved in bringing NR2A to the synapse has been identified in the cytoplasmic carboxyl terminal (Steigerwald *et al*, 2000). Furthermore, interactions between NMDAR subunits and PSD proteins appear to play a pivotal role in synaptic targeting. Membrane-associated guanylate kinases (MAGUKs), such as PSD-93, PSD-95 and SAP-102, are involved in the clustering and anchoring of NMDARs at the synapse and in subsequent signal transduction processes (reviewed by Ziff, 1997; Grant and O'Dell, 2001; Sheng and Kim, 2002). SAP-102 was reported to be abundant at hippocampal CA1 synapses in early postnatal development, coinciding with the expression of NR2B (Sans *et al*, 2000). At older synapses, high expression levels of PSD-93 and PSD-95 coincided with NR2A expression. Multiple MAGUKs could be expressed at the same synapse and further co-immunoprecipitation experiments supported a preference for complexes of NR2A with PSD-93/95 and NR2B with SAP-102. Selective interaction with MAGUKs may therefore be one of the mechanisms responsible for the delivery of specific NMDAR subunits to synaptic sites at different stages in development.

Barria and Malinow (2002) recently elucidated further details on the variables affecting the number and subunit composition of NMDARs at hippocampal synapses. The trafficking of NR2A-containing receptors was dependent on synaptic activity and agonist binding. Increased NR2A expression led to a reduction in the magnitude of synaptic NMDAR currents, faster decay kinetics

and reduced ifenprodil sensitivity. These effects are similar to the developmental changes observed in the present study at the parallel fibre-Golgi cell synapse, and are consistent with a developmentally-regulated replacement of NR2B receptors with NR2A-containing receptors at synapses.

Besides dynamic NMDAR targeting during development, evidence is also accumulating that NMDARs in the plasma membrane may not be as static as they were once thought to be. NMDARs at synaptic sites have been demonstrated to undergo constant internalisation during early development in hippocampal cultures (Roche *et al*, 2001). The internalisation process decreased with maturation and was blocked by the co-expression of PSD-95. Coincidentally, PSD-95 is expressed at higher levels later in development (see above; Sans *et al*, 2000). Furthermore, NMDARs may be able to move laterally between 'synaptic' and 'extrasynaptic' sites. Tovar and Westbrook (2002) reported a recovery of the NMDAR-EPSC after block of 'synaptic' receptors by MK801. We did not observe this in our experiments and it is possible that by P15-18 in mouse cerebellar Golgi cell development, NMDAR receptors are more stabilised e.g. by postsynaptic proteins. Both the internalisation and lateral movement of NMDARs were observed relatively early in development (primary hippocampal cultures: 3-5 and 6-9 days in vitro (DIV), respectively), before NR2A was reported to dominate at these synapses (>12 DIV; Tovar and Westbrook, 1999). So, the processes of NMDAR targeting, localisation and stabilisation appear to be developmentally regulated and dynamically inter-linked.

4.4.4.1 *Published evidence supporting the differential localisation of NMDARs*

This study shows that perisynaptic receptors at the parallel fibre to Golgi cell synapse, activated by a high-frequency train of stimuli, can be of different subunit composition compared with those receptors located directly adjacent to the presynaptic terminal. Perisynaptic receptors, in comparison with somatic receptors, are much more likely to be involved in synaptic transmission. At the parallel fibre to Golgi cell synapse, just three stimuli at 100Hz at room temperature were enough to affect the duration of EPSCs. Of course, whether this occurs at physiological temperature is unknown as one would have to take into consideration the differences in passive diffusion and glutamate uptake. It is also yet unknown what the average firing frequency of parallel fibres is *in vivo*. Granule cells are able to sustain high-frequency spiking (>100Hz; D'Angelo *et al*, 1995; D'Angelo *et al*, 2001; Cathala L, personal communication) and microelectrode recordings in anaesthetised cats have shown that the firing frequency of mossy fibre units can exceed 1000Hz (within bursts) in response to natural stimulation of the receptive fields (Garwicz *et al*, 1998; Ekerot and Jörntell, 2001).

Several studies have compared the properties of somatic NMDARs with those of synaptic ones. An immunocytochemical analysis of the localisation of NMDARs in cultured cortical neurons showed that NR2B subunits were present at both synaptic and extrasynaptic sites while NR2A subunits clustered preferentially at synaptic sites (Li *et al*, 1998). Rumbaugh and Vicini (1999) demonstrated that although synaptic currents from rat cerebellar granule cells became insensitive to the NR2B-selective inhibitor CP101,606 by P10, currents through nucleated patches were still highly sensitive after P18. But, Cathala *et al* (2000) reported a

loss in ifenprodil sensitivity of somatic NMDARs during the same stage of granule cell development. In adult rat dorsal horn neurons, somatic NMDAR channels were of the high-conductance type and were highly sensitive to ifenprodil. However, synaptic currents were unaffected by ifenprodil and exhibited decay kinetics indicative of NR2A-containing NMDARs (Momiyama, 2000). Furthermore, in a study by Tovar and Westbrook (1999), the ifenprodil sensitivity of whole-cell currents was compared with that of synaptic currents in cultured hippocampal neurons. At a developmental stage when NR2A is known to be expressed at these synapses, ifenprodil sensitivity was higher for whole-cell currents compared with synaptic currents. However, a whole-cell current includes the currents through all receptors and may still be largely dominated by somatic receptors. The current study shows that the boundary of the differential distribution of NR2A- and NR2B-NMDARs is likely to be close to the synapse, and that differential localisation of NMDARs can be of immediate relevance to synaptic transmission.

CHAPTER 5

ANALYSIS OF NMDARs IN WILD-TYPE AND NR2D-KNOCKOUT MICE

5.1 Summary

1. Single-channel openings activated by NMDA were recorded in outside-out patches excised from cerebellar Golgi cells of P7-10 wild-type and NR2D-knockout mice. Both high conductance (~50 and ~40pS) and low conductance (~40 and ~20pS) channels were resolved in wild-type Golgi cells, while patches from NR2D-knockout mice contained only high conductance openings.

2. Comparing the kinetic properties of high conductance openings between the two strains, we found the weighted mean open-period to be briefer in patches from wild-type Golgi cells (τ = 2.4 ± 0.2ms, n=15; NR2D-knockout, τ = 3.4 ± 1.5ms, n=14). The probability of a high conductance channel being open ($P_{OPEN(HIGH)}$) was thus significantly greater in NR2D-knockout (0.04 ± 0.004) than in wild-type (0.02 ± 0.004) mice.

3. The presence of NR2D also affected the pharmacological properties of high conductance openings. The ifenprodil sensitivity was greater in the absence of NR2D. In the presence of 0.1μM ifenprodil, $P_{OPEN(HIGH)}$ was reduced by only 31.2 ± 8.7% (n=7) in wild-type *vs* 58.9 ± 7.5% (n=8) in NR2D-knockout mice.

4. To investigate whether NR2D is involved in synaptic transmission, miniature EPSCs (mEPSCs) were recorded in cerebellar Golgi cells from P7-10 wild-type and NR2D-ablated mice. The amplitude, charge transfer and decay kinetics of the NMDAR-mediated component were found to be similar between the two animal strains. Furthermore, the amplitude and decay kinetics of sEPSCs were the same as those of mEPSCs.

5. We next investigated the ifenprodil sensitivity of sEPSCs and found that NMDAR-sEPSCs from wild-type and mutant mice were inhibited to the same extent by 0.1μM (21.4 ± 3.2% and 24.9 ± 7.7%, respectively) and 10μM ifenprodil (54.0 ± 11.2% and 51.8 ± 8.5%, respectively).

6. Trains of stimuli (5 stimuli at 50Hz) were used to activate a greater proportion of extrasynaptic receptors. No differences were found in the NMDAR-EPSC charge transfer, decay kinetics or ifenprodil sensitivity between wild-type and NR2D-knockout animals.

7. Taken together, these results are consistent with the presence of a distinct population of triheteromeric NR1/NR2B/NR2D channels in the somatic membrane of wild-type Golgi cells. The presence of NR2D in the receptor assembly altered the kinetic and pharmacological properties but had no effect on conductance levels. Furthermore, NR2D-containing receptors appear to be absent from synaptic and perisynaptic sites in cerebellar Golgi cells at this age.

5.2 Introduction

Previous work from this group demonstrated the functional expression of NR2D-containing NMDARs in the cell bodies of P14 rat Golgi cells (Misra *et al*, 2000a). *In situ* hybridisation studies have shown expression of the NR2D subunit in thalamic and midbrain areas and in interneurons throughout the brain, and expression levels are highest during embryonic and early postnatal development (Akazawa *et al*, 1994; Monyer *et al*, 1994; Watanabe *et al*, 1994; Dunah *et al*, 1996; Wenzel *et al*, 1996). NMDARs containing the NR2D subunit have several characteristic properties, such as very slow deactivation kinetics (Monyer *et al*, 1994; Wyllie *et al*, 1998; Misra *et al*, 2000b), a higher affinity for glutamate and a lower sensitivity to the voltage-dependent channel block by Mg^{2+} (Ikeda *et al*, 1992; Kuner and Schoepfer, 1996; see Table 1.1).

Low conductance (~30 and ~18pS) channel openings exhibiting asymmetry (i.e. there are more transitions from 30pS to 18pS than vice versa) were observed in somatic outside-out patches from Purkinje cells and deep cerebellar nuclei neurons (Momiyama *et al*, 1996). Comparison of these openings with the subsequent single-channel characterisation of NR1/NR2D receptors (Wyllie *et al*, 1998) supported that these were activations of NR2D receptors. Single-channel openings with similar properties have also been reported in somatic patches from cerebellar Golgi cells (Misra et al, 2000a), cerebellar stellate cells (Momiyama, Clark and Cull-Candy, unpublished observations), dorsal horn neurons (Momiyama, 2000) and hippocampal granule cells (Piña-Crespo and Gibb, 2002).

Further confirmation that these single-channel openings reflect activation of NR2D receptors can be obtained by analysing NR2D-knockout mice (Ikeda *et al*, 1995). We compared single-channel openings in somatic patches from P7-P10 Golgi cells of wild-type and NR2D-knockout mice. The single-channel conductance, kinetics and ifenprodil sensitivity of these openings were examined.

Although NR2D receptors have been shown to be present in the soma of several cell types, there is still no evidence for their presence at synapses. The very slow deactivation kinetics of currents through NR2D-containing NMDARs, of about 4 seconds (Wyllie *et al*, 1998; Misra *et al*, 2000b), does not correlate with the decay kinetics of synaptic currents. Because of this, it is generally believed that the NR2D subunit is excluded from synaptic sites and does not play a role in synaptic transmission. We decided to test for the presence of NR2D at synapses by comparing the kinetic and pharmacological properties of NMDAR-mediated synaptic currents in Golgi cells of wild-type and NR2D-knockout mice.

5.3 Results

5.3.1 *Single-channel analysis of outside-out patch recordings*

This section summarises the single-channel analysis results from joint experiments with Dr Charu Misra and Dr Stephen Brickley. My main contribution to this project is described in section 5.3.2 where the properties of synaptic NMDARs in wild-type and NR2D-knockout mice are compared.

5.3.1.1 *Single-channel conductance*

Single-channel recordings were carried out in nominally Mg^{2+}-free bathing solution containing 1mM Ca^{2+}, and in the presence of CNQX (5μM), bicuculline (10μM) and strychnine (500nM) to block non-NMDA-, GABA- and glycine receptors, respectively. At the holding potential of -60mV, steady state application of 10μM NMDA (together with 10μM glycine) to outside-out patches excised from the soma of P7-P10 Golgi cells activated discrete NMDAR single-channel openings. In wild-type mice, openings to the 50pS state were observed (53.5 ± 0.8pS; n=15). Many of these openings were associated with a brief ~40pS sub-conductance state characteristic of conventional 'high conductance' NMDAR-openings (reviewed in Cull-Candy *et al*, 2001). As is apparent in Figure 5.1A, 'low' conductance (40 and 20pS) NMDAR-openings were also resolved and were characterised by frequent direct transitions between levels. We have previously observed a similar pattern of NMDAR channel openings in *rat* Golgi cells (Misra *et al*, 2000a), and other central neurons (Momiyama *et al*, 1996). As in the rat, the occurrence of these low conductance openings was much less frequent than the

high conductance openings, reflecting the low open probability of this NR1/NR2D channel population (Wyllie *et al,* 1998; Misra *et al,* 2000a).

Time-course fitting of single-channel data revealed three discrete peaks in the amplitude histograms constructed from wild-type outside-out patches (Figure 5.1A, bottom left panel). Pooled data (from all patches) showed 48.9 ± 5.8% of openings were to the high conductance (50pS) state. Low conductance openings occurred in isolation (i.e. not linked to the high conductance 50pS state), indicating that they arose from a separate NMDAR population. Low conductance openings with mean conductance states of 43.4 ± 1.2pS and 23.1 ± 0.7pS were present in all patches examined (n=15) and resembled those previously described in outside-out patches from rat Golgi cells (Misra *et al*, 2000a). Moreover, when we analysed 1,113 direct transitions that occurred between the main- and sub-conductance state of the low conductance channels, 65.6 ± 2.5% arose as transitions from the 40 to the 20 pS state, corresponding well to the transition rate of 64 % reported previously for low conductance NMDAR-openings in rat Golgi- and Purkinje cells (Momiyama *et al*, 1996; Misra *et al*, 2000a).

As shown in Fig. 5.1B, in contrast to data from wild-type mice, amplitude histograms constructed from NMDAR single-channel openings from NR2D-knockout mice exhibited only high conductance openings (50pS, with infrequent sojourns to the 40pS sub-conductance state). On average, the main single-channel conductance in these cells was 53.9 ± 1.7pS (n=14) with a sub-conductance state of 46.3 ± 1.3pS (contributing less than 10% of the total number of events). The main and sub- conductance states were always linked by a direct transition, indicating that these two states arose from activation of a single type of NMDAR channel.

5.3.1.2 *Kinetic properties of high conductance NMDAR channels are modified in NR2D-knockout mice*

We next considered whether the kinetic properties of the high conductance openings were affected by the presence of the NR2D subunit. For the purpose of our analysis, we considered the open-period of the channel to be the total time it remained open at its various conductance levels between full closures. A full closure was deemed to have occurred once the channel had closed for a period exceeding twice the filter rise time. In the present study, we analysed the open-periods of the high conductance (50pS) openings (open-period$_{HIGH}$) in isolation by defining critical amplitudes that separate the high conductance (50pS) openings from the other (20/40pS) states. For example, the multiple peaks present in the wild-type data shown in Figure 5.1A (bottom left panel) were described by the sum of three Gaussian distributions. A critical amplitude (A_{crit}) was defined from the fit of these Gaussian distributions, such that >90% of openings (wild-type, 92 ± 1% *n*=14; NR2D-knockout, 91 ± 2 % n=14) were of the high conductance (50pS) type (see Howe *et al*, 1991).

It is worth noting that only a small proportion of events in the 40pS group will come from NR1/NR2D-like openings (i.e. the 20/40pS group) as this channel population has a low open probability (Wyllie *et al*, 1998; Misra *et al*, 2000a). For example, in 7 wild-type patches where a sufficient number of low- and high conductance openings were present within the same patch, time-course fitting of NMDAR channel openings demonstrated that the average proportion of low conductance (20/40pS) events was 8.0 ± 1.5 % (range 5.2 - 15.9%). Only a fraction of these events will then contribute to the 'misclassified openings' as the majority of the 40pS group arises from the sub-conductance state of the 50pS openings.

From a cursory examination of the single-channel currents in patches from wild-type and NR2D-knockout mice (Figure 5.2A and B), the kinetic properties of high conductance openings were clearly changed in the absence of the NR2D subunit. The high conductance NMDAR channel openings observed in wild-type patches were noticeably briefer than those observed in patches from the NR2D-knockout strain. Indeed, open $period_{HIGH}$ analysis demonstrated a significant difference in the kinetics of high conductance events in the two strains. This change in kinetics following loss of the NR2D subunit is evident in the open $period_{HIGH}$ distributions shown in Figure 5.1. For both strains, the distribution of open $period_{HIGH}$ was best described by a double exponential fit. When data from a wild-type animal was plotted on a logarithmic scale this distribution has two clear peaks. In contrast, though the distribution of open periods for high conductance openings from NR2D-knockout animals was also best described by a fast and slow component, the magnitude of the fast component was much reduced (see Figure 5.1B, bottom right). This was true for all NR2D-knockout patches. Consequently, in wild-type mice, the fast component (τ_{fast}= 732.6 ± 122.6μs; n=15) contributed 37.7 ± 5.6 % to the open-periods, whereas, in NR2D-knockout mice it contributed only 15.4 ± 5.8 % (τ_{fast} = 971.7 ± 203.6 μs; n=14). We found no significant change in the time constant of either the fast- or slow components (τ_{slow} = 3.3 ± 0.2 ms in wild-type, *vs* τ_{slow} = 3.8 ± 5.8 ms in NR2D-knockout mice). Therefore, at this concentration of NMDA (10 μM), the weighted mean open-period for high conductance events was τ = 2.4 ± 0.2 ms (n=15) in wild-type mice, compared with 3.4 ± 0.2 ms (n=14) in NR2D-knockout mice ($p < 0.01$, unpaired Student's t test).

As a result of the difference in open periods, the probability of a high conductance channel being open ($Popen_{HIGH}$) was significantly greater in NR2D-knockout

(0.04 ± 0.004) than in wild-type mice (0.02 ± 0.004; $p < 0.05$, unpaired Student's *t* test). This observation is consistent with the idea that the NR2D subunit co-assembles with NR2B to form a native triheteromeric NR1/NR2B/NR2D receptor with distinct single-channel kinetics, but with a conductance that is indistinguishable from the diheteromeric NR1/NR2B receptor. The frequency of the *high conductance* openings was also not significantly different between wild-type (8.5 ± 1.6 Hz) and NR2D-knockout (11.2 ± 1.8 Hz; $p > 0.2$, unpaired Student's *t* test) animals. Further, the shut-time distribution of high conductance events was similar between strains (data not shown). In both cases the shut-time distribution was well fitted with the sum of three exponential components, with weighted mean shut-times of τ = 133.2 ± 72.9 ms (n=14) for wild-type, and τ = 77.0 ± 13.1 ms (n=14) for NR2D-knockout animals. These values were not significantly different ($p > 0.4$, unpaired Student's *t* test).

5.3.1.3 *Ifenprodil sensitivity of high conductance openings is modified by NR2D*

Co-assembly of NR2B and NR2D subunits in Golgi cells might also be expected to influence the pharmacology of the high-conductance (NR2B-containing) receptor. We therefore examined the effect of the NR2B-selective antagonist ifenprodil on high-conductance openings activated by 10 μM NMDA. In patches from both wild-type and NR2D-knockout mice, 0.1μM ifenprodil caused a marked reduction in $Popen_{HIGH}$. However, as shown in Figure 5.2A, the degree of block was significantly greater in the absence of the NR2D subunit. Thus, comparison of the change in $P_{OPEN(HIGH)}$, following bath application of 0.1μM ifenprodil, revealed a reduction of only 31.2 ± 8.7% (n=7) in wild type *vs* 58.9 ± 7.5% (n=8) in NR2D-knockout mice.

Figure 5.2C illustrates the concentration-response relationship for the inhibitory action of ifenprodil, constructed from charge transfer analysis of all NMDAR openings (i.e. both high and low conductance) in patches from wild-type and NR2D-knockout mice. The low open probability and low single-channel conductance of the NR1/NR2D NMDARs would imply that they contribute little to the charge transfer data. To confirm this, we compared charge transfer and time-course fitting analysis on the same patches. The reduction in $P_{OPEN(HIGH)}$ was very similar to the reduction in the total charge transfer. When 0.1μM ifenprodil was applied to patches from wild-type mice, $P_{OPEN(HIGH)}$ analysis gave a reduction of 31±8%, while total charge transfer analysis gave a reduction of 30±7% (n=7). In NR2D-knockout mice, P_{OPEN} analysis gave a reduction of 60±9%, while total charge transfer analysis gave a reduction of 63±5% (n=7).

Concentration-response relationships for ifenprodil inhibition of NMDARs in patches from wild-type mice (Figure 5.2C) were best fitted with a modified form of the Hill equation with two IC_{50} components (see section 2.6.2). The identification of an additional component with apparent low affinity extends our previous observations on rat Golgi cell NMDARs which were fitted with a single component Hill equation (Misra *et al*, 2000a). In the present study, the IC_{50} value for the apparent high affinity component was 129nM with a Hill slope of 0.6, and $I_{max(H)}$ of 71.5%, whereas the apparent low affinity component had an IC_{50} of 45μM with a Hill slope of 1.8 and $I_{max(L)}$ of 28.5%. Although the high affinity component was present in both strains of mice, the lower affinity component was absent in patches from NR2D-knockout animals. Therefore, these data were best fitted with a single Hill equation (IC_{50} = 37 nM; Hill slope = 0.4). Once again, the reduced blocking action of ifenprodil in patches from wild-type mice is consistent with the

presence of a pharmacologically distinct population of channels, containing co-assembled NR2B and NR2D subunits.

In Chapter 3, we showed that the NR2A subunit contributes to the synaptic population of NMDARs later in Golgi cell development. To address the possibility that NR2A might contribute to the somatic NMDAR population in these cells, we examined the actions of the Zn^{2+} chelator TPEN on NMDAR channel openings in outside-out Golgi cell patches from P7-10 wild-type mice. Consistent with our data from the rat (Misra *et al*, 2000a), we found no significant change in charge transfer (-93 ± 57fC *vs* -117 ± 90fC; n=5) when patches were exposed to 1 μM TPEN.

Figure 5.1 *'Low' conductance openings were not observed in Golgi cell outside-out patches from NR2D knockout*

A, single-channel openings from an outside-out patch excised from a P8 wild-type Golgi cell and voltage-clamped at -60mV. NMDA (10μM) was applied in the presence of 10μM glycine, 10μM bicuculline, 1μM strychnine, and 5μM CNQX. Three conductance states were resolved and the histogram was best described by three Gaussian distributions (*bottom left*, corresponding to 50, 40 and 20pS). The open period distribution of high conductance openings (of amplitude greater than A_{crit}) was best fitted by two components, giving a weighted mean open period of 2.43 ± 0.21ms (n=15; *bottom right*).

B, the properties of single-channel openings recorded from outside-out patches from NR2D-knockout mice. The open point histogram shows that 'low' conductance openings were absent, resolving mainly 50pS openings (*bottom left*), and that the proportion of short open periods (*bottom right*) was smaller than for recordings from wild-type animals. The weighted mean open period was 3.42 ± 0.22ms (n=14).

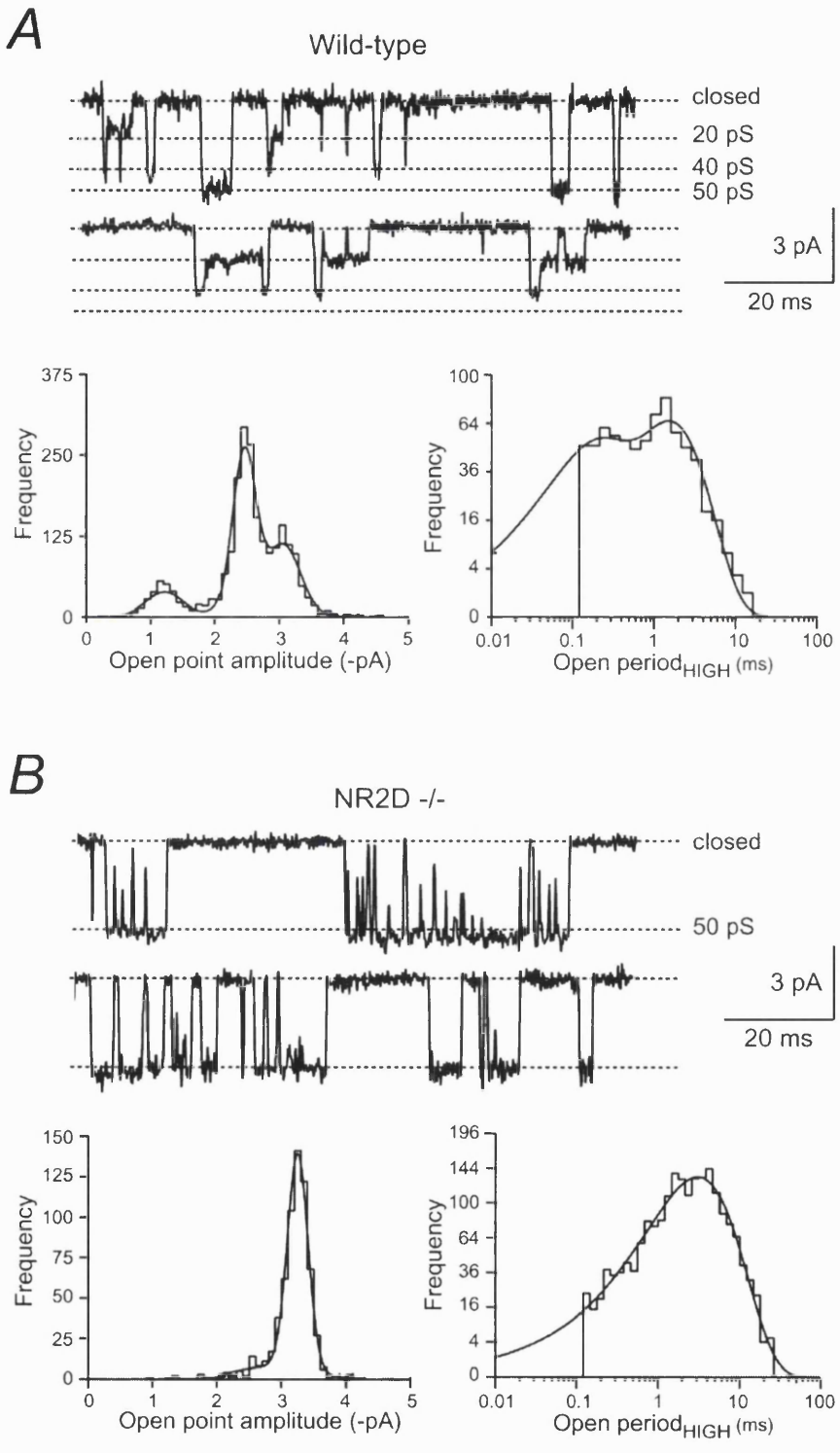
A
Wild-type
closed
20 pS
40 pS
50 pS
3 pA
20 ms
Frequency
375
250
125
0
0 1 2 3 4 5
Open point amplitude (-pA)
100
64
36
16
4
0
0.01 0.1 1 10 100
Open period HIGH (ms)
B
NR2D -/-
closed
50 pS
3 pA
20 ms
150
125
100
75
50
25
196
144
100
64
36
16

Figure 5.2 *Higher ifenprodil sensitivity of high conductance openings from NR2D-knockout Golgi cells compared with wild-type*

A, the effect of ifenprodil (0.1μM) on single-channel openings in somatic patches excised from wild-type (*right*) and NR2D-knockout (*left*) Golgi cells. Cursory inspection of the raw data suggested that ifenprodil at 0.1μM had a greater inhibitory effect on the charge transfer of openings from NR2D-knockout animals compared with wild-type.

B, in the presence of 0.1μM ifenprodil, high-conductance openings from NR2D-knockout Golgi cells were inhibited to a greater degree. $P_{open(HIGH)}$ was reduced by 31.2 ± 8.7% (n=7) in wild-type *vs* 58.9 ± 7.5% (n=8) in NR2D-knockout mice.

C, concentration-response relationship for the inhibitory effect of ifenprodil on high conductance single-channel openings from wild-type (*open circles*) and NR2D-knockout animals (*filled circles*). For the wild-type data, the relationship was best described by the sum of two Hill functions, giving a high-affinity component of IC_{50} = 129nM (Hill slope 0.6, $I_{max(H)}$ 71.5%) and a low-affinity component of IC_{50} = 45μM (Hill slope 1.8, $I_{max(H)}$ 28.5%). The concentration-response curve was shifted to the left, indicating a greater effect by ifenprodil on NR2D-knockout patches. Best described by a single Hill function, the IC_{50} of ifenprodil for NR2D-knockout Golgi cells was 37nM (Hill slope 0.4). For comparison, a data point showing the degree of ifenprodil block (0.1μM) for NMDARs recorded in migrating cerebellar granule cells (Misra *et al,* 2000a) has been added to this plot (*grey square*).

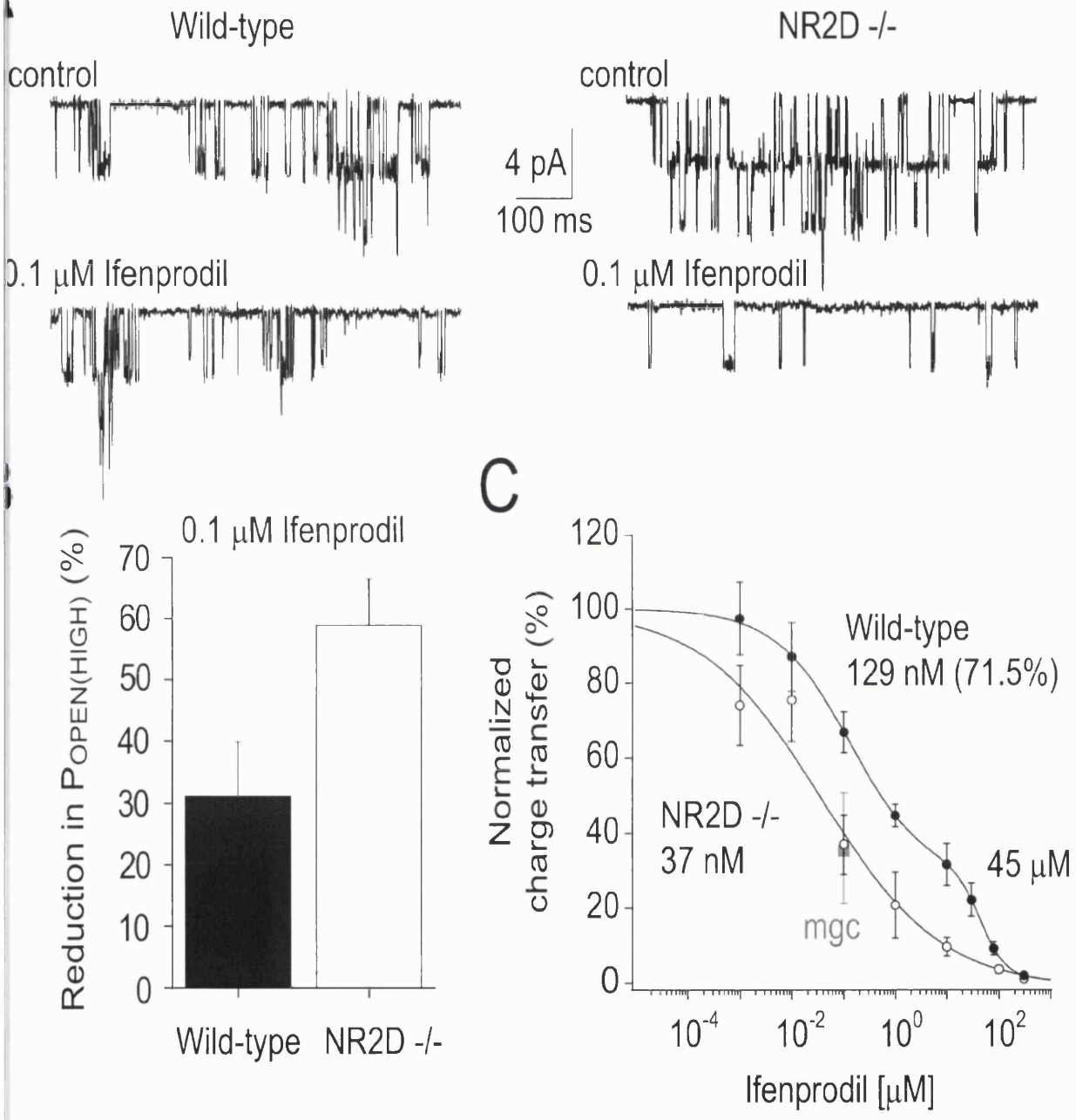
Wild-type
NR2D -/-
control
control
4 pA
100 ms
0.1 μM Ifenprodil
0.1 μM Ifenprodil
0.1 μM Ifenprodil
Reduction in POPEN(HIGH) (%)
70
60
50
40
30
20
10
0
Wild-type
NR2D -/-
C
Normalized charge transfer (%)
120
100
80
60
40
20
0
Wild-type
129 nM (71.5%)
NR2D -/-
37 nM
45 μM
mgc
10-4
10-2
100
102
Ifenprodil [μM]

5.3.2 *Comparing synaptic currents in wild-type and NR2D-knockout mice*

5.3.2.1 *Miniature EPSCs*

To test whether the NR2D subunit contributes to NMDARs involved in synaptic transmission, we first compared the properties of miniature EPSCs (mEPSCs) in Golgi cells of wild-type and NR2D-knockout mice (Figure 5.3). mEPSCs were recorded in Mg^{2+}-free bathing solution, in the presence of 0.5μM TTX, 10μM SR95531, 1μM strychnine and 10μM glycine at the holding potential of -30mV (Figure 5.3A and B). As summarised in Figure 5.3C and Table 5.1, we found no differences in: (a) mEPSC frequency; (b) NMDAR-mEPSC amplitude; (c) NMDAR-mEPSC charge transfer; (d) NMDAR-mEPSC decay time constant (single-component fit); and (e) non-NMDAR mEPSC amplitude. This suggests that the NR2D subunit does not significantly contribute to NMDAR-mediated quantal events in the Golgi cell.

5.3.2.2 *Comparing mEPSCs and sEPSCs*

Most granule cells are inactive in the slice (Cathala L and Brickley S, personal communication) as the mossy fibre inputs are severed and inhibition is still being mediated by spontaneously-firing Golgi cells. Spontaneously-occurring EPSCs recorded from Golgi cells are therefore likely to arise from action potential-independent release at parallel fibre terminals. Indeed, Dieudonné (1998) showed that sEPSCs are the same as mEPSCs in terms of non-NMDAR-mediated amplitude. We compared the NMDAR-mediated components of mEPSCs and sEPSCS in P7-10 Golgi cells.

The frequency of mEPSCs was approximately 20% lower than that of sEPSCs in wild-type Golgi cells (0.13 ± 0.03Hz (n=6) *vs* 0.18 ± 0.01Hz (n=3), respectively; $p > 0.1$, Mann-Whitney U). We found no differences between sEPSCs and mEPSCs recorded from wild-type Golgi cells in terms of the NMDAR-EPSC amplitude, charge transfer and decay time constant. The properties of the non-NMDAR component (peak amplitude, 10-90% rise and τ_w) were also similar between sEPSCs and mEPSCs (Table 5.1).

In a similar fashion, there were no significant differences between sEPSCs and mEPSCs from NR2D-knockout mice nor were there differences in sEPSCs between wild-type and NR2D-knockout mice (Table 5.1; $p > 0.05$, unpaired Student's *t* test or Mann-Whitney U). This indicates that Golgi cell sEPSCs are mostly quantal events.

5.3.2.3 *Ifenprodil sensitivity of sEPSCs*

We next compared the ifenprodil sensitivity of synaptic currents recorded from the two strains. Because of the higher frequency of sEPSCs, it was more practical to record sEPSCs rather than mEPSCs for this set of experiments. Ifenprodil (10μM) inhibited the NMDAR-sEPSC charge transfer by the same degree in wild-type and mutant mice (wild-type, 54.0 ± 11.2%, n=7; NR2D-knockout, 51.8 ± 8.5%, n=8; $p > 0.5$, unpaired Student's *t* test; Figure 5.4B). There was also no difference in the amount of inhibition by 0.1μM ifenprodil between wild-type and NR2D-ablated animals (wild-type, 21.4 ± 3.2%, n=3; NR2D-knockout, 24.9 ± 7.7%, n=5; $p > 0.6$, unpaired Student's *t* test). This result is also consistent with the idea that NR2D-containing receptors are not located at synaptic sites.

5.3.2.4 *High-frequency train stimulation: no differences in kinetic or pharmacological properties between wild-type and NR2D-knockout mice*

The possibility that NR2D-containing receptors are located perisynaptically prompted us to examine the properties of currents generated by a high frequency train of stimuli at parallel fibre-Golgi cell synapses. To activate a substantial proportion of extrasynaptic receptors, we decided to use a stimulation intensity that was twice threshold and to adopt a stimulation protocol of 5 stimuli at 50Hz. There was no significant difference in the charge transfer (wild-type, 9834 ± 2197fC, n=10; NR2D-knockout, 5702 ± 1047fC, n=7; $p > 0.1$, unpaired Student's *t* test) or in the decay kinetics (wild-type, 332.6 ± 49.0ms; NR2D-knockout, 236.3 ± 30.3ms; $p > 0.1$, unpaired Student's *t* test) of the train of NMDAR-EPSCs between the two strains. The sensitivity of the charge transfer to ifenprodil was the same between NR2D-ablated and wild-type animals, at both 0.1μM (wild-type, 5.4 ± 6.2%, n=9; NR2D-knockout, 25.2 ± 20.2%, n=5; $p > 0.3$, unpaired Student's *t* test) and 10μM (wild-type, 60.7 ± 7.2%, n=9; NR2D-knockout, 65.8 ± 10.4%, n=7; p>0.5, unpaired Student's *t* test; Figure 5.4B). This set of results suggest that, not only are NR2D-containing receptors absent from synaptic sites, but that they are also absent from perisynaptic locations.

Figure 5.3 *Golgi cell mEPSCs from NR2D-knockout mice were the same as mEPSCs from wild-type animals*

A, *left*, traces of mEPSC recordings from a P9 wild-type Golgi cell under control conditions (*top*) and in the presence of 50μM D-AP5 (*bottom*). This recording was made in the presence of 0.5μM TTX, 10μM SR93351, 1μM strychnine and 10μM glycine, at a holding potential of -30mV. *Right*, average waveform (of at least 100 individual mEPSCs) from the same recording under control conditions (*black*) and in 50μM D-AP5 (*grey*). *Inset*, The NMDAR-mediated component of the average mEPSC was best fitted by a single exponential and had a decay time constant (τ) of 94.6ms.

B, *left*, trace of mEPSC recording from a P7 NR2D-knockout Golgi cell under control conditions. *Right*, average waveform from the same recording under control conditions (*black*) and in 50μM D-AP5 (*grey*). *Inset*, The NMDAR-mediated component of the average mEPSC was best fitted by a single exponential and had a decay time constant (τ) of 75.8ms.

C, there were no differences between wild-type and NR2D-knockout animals in terms of mEPSC frequency, NMDAR amplitude, NMDAR charge transfer, NMDAR decay time-course and non-NMDAR amplitude. Each bar in the graph represents the value from mutant animals (n=8) expressed as a percentage of the mean value from wild-type mEPSC recordings (n=6).

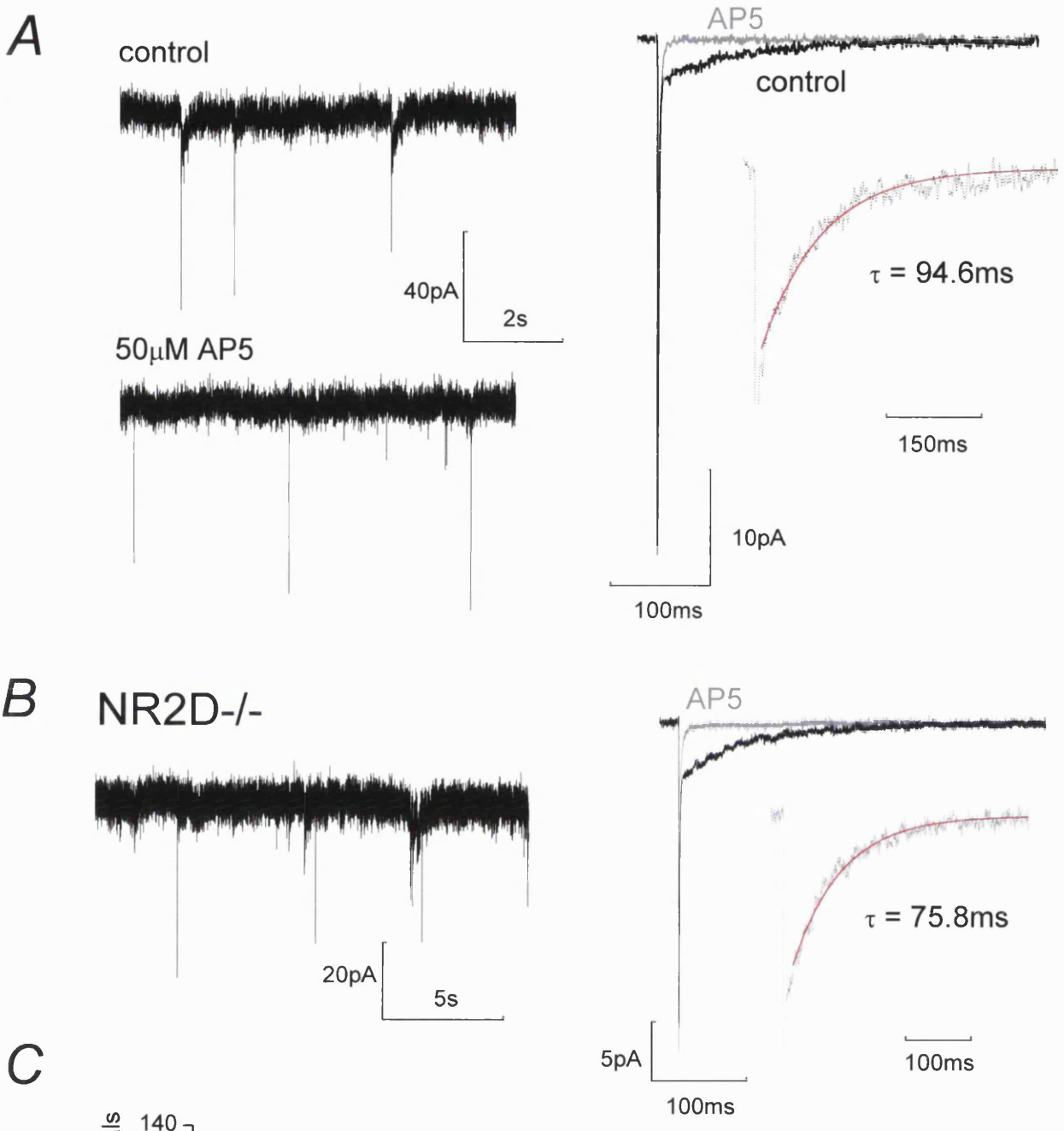
A
control
40pA
2s
50μM AP5
AP5
control
τ = 94.6ms
150ms
10pA
100ms
B
NR2D-/-
20pA
5s
AP5
τ = 75.8ms
5pA
100ms
100ms
C
% of mean value from wild-type animals
140
120
100
80
60
40
20
0
mEPSC frequency
NMDAR amplitude
NMDAR charge transfer
NMDAR decay time constant
non-NMDAR amplitude

Figure 5.4 *Ifenprodil sensitivity of sEPSCs and parallel fibre-Golgi cell EPSCs generated by 5 pulses at 50Hz*

A, EPSCs elicited by a train stimulus of 5 pulses at 50Hz (stimulation intensity, 15V above threshold) recorded from a P8 NR2D-knockout mouse. *black trace*, control conditions; *blue trace*, in 10μM ifenprodil; and *grey trace*, in 50μM D-AP5.

B, the degree of inhibition by 10μM ifenprodil was similar between sEPSCs and EPSCs produced by a train of stimuli. There were also no differences between the wild-type (*open bars*) and mutant (*grey bars*) animals.

A

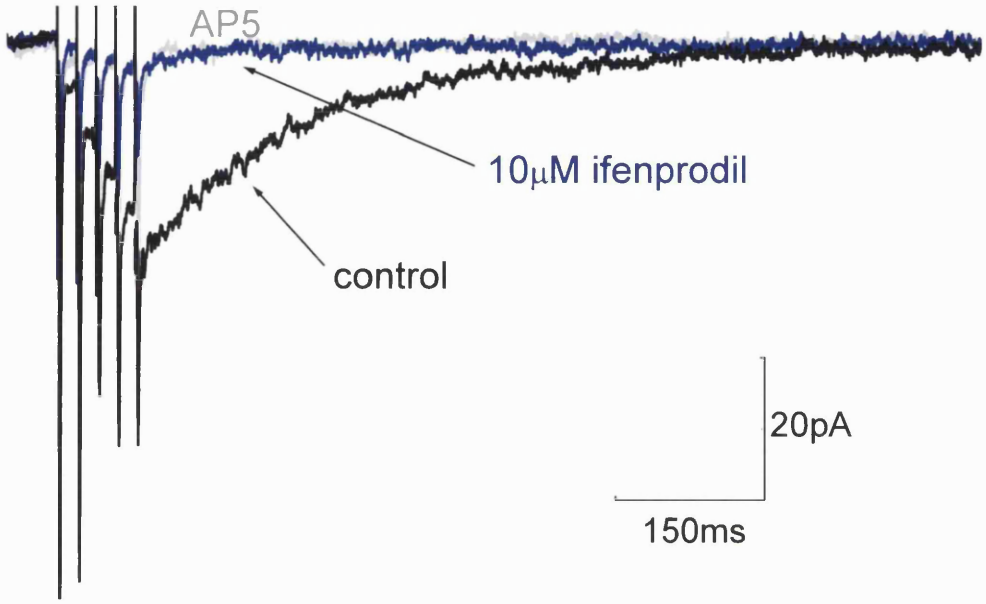
AP5
10μM ifenprodil
control
20pA
150ms

B

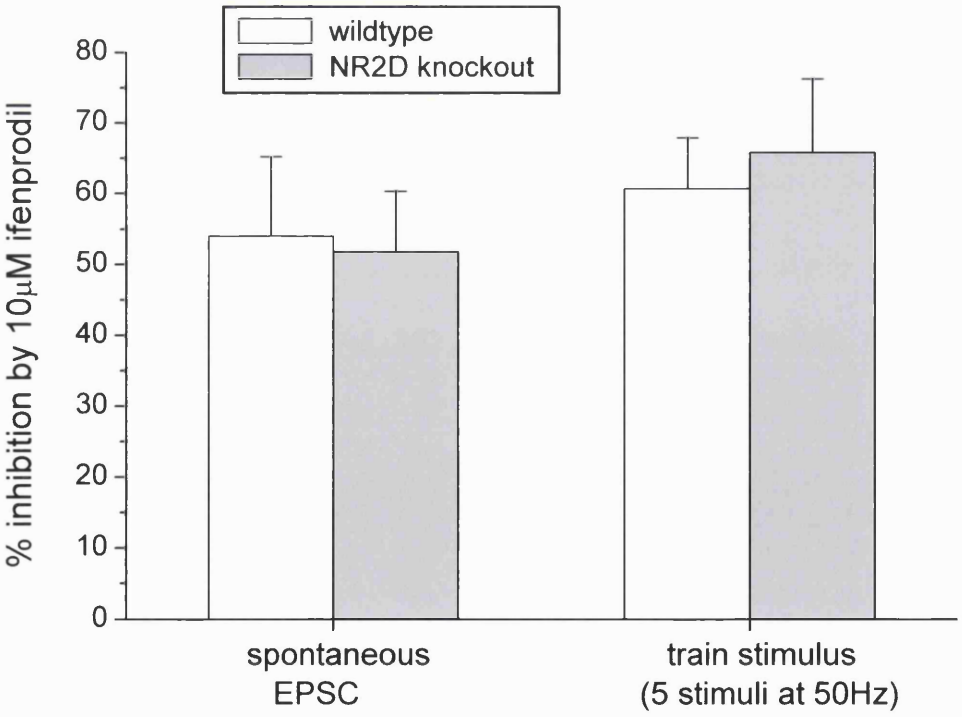
wildtype
NR2D knockout
% inhibition by 10μM ifenprodil
0
10
20
30
40
50
60
70
80
spontaneous EPSC
train stimulus (5 stimuli at 50Hz)

Table 5.1 *The kinetic properties of synaptic currents are similar between wild-type and NR2D-knockout mice, and between mEPSCs and sEPSCs*

		Wild-type	NR2D-knockout
mEPSCs	Frequency (Hz)	0.134 ± 0.03 (6)	0.133 ± 0.02 (8)
	NMDAR amplitude (pA)	-5.36 ± 1.87	-5.23 ± 0.60
	NMDAR charge transfer (fC)	842.4 ± 201.2	893.1 ± 157.7
	NMDAR decay τ (ms)	100.4 ± 6.2	86.0 ± 4.3
	Non-NMDAR amplitude (pA)	-30.9 ± 3.4	-33.2 ± 2.8
	Non-NMDAR 10-90% rise (μs)	365.7 ± 20.1	352.2 ± 23.6
	Non-NMDAR decay τ_w (ms)	1.45 ± 0.14	1.36 ± 0.14
sEPSCs	Frequency (Hz)	0.176 ± 0.01 (3)	0.175 ± 0.01 (8)
	NMDAR amplitude (pA)	-4.34 ± 1.24	-3.92 ± 0.29
	NMDAR charge transfer (fC)	-736.4 ± 268.0	-566.3 ± 100.7
	NMDAR decay τ (ms)	104.8 ± 24.7	106.5 ± 16.9
	Non-NMDAR amplitude (pA)	-26.4 ± 1.5	-28.1 ± 1.6
	Non-NMDAR 10-90% rise (μs)	433.7 ± 18.6	478.5 ± 34.4
	Non-NMDAR decay τ_w (ms)	1.83 ± 0.41	1.52 ± 0.15

Mean ± S.E.M. (number of cells)

No significant differences between wild-type and NR2D-knockout animals for all parameters analysed ($p > 0.1$, unpaired Student's t test or Mann-Whitney U). Also, no significant differences between mEPSC and sEPSC for both wild-type and NR2D-knockout Golgi cells ($p > 0.1$, unpaired Student's t test or Mann-Whitney U).

Table 5.2 *Ifenprodil sensitivity of synaptic and spillover currents from wild-type and NR2D-knockout mice*

		Wild-type	NR2D-knockout
sEPSCs	% inhibition by 0.1μM ifenprodil	21.4 ± 3.2 (3)	24.9 ± 7.7 (5)
	% inhibition by 10μM ifenprodil	54.0 ± 11.2 (7)	51.8 ± 8.5 (8)
High-frequency trains	% inhibition by 0.1μM ifenprodil	5.4 ± 6.2 (9)	25.2 ± 20.2 (5)
	% inhibition by 10μM ifenprodil	60.7 ± 7.2 (9)	65.8 ± 10.4 (7)

Number of cells in parentheses

No significant differences between wild-type and NR2D-knockout animals for all parameters analysed ($p>0.1$)

5.4 Discussion

5.4.1 *Summary of results*

Our experiments provide three main findings. First, they demonstrate that low-conductance NMDAR-channels are lost in cells that lack the NR2D subunit. Second, our analysis of the biophysical and pharmacological properties of NMDAR-channels in NR2D-knockout mice indicates that NR2D and NR2B co-assemble to form a population of functionally distinct receptors. Third, NR2D-containing receptors do not appear to be present at synapses in the Golgi cell. On comparison of synaptic currents of wild-type and NR2D-ablated animals, we found no differences in the magnitude or kinetics of the NMDAR-mediated component of mEPSCs. The ifenprodil sensitivity of synaptic currents was also comparable in the two strains. Furthermore, currents generated by high-frequency stimulation of parallel fibres revealed no biophysical or pharmacological differences between the two strains. This suggests that the NR2D subunit does not play a significant role in synaptic transmission in the Golgi cell, and that the NR2D subunit appears to be selectively expressed at somatic locations in the young (P7-P10) cerebellar Golgi cell.

5.4.2 *Functional expression of triheteromeric NMDARs*

Our previous experiments on rat cerebellar Golgi cells identified high-conductance (~50 pS) NMDAR-channels that are sensitive to the NR2B-selective antagonist ifenprodil, and low-conductance channels (20/40pS) that exhibit asymmetric gating between conductance states (Misra *et al*, 2000a), characteristic

of NR1/NR2D receptors (Wyllie *et al*, 1996). The present experiments indicate that mouse Golgi cells express a similar repertoire of NMDAR channels. Moreover, the selective loss of 20/40pS channels in Golgi cells lacking the NR2D subunit (while 50/40pS openings remain intact), provides direct evidence for the idea that these low-conductance NMDAR-channels constitute the native form of NR1/NR2D-subunit containing receptors (Momiyama *et al,* 1996; Misra *et al,* 2000a, 2000b).

In the present study, analysis of single-channel currents, recorded from cerebellar Golgi cells in wild-type and NR2D-knockout mice, directly demonstrated that expression of the NR2D subunit altered both the kinetics and ifenprodil sensitivity of high conductance NMDAR channels. This result suggests the existence of a triheteromeric assembly containing NR1/NR2B/NR2D subunits, implying that at least three types of NMDAR are present in cerebellar Golgi cell bodies at this stage of development. While NR1/NR2D and NR1/NR2B containing receptors gives rise to low (20/40pS) and high conductance events (50pS) respectively, the triheteromeric assembly (NR1/NR2B/NR2D) generates 50pS channels but with distinct kinetic behavior and pharmacological properties.

Immunoprecipitation and molecular studies suggest that more than one type of NR2 subunit can be contained within NMDAR assemblies (Sheng *et al.*, 1994; Chazot and Stephenson, 1997; Dunah *et al*, 1998). A growing body of evidence also supports the view that triheteromeric assemblies give rise to discrete receptor subtypes. For example, recombinant NMDARs in cells transfected with NR1, NR2A and NR2B subunits display reduced ifenprodil sensitivity (Vicini *et al*, 1998; Tovar and Westbrook, 1999; but see Kew *et al*, 1998). Patches from *Xenopus* oocytes co-transfected with NR1, NR2A and NR2D subunits exhibited

channels with direct transitions between low and high conductance states (~30, 40 & 50 pS; Cheffings and Colquhoun, 2000). However, despite the widespread distribution of the NR2D subunit in the CNS, it is not known whether triheteromeric NR2D- containing NMDAR assemblies exist *in vivo* and whether the inclusion of NR2D in such an assembly imparts distinct single-channel properties. These questions are particularly relevant to the developing nervous system, given that NR2D and NR2B are co-expressed in many immature neurons (Akazawa *et al*, 1995; Monyer *et al*, 1994; Watanabe *et al*, 1994). Furthermore, immunohistochemical data suggests that all NR2D-containing receptors in the adult midbrain may be triheteromeric (Dunah *et al*, 1998).

The expression of a functionally distinct triheteromeric receptor subtype clearly increases the potential for receptor diversity. In this context it is of interest that earlier studies have shown that recombinant triheteromeric receptors display properties intermediate between the NR2 subunits expressed. For example, NR1/NR2A/NR2B receptors exhibit a slow deactivation time and decreased haloperidol sensitivity (Vicini *et al*, 1998). Furthermore, NR1/NR2A/NR2D receptors display extended total activation times, but with reduced channel open probability, when compared with NR1/NR2A receptors (Cheffings and Colquhoun, 2000). Our observations suggest a similar phenomenon occurs with NR1/NR2B/NR2D receptors, since the presence of NR2D resulted in a significant decrease in open $period_{(HIGH)}$. However, unlike the recombinant NR1/NR2A/NR2D receptors (Cheffings & Colquhoun, 2000), we detected no additional conductance states for the native NR1/NR2B/NR2D assembly.

It is notable that in almost all neurons where NR2D (or NR2C) are expressed together with other NR2 subunits, only two types of single-channel openings have

been reported (Farrant *et al*, 1994; Momiyama *et al*, 1996; Takahashi *et al*, 1996; Plant *et al*, 1997; Misra *et al*, 2000a; Momiyama, 2000; but see Ebralidze *et al*, 1996). The high- (~50pS) conductance events are believed to arise from native NR2A- and NR2B-containing receptors, while low-conductance (38-18 pS) events arise from NR2C- and NR2D-containing receptors. Our experiments suggest that the absence of other conductance levels does not indicate a lack of triheteromeric receptors as NR1/NR2B/NR2D and NR1/NR2B assemblies exhibit similar single-channel conductances.

Not all low conductance events necessarily arise from NR1/NR2D or NR1/NR2C containing NMDARs. For example, there is compelling evidence that the NR3A subunit can co-assemble with NR1/NR2 receptors to produce a functionally distinct recombinant NR1/NR2A/NR3A receptor with low-conductance channel openings (Das *et al*, 1998; Perez-Otano *et al*, 2001). Therefore, it is only in the absence of NR3 (as in the cerebellum) that low-conductance NMDAR-openings provide an unambiguous *single-channel signature* for NR2C- or NR2D-containing diheteromeric receptors. In this respect it is notable that other native NMDAR channel conductance levels have been described, with subunit compositions that remain to be identified (Palecek *et al*, 1999). Also, in a recent study of NMDAR channels in neonatal rat hippocampal neurons thought to express NR2D, it has been suggested that a single type of triheteromeric receptor may switch between two states, giving rise both to *high* and *low* conductance modes (Piña-Crespo and Gibb, 2002). It is therefore conceivable that a proportion of the low conductance events observed in Golgi cells may reflect modal gating of the triheteromeric NR2D-containing receptor.

5.4.3 *NR2D-containing NMDARs are absent from Golgi cell synapses*

While the low conductance NR2C-containing NMDAR has been shown to participate in synaptic transmission at the mossy fibre-granule cell relay (Takahashi *et al*, 1996; Cathala *et al*, 2000), there is currently no evidence suggesting the presence of NR2D at any central synapse. If present at synapses, NR1/NR2D NMDARs might be recognized by their conspicuously slow decay which would last seconds rather than hundreds of milliseconds (Monyer *et al*, 1994; Vicini *et al*, 1998; Wyllie *et al*, 1998; Misra *et al*, 2000b). The current study demonstrates that high conductance openings from NR1/NR2B/NR2D assemblies should also exhibit altered deactivation kinetics compared with conventional NR1/NR2B ones. However, the kinetics of NMDAR-mediated miniature, spontaneous and evoked EPSCs were found to be no different in NR2D-knockout mice, suggesting that the NR2D subunit does not significantly contribute to synaptic currents in P7-P10 cerebellar Golgi cells. The ifenprodil sensitivity of the synaptic response was also unaffected. In addition, high frequency stimulation of parallel fibre inputs did not result in an NMDAR response with altered kinetics or pharmacology. This would suggest that those perisynaptic NMDARs activated by diffusion of glutamate also lacked the NR2D subunit. Therefore, NR2D-containing NMDARs do not appear to be targeted to the vicinity of parallel fibre-Golgi cell synapses at this age.

In Chapter 3 we showed a reduction in ifenprodil sensitivity of synaptic currents between P7-8 and P15-18 Golgi cells. We argued for the increased expression of NR2A at P15-18 as currents exhibited faster decay kinetics and increased sensitivity to TPEN at this age. Could this interpretation of our results be affected in light of the possibility of NR1/NR2B/NR2D receptors? Although the presence

of NR1/NR2B/NR2D receptors would reduce ifenprodil sensitivity (see Figure 5.2C), it is yet unknown how the presence of NR2D in triheteromeric receptors may affect the decay kinetics of macroscopic currents. Furthermore, it is very unlikely NR1/NR2B/NR2D receptors are sensitive to TPEN as the charge transfer of single-channel openings in wild-type outside-out patches were unaffected by 1μM TPEN (section 5.3.1.3). For the moment, the most likely interpretation of our results presented in Chapter 3 is that of a developmental increase in NR2A expression at Golgi cell synapses.

As mentioned in Chapters 1 and 4, the interactions between the carboxyl terminals of NR2 subunits and PSD proteins are now thought to be important in the targeting of NMDARs to synaptic sites. NR2A and NR2B subunits contain PDZ-binding motifs in their cytoplasmic tails that are involved in receptor delivery to the plasma membrane and targeting of these receptors to synaptic sites (Kornau *et al*, 1995; Niethammer *et al*, 1996; Steigerwald *et al*, 2000; Roche *et al*, 2001). The intracellular domains of NR2C and NR2D subunits are shorter by 150-200 amino acid residues (Ishii *et al*, 1993) and would therefore lack at least some of the PDZ-binding motifs. Perhaps this is the mechanism by which NR2D receptors are excluded from synapses.

NR2D expression is most prominent during embryonic and early postnatal development (Monyer *et al*, 1994; Watanabe *et al*, 1994; Dunah *et al*, 1996; Wenzel *et al*, 1996), suggesting participation in neuronal development. Although RNase protection experiments indicate two splice variants of the NR2D subunit (Ishii *et al*, 1993), only the NR2D-2 variant (corresponding to the sequence identified originally by Ikeda *et al*, 1992) has been detected in the brain (Wenzel

et al, 1996). The level of NR2D mRNA in the rat brain declines directly after birth while protein expression of NR2D continues to increase until P10 before declining (Wenzel *et al*, 1996). This suggests that NR2D expression may be regulated at the transcription level.

5.4.4 *Possible functional significance of NR2D-containing extrasynaptic receptors*

Although the properties of extrasynaptic NMDA receptors have been extensively studied, the function of these receptors remains largely unknown. Tonically-active NMDARs have been suggested to promote neuronal excitability (Sah *et al*, 1989). Due to their high glutamate affinity and low Mg^{2+} block sensitivity, NR1/NR2D receptors are likely to be activated by ambient levels of glutamate. Spontaneous Ca^{2+} oscillations in astrocytes have been linked to long-lasting NMDAR-mediated currents (with decay time constants of around 3 seconds) in thalamic neurons. As NR2D is abundantly expressed in these neurons in early postnatal development, it is possible that extrasynaptic NR2D-containing receptors are activated by Ca^{2+}-induced glutamate release from surrounding astrocytes (Parri *et al*, 2001).

Intense NR2D protein staining was recently reported in the hippocampal stratum lucidum, suggesting the expression of NR2D at presynaptic sites (Thompson *et al*, 2002). Indeed, presynaptic NMDARs have been described at cerebellar synapses. Glitsch and Marty (1999) demonstrated that the frequency of IPSCs recorded from Purkinje cells and stellate cells was reduced on perfusion of D-AP5. As molecular layer interneurons stain positive for NR2D mRNA (Akazawa *et al*, 1994) and low conductance channels indicative of NR1/NR2D receptors have been recorded in patches from stellate cells (Momiyama, Clark and Cull-Candy, unpublished observations), it is tempting to speculate that NR2D receptors may be located at

axon terminals. Indeed, I attempted to address this possibility of presynaptic NR2D receptors by examining the effect of D-AP5 on the frequency of miniature IPSCs recorded from deep cerebellar nuclei (DCN) neurons. Purkinje cells, which express NR2D and no other NR2 subunit during the first postnatal week (Akazawa *et al*, 1994; Momiyama *et al*, 1996), form GABAergic synapses onto DCN neurons. In terms of NR2D subunits, this would be a good system to test the hypothesis of NR2D presynaptic NMDARs. However, several practical complications arose. Principal neurons in the DCN are very large (whole-cell capacitance, 20-70pF) and have a substantial AP5-sensitive leak current. In the presence of D-AP5, more small-amplitude mIPSCs were detected, possibly due to the quieter baseline and improved resolution. This may underlie the observed increase in mIPSC frequency and we decided this system was not suitable for rigorous and reliable analysis of mIPSC frequency. Further complications included the heterogeneity of DCN neurons and the presence of interneurons within the DCN which may contribute to the mIPSCs recorded.

The possible significance of the NR2D subunit in behaviour has also been investigated in NR2D-knockout mice (Ikeda *et al*, 1995). Although general spontaneous activity was significantly lower than in heterozygous littermates, no abnormality was detected in motor activity or anxiety. The disruption of NR2D expression was suggested to affect the formation of whisker-related patterns as this subunit is highly expressed in the embryonic and neonatal brainstem. However, no difference was found, either because the NR2D subunit is not involved in this process or because of compensatory mechanisms. No gross differences were found in the mRNA expression of NR1, NR2A, NR2B or NR2C. Nevertheless, it is very interesting to note that NR2D may be linked to schizophrenia. A relative 50% increase in the level of NR2D mRNA was observed

in the prefrontal cortex of schizophrenics (Akbarian *et al*, 1996). It still remains to be seen what functions the NR2D subunit holds, and by what mechanisms the selective expression or exclusion of the NR2D subunit is controlled.

CHAPTER 6

GENERAL DISCUSSION

6.1 *NMDA receptors in the cerebellar Golgi cell: differential localisation and developmental changes*

Taking together the results of Chapters 3, 4 and 5, we summarise the differential localisation of NMDARs in the cerebellar Golgi cell during the first three weeks of murine postnatal development (Figure 6.1). At the end of the first postnatal week (P7-8), NR2B receptors dominate at (parallel fibre-) Golgi cell synapses. Meanwhile, NR1/NR2B, NR1/NR2D and NR1/NR2B/NR2D receptors are functionally expressed on the cell body. Furthermore, the NR2D subunit appears to be absent from synaptic and perisynaptic locations.

At the beginning of the third postnatal week (P15-18), NR2A-containing receptors (either diheteromeric NR1/NR2A or triheteromeric NR1/NR2A/NR2B ones) participate in synaptic transmission. However, this change in the subunit composition of NMDARs from mainly NR2B-NMDARs to more NR2A-containing receptors does not occur in the perisynaptic membrane. At both P7-8 and P15-18, NMDARs located in the periphery of parallel fibre-Golgi cell synapses are of the NR2B subtype. This study shows that synaptic NMDARs are developmentally regulated and that a number of NMDAR subtypes are differentially distributed in the mouse cerebellar Golgi cell. Further work is needed to elaborate on this characterisation and to ascertain what specific roles these NMDAR subtypes may serve in the function of central neurons.

Figure 6.1 *Summary of the different NMDAR subtypes functionally expressed in the cerebellar Golgi cell*

At P7-8 (top), properties of the synaptic currents indicate that NR2B receptors dominate at Golgi cell synapses. It also appears that these receptors are present perisynaptically and can be activated by a high-frequency train of stimuli. Single-channel recordings provide evidence for the functional expression of three NMDAR subtypes in the cell soma: NR1/NR2B, NR1/NR2D and NR1/NR2B/NR2D.

At P15-18 (bottom), changes in the properties of synaptic currents are consistent with an increase in NR2A-containing NMDARs at Golgi cell synapses. This change in subunit composition appears to be targeted at synapses. Perisynaptic NMDARs remain of the NR2B subtype.

P7-8

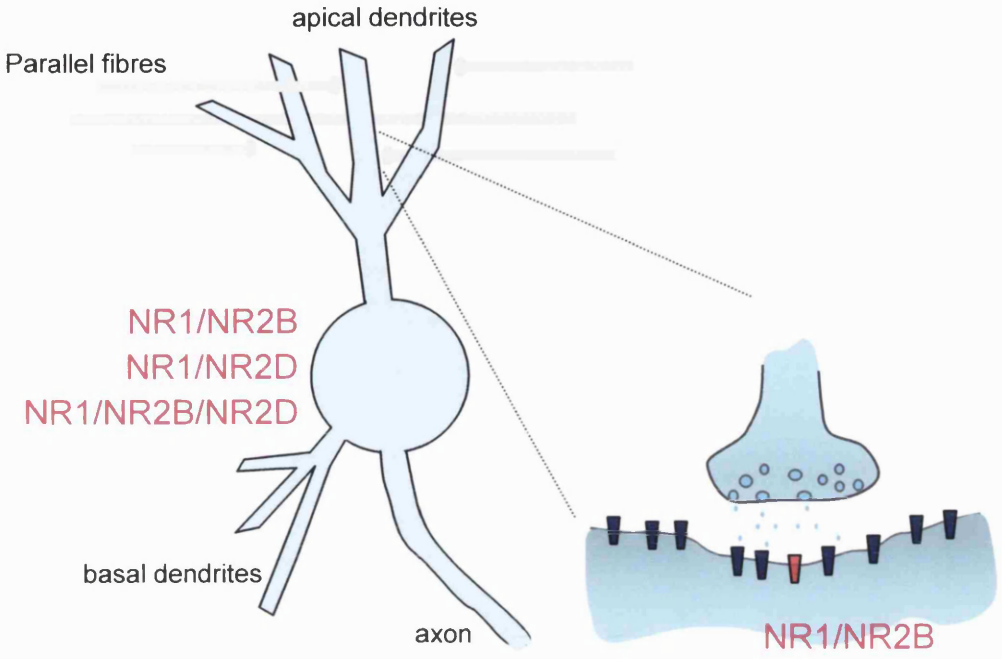
apical dendrites
Parallel fibres
NR1/NR2B
NR1/NR2D
NR1/NR2B/NR2D
basal dendrites
axon
NR1/NR2B

P15-18

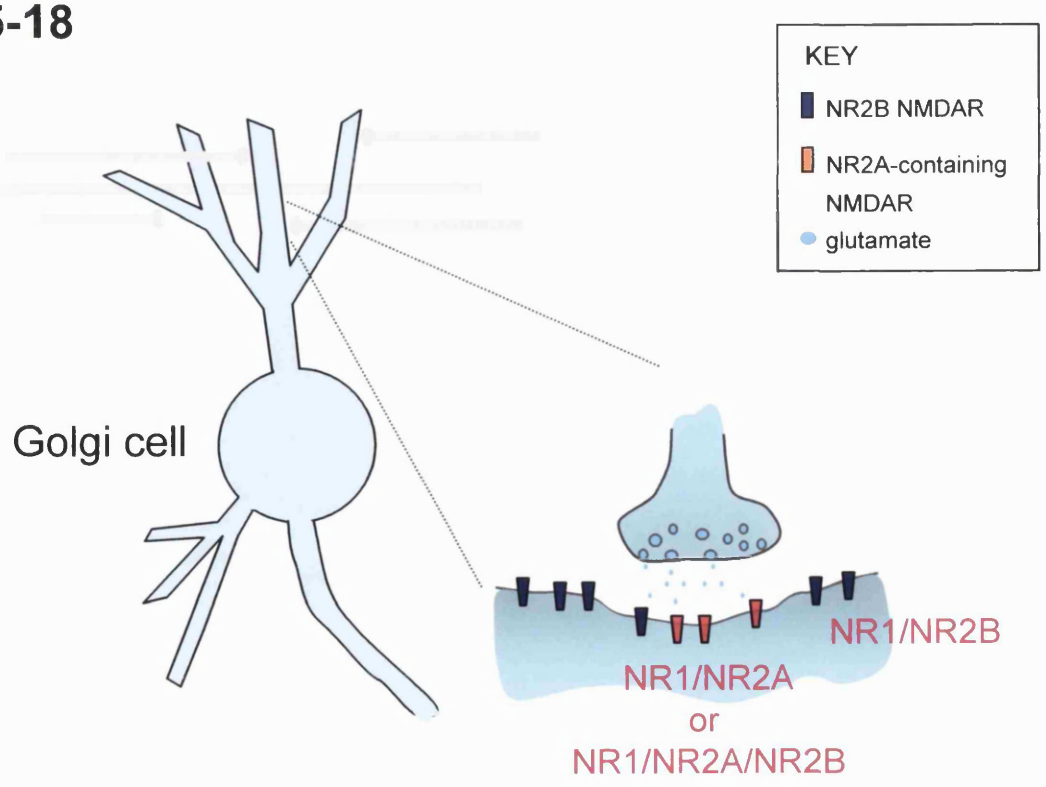
KEY
NR2B NMDAR
NR2A-containing NMDAR
glutamate
Golgi cell
NR1/NR2B
NR1/NR2A
or
NR1/NR2A/NR2B

6.2 *Possible future directions*

A number of interesting points have arisen from the work presented in this thesis. Further investigation of these questions would not only elaborate on the properties of NMDARs, it would also provide us with a more detailed picture of the cerebellar Golgi cell.

- NR1/NR2A receptors have been shown to be tonically inhibited by Zn^{2+} (Paoletti *et al*, 1997) but are not sensitive to the antagonist ifenprodil (Williams, 1993). We showed in section 3.3.4.3 that, at P15-18, percentage inhibition of synaptic NMDARs by ifenprodil was greater in the presence of the Zn^{2+} chelator TPEN. In order to interpret this result in terms of possible coassembly of NR2A and NR2B, we need to know whether NR2A-containing receptors are sensitive to inhibition by ifenprodil when tonic Zn^{2+} inhibition has been removed. As ifenprodil inhibition of NR2B receptors and (the voltage-independent component of) Zn^{2+} inhibition of NR2A receptors are thought to act by enhancing proton sensitivity (Mott *et al*, 1998; Choi and Lipton, 1999; Low *et al*, 2000; Zheng *et al*, 2001), interactions between Zn^{2+} inhibition and ifenprodil inhibition are plausible.

To address this question, one could investigate whether recombinant NR1/NR2A receptors become sensitive to ifenprodil inhibition in the presence of TPEN (i.e. in the absence of Zn^{2+}). It would also be interesting to see if recombinant NR1/NR2A/NR2B receptors are sensitive to high-affinity voltage-independent inhibition by Zn^{2+}, and if so, whether this Zn^{2+} inhibition affects the receptors' sensitivity to ifenprodil.

- It would also be interesting to investigate further the role of glutamate transporters in determining the kinetics and magnitude of synaptic currents in the Golgi cell. First of all, experiments would have to be conducted at physiological temperature as glutamate uptake is highly temperature-dependent. As we saw in section 4.3.5, bath perfusion of the glutamate transporter inhibitor TBOA was detrimental to Golgi cells in slices from P15-18 mice. Local perfusion of TBOA in the vicinity of the stimulation electrode would be a less invasive method. As the stimulation electrode is usually placed on the surface of the molecular layer, it is likely that TBOA will easily diffuse to the synapses being activated.

- I am also very curious as to whether the NMDAR-mediated component affects the properties of excitatory postsynaptic potentials (EPSPs) in Golgi cells. How do the developmental changes in the size and the duration of the NMDAR current affect the shape of the EPSP? To address this, one could record EPSPs in current-clamp (at physiological temperature) and see how the NMDAR antagonist D-AP5 affects the amplitude and decay kinetics.

- Are extrasynaptic NMDARs activated by high-frequency bursts of stimuli at physiological temperature? Furthermore, how does the activation of perisynaptic NMDA receptors affect Golgi cell firing?

The first question can be addressed by repeating, at physiological temperature, the experiments outlined in Chapter 4. The second question may be a little more difficult to answer. In current-clamp at physiological temperature, one could record Golgi cell firing in response to a train of afferent stimuli. As synaptic NMDARs are relatively insensitive to ifenprodil at P15-18, one could explore how ifenprodil affects the firing response at this age. A complication does arise

because the Golgi cell also expresses many NR2B-NMDARs on the cell body. Inhibition of these receptors by ifenprodil may affect cell excitability by making the cell membrane less leaky. To circumvent this complication, one could locally perfuse ifenprodil along the parallel fibres in the vicinity of the stimulation electrode.

- Another aspect of synaptic transmission I would be interested in investigating is whether Golgi cell synapses are plastic. In light of the possibility of LTP at the mossy fibre-granule cell synapse (D'Angelo *et al*, 1999) and activity-induced changes in AMPA receptor calcium permeability at the parallel fibre-stellate cell synapse (Liu and Cull-Candy, 2000), it would be interesting to further test the possibility of activity-dependent changes at Golgi cell synapses. Preliminary work suggests that the parallel fibre-Golgi cell synapse does not undergo LTP. No changes to synaptic currents were observed in response to theta-burst or sustained stimulation.

- The Golgi cell in the cerebellum expresses a wide variety of glutamate receptors. Besides AMPA and NMDA receptors, the Golgi cell also expresses kainate receptors and metabotropic glutamate receptors. Kainate receptors have been reported to be activated by synaptic activity at the parallel fibre-Golgi cell synapse (Bureau *et al*, 2000). Golgi cells express the metabotropic glutamate receptors mGluR2 and mGluR5, as supported by immunostaining and radioligand binding studies (Neki *et al*, 1996; Knoflach *et al*, 2001). The mGluR2 receptors are located on the cell bodies and the proximal parts of their dendrites, while mGluR5 immunoactivity could be traced throughout the molecular layer (Neki *et al*, 1996). Indeed, mGluRs have been shown to play a role in synaptic transmission at the Golgi cell to granule cell synapse (Mitchell and Silver, 2000)

and it is possible that parallel fibre activity can activate mGluR5. Further work would be required to elucidate whether kainate receptors and mGluRs modulate synaptic activity or synaptic plasticity in the cerebellar Golgi cell.

REFERENCES

AND

BIBLIOGRAPHY

Aizenman E, Lipton SA & Loring RH (1989) Selective modulation of NMDA responses by reduction and oxidation. *Neuron* **2**: 1257-1263

Akazawa C, Shigemoto R, Bessho Y, Nakanishi S, Mizuno N (1994) Differential expression of five *N*-methyl-D-aspartate receptor subunit mRNAs in the cerebellum of developing and adult rats. *J Comp Neurol* **347**:150-160

Akbarian S, Sucher NJ, Bradley D, Tafazzoli A, Trinh D, Hetrick WP, Potkin SG, Sandman CA, Bunney WE Jr & Jones EG (1996) Selective alterations in gene expression for NMDA receptor subunits in prefrontal cortex of schizophrenics. *J Neurosci* **16**:19-30

Albus JS (1971) A theory of cerebellar function. *Math Biosci* **10**:25-61

Altman J & Bayer SA (1997) Development of the cerebellar system in relation to its evolution structure and functions. CRC Press, Boca Raton, USA.

Arnth-Jensen N, Jabaudon D & Scanziani M (2002) Cooperation between independent hippocampal synapses is controlled by glutamate uptake. *Nature Neurosci* **5**:325-331

Arriza JL, Fairman WA, Wadiche JI, Murdoch GH, Kavanaugh MP & Amara SG (1997) Functional comparisons of three transporter subtypes cloned from human motor cortex. *J Neurosci* **14**:5559-5569

Arriza JL, Eliasof S, Kavanaugh MP & Amara SG (1997) Excitatory amino acid transporter 5, a retinal glutamate transporter coupled to a chloride conductance. *Proc Natl Acad Sci USA* **4**:4155-4160

Arslan P, Di Virgilio F, Beltrame M, Tsien RY, Pozzan T (1985) Cytocolic Ca^{2+} homeostasis in Ehrlich and Yoshida carcinomas. *J Biol Chem* **260**:2719-2727

Assaf SY & Chung SH (1984) Release of endogenous Zn^{2+} from brain tissue during activity. *Nature* **308**:734-736

Asztely F, Erdemli G & Kullmann DM (1997) Extrasynaptic glutamate spillover in the hippocampus: dependence on temperature and the role of active glutamate uptake. *Neuron* **18**:281-293

Atluri PP & Regehr WG (1998) Depayed release of neurotransmitter from cerebellar granule cells. *J Neurosci* **18**:8214-8227

Barbour B, Keller BU, Llano I & Marty A (1994) Prolonged presence of glutamate during excitatory synaptic transmission to cerebellar Purkinje cells. *Neuron* **12**:1331-1343

Barria A & Malinow R (2002) Subunit-specific NMDA receptor trafficking to synapses. *Neuron* **35**:345-353

Barth AL & Malenka RC (2001) NMDAR EPSC kinetics do not regulate the critical period for LTP at thalamocortical synapses. *Nature Neurosci* **4**:235-236

Baude A, Nusser Z, Roberts JD, Mulvihill E, McIllinney RA & Somogyi P (1993) The metabotropic glutamate receptor (mGluR1α) is concentrated at perisynaptic membrane of neuronal subpopulations as detected by immunogold reaction. *Neuron* **11**: 771-787

Bear MF & Malenka RC (1994) Synaptic plasticity: LTP and LTD. *Curr Op Neurobiol* **4**: 389-399

Béhé P, Stern P, Wyllie DJA, Nassar M, Schoepfer R & Colquhoun D (1995) Determination of NMDA NR1 subunit number in recombinant NMDA receptors. *Proc R Soc Lond Ser B* **262**:205-213

Bennett JA & Dingledine R (1995) Topology profile for a glutamate receptor: three trans-membrane segments and a channel-lining re-entrant membrane loop. *Neuron* **14**:373-384

Benveniste M & Mayer ML (1993) Multiple effects of spermine on *N*-methyl-D-aspartatic acid receptor responses of rat cultured hippocampal neurons. *J Physiol* **464**:131-163

Berger ML & Rebernik P (1999) Zinc and ifenprodil allosterically inhibit two separate polyamine-sensitive sites at *N*-methyl-D-asparate receptor complex. *J Pharmacol Exp Ther* **289**:1584-1591

Bergles DE & Jahr CE (1997) Synaptic activation of glutamate transporters in hippocampal astrocytes. *Neuron* **19**:1297-1308

Bergles DE, Diamond JS & Jahr CE (1999) Clearance of glutamate inside the synapse and beyond. *Curr Opin Neurobiol* **9**:293-298

Bettler B & Mulle C (1996) Review: Neurotransmitter receptors. II. AMPA and kainate receptors. *Neuropharmacology* **34**:123-139

Billups D, Liu Y-B, Birnstiel S & Slater NT (2002) NMDA receptor-mediated currents in rat cerebellar granule and unipolar brush cells. *J Neurophysiol* **87**:1948-1959

Bliss TVP & Lømo T (1973) Long-lasting potentiation of synaptic transmission in the dentate area of the anaesthetized rabbit following stimulation of the perforant pathway. *J Physiol* **232**:331-356

Bliss TVP & Collingridge GL (1993) A synaptic model of memory: long-term potentiation in the hippocampus. *Nature* **361**:31-39

Borges K & Dingledine R (1998) AMPA receptors: molecular and fuctional diversity. *Prog Brain Res* **116**:140-157

Brasjno G & Otis TS (2001) Neuronal glutamate transporters control activation of postsynaptic metabotropic glutamate receptors and influence cerebellar long-term depression. *Neuron* **31**:607-616

Brimecombe JC, Boeckman FA & Aizenman E (1997) Functional consequences of NR2 subunit composition in single recombinant *N*-methyl-D-aspartate receptors.

Bureau I, Dieudonne S, Coussen F & Mulle C (2000) Kainate receptor-mediated synaptic currents in cerebellar Golgi cells are not shaped by diffusion of glutamate. *Proc Natl Acad Sci USA* **94**:11019-11024

Burnashev N, Monyer H, Seeburg PH & Sakmann B (1992a) Divalent ion permeability of AMPA receptor channels is dominated by the edited form of a single subunit. *Neuron* **8**:189-198

Burnashev N, Schoepfer R, Monyer H, Ruppersberg JP, Gunther W, Seeburg PH & Sakmann B (1992b) Control by asparagines residues of calcium permeability and magnesium blockade in the NMDA receptor. *Science* **257**:1415-1419

Carmignoto G & Vicini S (1992) Activity-dependent decrease in NMDA receptor responses during development of the visual cortex. *Science* **258**:1007-1011

Carroll RC, Lissin DV, von Zastrow M, Nicoll RA & Malenka RC (1999) Rapid redistribution of glutamate receptors contributes to long-term depression in hippocampal cultures. *Nature Neurosci* **2**:454-460

Carter AG & Regehr WG (2000) Prolonged synaptic currents and glutamate spillover at the parallel fiber to stellate cell synapse. *J Neurosci* **20**:4423-4434

Carter AG & Regehr WG (2002) Quantal events shape cerebellar interneuron firing. Nature Neurosci 5:1309-1317

Carter CJ, Lloyd KG, Zivkovic B & Scatton B (1990) Ifenprodil and SL 82.0715 as cerebral antiischemic agents. III. Evidence for antagonistic effects at the polyamine modulatory site within the *N*-methyl-D-aspartate receptor complex. *J Pharmacol Exp Ther* **253**:475-482

Cathala L, Misra C & Cull-Candy SG (2000) Developmental profile of the changing properties of NMDA receptors at cerebellar mossy fiber-granule cell synapses. *J Neurosci* **20**:5899-5905

Chapman PF, Atkins CM, Allen MT, Haley JE & Steinmetz JE (1992) Inhibition of nitric oxide synthesis impairs two different forms of learning. *Neuroreport* **3**:567-570

Chaudry FA, Lehre KP, van Lookeren-Campagne M, Ottersen OP, Danbolt NC & Storm-Mathisen J (1995) Glutamate transporters in glial plasma membranes: highly differentiated localizations revealed by quantative ultrastructural immuno-cytochemistry. *Neuron* **15**:711-720

Chazot PL, Coleman SK, Cik M & Stephenson FA (1994) Molecular characterisation of *N*-methyl-D-aspartate receptors expressed in mammalian cells yields evidence for the coexistence of three subunit types within a discrete receptor molecule. *J Biol Chem* **269**:24403-24409

Chazot PL & Stephenson FA (1997) Molecular dissection of native mammalian forebrain NMDA receptors containing the NR1 C2 exon: direct demonstration of NMDA receptors comprising NR1, NR2A and NR2B subunit within the same complex. *J Neurochem* **69**:2138-2144

Cheffings CM & Colquhoun D (2000) Single channel analysis of a novel NMDA channel from *Xenopus* oocytes expressing recombinant NR1a, NR2A and NR2D subunits. *J Physiol* **526**:481-491

Chen L & Huang L-YM (1992) Protein kinase C reduces Mg^{2+} block of NMDA-receptor channels as a mechanism of modulation. *Nature* **356**:521-523

Chen N, Moshaver A & Raymond LA (1997) Differential sensitivity of recombinant N-methyl-D-aspartate receptor subtypes to zinc inhibition. *Mol Pharmacol* **51**:1015-1023

Chen S & Diamond JS (2002) Synaptically released glutamate activates extra-synaptic NMDA receptors on cells in the ganglion cell layer of rat retina. *J Neurosci* **22**:2165-2173

Chenard BL, Bordner J, Butler TW, Chambers LK, Collins MA, De Costa DL, Ducat MF, Dumont ML, Fox CB, Mena EE, Menniti FS, Nielson J, Pagnozzi MJ, Richter KEG, Ronau RT, Shalaby IA, Stemple JZ & While WF (1995) (1*S*,2*S*)-1-(4-hydroxyphenyl)-2-(4-hydroxy-4-phenylpiperidino)-1-propanol: a potent neuroprotectant which blocks *N*-methyl-D-aspartate responses. *J Med Chem* **38**:3138-3145

Choi DW (1995) Calcium: still center-stage in hypoxic-ischemic neuronal death. *Trends Neurosci* **18**:58-60

Choi Y-B, Chen H-SV & Lipton SA (2001) Three pairs of cysteine residues mediate both redox and Zn^{2+} modulation of the NMDA receptor. *J Neurosci* **21**:392-400

Christine CW & Choi DW (1990) Effect of zinc on NMDA receptor-mediated channel currents in cortical neurons. *J Neurosci* **10**:108-116

Church J, Fletcher EJ, Baxter K & MacDonald JF (1994) Blockade by ifenprodil of high voltage-activated Ca^{2+} channels in rat and mouse cultured hippocampal pyramidal neurones: comparison with *N*-methyl-D-aspartate receptor antagonist actions. *Br J Pharmacol* **113**:499-507

Ciabarra AM, Sullivan JM, Gahn LG, Pecht G, Heinemann S & Sevarino KA (1995) Cloning and characterisation of χ-1: A developmentally regulated member of a novel class of the ionotropic glutamate receptor family. *J Neurosci* **15**:6498-6508

Clark BA, Farrant M & Cull-Candy SG (1997) A direct comparison of the single-channel properties of synaptic and extrasynaptic NMDA receptors. *J Neurosci* **17**:107-116

Clark BA & Cull-Candy SG (2002) Activity-dependent recruitment of extrasynaptic NMDA receptor activation at an AMPA receptor-only synapse. *J Neurosci* **22**:4428-4436

Clark GD, Clifford DB & Zorumski CF (1990) The effect of agonist concentration, membrane voltage and calcium on *N*-methyl-D-aspartate receptor desensitisation. *Neuroscience* **39**:787-797

Clements JD, Lester RAJ, Tong G, Jahr CE & Westbrook, GL (1992) The time course of glutamate in the synaptic cleft. *Science* **258**:1498-1501

Clements JD (1996) Transmitter timecourse in the synaptic cleft: its role in central synaptic function. *Trends Neurosci* **19**:163-171

Collingridge GL, Kehl SJ & McLennan H (1983) Excitatory amino acids in synaptic transmission in the Schaffer-collateral commissural pathway of the rat hippocampus. *J Physiol* **334**:33-46

Collingridge GL & Lester RA (1989) Excitatory Amino acid receptors in the vertebrate central nervous system. Pharmacol Rev 40:143-210

Collingridge GL & Watkins JC (1994) The NMDA receptor. Oxford University Press

Conn PJ & Pin JP (1997) Pharmacology and functions of metabotropic glutamate receptors. *Annu Rev Pharmacol Toxicol* **37**:205-37

Conti F and Weinberg RJ (1999) Shaping excitation at glutamatergic synapses. *Trends Neurosci* **22**:451-458

Cull-Candy SG & Usowicz MM (1987) Multiple conductance channels activated by excitatory amino acids in cerebellar neurons. *Nature* **325**:525-28

Cull-Candy SG, Brickley SG, Misra C, Feldmeyer D, Momiyama A & Farrant M (1998) NMDA receptor diversity in the cerebellum: identification of subunits contributing to functional receptors. *Neuropharmacology* **37**:1369-1380

Cull-Candy SG, Brickley S & Farrant M (2001) NMDAR receptor subunits: diversity, development and disease. *Curr Opin Neurobiol* **11**: 327-335

Cummings JA, Mulkey RM, Nicoll RA & Malenka RC (1996) Ca^{2+} signalling requirements for long-term depression in the hippocampus. *Neuron* **16**:825-833

Das S, Sasaki YF, Rothe T, Premkumar LS, Takasu M, Crandall JE, Dikkes P, Conner DA, Rayadu PV, Cheung W, Chen HSV, Lipton SA & Nakanishi N (1998) Increased NMDA current and spine density in mice lacking the NMDA receptor subunit NR3A. *Nature* **393**:373-381

D'Angelo E, De Filippi G, Rossi P & Taglietti V (1995) Synaptic excitation of individual rat cerebellar granule cells in situ: evidence for the role of NMDA receptors. *J Physiol* **484**:397-413

D'Angelo E, Rossi P, Armano S & Taglietti V (1999) Evidence for NMDA and mGlu receptor-dependent long-term potentiation of mossy fiber-granule cell transmission in rat cerebellum. *J Neurophysiol* **81**:277-287

D'Angelo E, Nieus T, Maffei A, Armano S, Rossi P, Taglietti V, Fontana A & Naldi G (2001) Theta-frequency bursting and resonance in cerebellar granule cells: experimental evidence and modelling of a slow K+-dependent mechanism. *J Neurosci* **21**:759-770

De Schutter E, Vos BP & Maex R (2000) The function of cerebellar Golgi cells revisited. *Prog Brain Res* **124**:81-93

De Zeeuw CI, Hansel C, Bian F, Koekkoek SKE, van Alphen AM, Linden DJ & Oberdick J (1998) Expression of a protein kinase C inhibitor in Purkinje cells blocks cerebellar LTD and adaptation of the vestibule-ocular reflex. *Neuron* **20**:495-508

Diamond JS & Jahr CE (1997) Transporters buffer synaptically released glutamate on a submillisecond time scale. *J Neurosci* **17**:4672-4687

Diamond JS (2001) Neuronal glutamate transporters limit activation of NMDA receptors by neurotransmitter spillover on CA1 pyramidal cells. *J Neurosci* **21**:8328-8338

Diamond JS (2002) A broad view of glutamate spillover. *Nature Neurosci* **5**: 291-292

Dieudonné S (1995) Glycinergic synaptic currents in Golgi cells of the rat cerebellum. *Proc Natl Acad Sci USA* **92**:1441-1445

Dieudonné S (1998) Submillisecond kinetics and low efficacy of parallel fibre-Golgi cell synaptic currents in the rat cerebellum. *J Physiol* **510**:845-866

Dieudonné S & Dumoulin A (2000) Serotonin-driven long-range inhibitory connections in the cerebellar cortex. *J Neurosci* **20**:1837-1848

DiGregorio DA, Nusser Z & Silver RA (2002) Spillover of glutamate onto synaptic AMPA receptors enhances fast transmission at a cerebellar synapse. *Neuron* **35**:521-533

Dingledine R, McBain CJ & McNamara JO (1990) Excitatory amino acid receptors in epilepsy. *Trends Pharmacol* **11**:334-338

Dingledine R, Borges K, Bowie D & Traynelis SF (1999) The glutamate receptor ion channels. *Pharmacol Revs* **51**:7-61

Diño MR, Nunzi MG, Anelli R & Mugnaini E (2000) Unipolar brush cells of the vestubilocerebellum: afferents and targets. *Prog Brain Res* **124**:123-137

Dumoulin A, Triller A & Diendonné S (2001) IPSC kinetics at identified GABAergic and mixed GABAergic and glycinergic synapses onto cerebellar Golgi cells. *J Neurosci* **21**:6045-6057

Dunah AW, Yasuda RP, Wang YH, Luo J, Dávila-García MI, Gbadegesin M, Vicini S & Wolff BB (1996) Regional and ontogenic expression of the NMDA receptor subunit NR2D protein in rat brain using a subunit-specific antibody. *J Neurochem* **67**:2335-2345

Dunah AW, Luo J, Wang YH, Yasuda RP & Wolff BB (1998) Subunit composition of *N*-methyl-D-aspartate receptors in the central nervous system that contain the NR2D subunit. *Mol Pharmacol* **53**:170-174

Durand GL, Gregor P, Zheng X, Bennett MVL, Uhl GR & Zukin RS (1992) Cloning of an apparent splice variant of the rat *N*-methyl-D-aspartate receptor NMDAR1 with altered sensitivity to polyamines and activators of protein kinase C. *Proc Natl Acad Sci* **89**:9359-9363

Durand GM, Kovalchuk Y & Konnerth A (1996) Long-term potentiation and functional synapse induction in developing hippocampus. *Nature* **381**:71-5

Ebralidze AK, Rossi DJ, Tonegawa S & Slater NT (1996) Modification of NMDA receptor channels and synaptic transmission by targeted disruption of the NR2C gene. *J Neurosci* **16**:5014-5025

Eccles JC, Llinás R & Sasaki K (1966) The mossy fibre-granule cell relay of the cerebellum and its inhibitory control by Golgi cells. *Exp Brain Res* **1**:82-101

Eccles JC, Ito M & Szentágothai J (1967) The cerebellum as a neuronal machine. Springer-Verlag.

Edgley SA & Lidierth M (1987) The discharges of cerebellar Golgi cells during locomotion in the cat. J Physiol 392:315-332

Ehlers MD, Fung ET, O'Brien RJ & Huganir RL (1998) Splice variant-specific interaction of the NMDA receptor subunit NR1 with neuronal intermediate filaments. *J Neurosci* **18**:720-730

Ekerot C & Jörntell H (2001) Parallel fibre receptive fields of Purkinje cells and interneurons are climbing fibre-specific. *Eur J Neurosci* **13**:1303-1310

Ekerot C-F & Kano M (1985) Long-term depression of parallel fibre synapses following stimulation of climbing fibres. *Brain Res* **342**:357-360

Fairman WA, Vandenberg RJ, Arriza JL, Kavanaugh MP & Amara SG (1995) An excitatory amino-acid transporter with properties of a ligand-gated chloride channel. *Nature* **375**:599-603

Farrant M, Feldmeyer D, Takahashi T & Cull-Candy SG (1994) NMDA-receptor channel diversity in the developing cerebellum. *Nature* **368**:335-339

Fayyazuddin A, Villaroel A, Le Goff A, Lerma J & Neyton J (2000) Four residues of the extracellular N-terminal domain of the NR2A subunit control high-affinity Zn^{2+} binding to NMDA receptors. *Neuron* **25**:683-694

Feldmeyer D & Cull-Candy SG (1993) Temperature dependence of NMDA receptor channel conductance levels in outside-out patches from isolated cerebellar granule cells of the rat. *J Physiol* **459**:284P

Fischer M, Kaech S, Wagner U, Brinkhaus H & Matus A (2000) Glutamate receptors regulate actin-based neurite growth in dendritic spines. *Nature Neurosci* **20**:5024-5036

Flint AC, Maisch US, Weishaupt JH, Kriegstein AR & Monyer H (1997) NR2A subunit expression shortens NMDA receptor synaptic currents in developing neocortex. *J Neurosci* **17**:2469-2476

Frederickson CJ, Klitenick MA, Manton WI & Kirkpatrick JB (1983) Cyto-architectonic distribution of zinc in the hippocampus of man and the rat. *Brain Res* **273**:335-339

Furuta A, Martin LJ, Lin C-LG, Dykes-Hoberg M & Rothstein JD (1997a) Cellular and synaptic localization of the neuronal glutamate transporters excitatory amino acid transporter 3 and 4. *Neuroscience* **81**:1031-1042

Furuta A, Rothstein JD & Martin LJ (1997b) Glutamate transporter protein subtypes are expressed differentially during rat CNS development. *J Neurosci* **17**:8363-8375

Futai K, Okada M, Matsuyama K & Takahashi T (2001) High-fidelity transmission acquired via a developmental decrease in NDMA receptor expression at an auditory synapse. *J Neurosci* **21**:3342-3349

Gabbiani F, Midtgaard J & Knopfel T (1994) Synaptic integration in a model of cerebellar granule cells. *J Neurophysiol* **72**:999-1009

Gallagher MJ, Huang H, Pritchett DB & Lynch DR (1996) Interactions between ifenprodil and the NR2B subunit of the *N*-methyl-D-aspartate receptor. *J Biol Chem* **271**:9603-9611

Garwicz M, Jörntell H & Ekerot C (1998) Cutaneous receptive fields and topography of mossy fibres and climbing fibres projecting to cat cerebellar C3 zone. *J Physiol* **512**:277-293

Gasparini S, Saviane C, Voronin LL & Cherubini E (2000) Silent synapses in the developing hippocampus: lack of functional receptors or low probability of glutamate release? *Proc Natl Acad Sci USA* **97**:9741-9746

Geurts FJ, Timmermans J-P, Shigemoto R & de Schutter E (2001) Morphological and neurochemical differentiation of large granule layer interneurons in the adult rat cerebellum. *Neuroscience* **104**:499-512

Gibb AJ & Colquhoun D (1992) Activation of *N*-methyl-D-aspartate receptors by L-glutamate in cells dissociated from adult rat hippocampus. *J Physiol* **456**:143-179

Grant SGN, O'Dell TJ, Karl KA, Stein PL, Soriano P & Kandel ER (1992) Impaired long-term potentiation, spatial learning, and hippocampal development in *fyn* mutant mice. *Science* **258**:1903-1910

Grant SGN & O'Dell TJ (2001) Multiprotein complex signalling and the plasticity problem. *Curr Opin Neurobiol* **11**:363-368

Grosshans DR, Clayton DA, Coultrap SJ & Browning MD (2002) LTP leads to rapid surface expression of NMDA but not AMPA receptors in adult rat CA1. N*ature Neurosci* **5**:27-33

Hall RA & Soderling TR (1997) Differential surface expression and phosphorylation of the *N*-methyl-D-aspartate receptor subunit NR1 and NR2 in cultured hippocampal neurons. *J Biol Chem* **272**: 4135-4140

Hamill OP, Marty A, Neher E & Sakmann B (1981) Improved patch-clamp techniques for high-resolution current recording from cells and cell-free membrane patches. *Pflugers Arch* **391**:85-100

Hámori J & Szentágothai J (1966) Participation of Golgi neuron processes in the cerebellar gloneruli: an electron microcope study. *Exp Br Res* **2**:35-48

Hardingham GE, Fulunaga Y & Bading H (2002) Extrasynaptic NMDARs oppose synaptic NMDARs by triggering CREB shut-off and cell death pathways. *Nature Neurosci* **5**:405-413

Hardingham GE & Bading H (2003) The yin and yang of NMDA receptor signalling. *Trends Neurosci* **26**:81-89

Harsch A & Robinson HPC (2000) Postsynaptic variability of firing in rat cortical neurons: the roles of input synchronization and synaptic NMDA receptor conductance. *J Neurosci* **20**:6181-6192

Hartmann MJ & Bower JM (1998) Oscillatory activity in the cerebellar hemispheres of unrestrained rats. *J Neurophysiol* **80**:1598-1604

Hestrin S (1992) Developmental regulation of NMDA receptor-mediated synaptic currents at a central synapse. *Nature* **357**:686-689

Hirano T (1990) Synaptic transmission between rat inferior olivary neurons and cerebellar Purkinje cells in culture. *J Neurophysiol* **63**:181-189

Hollmann M, Boulter J, Maron C, Beasley L, Sullivan J, Pecht G & Heinemann S (1993) Zinc potentiates agonist-induced currents at certain splice variants of the NMDA receptor. *Neuron* **10**:943-954

Hollmann M & Heinemann M (1994) Cloned glutamate receptors. *Annu Rev Neurosci* **17**:31-108

Hollmann M, Maron C & Heinemann S (1994) N-glycosylation site tagging suggests a three transmembrane segment topology for the glutamate receptor GluR1. *Neuron* **13**:1331-1343

Howe JR, Cull-Candy SG & Colquhoun D (1991) Currents through single glutamate receptor channels in outside-out patches from rat cerebellar granule cells. *J Physiol* **432**:142-202

Howell GA, Welch MG & Frederickson CJ (1984) Stimulation-induced uptake and release of zinc in hippocampal slices. *Nature* **308**:736-738

Huettner JE & Bean BP (1988) Block of *N*-methyl-D-aspartate-activated current by the anticonvulsant MK-801: selective binding to open channels. *Proc Natl Acad Sci USA* **85**:1307-1311

Hume RI, Dingledine R & Heinemann SF (1991) Identification of a site in glutamate receptor subunits that controls calcium permeability. *Science* **253**:1028-1031

Ichise T, Kano M, Hashimoto K, Yanagihara D, Nakao K, Shigemoto R, Katsuki M & Aiba A (2000) mGluR1 in cerebellar Purkinje cells essential for long-term depression, synapse elimination and motor coordination. *Science* **288**:1832-1835

Ikeda K, Magasawa M, Mori H, Araki K, Sakimura K, Watanabe M, Inoue Y & Mishina M (1992) Cloning and expression of the $\epsilon 4$ subunit of the NMDA receptor channel. *FEBS Lett* **313**:34-38

Ikeda K, Araki K, Takayama C, Inoue Y , Yagi T, Aizawa S & Mishina M (1995) Reduced spontaneous activity of mice defective in the $\varepsilon 4$ subunit of the NMDA receptor channel. *Mol Brain Res* **33**:61-71

Ilyin VI, Whittemore ER, Guastella J, Weber E & Woodward RM (1996) Subtype-selective inhibition of *N*-methyl-D-aspartate receptors by haloperidol. *Mol Pharm* **50**:1541-1550

Imamura Y, Inokawa H, Ito A, Kadotani H, Toyama K, Noda M, Nakanishi S & Hirano T (2000) Roles of GABAergic inhibition and NMDA receptor subunits in the spatio-temporal integration in the cerebellar cortex of mice. *Neurosci Res* **38**:289-301

Isaac JT, Nicoll RA & Malenka RC (1995) Evidence for silent synapses: implications for the expression of LTP. *Neuron* **15**:427-434

Isaacson JS (1999) Glutamate spillover mediates excitatory transmission in the rat olfactory bulb. *Neuron* **23**:377-384

Isaacson JS & Murphy GJ (1999) Glutamate-mediated extrasynaptic inhibition: direct coupling of NMDA receptors to Ca^{2+}-activated K^{+} channels. *Neuron* **31**:1027-1034

Ishii T, Moriyoshi K, Sugihara H, Sakurada K, Kadotani H, Yokoi M, Akazawa C, Shigemoto R, Mizuna N, Masu M & Nakanishi S (1993) Molecular characterisation of the family of *N*-methyl-D-aspartate receptor subunits. *J Biol Chem* **268**:2836-2843

Ito M (2000) Mechanisms of motor learning in the cerebellum. Brain Res 886:237-245

Ito M (2001) Cerebellar long-term depression: characterisation, signal transduction and functional roles. Physiol Rev 81:1143-1195

Ito M & Kano M (1982) Long-lasting depression of parallel fiber-Purkinje cell transmission induced by conjunctive stimulation of parallel fibers and climbing fibers in the cerebellar cortex. *Neurosci Lett* **33**:253-258

Ito M, Sakurai M & Tongroach P (1982) Climbing fibre induced depression of both mossy fibre responsiveness and glutamate sensitivity of cerebellar Purkinje cells. *J Physiol* **324**:113-134

Jahr CE (1992) High probability opening of NMDA receptor channels by L-glutamate. *Science* **255**:470-472

Jahr CE & Stevens CF (1987) Glutamate activates multiple single channel conductances in hippocampal neurons. *Nature* **325**:522-525.

Johnson JW & Ascher P (1987) Glycine potentiates the NMDA response in cultured nouse brain neurons. *Nature* **325**:529-531

Kadotani H, Hirano T, Masugi M, Nakamura K, Nakao K, Katsiki M & Nakanishi S (1996) Motor discoordination results from combined gene disruption of the NMDA receptor NR2A and NR2C subunits, but not from single disruption of the NR2A or NR2C subunit. *J Neurosci* **16**: 7859-5867

Kakizawa S, Yamasaki M, Watanabe M & Kano M (2000) Critical period of activity-dependent synapse elimination in developing cerebellum. *J Neurosci* **20**:4954-4961

Kanai Y & Hediger MA (1992) Primary structure and functional characterization of a high affinity glutamate transporter. *Nature* **360**:467-471

Kandel ER, Schwartz JH & Jessel TM (1991) Principles of neural science (3rd edition). Prentice Hall International Inc.

Kano M, Kato M & Chang HS (1988) The glutamate receptor subtype mediating parallel fibre-Purkinje cell transmission in rabbit cerebellar cortex. *Neurosci Res* **5**:325-337

Kew JN, Trube G & Kemp JA (1996) A novel mechanism of activity-dependent NMDA receptor antagonism describes the effect of ifenprodil in rat cultured cortical neurons. *J Physiol* **497**:761-772

Kew JN, Richards JG, Mutel V & Kemp JA (1998) Developmental changes in NMDA receptor glycine affinity and ifenprodil sensitivity reveal three distinct populations of NMDA receptors in individual rat cortical neurons. J Neurosci 18:1935-1943

Kim W-K, Choi Y-B, Rayudu PV, Das P, Asaad W, Arnelle DR, Stamler JS & Lipton SA (1999) Attenuation of NMDA receptor activity and neurotoxicity by nitroxyl anion, NO^-. *Neuron* **24**:461-469

Kinney GA, Overstreet LS & Slater NT (1997) Prolonged physiological entrapment of glutamate in the synaptic cleft of cerebellar unipolar brush cells. *J Neurophysiol* **78**:1320-1333

Kirson ED & Yaari Y (1996) Synaptic NMDA receptors in developing mouse hippocampal neurones: functional properties and sensitivity to ifenprodil. *J Physiol* **497**:437-455

Kirson ED & Yaari Y (2000) Unique properties of NMDA receptors enhance synaptic excitation of radiatum giant cells in rat hippocampus. *J Neurosci* **20**:4844-4854

Kiyama Y, Manabe T, Sakimura K, Kawakami F, Mori H & Mishina M (1998) Increased thresholds for long-term potentiation and contextual learning in mice lacking the NMDA-type glutamate receptor ε1 subunit. *J Neurosci* **18**:6704-6712

Kleckner NW & Dingledine R (1988) Requirement for glycine in activation of NMDA receptors expressed in *Xenopus* oocytes. *Science* **241**:835-837

Knoflach F, Woltering T, Adam G, Mutel V & Kemp JA (2001) Pharmacological properties of native metabotropic glutamate receptors in freshly dissociated Golgi cells of the rat cerebellum. *Neuropharmacology* **40**:163-169

Köhr G, Eckardt S, Luddens H, Monyer H & Seeburg PH (1994) NMDA receptor channels: subunit-specific potentiation by reducing agents. *Neuron* **12**:1031-1040

Köhr G & Seeburg PH (1996) Subtype-specific regulation of recombinant NMDA receptor-channels by protein tyrosine kinases of the *src* family. *J Physiol* **492**:445-452

Komura H & Rakic P (1993) Modulation of neuronal migration by NMDA receptor. *Science* **260**:95-97

Kornau H, Schenker LT, Kennedy MB & Seeburg P (1995) Domain interaction between NMDA receptor subunits and the postsynaptic density protein PSD-95. *Science* **269**:1737-1740

Kreitzer AC & Regehr WG (2000) Modulation of transmission during trains at a cerebellar synapse. *J Neurosci* **20**:1348-1357

Krupp JJ, Vissel B, Heinemann SF & Westbrook GL (1996) Calcium-dependent inactivation of recombinant *N*-methyl-D-asparate receptors is NR2 subunit specific. *Mol Pharmacol* **50**:1680-1688

Kuner T & Schoepfer R (1996) Multiple structural elements determine subunit specificity of Mg^{2+} block in NMDA receptor channels. *J Neurosci* **16**:3549-3558

Kuner T, Schoepfer R & Korpi ER (1993) Ethanol inhibits glutamate-induced currents in heteromeric NMDA receptor subtypes. *Neuroreport* **5**:297-300

Kullmann DM & Asztely F (1998) Extrasynaptic glutamate spillover in the hippocampus: evidence and implications. *Trends Neurosci* **21**:8-14

Kutsuwada T, Kashiwabuchi N, Mori H, Sakimura K, Kushiya E, Araki K, Meguro H, Masaki H, Kumanishi T, Arakawa M & Mishina M (1992) Molecular diversity of the NMDA receptor channel. *Nature* **358**:36-41

Lainé J & Axelrad H (2002) Extending the cerebellar Lugaro cell class. *Neuroscience* **115**:363-374

Lan JY, Skeberdis VA, Jover T, Grooms SY, Lin Y, Araneda RC, Zheng X, Bennett MVL & Zukin RS (2001) Protein kinase C modulates NMDA receptor trafficking and gating. *Nature Neurosci* **4**:382-390

Laube B, Kuhse J & Betz H (1998) Evidence for a tetrameric structure of recombinant NMD ceptors. *J Neurosci* **18**:2954-2961

Lau LF & Huganir RL (1995) Differential tyrosine phosphorylation of N-methyl-D-aspartate receptor subunits. *J Biol Chem* **270**:20036-20041

Laurie DJ & Seeburg PH (1994a) Regional and developmental heterogeneity in splicing of the rat brain NMDAR1 mRNA. *J Neurosci* **13**:3180-3194

Laurie DJ & Seeburg PH (1994b) Ligand affinities at recombinant *N*-methyl-D-aspartate receptors depend on subunit composition. *Eur J Pharmacol* **268**:335-345

LeBrun B, Sakaitani M, Shimamoto K, Yasuda-Kamatani Y & Nakajima T (1997) New β-hydroxyaspartate derivatives are competitive blockers for the bovine glutamate/aspartate transporter. *J Biol Chem* **272**:20336-20339

Legendre P & Westbrook GL (1990) The inhibition of single *N*-methyl-D-aspartate-activated channels by zinc ions on cultured rat neurones. *J Physiol* **429**:429-449

Legendre P & Westbrook GL (1991) Ifenprodil blocks *N*-methyl-D-aspartate receptors by a two-component mechanism. *Mol Pharmacol* **40**:289-298

Legendre P, Rosenmund C & Westbrook GL (1993) Inactivation of NMDA channels on hippocampal neurons by intracellular calcium. *J Neursci* **13**:674-684

Lehre KP, Levy LM, Ottersen OP, Storm-Mathisen J & Danbolt NC (1995) Differential expression of two glial glutamate transporters in the rat brain: quantitative and immunosytochemical observations. *J Neurosci* **15**:1835-1853

Lei SB, Czerwinska E, Czerwinski W, Walsh MP & MacDonald JF (2001) Regulation of NMDA receptor activity by F-actin and myosin light chain kinase. *J Neurosci* **21**:8464-8472

Lei SB & McBain CJ (2002) Distinct NMDA receptors provide differential modes of transmission at mossy fiber-interneuron synapses. *Neuron* **33**:921-933

Lei SZ, Pan ZH, Aggarwal SK, Hartman J, Sucher NJ & Lipton AS (1992) Effect of nitric oxide production on the redox modulatory site of the NMDA-receptor-channel complex. *Neuron* **8**:1087-1099

Leonard AS & Hell JW (1997) Cyclic-AMP-dependent protein kinase and protein kinase C phosphorylate *N*-methyl-D-aspartate receptors at different sites. *J Biol Chem* **272**:12107-12115

Lester RAJ, Clements JD, Westbrook GL & Jahr CE (1990) Channel kinetics determine the time course of NMDA receptor-mediated synaptic currents. *Nature* **346**:565-567

Leszkiewicz DN, Kandler K & Aizenman E (2000) Enhancement of NMDA receptor-mediated currents by light in rat neurones in vitro. *J Physiol* **524**:365-374

Li B, Chen N, Luo T, Otsu Y, Murphy TH & Raymond LA (2002) Differential regulation of synaptic and extrasynaptic NMDA receptors. *Nature Neurosci* **5**:833-834

Li J, Smith SS & McElligott JG (1995) Cerebellar nitric oxide is necessary for vestibule-ocular reflex adaptation, a sensimotor model of learning. *J Neurophysiol* **74**:489-494

Li JH, Wang YH, Wolfe BB, Krueger KE, Corsi L, Stocca G & Vicini S (1998) Developmental changes in localization of NMDA receptor subunits in primary cultures of cortical neurons. *Eur J Neurosci* **10**:1704-1715

Li Y, Hough CJ, Frederickson CJ & Sarvey JM (2001) Induction of mossy fibre-CA3 long-term potentiation requires translocation of synaptically released Zn^{2+}. *J Neurosci* **21**:8015-8025

Liao D, Hessler NA & Malinow R (1995) Activation of postsynaptically silent synapses during pairing-induced LTP in CA1 region of hippocampal slice. *Nature* **375**:400-404

Lin S-Y & Constantine-Paton M (1998) Supression of sprouting: an early function of NMDA receptors in the absence of AMPA/kainate receptor activity. *J Neurosci* **18**: 3725-3737

Lin DD, Cohen AS & Coulter DA (2001) Zinc-induced augmentation of excitatory synaptic currents glutamate receptor response in hippocampal CA3 neurons. *J Neurophysiol* **85**:1185-1196

Lipton SA, Choi Y-B, Pan Z-H, Lei SZ, Chen H-SV, Sucher NJ, Loscalzo J, Singel DJ & Stamler JS (1993) A redox-based mechanism for the neuroprotective and neurodestructive effects of nitric oxide and related nitroso-compounds. *Nature* **364**:626-632

Liu S-QJ & Cull-Candy (2000) Synaptic activity at calcium-permeable AMPA receptors induces a switch in receptor subtype. *Nature* **405**:454-458

Lodge D, edited by (1988) Excitatory amino acids in health and disease. J. Wiley & Sons

Lopez de Armentia M & Sah P (2002) NMDA receptors in central amygdale neurons in adult rats contain NR2B subunits. *Soc Neuro Abstract* 747.5

Low C-M, Zheng F, Lyuboslavsky P & Traynelis SF (2000) Molecular determinants of coordinated proton and zinc inhibition of *N*-methyl-D-asparate NR1/NR2A receptors. *Proc Natl Acad Sci* **97**:11062-11067

Lu H-C, Gonzalez E & Crair MC (2001) Barrel cortex critical period plasticity is independent of changes in NMDA receptor subunit composition. *Neuron* **32**:619-634

Lu W-Y, Man H-Y, Ju W, Trimble WS, MacDonald JF & Wang YT (2001) Activation of synaptic NMDA receptors induces membrane insertion of new AMPA receptors and LTP in cultured hippocampal neurons. *Neuron* **29**:243-254

Lu YM, Roder JC, Davidow J & Salter MW (1998) Src activation in the induction of long-term potentiation in CA1 hippocampal neurons. *Science* **279**:1363-1367

Lu YM, Taverna FA, Tu R, Ackerley CA, Wang Y-T & Roder J (2000) Endogenous Zn2+ is required for the induction of long-term potentiation at rat hippocampal mossy fiber-CA3 synapses. *Synapse* **38**:187-197

Luo J-H, Wang Y-H, Yasuda RP, Dunah AW & Wolfe BB (1997) The majority of *N*-methyl-D-aspartate receptor complexes in the adult rat cerebral cortex contain at least three different subunits (NR1/NR2A/NR2B). *Mol Pharmacol* **51**:79-86

Luo J-H, Fu Z-Y, Losi G, Kim BG, Prybylowski K, Vissel B & Vicini S (2002) Functional expression of distinct NMDA channel subunits tagged with green fluorescent protein in hippocampal neurons in culture. *Neuropharmacol* **42**:306-318

Lüscher C, Nicoll RA, Malenka RC & Muller D (2000) Synaptic plasticity and dynamic modulation of the postsynaptic membrane. *Nature Neurosci* **3**: 545-550

Lüthi A, Schwyzer L, Mateos JM, Gähwiler BH & McKinney RA (2001) NMDA receptor activation limits the number of synaptic connections during hippocampal development. *Nature Neurosci* **4**:1102-1107

Maccaferri G & Dingledine R (2002) Control of feedforward dendritic inhibition by NMDA receptor-dependent spike timing in hippocampal interneurons. *J Neurosci* **22**:5462-5472

MacDermott AB, Mayer ML, Westbrook GL, Mith Sj & Barker JL (1986) NMDA-receptor activation increases cytoplasmic calcium concentration in cultured spinal cord neurones. *Nature* **321**:519-522

Maex R & de Schutter E (1998) Synchronization of Golgi and granule cell firing in a detailed network model of the cerebellar granule cell layer. *J Neurophysiol* **80**:2521-2537

Magee JC (2003) A prominent role for intrinsic neuronal properties in temporal coding. *Trends Neurosci* **26**:14-16

Mainen ZF & Sejnowski TJ (1995) Reliability of spike timing in neocortical neurons. *Science* **268**:1503-1506

Marr D (1969) A theory of cerebellar cortex. *J Physiol* **202**:437-470

Mauk MD (1997) Roles of cerebellar cortex and nuclei in motor learning: contradictions and clues? *Neuron* **18**:343-346

Mauk MD, Medina JF, Nores WL & Ohyama T (2000) Cerebellar function: coordination, learning or timing? *Curr Biol* **10**:R522-525

Mayer ML & Westbrook GL (1985) The activation of *N*-methyl-D-aspartic acid on mouse spinal neurons in culture. *J Physiol* **361**:65-90

Mayer ML, Vyklicky L & Westbrook GL (1989) Modulation of excitatory amino acid receptors by group IIB metal cations in cultured mouse hippocampal neurones. *J Physiol* **415**:329-350

McBain CJ & Mayer ML (1994) *N*-methyl-D-aspartic acid receptor structure and function. *Physiol Revs* **74**:723-760

McLennan H (1983) Receptors for the excitatory amino acids in the mammalian central nervous system. *Prog Neurobiol* **20**:251-271

Medina I, Filippova N, Charton G, Rougeole S, Ben-Ari Y, Khrestchatisky M & Bregestovski P (1995) Calcium-dependent inactivation of heteromeric NMDA receptor channels expressed in human embryonic kidney cells. *J Physiol* **482**:567-573

Meguro H, Mori H, Araki K, Kushiya E, Kutsuwada T, Yamazaki M, Kumanishi T, Arakawa M, Sakimura K & Mishina M (1992) Functional characterization of a heteromeric NMDA receptor channel expressed from cloned cDNAs. *Nature* **357**:70-74

Meldrum B & Garthwaite J (1990) Excitatory amino acid neurotoxicity and neurodegenerative disease. *Trends Pharmacol Sci* 11:379-387

Minelli A, Barbaresi P, Reimer RJ, Edwards RH & Conti F (2001) The glial glutamate transporter GLT-1 is localized both in the vicinity of and at distance from axon terminals in the rat cerebral cortex. *Neuroscience* **108**:51-59

Misra C, Brickley SG, Farrant M & Cull-Candy SG (2000a) Identification of subunits contributing to synaptic and extrasynaptic NMDA receptors in Golgi cells of the rat cerebellum. *J Physiol* **524**:147-162

Misra C, Brickley SG, Wyllie DJ & Cull-Candy SG (2000b) Slow deactivation kinetics of NMDA receptors containing NR1 and NR2D subunits in rat cerebellar Purkinje cells. *J Physiol* **525**:299-305

Mitchell SJ & Silver RA (2000) Glutamate spillover suppresses inhibition by activating presynaptic mGluRs. *Nature* **404**:498-502

Momiyama A, Feldmeyer D & Cull-Candy SG (1996) Identification of a native low-conductance NMDA channel with reduced sensitivity to Mg^{2+} in rat central neurones. *J Physiol* **494**:479-492

Momiyama A (2000) Distinct synaptic and extrasynaptic NMDA receptors identified in dorsal horn neurones of the adult rat spinal cord. *J Physiol* **523**:621-628

Monaghan DT & Cotman CW (1986) Identification and properties of N-methyl-D-aspartate receptors in rat brain synaptic plasma membranes

Monaghan DT, Andaloro VJ & Skifter DA (1998) Molecular determinants of NMDA receptor pharmacological diversity. Prog Brain Res 116: 171-189

Monyer H, Seeburg PH & Wisden W (1991) Glutamate-operated channels: developmentally early and mature forms arise by alternative splicing. *Neuron* **6**:779-810

Monyer H, Sprengel R, Schoepfer R, Herb A, Higuchi M, Lomeli H, Burnashev N, Sakmann B & Seeburg PH (1992) Heteromeric NMDA receptors: molecular and functional distinctions of subtypes. *Science* **256**:1217-1221

Monyer H , Burnashev N, Laurie DJ, Sakmann B & Seeburg PH (1994) Developmental and regional expression in the rat brain and functional properties of four NMDA receptors. *Neuron* **12**:529-540

Moon IS, Apperson ML & Kennedy MB (1994) The major tyrosine-phosphorylated protein in the postsynaptic density fraction is *N*-methyl-D-aspartate receptor subunit 2B. *Proc Natl Acad Sci* **91**: 3954-3958

Mori H, Masaki H, Yamakura T & Mishina M (1992) Identification by mutagenesis of a Mg^{2+}-block site of the NMDA receptor channel. *Nature* **358**:673-675

Moriyoshi K, Masu M, Ishii T, Shigemoto R, Mizuno N & Nakanishi S (1991) Molecular cloning and characterization of the rat NMDA receptor. *Nature* **354**:31-37

Mott DD, Doherty JJ, Zhang S, Washburn MS, Fendley MJ, Lyuboslavsky P, Traynelis SF & Dingledine R (1998) Phenylethanolamines inhibit NMDA receptors by enhancing proton inhibition. *Nature Neurosci* **1**:659-667

Mugnaini E & Floris A (1994) The unipolar brush cell: a neglected neuron of the mammalian cerebellar cortex. *J Comp Neurol* **339**:174-180

Nabekura J, Ueno T, Katsurabayashi S, Furuta A, Akaike N & Okada M (2002) Reduced NR2A expression and prolonged decay of NMDA receptor-mediated synaptic current in rat vagal motoneurons following axotomy. *J Physiol* **539**:735-741

Napper RM & Harvey RJ (1988) Number of parallel fiber synapses on an individual Purkinje cell in the cerebellum of the rat. *J Comp Neurol* **274**:168-177

Neher E & Sakmann B (1995) In *Single-channel recording*. 2nd edition. Eds. Neher E & Sakmann B.

Neki A, Ohishi H, Kaneko T, Shigemoto R, Nakanishi S & Mizuno N (1996) Metabotropic glutamate receptors mGluR2 and mGluR5 expressed in two non-overlapping populations of Golgi cells in the rat cerebellum. *Neuroscience* **75**:815-826

Niethammer M, Kim E & Sheng M (1996) Interaction between the C terminus of NMDA receptor subunits and multiple members of the PSD-95 family of membrane-associated guanylate kinases. *J Neurosci* **16**:2157-2163

Nowak LM, Bregestovski P, Ascher P, Herbet A & Prochiantz A (1984) Magnesium gates glutamate-activated channels in mouse central neurones. *Nature* **307**:263-465

O'Dell TJ, Kandel ER & Grant SG (1991) Long-term potentiation in the hippocampus is blocked by tyrosine kinase inhibitors. *Nature* **353**:558-560

Okabe S, Collin C, Auerbach JM, Neiri N, Bengzon J, Kennedy MB, Segal M & McKay RDG (1998) Hippocampal synaptic plasticity in mice overexpressing an embryonic subunit of the NMDA receptor. *J Neurosci* **18**:4177-4188

Otis TS (2002) Helping thy neighbors: spillover at the mossy fiber glomerulus. *Neuron* **35**: 412-414

Otis TS, Wu Y-C & Trussell LO (1996) Delayed clearance of transmitter and the role of glutamate transporters at synapses with multiple release sites. *J Neurosci* **16**:1634-1644

Overstreet LS, Kinney GAm Liu Y-B, Billups D & Slater NT (1999) Glutamate transporters contribute to the time course of synaptic transmission in cerebellar granule cells. *J Neurosci* **19**:9663-9673

Palay SL & Chan-Palay V (1974) Cerebellar cortex: cytology and organisation. Springer-Verlag, Berlin.

Palecek JI, Abdrachmanova G, Vlachova V & Vyklick L Jr. (1999) Properties of NMDA receptors in rat spinal cord motoneurons. *Eur J Neurosci* **11**: 827-36

Paoletti P, Ascher P & Neyton J (1997) High-affinity zinc inhibition of NMDA NR1-NR2A receptors. *J Neurosci* **17**:5711-25

Paoletti P, Perin-Dureau F, Fayyazuddin A, Le Goff A, Callebaut I & Neyton J (2000) Molecular organization of a zinc binding N-terminal modulatory domain in a NMDA receptor subunit. *Neuron* **28**:911-925

Parri HR, Gould TM & Crunelli V (2001) Spontaneous astrocytic Ca^{2+} oscillations in situ drive NMDAR-mediated neuronal excitation. *Nature Neurosci* **4**:803-811

Perez-Clausell J & Danscher G (1985) Intravesicular localization of zinc in telecephalon boutons. A histochemical study. *Brain Res* **337**:91-98

Perez-Otano I, Schulties CT, Contractor A, Lipton SA, Trimmer JS, Sucher NJ & Heinemann SF (2001) Assembly with NR1 subunit is required for surface expression of NR3A-containing NMDA receptors. *J Neurosci*, **21**:175-218.

Perkel DJ, Hestrin S, Sah P & Nicoll RA (1990) Excitatory synaptic currents in Purkinje cells. *Proc R Soc Lond B Biol Sci* **241**:116-121

Peters S, Koh J & Choi DW (1987) Zinc selectively blocks the action of *N*-methyl-D-aspartate on cortical neurons. *Science* **236**:589-593

Petralia RS, Wang Y-X, Singh S, Chun W, Shi L-G, Wei J & Wenthold RJ (1997) A monoclonal antibody shows discrete cellular and subcellular localizations of mGluRα metabotropic glutamate receptors. *J Chem Neuroanat* **13**:77-93

Philpot BD, Sekhar AK, Shouval HZ & Bear MF (2001a) Visual experience and deprivation bidirectionally modify the composition and function of NMDA receptors in visual cortex. *Neuron* **29**:157-169

Philpot BD, Weisberg MP, Ramos MS, Sawtell NB, Tang Y-P, Tsien JZ & Bear MF (2001b) Effect of transgenic overexpression of NR2B on NMDA receptor function and synaptic plasticity in visual cortex. *Neurophamacol* **41**:762-770

Pichitpornchai C, Rawson JA & Rees S (1994) Morphology of parallel fibers in the cerebellar cortex of the rat: an experimental light and electron microscopic study with biocytin. *J Comp Neurol* **342**:206-220

Pines G, Danbolt NC, Bjørás M, Zhang Y, Bendahan A, Eide L, Koepsell H, Storm-Mathisen J, Seeburg E & Kanner BI (1992) Cloning and expression of a rat brain L-glutamate transporter. *Nature* **360**: 464-467

Piña-Crespo JC & Gibb AJ (2002) Subtypes of NMDA receptors in new-born rat hippocampal granule cells. *J Physiol* **541**:41-64

Plant T, Schirra C, Garaschuk O, Rossier J & Konnerth A (1997) Molecular determinants of NMDA receptor function in GABAergic neurones of rat forebrain. *J Physiol* **499**:47-63

Premkumar LS & Auerbach A (1997) Stoichiometry of recombinant *N*-methyl-D-aspartate receptor channels inferred from single-channel current patterns. *J Gen Physiol* **110**:485-502

Priestley T, Laughton P, Myers J, Le Bourdellés B, Kerby J & Whiting PJ (1995) Pharmacological properties of recombinant human *N*-methyl-D-aspartate receptors comprising NR1a/NR2A and NR1a/ NR2B subunit assemblies expressed in permanently transfected mouse fibroblast cells. *Mol Pharmacol* **48**:841-848

Prybylowski KL & Wolfe BB (2000) Developmental differences in alternative splicing of the NR1 protein in rat cortex and cerebellum. *Dev Brain Res* **123**:143-150

Quinlan EM, Philpot BD, Huganir RL & Bear MF (1999) Rapid, experience-dependent expression of synaptic NMDA receptors in visual cortex in vivo. *Nature Neurosci* **2**:352-357

Rabacchi S, Bailly Y, Delhaye-Bouchaud N & Mariani J (1992) Involvement of the *N*-methyl-D-aspartate (NMDA) receptor in synapse elimination during cerebellar development. *Science* **256**:1823-1825

Raman IM, Tong G & Jahr CE (1996) β-adrenergic regulation of synaptic NMDA receptors by cAMP-dependent protein kinase. *Neuron* **16**:415-421

Ramón y Cajal S (1911) Histologie du système nerveux de l'homme et des vertébrés. Tome II. Paris: Maloine. (Histology of the nervous system of man and vertebrates, volume 2 (1995); translated from the French by Neely Swanson and Larry W. Swanson. New York : Oxford University Press)

Renger JJ, Egles C & Liu GS (2001) A developmental switch in neurotransmitter flux enhances synaptic efficacy by affecting AMPA receptor activation. *Neuron* **29**:469-484

Roberts EB & Ramoa AS (1997) Enhanced NR2A subunit expression and decreased NMDA receptor decay time at the onset of ocular dominance plasticity in the ferret. *J Neurophysiol* **81**:2587-2591

Roche KW, Standley S, McCallum J, Dune C, Ehlers MD & Wenthold RJ (2001) Molecular determinants of NMDA receptor internalization. *Nature Neurosci* **4**:794-802

Rossi DJ, Alford S, Mugnaini E & Slater NT (1995) Properties of transmission at a giant glutamatergic synapse in cerebellum: the mossy fiber-unipolar brush cell synapse. *J Neurophysiol* **74**:24-42

Rothstein JD, Martin L, Levey AI, Dykes-Hoberg M, Jin L, Wu D, Nash N & Kuncl RW (1994) Localization of neuronal and glial glutamate transporters. *Neuron* **13**:713-725

Rumbaugh G & Vicini S (1999) Distinct synaptic and extrasynaptic NMDA receptors in developing cerebellar granule neurons. *J Neurosci* **19**:10603-10610

Rumbaugh G, Prybylowski K, Wang JF & Vicini S (2000) Exon 5 and spermine regulate deactivation of NMDA receptor subtypes. *J Neurophysiol* **83**:1300-1306

Rusakov DA & Kullmann DM (1998) Extrasynaptic glutamate diffusion in the hippocampus: ultrastructural constraints, uptake and receptor activation. *J Neurosci* **18**:3158-3170

Sah P, Hestrin S & Nicoll RA (1989) Tonic activation of NMDA receptors by ambient glutamate enhances excitability of neurons. *Nature* **246**:815-818

Sahin M & Hockfield S (1990) Molecular identification of the Lugaro cell in the cat cerebellar cortex. *J Comp Neurol* **301**:575-584

Sakimura K, Kutsuwada T, Ito I, Manabe T, Takayama C, Kushiya E, Yagi T, Aizawa S, Inoue Y, Sugiyama H & Mishina M (1995) Reduced hippocampal LTP and spatial learning in mice lacking NMDA receptor ε1 subunit. *Nature* **373**:151-155

Sans N, Petralia RS, Wang Y-X, Blahos J II, Hell JW & Wenthold RJ (2000) A developmental change in NMDA receptor-associated proteins at hippocampal synapses. *J Neurosci* **20**:1260-1271

Sarantis M, Ballerini L, Miller B, Siler RA, Edwards M & Attwell D (1993) Glutamate uptake from the synaptic cleft does not shape the decay of the non-NMDA component of the synaptic current. *Neuron* **11**:541-549

Scott DB, Blanpied TA, Swanson GT, Zhang C & Ehlers MD (2001) An NMDA receptor ER retention signal regulated by phosphorylation and alternative splicing. *J Neurosci* **21**:3063-3072

Seeburg PH (1996) The role of RNA editing in controlling glutamate receptor channel properties. *J Neurochem* **66**:1-5

Sheng M, Cummings J, Roldan LA, Jan YN & Jan LY (1994) Changing subunit composition of heteromeric NMDA receptors during development of rat cortex. *Nature* **368**:144-147

Sheng M & Kim MJ (2002) Postsynaptic signaling and plasticity mechanisms. *Science* **298**:776-780

Shi S-H, Hayashi Y, Petralia RS, Zaman SH, Wenthold RJ, Szoboda K & Malinow R (1999) Rapid spine delivery and redistribution of AMPA receptors after synaptic NMDA receptor activation. *Science* **284**:1811-1816

Shibuki K, Gomi H, Chen L, Bao S, Kim JJ, Wakatsuki H, Fujisaki T, Fujimoto K, Katoh A, Ikeda T, Chen C, Thompson RF & Itohara S (1996) Deficient cerebellar long-term depression, impaired eyeblink conditioning, and normal motor coordination in GFAP mutant mice. *Neuron* **16**:587-599

Shimamoto K, LeBrun B, Yasuda-Kamatani Y, Sakaitani M, Shigeri Y, Yumoto N & Nakajima T (1998) DL-*threo*-β-Benzyloxyaspartate, a potent blocker of excitatory amino acid transporters. *Mol Pharmacol* **53**:195-201

Shirasaki T, Harata N & Akaike N (1994) Metabotropic glutamate response in acutely dissociated hippocampal CA1 pyramidal neurones of the rat. *J Physiol* **475**:439-453

Silver RA, Traynelis SF & Cull-Candy SG (1992) Rapid-time-course miniature and evoked excitatory currents at cerebellar synapses *in situ*. Nature, 355:163-6

Sin WC, Haas K, Ruthazer ES & Cline HT (2002) Dendrite growth increased by visual activity requires NMDA receptor and Rho GTPases. *Nature* **419**:475-480

Sinor JD, Du S, Venneti S, Blitzblau RC, Leszkiewicz, Rosenberg PA & Aizenman E (2000) NMDA and glutamate evoke excitotoxicity at distinct cellular locations in rat cortical neurons *in vitro*. *J Neurosci* **20**:8831-8837

Soderling TR & Derkach VA (2000) Postsynaptic protein phosphorylation and LTP. Trends Neurosci 23:75-80

Sommer B, Keinänen K, Verdoorn TA, Wisden W, Burnashev N, Herb A, Köhler M, Takagi T, Sakmann B & Seeburg PH (1990) Flip and flop: a cell-specific functional switch in glutamate-operated channels of the CNS. *Science* **249**:1580-1585

Steigerwald F, Schulz TW, Schenker LT, Kennedy MB, Seeburg PH & Köhr G (2000) C-terminal truncation of NR2A subunits impairs synaptic but not extrasynaptic localization of NMDA receptors. *J Neurosci* **20**:4573-4581

Stern P, Béhé P, Schoepfer R & Colquhoun D (1992) Single-channel conductances of NMDA receptors expressed from cloned cDNAs: comparison with native receptors. *Proc R Soc Lond B* **250**:271-277

Stevens CF & Zador AM (1998) Input synchrony and the irregular firing of cortical neurons. *Nature Neurosci* **1**:210-217

Stocca G & Vicini S (1998) Increased contribution of NR2A subunit to synaptic NMDA receptors in developing rat cortical neurons. *J Physiol* **507**:13-24

Storck T, Schulte S, Hofmann K & Stoffel W (1992) Structure, expression and functional analysis of a Na^+-dependent glutamate/aspartate transporter from rat brain. *Proc Natl Acad Sci USA* **89**:10955-10959

Sucher NJ, Akbarian S, Chi CL, Leclerc CL, Awobuluyi M, Deitcher DL, Wu MK, Yuan JP, Jones EG & Lipton SA (1995) Developmental and regional expression pattern of a novel NMDA receptor-like subunit (NMDAR-L) in the rodent brain. *J Neurosci* **15**:6509-6520

Sugihara H, Moriyoshi K, Ishii T, Masu M & Nakanishi S (1992) Structures and properties of seven isoforms of the NMDA receptor generated by alternative splicing. *Biochem Biophys Res Commun* **185**:826-832

Takahashi T, Feldmeyer D, Suzuki N, Onodera K, Cull-Candy SG, Sakimura K & Mishina M (1996) Functional correlation of NMDA receptor ε subunits

expression with the properties of single-channel and synaptic currents in the developing cerebellum. *J Neurosci* **16**:4376-4382

Takeuchi T, Kiyama Y, Nakamura K, Tsujita M, Matsuda I, Mori H, Munemoto Y, Kuriyama H, Natsume R, Sakimura K & Mishina M (2001) Roles of the glutamate receptor epsilon2 and delta2 subunits in the potentiation and prepulse inhibition of the acoustic startle reflex. *Eur J Neurosci* **14**: 153-60.

Tang YP, Shimizu E, Dube GR, Rampon C, Kercher GA, Zhuo M, Liu G & Tsien JZ (1999) Genetic enhancement of learning and memory in mice. *Nature* **401**:63-69

Taschenberger H & von Gersdorff H (2000) Fine-tuning an auditory synapse for speed and fidelity: developmental changes in presynaptic waveform, EPSC kinetics and synaptic plasticity. *J Neurosci* **20**:9162-9173.

Thompson CL, Dreqery DL, Atkins HD, Stephenson FA & Chazot PL (2002) Immunohistochemical localization of *N*-methyl-D-aspartate receptor subunits in the adult murine hippocampal formation: evidence for a unique role of the NR2D subunit. *Mol Brain Res* **102**:55-61

Tingley WG, Ehlers MD, Kameyama K, Doherty C, Ptak JB, Riley CT & Huganir RL (1997) Characterization of protein kinase A and protein kinase C phosphorylation of the *N*-methyl-D-asparate receptor NR1 subunit using phosphorylation site-specific antibodies. *J Biol Chem* **272**:5157-5166

Tóth K & McBain CJ (1998) Afferent-specific innervatino of two distinct AMPA receptor subtypes on single hippocampal interneurons. *Nature Neurosci.* **1**:572-578

Tovar KR & Westbrook GL (1999) The incorporation of NMDA receptors with a distinct subunit composition at nascent hippocampal synapses *in vitro*. *J Neurosci* **19**:4180-4188

Tovar KR & Westbrook GL (2000) Fast NMDA receptor-mediated synaptic currents in neurones from mice lacking the ε2 (NR2B) subunit. *J Neurophysiol* **83**:616-620

Tovar KR & Westbrook GL (2002) Mobile NMDA receptors at hippocampal synapses. *Neuron* **34**:255-264

Traynelis SF & Cull-Candy SG (1991) Pharmacological properties and H^+ sensitivity to excitatory amino acid receptor channels in rat cerebellar granule neurones. *J Physiol* **433**:727-763

Traynelis SF, Hartley M & Heinemann S (1995) Control of proton sensitivity of the NMDA receptor by RNA splicing and polyamines. *Science* **268**:873-876

Traynelis SF, Burgess MF, Zheng F, Lyuboslavsky P & Powers JL (1998) Control of voltage-independent zinc inhibition of NMDA receptors by the NR1 subunit. *J Neurosci* **18**:6163-6175

Vicini S, Wang JF, Li JH, Zhu WJ, Wang TH, Luo JH, Wolfe BB & Grayson DR (1998) Functional and pharmacological differences between recombinant *N*-methyl-D-aspartate receptors. *J Neurophysiol* **79**:555-566

Vissel B, Krupp JJ, Heinemann SF & Westbrook GL (2001) A use-dependent tyrosine dephosphorylation of NMDA receptors is independent of ion flux. *Nature Neurosci* **4**:587-596

Vogt K, Mellor J, Tong G & Nicoll R (2000) The actions of synaptically released zinc at hippocampal mossy fiber synapses. *Neuron* **26**:187-196

Vos BP, Maex R, Volny-Luraghi A & de Schutter E (1999) Parallel fibres synchronize spontaneous activity in cerebellar Golgi cells. *J Neurosci* **19**:RC6 (1-5)

Wadiche JI, Amara SG & Kavanaugh MP (1995) Ion fluxes associated with excitatory amino acid transport. Neuron 15:721-728

Wafford KA, Bain CJ, Le Bourdelles B, Whiting PJ & Kemp JA (1993) Preferential co-assembly of recombinant NMDA receptors composed of three different subunits. *NeuroReport* **4**:1347-1349

Wang LY, Orser BA, Brautigan DL & MacDonald JF (1994) Regulation of NMDA receptors in cultured hippocampal neurons by protein phosphatases 1 and 2A. *Nature* **369**:230-232

Wang YT & Salter MW (1994) Regulation of NMDA receptors by tyrosine kinases and phosphatases. *Nature* **369**:233-235

Watanabe D, Inokawa H, Hashimoto K, Suzuki N, Kano M, Shigemoto R, Hirano T, Toyama K, Kaneko S, Yokoi M, Moriyoshi K, Suzuki M, Kobayashi K, Nagatsu T, Kreitman RJ, Pastan I & Nakanishi S (1998) Ablation of cerebellar

Golgi cells disrupts synaptic integration involving GABA inhibition and NMDA receptor activation in motor cooridination. *Cell* **95**:17-27

Watanabe M, Mishina M & Inoue Y (1994) Distinct spatiotemporal expression of five NMDA receptor channel subunit mRNAs in the cerebellum. *J Comp Neurol* **343**:513-519

Watkins JC & Evans RH (1981) Excitatory amino acid transmitters. *Ann Rev Pharmacol Toxicol* **21**:165-204

Wenzel A, Villa M, Mohler H & Benke D (1996) Developmental and regional expression of NMDA receptor subtypes containing the NR2D subunit in rat brain. *J Neurochem* **66**:1240-1248

Wenzel A, Fritschy JM, Mohler H & Benke D (1997) NMDA receptor heterogeneity during postnatal development of the rat brain: differential expression of the NR2A, NR2B and NR2C subunit proteins. *J Neurochem* **68**:469-478

Westbrook GL & Mayer ML (1987) Micromolar concentration of Zn^{2+} antagonize NMDA and GABA responses of hippocampal neurons. *Nature* **328**:640-643

Wheal H and Thomson A, edited by (1991) Excitatory amino acids and synaptic transmission. Academic Press

Williams K (1993) Ifenprodil discriminates subtypes of the *N*-methyl-D-aspartate receptor: selectivity and mechanisms at recombinant heteromeric receptors. *Mol Pharmacol* **44**:851-859

Williams K, Russell SL, Shen YM & Molinoff PB (1993) Developmental switch in the expression of NMDA receptors occurs *in vivo* and *in vitro*. *Neuron* **10**:267-278

Williams K (1994) Mechanisms influencing stimulatory effects of spermine at recombinant N-methyl-D-aspartate receptors. *Mol Pharmacol* **45**:803-809

Williams K (1995) Pharmacological properties of recombinant *N*-methyl-D-aspartate (NMDA) receptors containing the ε4 (NR2D) subunit. *Neurosci Lett* **184**:181-184

Williams K (1996) Separating dual effects of zinc at recombinant *N*-methyl-D-aspartate receptors. *Neurosci Lett* **215**:9-12

Wu G-Y, Malinow R & Cline HT (1996) Maturation of a central glutamatergic synapse. *Science* **274**:972-976

Wyllie DJA, Béhé P, Nassar M, Schoepfer R & Colquhoun D (1996) Single-channel currents from recombinant NMDA NR1a/NR2D receptors expressed in *Xenopus* oocytes. *Proc Royal Soc* B **263**: 1079-1086

Wyllie DJA, Béhé P & Colquhoun D (1998) Single-channel activations and concentration jumps: comparison of recombinant NR1a/NR2A and NR1a/NR2D NMDA receptors. *J Physiol* **510**:1-18

Xiong Z-G, Pelkey KA, Lu WY, Lu YM, Roder JC, MacDonald JF & Salter MW (1999) Src potentiation of NMDA receptors in hippocampal and spinal neurons is not mediated by reducing zinc inhibition. *J Neurosci* **19**:5889-5997

Yu X-M & Salter MW (1998) Gain control of NMDA-receptor currents by intracellular sodium. *Nature* **396**:469-474

Zhang L & Goldman JE (1996) Generation of cerebellar interneurons from dividing progenitors in white matter. *Neuron* **16**:47-54

Zhang X-X, Bunney BS & Shi W-Z (2000) Enhancement of NMDA-induced current by the putative NR2B selective antagonist ifenprodil. *Synapse* **37**:56-63

Zheng F, Gingrich MB, Traynelis SF & Conn PJ (1998) Tyrosine kinases potentiates NMDA receptor current by reducing tonic Zn^{2+} inhibition. *Nature Neurosci* **1**:185-191

Zheng F, Erreger K, Low C-M, Banke T, Lee CJ, Conn PJ & Traynelis SF (2001) Allosteric interaction between the amino terminal domain and the ligand binding domain of NR2A. *Nature Neurosci* **4**:894-901

Zhong J, Carrozza DP, Williams K, Pritchett DB, Molinoff PB (1995) Expression of mRNAs encoding subunits of the NMDA receptor in the developing rat brain. *J Neurochem* **64**:531-539

Ziff EB (1997) Enlightening the postsynaptic density. *Neuron* **19**:1163-1174

Zucker RS (1999) Calcium- and activity-dependent synaptic plasticity. *Curr Opin Neurobiol* **9**:305-313

Zukin RS & Bennett MVL (1995) Alternatively spliced isoforms of the NMDAR1 receptor subunit. *Trends Neurosci* **18**:306-313